THE GENERATION OF DUAL-WAVELENGTH FIBER LASERS AND THEIR APPLICATIONS

AMIRAH BINTI ABD. LATIF

THESIS SUBMITTED IN FULFILLMENT OF THE REQUIREMENT FOR THE DEGREE OF DOCTOR OF PHILOSOPHY

DEPARTMENT OF PHYSICS
FACULTY OF SCIENCE
UNIVERSITY OF MALAYA
KUALA LUMPUR

2013

UNIVERSITI MALAYA
ORIGINAL LITERARY WORK DECLARATION

Name of Candidate: **AMIRAH BINTI ABD. LATIF** (I.C/Passport No:)

Registration/Matric No:**SHC100033**

Name of Degree: **DOCTOR OF PHILOSOPHY**

Title of Project Paper/Research Report/Dissertation/Thesis ("this Work"):

THE GENERATION OF DUAL-WAVELENGTH FIBER LASERS AND THEIR APPLICATIONS

Field of Study: **INFORMATION TECHNOLOGY AND COMMUNICATION**

I do solemnly and sincerely declare that:

(1) I am the sole author/writer of this Work;
(2) This Work is original;
(3) Any use of any work in which copyright exists was done by way of fair dealing and for permitted purposes and any excerpt or extract from, or reference to or reproduction of any copyright work has been disclosed expressly and sufficiently and the title of the Work and its authorship have been acknowledged in this Work;
(4) I do not have any actual knowledge nor do I ought reasonably to know that the making of this work constitutes an infringement of any copyright work;
(5) I hereby assign all and every rights in the copyright to this Work to the University of Malaya ("UM"), who henceforth shall be owner of the copyright in this Work and that any reproduction or use in any form or by any means whatsoever is prohibited without the written consent of UM having been first had and obtained;
(6) I am fully aware that if in the course of making this Work I have infringed any copyright whether intentionally or otherwise, I may be subject to legal action or any other action as may be determined by UM.

Candidate's Signature Date

Subscribed and solemnly declared before,

Witness's Signature Date

Name:

Designation:

ABSTRACT

This thesis describes the methods and processes of generating tunable single wavelength and dual-wavelength fiber lasers by using two different types of gain media. They are erbium doped fiber (EDF) and semiconductor optical amplifier (SOA) with each of them working as near to homogeneous and inhomogeneous broadening transition gain media respectively.

Various single wavelength and dual-wavelength fiber lasers (DWFLs) designs using different selective elements namely tunable banpass filter (TBF), compression and tensile strain FBGs (CTS-FBGs) and arrayed waveguide grating (AWG) are also discussed and compared in the thesis in terms of their output power, side mode suppression ratio (SMSR) and tunability. To generate single wavelength fiber lasers is not a problem compared to the generation of dual-wavelength fiber laser in a homogeneous gain medium. Therefore, cavity loss control method, as a new and novel approach is proposed to overcome the mode competition issue faced by EDF for generation of balanced dual-wavelength output. The generation of DWFL by using SOA is also presented in the thesis which is free from mode competition issue, which however fairs badly in terms of output power performance. This is presented as an alternative way of generating the DWFL.

The DWFLs have a lot of applications in various fields including fiber sensors and communications.In this study, new designs of DWFLs for various applications are presented. They are the generation of single longitudinal mode fiber laser for potential application in

Terahertz ray, the generation of DWFL for wavelength conversion, the generation of DWFL for a minute shifts temperature sensor and also the generation of DWFL for microwaves generation. This is achievable due to a high stability and high quality of the fiber laser in terms of output powers and high value of SMSR.

ABSTRAK

Tesis ini menerangkan kaedah dan proses penjanaan fiber laser bagi panjang gelombang tunggal dan juga dwi-panjang gelombang, dengan menggunakan dua jenis medium gandaan yang berbeza. Dua jenis medium gandaan ini adalah fiber berdop-erbium (EDF) dan pengganda semikonduktor optik (SOA) dengan masing-masing berfungsi sebagai media gandaan dengan lebar peralihan yang menghampiri keadaan homogen dan tak homogen.

Pelbagai jenis fiber laser berpanjang gelombang tunggal dan dwi-gelombang telah direkabentuk dengan menggunakan pelbagai jenis alat pemilih gelombang yang terdiri dari penapis boleh laras (TBF), FBG dengan kawalan secara mampatan dan terikan (CTS-FBGs) dan parutan gelombang teratur (AWG) yang diperbincangkan dan dibandingkan dari segi kuasa keluarannya, nisbah penyekatan mode bersebelahan (SMSR) dan kebolehan pelarasannya. Tidak menjadi satu masalah untuk menjana fiber laser gelombang tunggal, berbanding dengan fiber laser dwi-gelombang (DWFL) di dalam medium penggandaan homogen. Oleh itu, kaedah pengawalan kehilangan rongga, sebagai satu pendekatan baru telah dicadangkan bagi mengatasi masalah ini. Penjanaan DWFL menggunakan SOA juga dibentangkan di dalam tesis ini yang bebas dari masalah persaingan mod, yang bagaimanapun mempunyai keburukan yang berseimbangan dari segi kuasa keluarannya yang rendah. Ini dibentangkan sebagai kaedah alternatif untuk menghasilkan fiber laser dwi-gelombang.

DWFL mempunyai banyak aplikasi di dalam bidang seperti fiber pengesan dan komunikasi. Di dalam kajian ini, suatu rekaan baru yang menggunakan aplikasi DWFL ini telah dibentangkan. Ini adalah termasuk penjanaan fiber laser dengan lebar mod tunggal yang mempunyai aplikasi berpotensi di dalam teknologi gelombang terahertz, untuk penukaran

panjang gelombang, DWFL untuk aplikasi pengesan suhu beresolusi tinggi, dan juga DWFL untuk kegunaan penjanaan gelombang mikro. Aplikasi-aplikasi ini berhasil kerana keluaran kuasa laser dan nilai SMSR yang berkualiti, yang dihasilkan oleh fiber laser yang telah direkabentuk.

ACKNOWLEDGEMENTS

I would like to express my deepest gratitude to my supervisor, Professor Dr. Harith Ahmad and my co-supervisor, Prof. Dr. Sulaiman Wadi Harun for their priceless guidance, ideas, criticisms, motivation, inspiration, knowledge and wisdom. Through the research, I have learnt in a hard way to be more independent, not only to gain good research ideas but also to succeed in life. I am indebted with Dr. Noor Azura Awang (Kak Zura) and Dr. Mohd Zamani Zulkifli for providing excellent discussion and for sharing their knowledge as well as giving helpful assistance throughout the progress of the research.

I would like to convey my sincere thanks to all of my friends in Photonics Research Center, Siti Fatimah Norizan, Muhd Hafizhin Jemangin, Muhd Imran Mustafa, Farah Diana Muhammad, Nor Ahya Hassan, Dr. Lim Kok Sing, Kavintheran, Dr. Pua Chang Hong, Dr. Norfizah Mohd Ali (Kak Fiza), Nor Munirah, Siti Sarah, Yap Yuen Kiat, Fauzan Ahmad and the others for their kind assistance. I could not name all of them here, but I am so thankful for their encouragement throughout my research study. I would also like to deliver my special thanks to my close friends, Nor Azlia, Noryushan and 'Physics United' for their moral support.

My personal full-hearted thanks also go to my family, especially for my mother, Pn. Asmah binti Sani and my eldest sister Amalina binti Abd. Latif, for supporting, encouraging and fully understanding, in order to make sure that I could pursue my degree till the end. Alhamdulillah…

LIST OF ISI PUBLICATIONS

1. Ahmad H, Zulkifli MZ, **Latif AA**, Harun SW. Tunable dual wavelength fiber laser incorporating AWG and optical channel selector by controlling the cavity loss. Optics Communications. 2009;282(24):4771-5.
2. **Latif AA**, Zulkifli MZ, Awang NA, Harun SW, Ahmad H. A simple linear cavity dual-wavelength fiber laser using AWG as wavelength selective mechanism. Laser Physics. 2010;20(11):2006-10.
3. **Latif AA**, Awang NA, Zulkifli MZ, Harun SW, Ghani ZA, Ahmad H. Dual-wavelength tunable fibre laser with a 15-dBm peak power. Quantum Electronics. 2011;41(8):709-14.
4. Ahmad H, Zulkifli MZ, **Latif AA**, Thambiratnam K, Harun SW. Bidirectional S-band continuous wave operation in a depressed-cladding erbium doped fiber amplifier. Journal of Optoelectronics and Advanced Materials. 2009;11(5):547-53.
5. Ahmad H, Zulkifli MZ, **Latif AA**, Thambiratnam K, Harun SW. Dual wavelength fibre laser with tunable channel spacing using an SOA and dual AWGs. Journal of Modern Optics. 2009;56(16):1768-73.
6. Ahmad H, Zulkifli MZ, **Latif AA**, Thambiratnam K, Harun SW. 17-channels S band multiwavelength Brillouin/Erbium Fiber Laser co-pump with Raman source. Laser Physics. 2009;19(12):2188-93.
7. Ahmad H, Zulkifli MZ, **Latif AA**, Hassan NA, Ghani ZA, Harun SW. 120 nm wide band switchable fiber laser. Optics Communications. 2010;283(21):4333-7.

8. **Latif AA**, Zulkifli MZ, Hassan NA, Harun SW, Ghani ZA, Ahmad H. A compact O-plus C-band switchable quad-wavelength fiber laser using arrayed waveguide grating. Laser Physics Letters. 2010;7(8):597-602.
9. Ahmad H, Zulkifli MZ, **Latif AA**, Harun SW. O-BAND MULTI-WAVELENGTH FIBER LASER. Journal of Nonlinear Optical Physics & Materials. 2010;19(2):229-36.
10. Ahmad H, Zulkifli MZ, **Latif AA**, Harun SW. Novel O-band tunable fiber laser using an array waveguide grating. Laser Physics Letters. 2010;7(2):164-7.
11. Awang NA, Ahmad H, **Latif AA**, Zulkifli MZ, Ghani ZA, Harun SW. O-band to C-band wavelength converter by using four-wave mixing effect in 1310 nm SOA. Journal of Modern Optics. 2010;57(21):2147-53.
12. Ahmad H, Awang NA, **Latif AA**, Zulkifli MZ, Ghani ZA, Harun SW. Wavelength conversion based on four-wave mixing in a highly nonlinear fiber in ring configuration. Laser Physics Letters. 2011;8(10):742-6.
13. Awang NA, Zulkifli MZ, **Latif AA**, Harun SW, Ahmad H. Stable power multi-wavelength fibre laser based on four-wave mixing in a short length of highly non-linear fibre. Journal of Optics. 2011;13(7).
14. Ahmad H, Zulkifli MZ, Hassan NA, **Latif AA**, Harun SW. High gain S-band semiconductors optical amplifier with double-pass configuration. Laser Physics. 2011;21(7):1208-11.
15. **Latif AA**, Ahmad H, Awang NA, Zulkifli MZ, Pua CH, Ghani ZA, et al. Tunable high power fiber laser using an AWG as the tuning element. Laser Physics. 2011;21(4):712-7.

16. Ahmad H, **Latif AA**, Norizan SF, Zulkifli MZ, Harun SW. Flat and compact switchable dual wavelength output at 1060 nm from ytterbium doped fiber laser with an AWG as a wavelength selector. Optics and Laser Technology. 2011;43(3):550-4.

17. Awang NA, Ahmad H, **Latif AA**, Zulkifli MZ, Harun SW. Four-wave mixing in dual wavelength fiber laser utilizing SOA for wavelength conversion. Optik. 2011;122(9):754-7.

18. Awang NA, Ahmad H, **Latif AA**, Zulkifli MZ, Ghani ZA, Harun SW. Wavelength conversion based on FWM in a HNLF by using a tunable dual-wavelength erbium doped fibre laser source. Journal of Modern Optics. 2011;58(7):566-72.

19. Zulkifli MZ, Tamchek N**, Latif AA**, Harun SW, Ahmad H. Flat output and switchable fiber laser using AWG and broadband FBG. Optics Communications. 2009;282(13):2576-9.

20. Muhammad FD, Zulkifli MZ, **Latif AA**, Harun SW, Ahmad H. Graphene-Based Saturable Absorber for Single-Longitudinal-Mode Operation of Highly Doped Erbium-Doped Fiber Laser. IEEE Photonics Journal. 2012;4(2):467-75.

21. Ahmad H, Awang NA, **Latif AA**, Harun SW. Generation of high power pulse of Bi-EDF and octave spanning supercontinuum using highly nonlinear fiber. Microwave and Optical Technology Letters. 2012;54(4):983-7.

22. Ahmad H, Awang NA, Paul MC, Pal M, **Latif AA**, Harun SW. All fiber passively mode locked zirconium-based erbium-doped fiber laser. Optics and Laser Technology. 2012;44(3):534-7.

23. Ahmad H, **Latif AA**, Zulkifli MZ, Awang NA, Harun SW. High power dual-wavelength tunable fiber laser in linear and ring cavity configurations. Chinese Optics Letters. 2012;10(1).

24. Ahmad H, Zulkifli MZ, **Latif AA**, Jemangin MH, Chong SS, Harun SW. Tunable single longitudinal mode S-band fiber laser using a 3 m length of erbium-doped fiber. Journal of Modern Optics. 2012;59(3):268-73.

25. Ahmad, H, **Latif AA**, Awang, N. A., Zulkifli, M. Z., Thambiratnam, K., Ghani, Z. A., & Harun, S. W. (2012). Wide-band fanned-out supercontinuum source covering O-, E-, S-, C-, L- and U-bands. Optics and Laser Technology, 44(7), 2168-2174.

26. Ahmad, H., **Latif, A. A.**, Zulkifli, M. Z., Awang, N. A., & Harun, S. W. (2012). Temperature Sensing Using Frequency Beating Technique From Single-Longitudinal Mode Fiber Laser. IEEE Sensors Journal, *12*(7), 2496-2500.

27. Chong SS, Ahmad H, Zulkifli MZ, **Latif AA**, Chong WY, Harun SW. Synchronous tunable wavelength spacing dual-wavelength SOA fiber ring laser using Fiber Bragg grating pair in a hybrid tuning package . Optics Communications. 2012;285:1326-1330.

LIST OF ORAL AND POSTER PRESENTATIONS

1. **A. A. Latif,** M. Z. Zulkifli, S. W. Harun and H. Ahmad, "Tunable Dual-Wavelength Fibre Laser" 2nd Topical Meeting on Laser and Optoelectronics 2010 (TMLO), Berjaya Redang Resort, Kuala Terangganu, 13th – 15th March 2010.
2. **A. A. Latif**, S. W. Harun and H. Ahmad, "Switchable Fibre Laser by Using an AWG" 5th Mathematics and Physical Sciences Graduate Congress 2009, Faculty of Science, Chulalongkorn University, Bangkok, Thailand, 7th – 9th December 2009.

LIST OF AWARDS

1. **A.A.Latif**, N.A.Hassan, M.Z.Zulkifli, N. A. Awang, S. F. Norizan, S.W.Harun and H.Ahmad. Novel O-band Tunable fibre laser using an AWG, Gold Medal in Innovation & Creativity Expo University Of Malaya 2010 at 1^{st} – 3^{rd} April 2010.
2. N. A. Awang, S. F. Norizan, **A.A.Latif**, N.A.Hassan, M.Z.Zulkifli, S.W.Harun and H.Ahmad. An All-Optical Frequency Up/Down-Converter Utilizing Stimulated Brillouin and Raman Scattering in a Truewave Reach Fibre and Dispersion Compensating Fibre for Radio Over Fibre Application, Gold Medal inInnovation & Creativity Expo University Of Malaya 2010 at 1^{st} – 3^{rd} April 2010.
3. **A.A.Latif**, N.A.Hassan, M.Z.Zulkifli, S. F. Norizan, S.W.Harun and H.AhmadTunanle Multiwavelength Fiber Laser using AWG and a BB-FBG, Silver Medal in Innovation & Creativity Expo University Of Malaya 2010 at 1^{st} – 3^{rd} April 2009.

CONTENTS

3. SWITCHABLE SINGLE WAVELENGTH FIBER LASERS

LIST OF FIGURES

2 Theoretical Background

3 Switchable Single-Wavelength Fiber Lasers

4 The Design of Dual-Wavelength Fiber Lasers

LIST OF TABLES

NOMENCLATURE

E	energy level
R	pumping rate
W_{21}	stimulated emission
W_{12}	Stimulatedabsorption
τ	fluorescence lifetime
N	number of ions
ρ	ion density
$\rho(\upsilon)$	the energy density at frequency υ
h	Planck constant
c	light propagating in vacuum
n_r	refractive index of the waveguide
ρ_v	radiation energy per unit volume
$l(\upsilon)$	transition lineshape function
dP_v	total power
A	cross-section area
dz	length of the waveguide travel by the wave
$\mathrm{g}_m(\upsilon)$	SOA gain coefficient
I	bias current
d	thickness active region
e	electronic charge
L	length of the waveguide active region

W	width of the active region
Γ	confinement factor
Ns_k^+	photon rates in the positive direction
Ns_k^-	photon rates in the negative direction
$\gamma(\upsilon)$	gain coefficient
υ_o	central frequency
$\Delta\upsilon$	emission linewidth
τ_{sp}	spontaneous lifetime
N_o	state population different
λ	wavelength of light in the medium

ACRONYMS

ASE	amplified spontaneous emission
ATT	attenuator
AWG	arrayed waveguide grating
BB-FBG	broadband FBG
BFA	Brillouin fiber amplifier
DFB	distributed feedback
DWDM	dense wavelength divisionmultiplexing
DWFL	dual-wavelength fiber laser
DWTFL	dual-wavelength tunable fiber laser
EDF	erbium doped fiber
EDFA	erbium doped fiber amplifiers
EDFL	erbium doped fiber laser
FBG	fiber Bragg grating
FWM	four wave mixing
MQW-SOA	multi-quantum well SOA
NDFA	neodymium doped fiber amplifier
OC	optical circulator
OCS	optical channel selector
OPM	optical power meter
OSA	optical spectrum analyzer
OTDM	optical time domain multiplexing
OVA	optical variable attenuator
OVC	optical variable coupler
PC	polarization controller
PMF	polarisation maintaining fiber
PMFBG	polarization maintaining FBG
POA	programmable optical attenuator
RFA	Raman fiber amplifier

SLM	single longitudinal mode
SMF	single mode fiber
SMSR	side mode suppression ratio
SOA	semiconductor optical amplifier
SOP	state of polarization
TBF	tunable bandpass filter
TDF	thulium doped fiber
TDM	time domain multiplexing
WDM	wavelength division multiplexing
YbDF	ytterbium doped fiber
RFSA	radio frequency spectrum analyzer
LIDAR	light detection and ranging
DW-SLM	dual-wavelength single longitudinal mode
SA	saturable absorbers
HNF	highly nonlinear fiber
TLS	tunable laser source
RTD	resistance temperature detectors
PRT	platinum resistance temperature
Zr-EDF	zirconia-based erbium-doped fiber
AOM	acousto-optic modulator
SLM-FL	single longitudinal mode fiber laser
SSG	synthesized signal generator
RBW	resolution bandwidth

CHAPTER 1

INTRODUCTION

1.1 The History of Optical Fiber Technology as a Telecommunication System

Telecommunication is actually a term coming from two words, which are '*tele*' and '*communis*'. The word '*tele*' comes from French's word meaning at distance, while '*communis*' comes from Latin's word, meaning to share. In physical practice, the word telecommunication is simply an activity of delivering information over significant distance by the electromagnetic means.

During the old times, smoke signals, Chappe telegraphs, signal flags and beacons were involved in the old long distance optical communications. During the time, the Ancient China's soldiers (Tang Dynasty Era during year 620s) were enforced to keep alert of the smoke signal, from tower to tower to get the information of any enemy attack. The smoke signal had to be lit to inform any security information at any particular tower. By doing so, no tower could be detained by the enemy without being realized by the other towers. One more example is the 'optical telegraph' invented by Claude Chappe in 1790s. The design was called as Chappe telegraphs with semaphores mounted on towers, to give information to the next tower and operated by human's power.

In 1880, the first optical wireless telephone system known as Photophone had been introduced and patented by Alexander Graham Bell [1]. However, the information

technology by using a modulated light for conversation was seemed to be not so practical to be applied for practical purposes as the transmission of his design could be easily interfered by clouds, fog, rain and snow. The idea of light guided by glass is actually arose in 1840s, when Daniel Colladon and Jacques Baabinet were first demonstrating the total internal reflection of light in jet of water. It seemed like the light was trapped in it, as long as the reflection of light was not overpass its critical angle. The idea was further improved by John Baird and Clarence Hansell in 1920s by demonstrating the light guided by transparent rod for facsimile systems.

The optical fiber technology was making a huge progress when the lamps were invented. This is possible since the light can be on and off in a very fast duration, thus can be used as a blinker light to pave the way for optical fiber technology growth. A major breakthrough of the technology undeniably was led by the invention of laser in the 1960s, which had triggered numerous developments in the field of optical fiber communication systems. Despite its initial high value of 20 dB/km [2], fiber losses in the long run dropped to less than 0.2 dB/km [3]. This was caused by the rapid development in fiber fabrication technology in the 1970s.

In the late 1970s, single mode fiber (SMF) operated at the wavelength of 800nm was commercially available for long distance applications with the signal coming from gallium-aluminum-arsenide laser diodes. It was called as the first window for optical fiber communication. For the second window, the information spacing was increased significantly by shifting the operating wavelength to 1300 nm region which was called the O-band region. It offers a lower loss of less than 1 dB/km and a minimum dispersion which is good for modulated signal. The optical fiber in the third window system operated at 1550

nm region and can be called as C-band region. In this region, the signal experienced even lower loss of less than 0.2 dB/km [4, 5] .

1.2 DWDM Communication Systems

Single-longitudinal mode lasers operating in C-band region was successfully designed in 1990 to cope with the increasing demand of capacity bared by the communication systems. However, the signal has to be amplified in order to preserve the data transfer after a few kilometres (typically around 60 km) of its propagation along the fiber. In the earlier stage, the repeater was used to regenerate the signal. The process of converting the data from optical to electrical has to be done. Then, it will be amplified electrically before being converted back to the optical signal. It is a process of optical-electrical-optical conversion, which becomes a tedious effort to work with.

The invention of optical amplifiers helped in significant growth of the optical fiber technology in subsequent years. The optical amplification process is possible during these years by virtue of erbium doped fiber amplifiers (EDFAs) with the optical amplification naturally in 1550 nm region. This allows the transmission of signal without being converted to the electrical signals. The data rates were around 2.5 Gbit/s. The rapid growth of the technology, subsequently, increased the bandwidth demand, thus introducing the wavelength division multiplexing (WDM) technology. The WDM technology clearly increases the information carrying capacity of a single fiber.

The time domain multiplexing (TDM) system was also introduced to enhance the bit rate of the existing channels with the data rates of 10 Gbit/s. The TDM system however has a

dispersion problem when it comes to the higher bit rate transfer [6] and makes it less preferred. The optical time domain multiplexing (OTDM) system was then introduced to improve the previous TDM system. The bits rates transfer from 80 Gbit/s to 320 Gbit/s have been reported during that time [7-11]. A transmission as fast as 640 Gbit/s was then reported by Nakazawa in 1998 [12].

To cope with the wavelength demand as the channel for transmitting data, the dense wavelength division multiplexing (DWDM) was then introduced. The improvement was necessary to transmit large number of relatively closely spaced channels along an optical fiber. Instead of 8 Channels provided by the conventional WDM systems, the DWDM system would typically provide 40 channels with 100 GHz spacing, or 80 channels of 50 GHz spacing. The WDM and DWDM are however working with the same principle by having a combination of multiple signal wavelengths, only in a single optical fiber. The only differed is their inter channel spacing, number of channels involved and the ability to do the optical amplification with combination of many channels.

1.3 Single Wavelength Fiber Lasers

Single wavelength fiber lasers have become more attractive nowadays, after the first invention of a fiber laser at 1060 nm by Elias Snitzer [13] in 1961 by using a flash lamp as a laser pump source. The invention influenced the world in profound ways due to its contribution especially in the field of material processing, spectroscopy, LIDAR, telecommunications including internet, interferometry, medical imaging technology and high power illuminator for directed energy weapon system. These various applications are possible by virtue of the fiber-based laser itself which gives a lot of advantages as

compared to the other type of lasers. They include fiber compatibility, low intensity noise, high output power, its compactness, high optical quality and narrow linewidth.

Since the growth of optical fiber technology, there have been a lot of studies in many aspects to make use of it. Despite extensive studies on its applications, studies on improving the signal quality guided by the fiber glass material are also involved. In achieving this aim, a few gain media have been identified that can be used as the optical amplifier for amplification in the optical telecommunication systems. They include erbium doped fiber amplifier (EDFA) and neodymium doped fiber amplifier (NDFA) for amplification in 1550 nm and 1060 nm respectively which was later found to be really useful in generating single wavelength fiber laser. This fiber compatibility is important, as the light is already being coupled to the fiber and can provide the best quality of single wavelength fiber laser outputs.

Without any external coupling from the bulk laser, the fiber laser system emits low intensity noise, giving a high quality beam which is really useful for any sensing purpose. The single wavelength fiber laser also can generate high output power. This can be done by using a long length of gain medium (as long as several kilometres) to achieve a high optical gain. This is useful for the high power applications including cutting and welding technology. The size is not a problem since the fiber can be spooled to a compact size, and therefore they are much smaller as compared to the other type of lasers such as solid state lasers, dye lasers and gas lasers.

The single wavelength fiber laser also emits a narrow linewidth output which is comparable to the other type of lasers such as semiconductor lasers. This is due to the fact that single wavelength fiber lasers emit low phase noise and high spectral purity. A narrow linewidth

laser is important in order to get a highly coherent output that can be used as sensors for long distance applications.

A lot of devices were proposed and experimented in order to generate single wavelength fiber laser. These were fiber Bragg grating (FBG), tunable bandpass filter (TBF) and arrayed waveguide grating (AWG) as the wavelength selective element. The generation of single wavelength fiber laser can be done typically by using a linear cavity and ring cavity configurations. A more attractive criteria which comes from the fiber based is that the single wavelength fiber laser can be tuned or switched into a few other wavelength options. By using the TBF, the wavelength selection can be done within the operating wavelength of the TBF. On the other hand the FBG can be compressed, stretched or cascaded together for variety wavelength options. The AWG on the other hand, can be made switchable by connecting it to the optical channel selector (OCS).

1.4 Dual-Wavelength Fiber Lasers

Multiwavelength fiber lasers and Dual-Wavelength Fiber Lasers (DWFLs) are well known to be useful for applications such as in the field of optical fiber sensors [14-16] which can be used for long haul sensing system and also for optical spectroscopy [17]. The sensing system is actually done by taking a wavelength as a reference and another signal which has almost the same wavelength is used as the sensor indicator for any slight changes which gives a shifting effect to the second wavelength of the fiber laser output. Most of the experiments are done by using FBGs as the wavelength selective elements. The optical spectroscopy application on the other hand, uses the multiwavelength fiber laser or DWFL for observing the wavelength absorption in order to determine the atom identity. This is due

to the fact that the wavelength of light is being absorbed is related to the specific energy transition by a specific atom.

Other applications are for microwaves photonics systems [18-20] and optical wavelength division multiplexing systems (WDM) [21, 22]. The microwave generation is basically using the dual-wavelength beating technique in order to generate the microwave signals. The technique is easy to setup and can be easily sensed by using a photodetector. The technique also becomes useful due to its advantage of noise reduction in the system. The DWFL and multiwavelength fiber laser, on the other hand, can act as the selectable wavelength laser source in the WDM systems which made them useful for these applications.

Other useful applications are for optical component testing, optics instrumentation and characterization of photonics component such as for chromatic dispersion measurement [23]. However the technology nowadays move forward to the generation of dual-wavelength fiber lasers (DWFLs) since DWFLs are attractive for advance applications that need only two synchronize wavelengths for many applications. Despite the usefulness of the multiwavelength fiber laser, the DWFLs are more attractive due to their potential to work as a high precision strain and temperature sensors, for wavelength conversion application [24, 25] to convert the signal from one communication band to another without using any active devices to make an optical- electrical-optical conversion thus can be effectively used to fulfil the communication demand with a low cost borne by the network providers, and also for terahertz generation [26, 27] signal that is quite notable in the new industrial process quality controls and for security monitoring applications. These three

applications however need a lot of efforts in order to generate the single longitudinal mode (SLM) DWFLs that exhibit a high spectral purity.

A lot of methods have been used to generate the multiwavelength fiber lasers and DWFLs. The gain media typically used in order to generate DWFLs in C-band region for telecommunication window are erbium doped fiber amplifiers (EDFAs). However, the generation of DWFL is quite cumbersome for the researchers to mull over. This is due to the mode competition caused by the cross-gain saturation and strong homogeneous line broadening faced by erbium doped fibers (EDFs).

Various means have been utilized to generate DWFL such as by cooling the EDF with liquid nitrogen [28, 29] and by using an elliptical EDF [30]. For the first method, the EDF is cooled to 77 K by using liquid nitrogen to reduce its homogeneous linewidth, as narrow as 1 nm. Thus a stable multiwavelength fiber laser can be easily generated. On the other hand, the elliptical EDF helps in generating multiwavelength fiber lasers and DWFLs by using the principle of anisotropic gain behavior of the elliptical core EDF. This is done by having the same output lasing threshold of the multiwavelength lasers, by adjusting the polarization controller (PC) to control the polarization state of the pump along the cavity axis. This subsequently generates a stable multiwavelength fiber laser source.

Another method is by using a polarization maintaining FBG (PMFBG) for wavelength selection [31] and a frequency shifter in the cavity [32]. In the paper, the DWFL is easily generated by using the PMFBG due to the polarization hole burning enhancement. This is an important effect since it is helping in increasing the inhomogeneous broadening effects thus providing a stable dual-wavelength oscillation in the cavity design. The technique also uses the PC to control the polarization state in the cavity, thus helps to balance the lasing of the DWFL. For the latter case, a frequency shifter is inserted in the cavity to prevent only a

single frequency oscillation which is caused by a single steady state lasing in order to generate a stable DWFL.

The other alternative ways are by using DFB fiber laser source with a separate resonance cavity [20] and four wave mixing effect (FWM) as a stabilizer [33]. The first method succeeded in generating the DWFL by the virtue of the spatially separated of two lasing wavelength and avoiding the mode competition to occur in the cavity. While the latter is using a highly nonlinear bismuth-oxide fiber to generate the FWM effect which shows a significant stability improvement compare to the cavity without the highly nonlinear fiber.

The other methods are by using the optical injection Fabry-Perot laser [34] and by using dual-ring fiber laser [35]. For the second method, the cavity is controlled separately by using two different PCs to achieve a stable DWFL.

All of the methods mentioned above use the EDF as the gain medium. Another alternative way to generate DWFLs is by using semiconductor optical amplifiers (SOAs) as the alternative gain medium [36,37]. However, SOAs does not provide the best solution in terms of lower output power and higher noise compared to using EDFs.

1.5 Objectives

The aim of the research presented in this thesis has been planned thoroughly and highlighted. The research work focus on the unsolved problem faced by the current device in the optical communication systems, subsequently to improve the weakness of the current design.

1.5.1 The Generation of Tunable Single Wavelength Fibre Lasers

The first objective of the research work is to design tunable single wavelength fiber lasers, as a single output source. One of a novel approach is by using an arrayed waveguide grating (AWG) is being discussed in the thesis with a few other designs as another option. Two types of gain media composed of a homogeneous and an inhomogeneous broadening gain media are used for comparison purpose of the output performance. The proposed single wavelength fiber laser designs are then being characterized for their output power, tunability and side mode suppression ratio (SMSR) value. It is important to provide a few options that can be utilized in the DWDM systems depending on any specific particular interest such as the range of the wavelength that can be tuned or the amount of loss the system can tolerate.

1.5.2 The Generation of Tunable Dual-Wavelength Fibre Lasers

The second motivation of the thesis is to design the tunable dual-wavelength fiber lasers. It is known that the EDF is a good amplifier in the C-band region of communication window. However, it has its own limitation of difficulty to provide dual-wavelength or

multiwavelength output due to the close to homogeneous broadening effects emitted by the EDF. A novel approach of using an AWG as the wavelength selective element and two OCS as the selector, with a cavity loss control method has been designed and reported by our group. The design is effective to overcome the limitation of mode competition inherited in the EDF to provide a balance dual-wavelength output power source. Some other few designs are also proposed by using the same technique but using different wavelength selective elements. To give a clear understanding, a semiconductor optical amplifier (SOA), another type of gain medium which emits inhomogeneous broadening effect is also being presented in the thesis for comparison. The two types of broadening are also being presented in Chapter 2 to give a clear understanding regarding this effect and the reason for the significant difference of output performance between the two.

1.5.3 Applications of Dual-Wavelength Fibre Lasers

The third objective is the main objective to see the significance of the new DWFL designs. This is done by proposing a few new applications that can be provided by the design invented. It has been proved by the research study that the DWFLs have a lot of functions and all of them are presented in Chapter 5 including for wavelength converter in communication systems, for temperature sensors by using the beating of the dual-wavelength output, microwaves generation for future optical to microwaves communication systems and single longitudinal mode DWFL for possible application in Terahertz generation.

1.6 Thesis Outline

There are six chapters in the thesis. Chapter 1 revolves around a brief understanding of optical fiber technology and its relation with the telecommunication system. Chapter 2 on the other hand, provides the theoretical background for the generation of fiber laser. It also provides the basic equations for spontaneous and stimulated emission from basic atomic rate equations for two different gain media. They are erbium doped fiber (EDF), as well as semiconductor optical amplifiers (SOA). The explanation is then followed by the difference of broadening effect between both of them.

Chapter 3 demonstrates the generation of tunable single wavelength fiber lasers. Different wavelength selective elements used comprise of a tunable bandpass filter (TBF), 6 fiber Bragg gratings (FBGs) with Sagnac loop mirror method, compression and tensile strain FBGs (CTS-FBGs); and an arrayed waveguide grating (AWG). The working principle of each wavelength selective elements is discussed in this chapter. The demonstration of the fiber laser generation is done by using a closely to homogeneous broadening and inhomogeneous broadening of EDFA and SOA respectively, as the gain media. The difference of output power and SMSR for each design is then being discussed in this chapter. There have been 6 publications as have been listed in Appendix 1 and 2 related and being improved from the design presented in this chapter.

Chapter 4 represents a few new designs of tunable dual wavelength fiber lasers which each constructed by different wavelength selective elements which uses the same gain media as in Chapter 3. The architectures are considered to be novel by the virtue of a cavity loss control method to solve the mode competition problem faced by the EDF gain medium with broadening of more to homogeneous broadening transition. Two cavity designs are

being presented, which are ring cavity and linear cavity configuration. The new design is found to be more cost effective as compared to the conventional tunable dual-wavelength laser source. The SOA is also presented as an alternative way to generate the DWFL without the mode competition issue. However it has lower output power performance and higher noise. This made the EDF being more preferable to the SOA. There have been 7 publications as have been listed also in Appendix 1 and 2 related and being improved from the design presented in the thesis.

Chapter 5 presents research work on application of the DWFL by the virtue of new findings that have been explained in Chapter 4. A few applications demonstrated in this research are considered as new and novel, since it is invented by using some new designs of the DWFL. A few new applications presented in this chapter are tunable dual-wavelength single longitudinal mode fiber laser, dual-wavelength as pump source for wavelength conversion in the SOA as a highly nonlinear gain medium, the DWFL as a temperature sensor and also the DWFL for the generation of microwaves signals. There are 5 publications as being listed in Appendix 1 and 2 related to the design proposed.

Finally, Chapter 6 concludes the thesis with a summary of the main contributions from the research work. Recommendations for future works in the field are also discussed as the extension of the works done in this research.

References

1. Mims, I.F.M., *Alexander Graham Bell and the Photophone: The Centennial of the Invention of Light-Wave Communications, 1880-1980.* Optics News, 1980. **6**(1): p. 8-16.
2. Kao, K.C. and G.A. Hockham, *Dielectric-fiber surface waveguides for optical frequencies.* Optoelectronics, IEE Proceedings J, 1986. **133**(3): p. 191-198.
3. Kato, T., et al., *Ultra-low nonlinearity low-loss pure silica core fiber for long-haul WDM transmission.* Electronics Letters, 1999. **35**(19): p. 1615-1617.
4. *Ultimate low-loss fibers.* Electronics and Power, 1979. **25**(2): p. 91.
5. Murata, H. and N. Inagaki, *Low-loss single-mode fiber development and splicing research in Japan.* Quantum Electronics, IEEE Journal of, 1981. **17**(6): p. 835-849.
6. Inoue, K., et al., *Crosstalk and power penalty due to fiber four-wave mixing in multichannel transmissions.* Lightwave Technology, Journal of, 1994. **12**(8): p. 1423-1439.
7. Kaman, V. and J.E. Bowers, *120 Gbit/s OTDM system using electroabsorption transmitter and demultiplexer operating at 30 GHz.* Electronics Letters, 2000. **36**(17): p. 1477-1479.
8. Marcenac, D.D., A.D. Ellis, and D.G. Moodie, *80 Gbit/s OTDM using electroabsorption modulators.* Electronics Letters, 1998. **34**(1): p. 101-103.
9. Moodie, D.G., et al., *Multiquantum well electroabsorption modulators for 80 Gbit/s OTDM systems.* Electronics Letters, 1995. **31**(16): p. 1370-1371.

10. Toliver, P., et al., *Simultaneous optical compression and decompression of 100-Gb/s OTDM packets using a single bidirectional optical delay line lattice.* Photonics Technology Letters, IEEE, 1999. **11**(9): p. 1183-1185.

11. Raybon, G., et al. *320 Gbit/s single-channel pseudo-linear transmission over 200 km of nonzero-dispersion fiber*. in *Optical Fiber Communication Conference, 2000*. 2000.

12. Nakazawa, M., et al., *TDM single channel 640 Gbit/s transmission experiment over 60 km using 400 fs pulse train and walk-off free, dispersion flattened nonlinear optical loop mirror.* Electronics Letters, 1998. **34**(9): p. 907-908.

13. Snitzer, E., *Optical Maser Action of Nd^{+3} in a Barium Crown Glass.* Physical Review Letters, 1961. **7**(12): p. 444-446.

14. Peng-Chun, P., T. Hong-Yih, and C. Sien, *Long-distance FBG sensor system using a linear-cavity fiber Raman laser scheme.* Photonics Technology Letters, IEEE, 2004. **16**(2): p. 575-577.

15. Bolognini, G., M.A. Soto, and F. Di Pasquale, *Fiber-Optic Distributed Sensor Based on Hybrid Raman and Brillouin Scattering Employing Multiwavelength Fabry Perot Lasers.* Photonics Technology Letters, IEEE, 2009. **21**(20): p. 1523-1525.

16. Talaverano, L., et al., *Multiwavelength fiber laser sources with Bragg-grating sensor multiplexing capability.* Lightwave Technology, Journal of, 2001. **19**(4): p. 553-558.

17. Joanna, M., S. George, and W. Gillian, *Design of a tunable L-band multi-wavelength laser system for application to gas spectroscopy.* Measurement Science and Technology, 2006. **17**(5): p. 1023.

18. Capmany, J., et al., *Multiwavelength single sideband modulation for WDM radio-over-fiber systems using a fiber grating array tandem device.* Photonics Technology Letters, IEEE, 2005. **17**(2): p. 471-473.

19. Yu, Y., et al., *Dual-wavelength erbium-doped fiber laser with a simple linear cavity and its application in microwave generation.* Photonics Technology Letters, IEEE, 2006. **18**(1): p. 187-189.

20. Jie, S., et al., *Stable Dual-Wavelength DFB Fiber Laser With Separate Resonant Cavities and Its Application in Tunable Microwave Generation.* Photonics Technology Letters, IEEE, 2006. **18**(24): p. 2587-2589.

21. Pan, J.J. *Multiwavelength photonic communications*. in *Telesystems Conference, 1993. 'Commercial Applications and Dual-Use Technology', Conference Proceedings., National*. 1993.

22. Xinhuan, F., et al. *WDM-PON using Fabry-Perot laser diodes injection locked by multiwavelength erbium-doped fiber laser*. in *OptoeElectronics and Communications Conference (OECC), 2011 16th*. 2011.

23. Maran, J.N., et al., *Chromatic dispersion measurement using a multiwavelength frequency-shifted feedback fiber laser.* Instrumentation and Measurement, IEEE Transactions on, 2004. **53**(1): p. 67-71.

24. Qureshi, K.K., et al., *Width-tunable pulse generation using four-wave mixing in bismuth based highly nonlinear fiber.* Optics Communications, 2007. **275**(1): p. 223-229.

25. Uchida, A., et al., *Wide-range all-optical wavelength conversion using dual-wavelength-pumped fiber Raman converter.* Lightwave Technology, Journal of, 1998. **16**(1): p. 92-99.

26. Alouini, M., et al., *Dual tunable wavelength Er,Yb:glass laser for terahertz beat frequency generation.* Photonics Technology Letters, IEEE, 1998. **10**(11): p. 1554-1556.

27. Jeon, M.Y., et al., *Widely tunable dual-wavelength Er3+-doped fiber laser for tunable continuous-wave terahertz radiation.* Opt. Express, 2010. **18**(12): p. 12291-12297.

28. Yamashita, S. and K. Hotate, *Multiwavelength erbium-doped fiber laser using intracavity etalon and cooled by liquid nitrogen.* Electronics Letters, 1996. **32**(14): p. 1298-1299.

29. Park, N. and P.F. Wysocki, *24-line multiwavelength operation of erbium-doped fiber-ring laser.* Photonics Technology Letters, IEEE, 1996. **8**(11): p. 1459-1461.

30. Das, G. and J.W.Y. Lit, *L-band multiwavelength fiber laser using an elliptical fiber.* Photonics Technology Letters, IEEE, 2002. **14**(5): p. 606-608.

31. Feng, S., et al., *Switchable single-longitudinal-mode dual-wavelength erbium-doped fiber ring laser based on one polarization-maintaining fiber Bragg grating incorporating saturable absorber and feedback fiber loop.* Optics Communications, 2009. **282**(11): p. 2165-2168.

32. Bellemare, A., et al., *Room temperature multifrequency erbium-doped fiber lasers anchored on the ITU frequency grid.* Lightwave Technology, Journal of, 2000. **18**(6): p. 825-831.

33. Fok, M.P. and C. Shu, *Tunable dual-wavelength erbium-doped fiber laser stabilized by four-wave mixing in a 35-cm highly nonlinear bismuth-oxide fiber.* Opt. Express, 2007. **15**(10): p. 5925-5930.

34. Chien-Hung, Y., et al., *Tunable Dual-Wavelength Fiber Laser Using Optical-Injection Fabry Perot Laser.* Photonics Technology Letters, IEEE, 2008. **20**(24): p. 2093-2095.

35. Yeh, C.-H., et al., *Stabilized dual-wavelength erbium-doped dual-ring fiber laser.* Opt. Express, 2007. **15**(21): p. 13844-13848.

36. Xiangfei, C., D. Zhichao, and Y. Jianping, *Photonic generation of microwave signal using a dual-wavelength single-longitudinal-mode fiber ring laser.* Microwave Theory and Techniques, IEEE Transactions on, 2006. **54**(2): p. 804-809.

37. Tanaka, S., et al. *Multi-Wavelength Tunable Fiber Laser using SOA: Application to Fiber Bragg Grating Vibration Sensor Array*. in *Sensors, 2007 IEEE*. 2007.

CHAPTER 2

THEORETICAL BACKGROUND

2.1 Introduction

The theoretical background for the generation of fiber lasers shall begin with a brief overview of optical amplification, which provides the basic equations for spontaneous and stimulated emission from basic atomic rate equations. The amplified optical signal is then placed inside an optical cavity, thereby providing optical feedback, thus generating a fiber laser. The basic processes of the optical amplifiers and fiber laser are therefore discussed in this chapter. Subsequently, laser transition processesin a fiber gain media, specifically in erbium doped fibers (EDFs), as well as in a semiconductor optical amplifier (SOA) are discussed in this chapter. This is followed by a discussion on the broadening effect on the EDF and SOA in the last section of the chapter, with a simple experiment given as an example in order to distinguish the broadening type of both media.

2.2 Interaction of photons with atoms

Optical amplification comprises of three basic processes, optical absorption, spontaneous emission, and stimulated emission processes. These three processes are elaborated in this section.

1. **Optical Absorption**: Consider a case where an atom is in its steady state condition and suddenly a photon is passing by. If the photon energy coincides with one particular bandgap energy of the atom, the photon may get 'absorbed' by the atom. This causes the energy of the atom to increase, as the atom is excited to an upper energy level. This photon-induced process is called 'optical absorption'.

2. **Spontaneous Emission**: This is a term to describe the process when the randomly excited atom from the upper state returns spontaneously to its ground state level without any given signal as the trigger, and thereby releasing energy in the form of photon. This is as shown in Figure 2.1(a). This is why it is called spontaneous emission, as the atom will decay 'spontaneously' to its initial state. However, since the de-excitation happens spontaneously, the photons travel in all direction with slightly different frequencies, leading to a variety of wavelength emissions in addition to contributing to noise. This signal is known as amplified spontaneous emission (ASE) and will be discussed in the following chapters.

3. **Stimulated Emission**: Stimulated emission is important in order to achieve optical amplification to form a laser system, which is characterized by a property called 'coherence', meaning that the output optical signal has the same frequency, wavelength and energy. To achieve this, an atom must be excited to a higher energy level denoted as E_2 from its ground level denote as E_1 by supplying energy in form of light such as with arc lamps, flash lamps or semiconductor laser diodes. In this condition, the excited atoms are not stable and prefer to occupy the ground state level which a much in stable state.

Suppose an external photon with energy equal to the energy difference of the excited state and ground state level was introduced in the system, the excited electron in E_2 tends to de-excited, and the relaxation process causes a release of a photon with similar energy, frequency and direction to the incoming photon. This is what we call as stimulated emission and can be illustrated in Figure 2.1(b). This process is crucial for signal amplification in C-band optical communication systems.

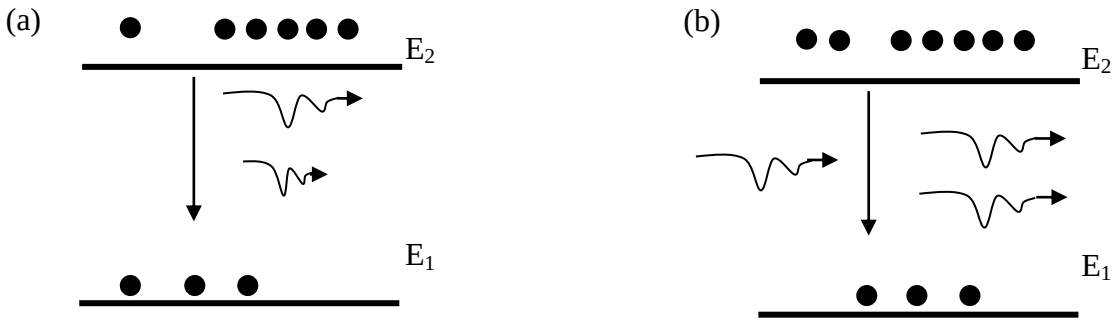

Figure 2.1: The processes of (a) spontaneous emission and (b) stimulated emission.

2.3 Types of Gain Media

There are several types of gain media used for optical amplification for realising fiber lasers, such as erbium doped fiber (EDF), semiconductor optical amplifier (SOA), Brillouin fiber amplifier (BFA) and Raman fiber amplifier (RFA). For our purposes, we focussed on the study of only EDF Amplifiers (EDFAs) and SOAs in the thesis, as these two provides different characteristics in generating fiber lasers as will be discussed later in this chapter.

2.3.1 Erbium Doped Fiber Amplifier (EDFA)

Research on the amplification of optical signals optically was undertaken beginning in the 1970's after a semiconductor laser amplifier was invented with considerably high noise level by Zeidler and Personick [1]. The study on optical fiber amplifiers, however, began slightly later, around mid-1980's, when neodymium (Nd) doped fibers, the first rare earth doped in a single mode fiber capable of amplifying light at 1060 nm, was invented by Broer and Simpson [2]. This was followed by the invention of erbium doped fiber amplifier (EDFA) in 1987 at the University of Southampton, ushering in a boom research on fiber amplifiers [3-5]. EDFs were then pumped by a 650 nm dye laser, and emitted light at 1550 nm. This region, called the C-band, proved to be very important, and is the current technology driving modern optical communication systems.

Erbium belongs to the Lanthanides groups, which consists of fifteen Lanthanides (atomic numbers from 57 until 71), and are also known as rare earth elements [6]. The elements in this group allow for the ability to provide the population inversion condition, the necessary condition in the generation of lasers, due to their 5s and 5f outer most electrons that accounts for the laser transitions. These Lanthanides typically appear in an ionic form of a trivalent state $(Ln)^{3+}$ with the atomic form of $(Xe)\ 4f^{N'}6s^2$ or $(Xe)\ 4f^{N'-1}5d6s^2$ [7] . The trivalent state is formed by eliminating three electrons, with two of the electron originating from the 6s orbital and the remaining one from either the 4f or 5d orbitals. In the case of erbium, the three electrons originate from the 6s and 4f orbitals.

The amplification by EDFA occurs with the transition of an electron from the metastable state, denoted as ${}^4I_{13/2}$, to the ground state level, denoted as ${}^4I_{15/2}$, from the 4f state. The

metastable state has a lifetime of 10 ms which is a sufficient amount of time for optical amplification to occur. Current, commercially available EDFA for modern applications typically employ either a 980 nm or 1480 nm semiconductor laser diode as the pump, which is also known as the pump laser diode. For fiber-based application, the pump laser diode is connected to the EDF through a 980/1550 nm or 1480/1550 nm wavelength division multiplexer (WDM) as depicted in Figure 2.2 below.

The signal used in this setup is in the C- or L-band region, depending on the length of the EDF. The isolator is used to prevent back reflections which contribute to noise during the amplification process. The optical spectrum analyzer (OSA) is used to observe the emitted optical spectrum and analyze the amount of gain provided by the EDFA.

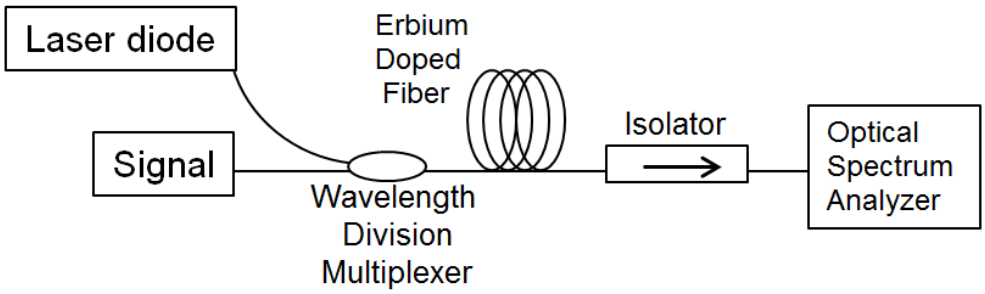

Figure 2.2: The setup of erbium doped fiber amplifier (EDFA).

2.3.1.1 Atomic Rate Equation for EDF

In this section, a quasi-three level energy system is employed to model the atomic rate equation for an EDF. These levels are illustrated in Figure 2.3, and has been discussed thoroughly by Desurvire [8]. The three energy levels are denoted as E_1 , E_2 and E_3, with E_1 being the ground state level where most of atom situated when no energy is being absorbed by the EDF, E_2 is the metastable state level with a transient life time denoted as τ,

and E_3 is the pumping level. Therefore, $E_3 > E_2 > E_1$. The pumping rate from E_1 to E_3 is denoted as R_{13}, while the stimulated emission ratefrom level E_3 to E_1 is denoted as R_{31} and the stimulated emission and absorption rates denoted as W_{21} and W_{12}, respectively. The spontaneous decay rate, A, can either correspond to radiated (A^R) and non-radiated (A^{NR}) emissions. For the case of unstable excitation at level E_3, the unstable electrons will decay immediately, following their excitation, through either radiative or nonradiative decay. A_{32}^R and A_{31}^R are the radiative decay rates for transition from E_3 to E_2 and E_3 to E_1, respectively, which has been clearly explained in ref [8] and reproduced here for completeness of the thesis.

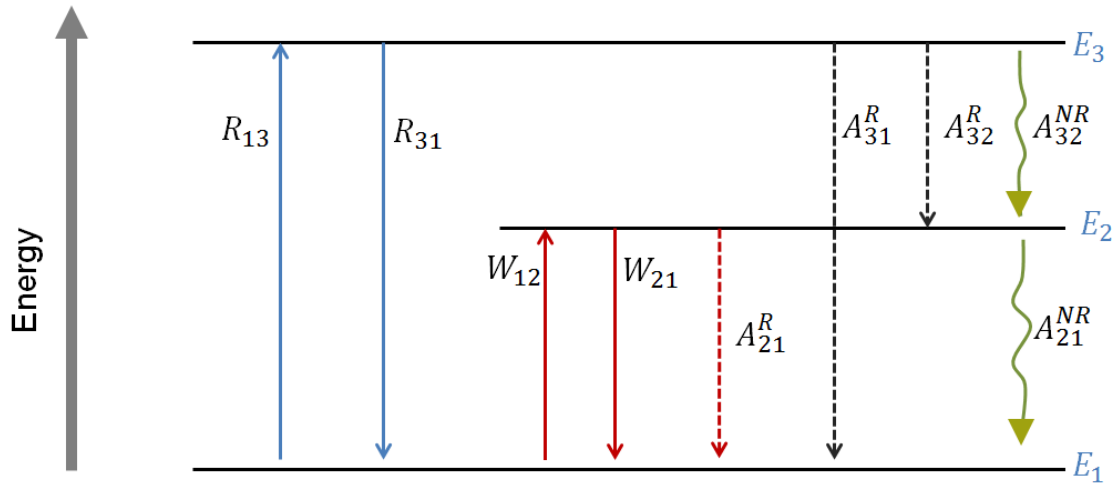

Figure 2.3: The illustration of three-level energy system for EDF [8].

If we assume that the nonradiative transition from E_3 to E_2, denoted as A_{32}^{NR} to be the largest contributor of decay from level E_3, then we can state that $A_{32}^{NR} \gg A_3^R$, where $A_3^R = A_{32}^R + A_{31}^R$. Therefore, the emission from level E_3 to E_2 is denoted as A_{32}^{NR} for simplicity.

However this is not the case for the transition from E_2 to E_1. In this process, the most dominant transition is the spontaneous radiative emission denoted as A_{21}^R rather than

spontaneous nonradiative emission, denoted as A_{21}^{NR} ($A_{21}^{R} \gg A_{21}^{NR}$). $A_{21}^{R} = \frac{1}{\tau}$, where τ is the fluorescence lifetime. Now, we denote N_1, N_2 and N_3 to be the number of ions at level E_1 , E_2 and E_3, respectively and ρ to be the laser ion density, where $\rho = N_1 + N_2 + N_3$. The atomic rate equations for the three-level energy system can then be expressed as [8]

$$\frac{dN_1}{dt} = -R_{13}N_1 + R_{31}N_3 - W_{12}N_1 + W_{21}N_2 + A_{21}N_2 \quad 2.1$$

$$\frac{dN_2}{dt} = W_{12}N_1 - W_{21}N_2 - A_{21}N_2 + A_{32}N_3 \quad 2.2$$

$$\frac{dN_3}{dt} = R_{13}N_1 - R_{31}N_3 - A_{32}N_3 \quad 2.3$$

Initially, the ion population is assumed to be constant and this state is called the steady state condition. This condition is satisfied when $\frac{dN_i}{dt} = 0$, where $i = 1, 2$ and 3, denoting the different energy levels.

We now define $a = (R_{31} + A_{32})$ and $b = (W_{21} + A_{21})$. Equations (2.2) and (2.3) then can be expressed as

$$W_{12}N_1 - bN_2 + A_{32}N_3 = 0 \quad 2.4$$

$$R_{13}N_1 - aN_3 = 0 \quad 2.5$$

Now, N_3can also be express as $N_3 = \rho - N_1 - N_2$. This allows equations (2.4) and (2.5) to be solved in order to find N_1 and N_2 as

$$N_1 = \rho \frac{ab}{b(a + R_{13}) + aW_{12} + R_{12}A_{32}} \quad 2.6$$

$$N_2 = \rho \frac{R_{13}A_{32} + aW_{12}}{b(a + R_{13}) + aW_{12} + R_{13}A_{32}} \quad 2.7$$

Employing the definitions for a and b and factorising A_{21} and A_{23}, we obtain

$$N_1 = \rho \frac{(1 + W_{21}\tau)(1 + \frac{R_{13}}{A_{32}})}{(1 + W_{21}\tau)\left(1 + \frac{R_{13}+R_{31}}{A_{32}}\right) + W_{12}\tau\left(1 + \frac{R_{31}}{A_{32}}\right) + R_{13}\tau} \quad 2.8$$

$$N_2 = \rho \frac{R_{13}\tau + W_{12}\tau(1 + \frac{R_{13}}{A_{32}})}{(1 + W_{21}\tau)\left(1 + \frac{R_{13}+R_{31}}{A_{32}}\right) + W_{12}\tau\left(1 + \frac{R_{31}}{A_{32}}\right) + R_{13}\tau} \quad 2.9$$

Assuming $A_{32} \gg R_{13}$, and $A_{32} \gg R_{31}$ therefore, $\frac{R_{13,31}}{A_{32}} \approx 0$. From the initial assumption that the nonradiative decay rate is dominant, equations (2.8) and (2.9) become

$$N_1 = \rho \frac{1 + W_{21}\tau}{1 + R\tau + W_{12}\tau + W_{21}\tau} \quad 2.10$$

$$N_2 = \rho \frac{R\tau + W_{12}\tau}{1 + R\tau + W_{21}\tau + W_{12}\tau} \quad 2.11$$

with $R = R_{13}$. From equation (2.10) and (2.11), $N_3 = \rho - N_1 - N_2 = 0$. This means the pump level population is neglected by the major contribution of nonradiative decay (A_{32}) from level E_3 to E_2, which is the metastable level.

These equations provide the basic conditions in order to achieve amplified stimulated emission, which is the key ingredient for the generation of lasers. The next subsection will investigate how semiconductor optical amplifier functions in order to achieve similar conditions.

2.3.2 Semiconductor Optical Amplifier (SOA)

SOAs are devices that have characteristics of both metal and glass. Metals such as copper are materials which allow the flow the electricity. Indeed, copper wires are still being widely used in modern communication systems due to its properties, especially for fixed-line telephone communication systems such as the one provided by Telekom Malaysia Berhad that covers the Peninsular Malaysia, Sabah and Sarawak. Glass, on the other hand, is a material that can guide light through the phenomenon called total internal reflection as in optical fiber, which was proposed in 1961 by E. Snitzer [9]. Since then, optical fibers have had a major role in the development of optical communication technology, such as the one employed by UniFi, which is also provided by Telekom Malaysia Berhad. Semiconductor materials, employed to build SOAs, on the other hand, are materials which exhibits properties of both glass and metal, and therefore can guide light yet at the same time allow electrons to flow through it. The material thus uniquely, allows the conversion of the flowing electrons into photons, and vice versa. This unique feature allows the development of a new field, optoelectronics, which combines optics and electronics.

The invention of SOAs is triggered by the development of semiconductor laser, when the first semiconductor laser was created by Robert Hall and his team in 1962 [10] which was based on a homojunction device. Since then a large number of studies have been undertaken in order to improve the laser emission [11-13]. In the 1970's the homojunction structure gave way to a heterostructure which improved the performance of homostructure laser diode [1, 14, 15]. Research in SOAs, however, only developed rapidly in the 1980's, when the anti-reflection coating which prevent reflection was invented, thereby creating a usable diode [16, 17]. This research continues up to this day [18]. However, due to relative infancy of this research field and the fact that this material has a relatively high loss, SOAs became less preferable as compared to the erbium doped fiber, the fiber amplifier that opened the communication window in 1550 nm region during that time.

With improvement of the p-n junction and coating in SOAs, the use of SOAs became more widespread due to their relatively large amplification window, especially in the C- and O-band regions, and, more recently, in the S- and L-band regions [19-22]. In contrast to fiber amplifiers, which employ rare earth-doped dopants inside the fibers' core to achieve amplification, SOAs use a combination of several materials to form semiconductor p-n junctions which then act as amplifiers. Amplification is achieved by creating excessive amounts of holes and electrons in order to obtain p-type or n-type semiconductors, respectively.

There are two basic types of SOAs, namely, Fabry-Perot SOAs and travelling-wave SOAs. Fabry-Perot SOAs operate with virtual 'mirrors' at the ends of the device, due to reflection at the facets, but operate below the lasing threshold. Reflections at the facets cause multiple interference in the cavity, leading to 'ripples' in the gain spectrum. Travelling-wave SOAs, on the other hand, operate without 'mirrors', which is done by inserting anti-reflection

coating with reflectivity less than 10^{-5} at the surface of the facets [23]. The performance of the travelling wave SOAs is better than the Fabry-Perot SOAs due to the fact that they sensitive less (which lead to fluctuation) to the surroundings.

2.3.2.1 Spontaneous and Stimulated Transition in SOA

In contrast to the three-level system used to describe EDFA's emission, SOAs employ a two-level system to achieve emission, due to the linear relationship amplification and the spontaneous and stimulated emissions of the SOA. The two-level laser system can be demonstrated as in Figure 2.4.

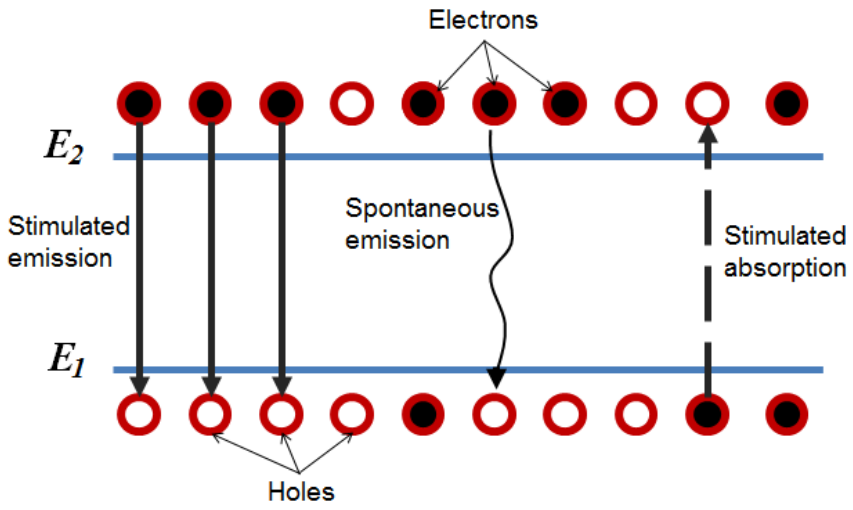

Figure 2.4: The illustration of electrons transition in a two-level laser system [23].

Let N_1 be the amount of electrons density at energy E_1, and N_2 be the number of electrons at energy E_2. As depicted in Figure 2.4, E_2 has a higher energy level as compared to E_1. The rate of spontaneous transition from the higher level to the lower level, or E_2 to E_1 can be described as [23]

$$\left.\frac{dN_{21}}{dt}\right|_{spon} = A_{21}N_2 \qquad 2.12$$

where A_{21} is the parameter of spontaneous emission from energy level of E_2 to E_1.

The rate of stimulated electron transition from E_2 to E_1 on the other hand is expressed as

$$\left.\frac{dN_{21}}{dt}\right|_{stim} = B_{21}\rho(C)N_2 \qquad 2.13$$

where B_{21} is the parameter of stimulated emission from E_2 to E_1 and $\rho(\upsilon)$ is the energy density at frequency υ. Trivially, the energy of the stimulated photon is equal to the energy difference between E_2 and E_1, from energy conservation. The rate of stimulated electron absorption from E_1 to E_2 can then be expressed as,

$$\left.\frac{dN_{12}}{dt}\right|_{stim} = B_{12}\rho(\upsilon)N_1 \qquad 2.14$$

where B_{12} is the parameter of stimulated absorption from E_1 to E_2. Quantum-mechanically, it has been proven that [24]

$$B_{12} = B_{21} \qquad 2.15$$

This therefore leads to the following expression:

$$\frac{A_{21}}{B_{21}} = \frac{8\pi n_r^3 h v^3}{c^3} \tag{2.16}$$

where c the speed of light propagating in vacuum, h is the Planck constant and n_r is the refractive index of the waveguide inside the SOA. By inserting (2.16) into equation (2.14), the following equation is obtained

$$\left.\frac{dN_{21}}{dt}\right|_{stim} = \frac{A_{21} c^3 \rho(v) N_2}{8\pi n_r^3 h v^3} \tag{2.17}$$

For stimulated emission from E_2 to E_1 centralized at a single frequency v, the equation becomes

$$\left.\frac{dN_{21}}{dt}\right|_{stim} = \frac{A_{21} c^3 \rho_v l(v) N_2}{8\pi n_r^3 h v^3} \tag{2.18}$$

where ρ_v is the radiation energy per unit volume, or energy density, due to the stimulated emission, and $l(v)$ is the transition lineshape function, $l(v)$ is normalized by the following procedure:

$$\int_{-\infty}^{\infty} l(v)dv = 1 \tag{2.19}$$

This gives the probability of spontaneous emission event between the frequencies$v$ and$(v + dv)$. The induced field intensity is then given as

$$I_v = \frac{c}{n_r}\rho_v \tag{2.20}$$

From this, the stimulated electron transition rate becomes

$$\left.\frac{dN_{21}}{dt}\right|_{stim} = \frac{A_{21}c^2 I_v l(v) N_2}{8\pi n_r^2 h v^3} \tag{2.21}$$

The total power, dP_v, can then be calculated by assuming that it can be modelled as a plane wave propagation as follows

$$dP_v = \left(\left.\frac{dN_{21}}{dt}\right|_{stim} - \left.\frac{dN_{12}}{dt}\right|_{stim}\right) hvA\, dz \tag{2.22}$$

where A is the cross-section area and dz is the length of the waveguide travel by the wave. This can be described as the total number of significant electrons that will contribute to emission, and therefore, would not absorbed by the gain medium. This will then allow us to calculate the total amount of radiation intensity, by multiplying the number of electrons contributing to emission with the transition energy, hv. To observe the power change by the change of length travelled by the photons, the equation can be expressed as

$$\begin{aligned}\frac{dP_v(z)}{dz} &= \left(\left.\frac{dN_{21}}{dt}\right|_{stim} - \left.\frac{dN_{12}}{dt}\right|_{stim}\right) hvA \\ &= \mathrm{g}_m(v) P_v \end{aligned} \tag{2.23}$$

where $\mathrm{g}_m(v)$ is the SOA gain coefficient given by [23]

$$\mathrm{g}_m(v) = \frac{A_{21}c^2 l(v)(N_2 - N_1)}{8\pi n_r^2 v^2} \tag{2.24}$$

It should be noted, however, that this expression is true only when the number of electron density at level E_2 is much larger than level E_1.

2.3.2.2 Electron Density Rate Equation in SOA

Amplification in the SOA is dependent on the amount of carrier or electrons, and is controlled by its bias current. This is quite different from the EDFA, as the amplification in the gain medium is provided by power injected into the EDF by the laser pump. Therefore, the spontaneous emission from SOA is a result of the bias current. The amount of electrons per volume at position *z* in the SOA can be expressed as [23]

$$\frac{dn(z)}{dt} = \frac{I}{edLW} - R(n) - \frac{\Gamma}{dw}\left\{\sum_{k=1}^{N_s} g_m(v_k, n)[Ns_k^+(z) + Ns_k^-(z)]\right\} - \frac{2\Gamma}{dw}\left\{\sum_{j=0}^{N_m-1} g_m(v_j, n)\left[N_j^+(z) + N_j^-(z)\right]\right\} \quad 2.25$$

where I is the bias current,d is the thickness active region, e is the electronic charge, L is the length of the waveguide active region, W is the width of the active region and Γ is the confinement factor. Ns_k^+ and Ns_k^- are the photon rates in the positive and negative z direction, respectively, while N_j^+ and N_j^- are the photon rates at positive and negative z direction with a particular polarization, and v_k and v_k are frequencies of each respective term.

The distribution of the current is presumed to be uniform across the waveguide. The first term in the right hand side, $\frac{I}{dLW}$, describes the addition of electron carriers resulting from an increase in the supplied bias current. The second term describes the process of radiative (spontaneous emission) and nonradiative recombination which produces loss in the gain medium. The third and fourth terms are the radiative recombination of the amplified signal and amplified spontaneous emission (ASE) respectively.

2.4 Homogeneous and Inhomogeneous Broadening Gain Media

There are two types of atomic transition for spectral broadening in an active gain media, namely, homogeneous and inhomogeneous spectral broadening, corresponding to homogeneous and inhomogeneous gain media, respectively. Homogeneous spectral broadening is explicitly exhibited by most rare earth doped fibers such as erbium doped fibers (EDFs) [25-27], ytterbium doped fibers (YbDFs) [28-30] and thulium doped fibers (TDFs), while inhomogeneous spectral broadening can be seen in devices such as the semiconductor optical amplifiers (SOAs). This doesn't mean that both of the gain media only exhibit homogeneous and inhomogeneous spectral broadening, but rather these two gain media exhibit gain profiles which are either dominantly homogeneously broadened or inhomogeneously broadened.

Here, the shapes of the atomic linewidth transitions, which are either Lorentzian or Gaussian, will be discussed in relation to either the homogeneous or inhomogeneous gain media. This will allow for a numerical interpretation for these two spectral linewidths. In the next subsection, the characteristics of these two broadening phenomena are studied through experimental work which will be explained further.

2.4.1 Homogeneous Gain Medium

The EDFs which will be used in the work, especially in Chapter 3, is a Metrogain-12 EDF provided by Fiber Core Company, due to its commercial availability. In general, all of rare earth doped fibers exhibit homogeneous broadening transition. As the present work will involve EDFs, they would be the primary method in investigating homogenously

broadened gain media [31]. However, it is worth noting that the EDFs still produce inhomogeneous broadened transitions in a relatively low amount, as compared to the homogeneous broadening.

Now, atomic transitions in EDFs are caused by a stimulated emission from the $^4I_{13/2}$ level to the $^4I_{15/2}$ level, when pumped by either a 980 nm or 1480 nm laser diode. This transition, however, experience Stark broadening, actually induced by Stark effect [8], which splits the energy levels into an upper and lower manifold, denoted as g_1 and g_2 respectively. This splitting of energy levels into upper and lower levels allows for an increase in the number of atomic transitions thereby causing a broadening of the laser transition. As mentioned previously, the characteristic of every transition is also different and not homogeneous. However, in the case of EDF, it can be viewed as homogeneous due to the fact that the energy sublevels are strongly coupled by the thermalization effect, which results in homogeneous broadening.

Homogenous broadened transition has a Lorentzian line shape as has been discussed before, and therefore causes a narrowing of the transition linewidth as depicted in Figure 2.5. The broadening also has an unambiguous dependence of the resonance frequency to the signal frequency, and due to the response of each individual ion in the collection, the signal is broadened equally and homogeneously [32]. Hence, the atomic transition will exhibit exactly the same lineshape if the right conditions are provided by the cavity and surroundings.

The Lorentzian gain coefficient,$\gamma(\upsilon)$can be expressed as[33];

$$\boldsymbol{\gamma(\upsilon) = \gamma(\upsilon_o)\frac{(\Delta\upsilon/2)^2}{(\upsilon-\upsilon_o)^2+(\Delta\upsilon/2)^2}} \quad 2.26$$

where $\gamma(\upsilon_o)$ is the gain coefficient at the central frequency, υ_o and $\Delta\upsilon$ is the emission linewidth.

The homogeneous broadening effect therefore leads to a uniform saturation of the gain across the whole spectrum, independent of frequency, with the lasing frequency selected from the conditions within the cavity. This effect is depicted in Figures 2.6(a) and 2.8(a), while Figure 2.6 (b) and Figure2.8 (b) are shown to depict the effect of inhomogeneous broadening to the gain curve for comparison.

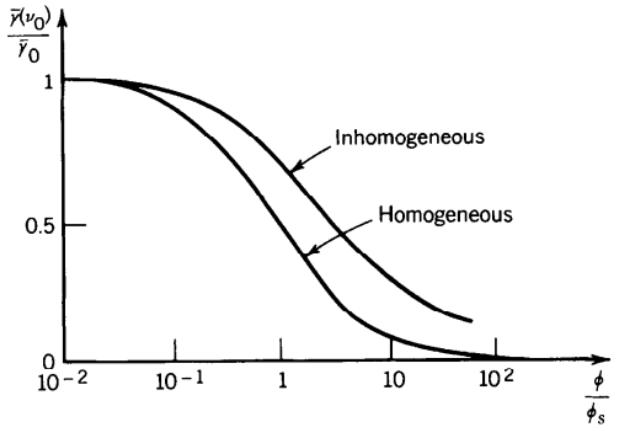

Figure 2.5: The Lorentzian and Gaussian lineshapeon normalized saturated gain coefficient versus normalized photon flux density [34].

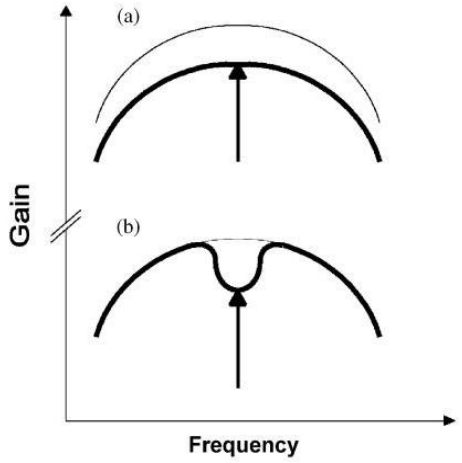

Figure 2.6: The effect of saturating signal on the gain curve for (a) Homogeneous and (b) Inhomogeneous spectral broadening. [After Ref. [31]]

2.4.2 Inhomogeneous Gain Medium

SOAs exhibit both of homogenous and inhomogeneous broadening effect. However, as has been proven by many research and experiments, the emission has a relatively large portion of inhomogeneously broadened transitions as compared to homogeneous broadening transitions [35, 36]. The SOA used in the work is a travelling wave multi-quantum well SOA (MQW-SOA) which was found to have an emission spectrum that is largely inhomogeneous broadened [37-40] as has been studied by many research group [41-46]. In contrast to homogeneously broadened transition, atoms in inhomogeneous broadening materials actin a different manner due to the fact that they have different orientations and lattice location [23], in addition to quantum well imperfections. This is manifested in the independent saturation of different frequencies for each mode in the steady state condition. Consequently, multi-longitudinal modes fiber laser can be established in inhomogeneously broadened lasers.

Inhomogeneously broadened gain media differ from homogeneously broadened gain media in that they exhibit a phenomenon known as the hole-burning effect, which occurs at the center of the saturating signal emitted by inhomogeneous gain medium. This is because the saturating signal will only affect the transition of atoms with similar frequencies. This then only allows a relatively small number of atoms to be homogeneously broadened and therefore having a reduced gain, while leaving other atoms free. The aggregation of these atoms then is an inhomogeneously broadened transition, as illustrated in Figure 2.7.

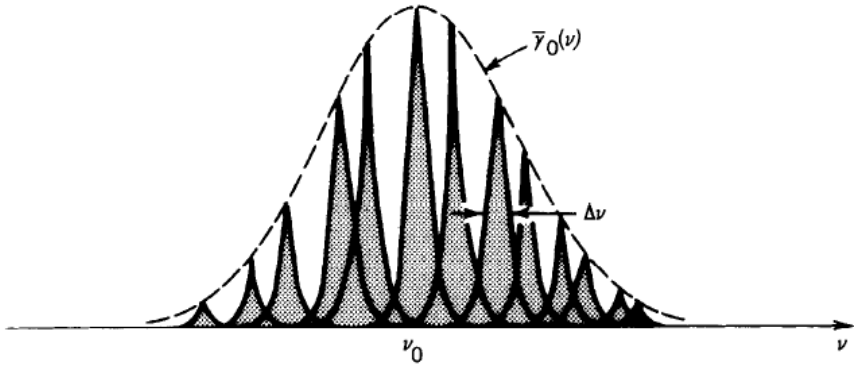

Figure 2.7: The lineshape of inhomogeneous broadened gain medium[33].

As SOAs generally is inhomogeneously broadened, they exhibit an inhomogeneously broadened lineshape, as shown in Figure 2.5. It also can be seen from the same figure that the inhomogeneous gain coefficient saturates slower than homogeneous gain coefficient.

The Gaussian gain coefficient, $\gamma(\upsilon)$ can be expressed as [33]

$$\gamma_\beta(\upsilon) = \frac{b(\Delta\upsilon/2\pi)}{(\upsilon - \upsilon_\beta - \upsilon_o)^2 + (\Delta\upsilon_s/2)^2} \qquad 2.27$$

where β is the subset of frequency, υ_β, $\Delta\upsilon$ is the emission linewidth, $\Delta\upsilon_s$ is the Lorentzian shape of width and υ_o is the central frequency. b is a constant and is defined as, $b = N_o(\lambda^2/8\,\pi\,\tau_{sp})$, with is τ_{sp} the spontaneous lifetime, N_o the steady state population different and λ the wavelength of light in the medium.

The hole-burning effect was also explained by Siegman [32] as an indispensable phenomenon in inhomogeneously broadened gain media when a strong signal is injected into the gain medium and causing saturation of only a sub-group of atoms with similar resonance frequencies as the signal. Other transitions at more distant frequencies will not be effected. This physical explaination can be clearly seen as illustrated in Figure 2.8(b).

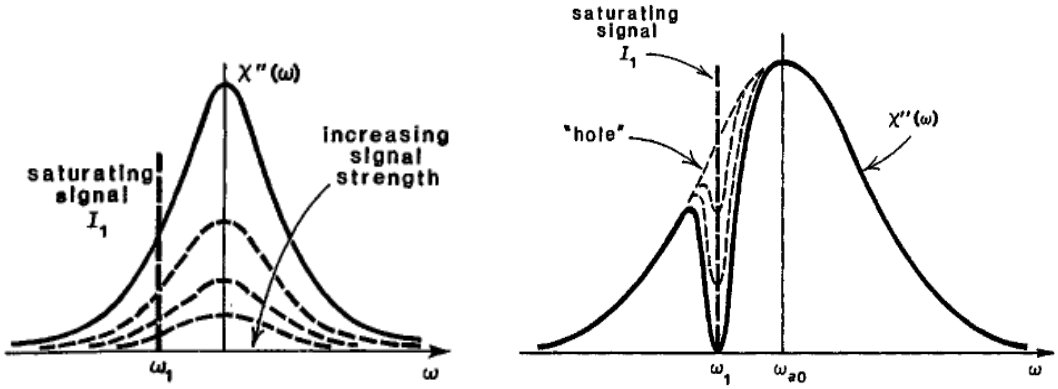

(a) (b)

Figure 2.8: The saturation condition for (a)homogeneous and (b)inhomogeneous profile [32].

2.4.3 Characterization of Homogeneous and Inhomogeneous Gain Media

In this section, the experimental work done in characterizing the homogeneous and inhomogeneous broadening emitted by the EDF and SOA, respectively, are presented.

2.4.3.1 Experimental Analysis

In order to analyze the homogeneous and inhomogeneous broadening phenomena, a saturating signal is injected into the gain media, and their spectrum profiles were then analyzed. However to obtain the saturation power for both of the gain media, a simple experiment was done as shown in Figure 2.9(a) for the EDFA and 2.9(b) for the SOA, respectively. The setup for the EDFA is comprised of a 980 nm laser diode, a 980/1550 nm wavelength division multiplexer (WDM) and a 5 m EDF. While the SOA comprises a single device with an input and output port connected to the SOA. An optical attenuator is used to control the input power entering the amplifiers. The gain measurements for both of the gain media were carried out and analyzed.

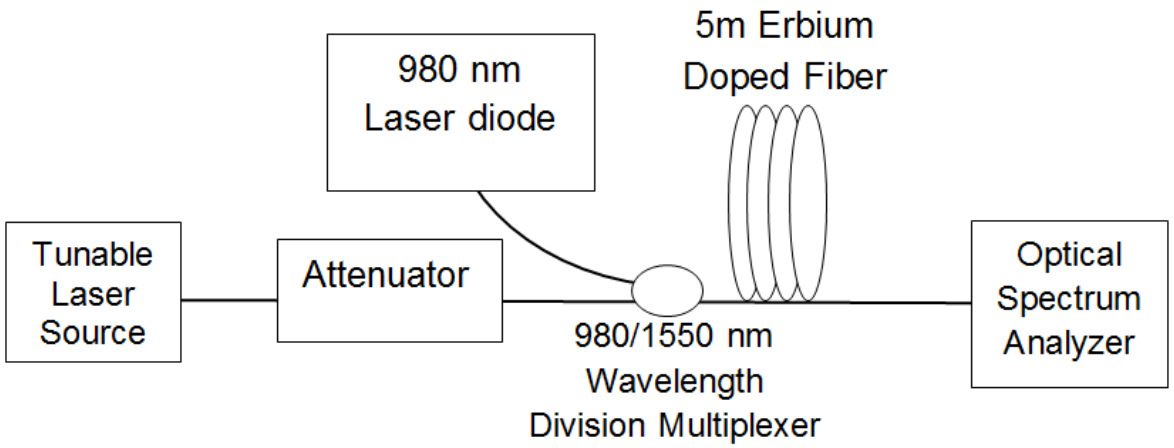

(a)

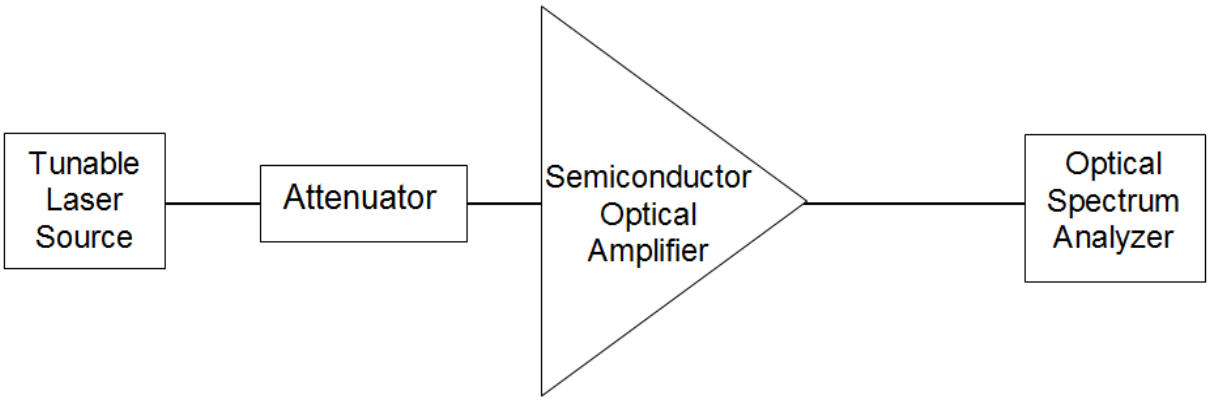

(b)

Figure 2.9: Experimental setup for gain measurement of (a) EDFA and (b) SOA.

The saturation input power for both gain media are determined by measuring the input power level when it has a 3dB gain attenuation from the maximum gain [8, 23]. Figure 2.10 shows the gain measurement as a function of signal power. By analyzing this graph, the saturation power for EDFA was found to be -5 dBm, while that of the SOA was at -20 dBm. The data presented in Figure 2.10 is in agreement with theoretical considerations which states that the more the injected signal power, the lower the gain shall be [8]. This is to be expected as if a higher input power higher than the saturation power is injected, there will be an increase in the depletion of the active region responsible for gain [23, 32].

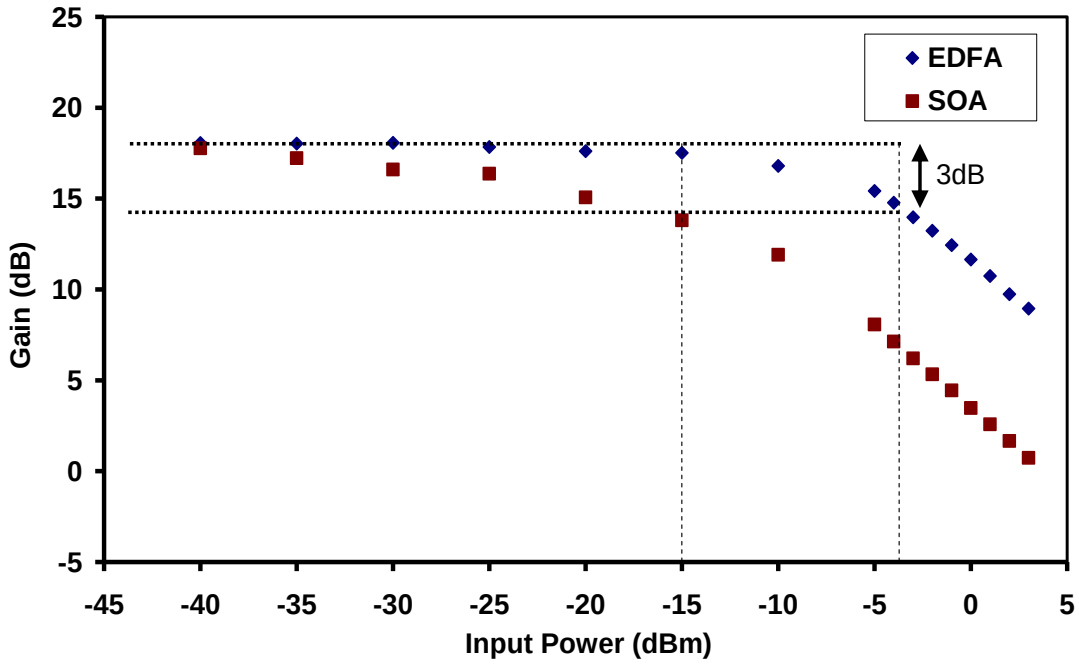

Figure 2.10: Results for gain measurement for EDFA and SOA.

Figure 2.11 shows the homogeneously broadened spectrum of the EDFA. Since the lasing frequency for the EDFA at room temperature is close to the frequency profile for homogeneous systems, the saturation effect is present in the entire spectrum. This therefore reduces the gain of the entire spectrum, preventing the observation of a ASE 'hole' in the spectrum, as is present in inhomogeneously broadened gain media.

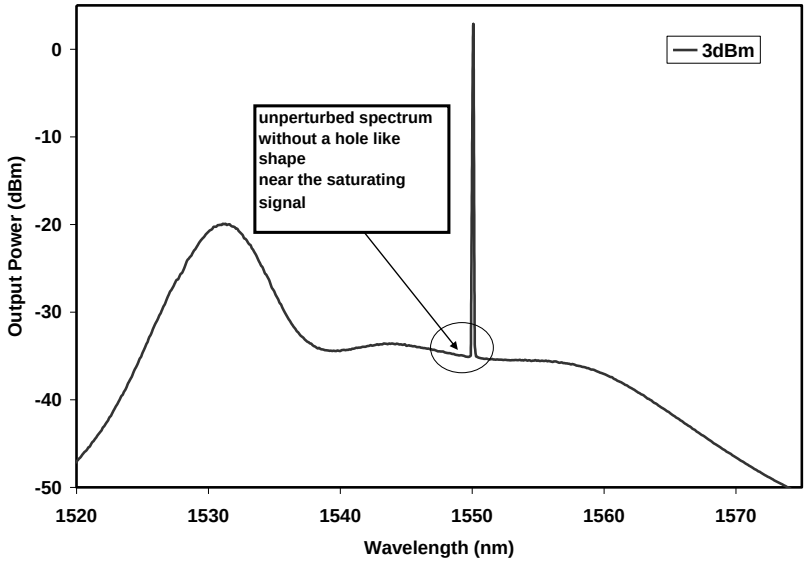

Figure 2.11: Homogeneous broadening effect in EDFA.

Comparing this to the inhomogeneous line broadening in the SOA, depicted in Figure 2.12, it is clear that a hole-like shape can be seen in addition to the injected signal. The reason for such phenomenon is that the lasing frequency for each wavelength is different from one to another, and therefore saturation happens only at certain wavelengths which have the same frequency as the oscillation. Both materials were injected with 3 dBm input signal as this amount of power is bigger than the saturation power for both EDFA and SOA as -5 dBm and -20 dBm of saturation power are obtained from the analysis respectively.

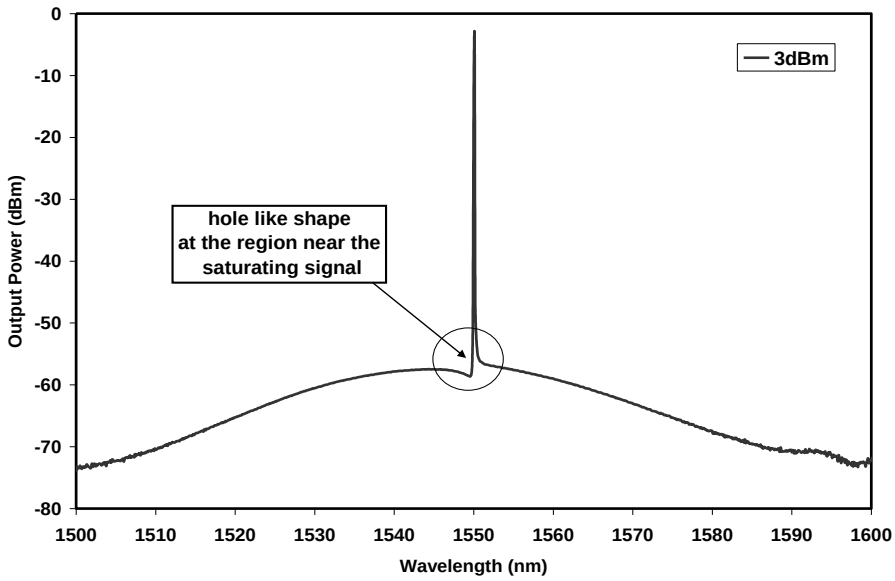

Figure 2.12: Inhomogeneous broadening effect in SOA.

2.5 Optical Fibre Lasers

LASER is an acronym for light amplification by stimulated emission of radiation. It is a device which allows for the generation of amplified light provided that three conditions are satisfied. First, the device must contain a laser medium such as atoms or molecules which acts as the active medium for amplification. Secondly, the device must contain an optical cavity which allows for circulation of photons inside the cavity, and therefore, causes population inversion. This enables the laser beam to propagate back and forth in the cavity, increasing the gain until saturation, before being extracted to obtain the output. The third condition is that the device must include a pumping method to allow excite the active medium and cause stimulated emission to take place inside the cavity. A simple configuration of a laser is shown in Figure 2.13.

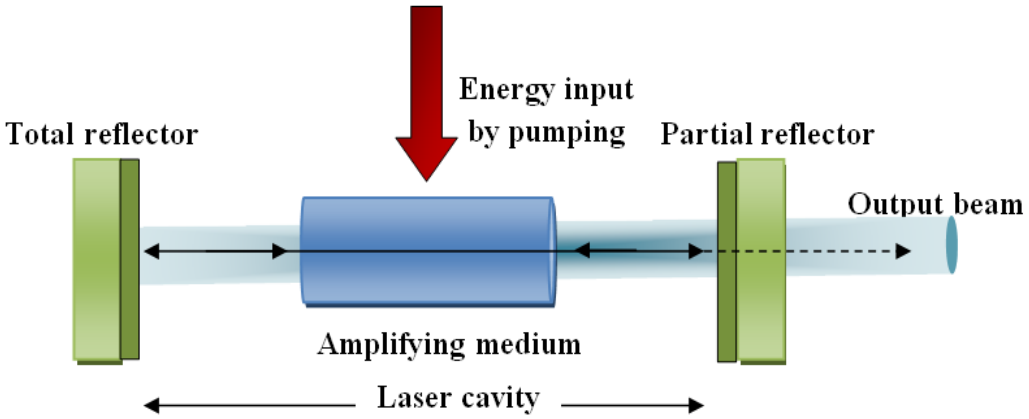

Figure 2.13: A simple free space laser cavity design

As was discussed previously, one of the most important aspects to be considered before a laser can be realized is population inversion. Population inversion can be achieved by increasing the amount of the excited atoms in a particular system to be higher than the amount of electrons in the ground state level. When the gain of the laser is higher than the cavity loss the lasing will start.

There are several types of lasers, such as solid state lasers, gas lasers, semiconductor lasers, dye lasers and optical fiber lasers. Optical fiber lasers are generally designed by inserting an active gain medium such as the EDFA or SOA into an optical cavity whose output is looped back to the input port the gain medium. This is illustrated in Figure 2.14. The laser is generated from the amplification of the optical gain medium output which has reached the lasing threshold, by reconnecting the output to the input via a WDM (see Figure 2.9(a)). The process continues until it reaches its highest output power when the gain saturation is reached. The condition is called as a steady state condition, where the fiber laser cannot produce any larger amount of output power.

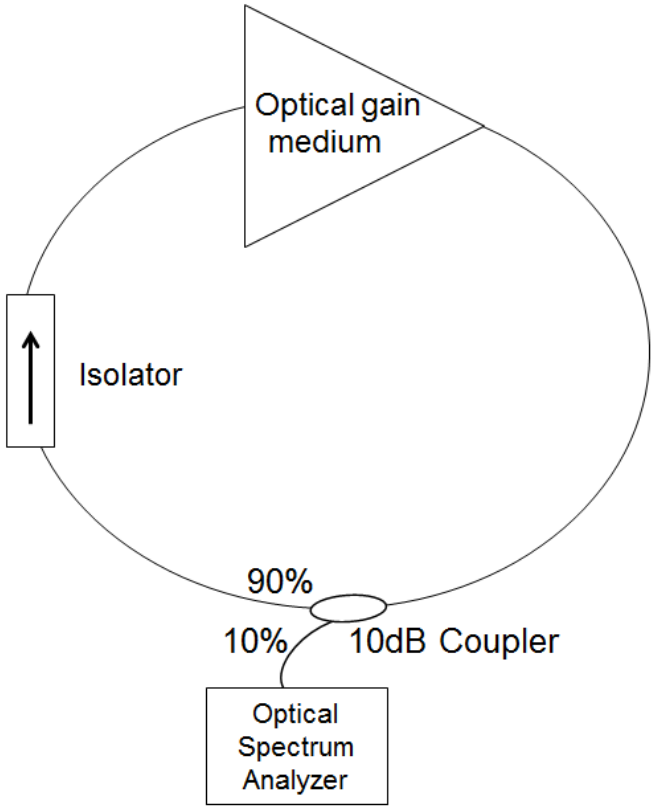

Figure 2.14: A configuration of a basic optical fiber laser

2.6 Characteristic of Fiber Lasers

The important characteristics to determine the performance of the fiber lasers are the output power, side mode suppression ratio (SMSR), tunability and stability. The output is considered to be a laser when the pump power is sufficiently high such that population inversion is achieved and therefore, the energy of the system has reached the lasing threshold. In other words, a laser is generated when the small-signal gain coefficient is higher than its loss coefficient. A stable performance of fiber laser typically has a minimum output power of -20 dBm. A high output power is crucial for the performance of the fiber laser.

The SMSR on the other hand is necessary to evaluate the degree of noise in the fiber laser. The SMSR can be defined as the intensity difference between the main longitudinal mode and the maximum side mode, and can be written as [47]

$$\begin{aligned} \mathrm{SMSR(dB)} &= 10\log\left(\frac{\mathrm{I_{main}}}{\mathrm{I_{side}}}\right) \\ &= \mathrm{I_{main}(dBm) - I_{side}(dBm)} \end{aligned} \qquad 2.28$$

A high value of SMSR indicates a good performance of a fiber laser. A conventional laser diode has a typical SMSR value of 40 dB. Therefore, in order to build a well performing laser, the SMSR value is required to be as high as possible, preferably with a minimum value of 40 dB. This is important in order to reduce the crosstalk in the WDM networks when they function as transmitters.

The tunability of a laser allows for the selection of wavelengths provided by the fiber laser. The wider the range, the better the fibre laser is and can be used for a number of applications, such as in DWDM communication system as a transmitter, in spectroscopy and as sensors, especially temperature and displacement sensors.

Stability is the measure of fluctuation of the output power with time. It is important to see whether a fiber laser is stable enough and operate for a long period of time. This is important, as a stable output power fiber laser is required for transmission purposes in communication systems to prevent extra cost.

2.6 Summary

In this chapter, two types of gain media, namely, the EDF and SOA were discussed. The rate equation of the EDF and SOA were presented in this chapter in order to gain some understanding the principle of amplification. The gain media can be classified into two categories, namely, homogeneous and inhomogeneous gain media. The EDF can be considered to be a homogeneously broadened gain media while SOA has an output profile which is closer to the inhomogeneously broadened gain media. A simple experiment was also conducted to observe the difference in the broadening effects between the EDF and the SOA. A clear distinction can be seen as the inhomogeneously broadened gain medium exhibits a phenomenon known as spectral hole burning, which is absent inhomogeneously broadened gain media, which are demonstrated in the following chapters.

This chapter also briefly discusses the generation of fiber lasers. The characteristics of fiber lasers including the output power, SMSR value, tunability and stability are also discussed in this chapter. These characteristics shall be important as they will be extensively employed in the next chapter in discussing the switchable and tunable fiber laser.

References

1. Zeidler, G. and D. Schicketanz, *Use of laser amplifiers in a glass-fibre communications system.* Radio and Electronic Engineer, 1973. **43**(11): p. 675-682.
2. Broer, M.M., et al., *Low-temperature optical dephasing of rare-earth ions in inorganic glasses.* Physical Review B, 1986. **33**(6): p. 4160-4165.
3. Poole, S.B., D.N. Payne, and M.E. Fermann, *Fabrication of low-loss optical fibres containing rare-earth ions.* Electronics Letters, 1985. **21**(17): p. 737-738.
4. Townsend, J.E., S.B. Poole, and D.N. Payne, *Solution-doping technique for fabrication of rare-earth-doped optical fibres.* Electronics Letters, 1987. **23**(7): p. 329-331.
5. Poole, S., et al., *Fabrication and characterization of low-loss optical fibers containing rare-earth ions.* Lightwave Technology, Journal of, 1986. **4**(7): p. 870-876.
6. Emsley, J., *Nature's Building Blocks: An A-Z Guide to the Elements*2001: Oxford University Press.
7. Becker, P.C., N.A. Olsson, and J.R. Simpson, *Erbium-Doped Fiber Amplifiers: Fundamentals and Technology*1999: Elsevier Science.
8. Desurvire, E., *Erbium-Doped Fiber Amplifiers* 1994, Canada: John Wiley and Sons, Inc. 770.
9. Snitzer, E., *Optical Maser Action of Nd^{+3} in a Barium Crown Glass.* Physical Review Letters, 1961. **7**(12): p. 444-446.
10. Hall, R.N., et al., *Coherent Light Emission From GaAs Junctions.* Physical Review Letters, 1962. **9**(9): p. 366-368.

11. Lasher, G. and F. Stern, *Spontaneous and Stimulated Recombination Radiation in Semiconductors.* Physical Review, 1964. **133**(2A): p. A553-A563.

12. Dumke, W.P., *Optical Transitions Involving Impurities in Semiconductors.* Physical Review, 1963. **132**(5): p. 1998-2002.

13. Leite, R.C.C., et al., *Injection Mechanisms in GaAs Diffused Electroluminescent Junctions.* Physical Review, 1965. **140**(7AB): p. AB4-AB4.

14. Nakamura, M., et al., *GaAs GaAlAs double-heterostructure injection lasers with distributed feed back.* Quantum Electronics, IEEE Journal of, 1975. **11**(7): p. 436-439.

15. Schicketanz, D. and G. Zeidler, *GaAs-double-heterostructure lasers as optical amplifiers.* Quantum Electronics, IEEE Journal of, 1975. **11**(2): p. 65-69.

16. Zah, C.E., et al., *1.3 μm GaInAsP near-travelling-wave laser amplifiers made by combination of angled facets and antireflection coatings.* Electronics Letters, 1988. **24**(20): p. 1275-1276.

17. Saitoh, T., T. Mukai, and O. Mikami, *Theoretical analysis and fabrication of antireflection coatings on laser-diode facets.* Lightwave Technology, Journal of, 1985. **3**(2): p. 288-293.

18. Reed, M., et al., *Antireflection-coated angled facet design.* Optoelectronics, IEE Proceedings, 1996. **143**(4): p. 214-220.

19. Dar-Zu, H., et al. *High-efficiency and wideband SOA-based wavelength converters by using four-wave-mixing with orthogonal pumps and an assisted beam*. in *Lasers and Electro-Optics, 2003. CLEO/Pacific Rim 2003. The 5th Pacific Rim Conference on*. 2003.

20. Lu, Z.G., et al. *Ultra-broadband quantum-dot semiconductor optical amplifier and its applications*. in *Optical Fiber Communication and the National Fiber Optic Engineers Conference, 2007. OFC/NFOEC 2007. Conference on*. 2007.

21. Assadihaghi, A., et al. *O-band semiconductor optical amplifier design for CWDM applications*. in *Microsystems and Nanoelectronics Research Conference, 2008. MNRC 2008. 1st*. 2008.

22. Kelly, A.E., et al., *High performance polarisation independent reflective semiconductor optical amplifiers in the S, C, and L bands.* Selected Areas in Communications, IEEE Journal on, 2010. **28**(6): p. 943-948.

23. Connelly, M.J., *Semiconductor Optical Amplifiers*2002, Boston: Kluwer Academic Publisher.

24. Suematsu, Y. and A.R. Adams, *Handbook of Semiconductor Lasers and Photonic*1994: Springer.

25. Sun, J., J. Qiu, and D. Huang, *Multiwavelength erbium-doped fiber lasers exploiting polarization hole burning.* Optics Communications, 2000. **182**(1–3): p. 193-197.

26. Yeh, C.H., et al., *Multiwavelength erbium-doped fiber ring laser employing Fabry–Perot etalon inside cavity operating in room temperature.* Optical Fiber Technology, 2009. **15**(4): p. 344-347.

27. Feng, X., et al., *Switchable multiwavelength erbium-doped fiber laser employing wavelength-dependent loss.* Optical Fiber Technology, 2011. **17**(2): p. 138-140.

28. Guan, W. and J.R. Marciante, *Dual-Frequency Operation in a Short-Cavity Ytterbium-Doped Fiber Laser.* Photonics Technology Letters, IEEE, 2007. **19**(5): p. 261-263.

29. Pan, L., I. Utkin, and R. Fedosejevs, *Two-wavelength ytterbium-doped fiber laser with sustained relaxation oscillation.* Appl. Opt., 2009. **48**(29): p. 5484-5489.

30. Zongjiu, Z. and Y. Liu. *Multiwavelength oscillations of Ytterbium-doped fiber laser*. in *Signals Systems and Electronics (ISSSE), 2010 International Symposium*. 2010.

31. Bellemare, A., *Continuous-wave silica-based erbium-doped fibre lasers.* Progress in Quantum Electronics, 2003. **27**(4): p. 211-266.

32. Siegman, A.E., *Lasers*1986: University Science Books.

33. Saleh, B.E.A. and M.C. Teich, *Fundamentals of photonics,* 2007: Wiley-Interscience.

34. Saleh, B.E.A., *Photonic,* 2007, Hoboken, New Jersey: John Wiley & Sons.

35. Tanaka, S., et al. *Multi-Wavelength Tunable Fiber Laser using SOA: Application to Fiber Bragg Grating Vibration Sensor Array*. in *Sensors, 2007 IEEE*. 2007.

36. Tang, M., et al., *Tunable terahertz-wave generation from DAST crystal pumped by a monolithic dual-wavelength fiber laser.* Opt. Express, 2011. **19**(2): p. 779-786.

37. Piprek, J., et al., *Saturation analysis of a monolithic wavelength converter.* 2004: p. 102-109.

38. Zilkie, A.J., et al., *Carrier Dynamics of Quantum-Dot, Quantum-Dash, and Quantum-Well Semiconductor Optical Amplifiers Operating at 1.55 μm.* Quantum Electronics, IEEE Journal of, 2007. **43**(11): p. 982-991.

39. Vlachos, K., et al., *Ultrafast semiconductor-based fiber laser sources.* Selected Topics in Quantum Electronics, IEEE Journal of, 2004. **10**(1): p. 147-154.

40. Kim, B., J. Han, and Y. Chung, *Tunable and switchable multi-wavelength fiber laser based on semiconductor optical amplifier and twin-core photonic crystal fiber.* 2012: p. 82570F-82570F.

41. Adachi, S., et al., *InGaAsP/InP heterostructure lasers with chemically etched mirrors.* Journal of Applied Physics, 1981. **52**(9): p. 5843-5845.

42. Adachi, S., *Material parameters of InGaAsP and related binaries.* Journal of Applied Physics, 1982. **53**(12): p. 8775-8792.

43. Adachi, S., *Optical dispersion relations for GaP, GaAs, GaSb, InP, InAs, InSb, AlGaAs, and InGaAsP.* Journal of Applied Physics, 1989. **66**(12): p. 6030-6040.

44. Broberg, B. and S. Lindgren, *Refractive index of InGaAsP layers and InP in the transparent wavelength region.* Journal of Applied Physics, 1984. **55**(9): p. 3376-3381.

45. Henry, C., et al., *Determination of the refractive index of InGaAsP epitaxial layers by mode line luminescence spectroscopy.* Quantum Electronics, IEEE Journal of, 1985. **21**(12): p. 1887-1892.

46. Fiedler, F. and A. Schlachetzki, *Optical parameters of InP-based waveguides.* Solid-State Electronics, 1987. **30**(1): p. 73-83.

47. Mynbaev, D.K. and L.L. Scheiner, *Fiber-Optic Communications Technology*, 2001: Prentice Hall.

CHAPTER 3

TUNABLE SINGLE WAVELENGTH FIBER LASERS

3.1 Introduction

Tunable Fiber Lasers have become one of the key technology that have been developed significantly recently to its potential applications in various fields such as sensing, communications systems, medicine, as well as industrial applications such as for cutting and welding and defense. The ability to tune the laser in order to get lasing at certain particular wavelength helps to maximize their use, by providing a compact and yet with a simple cavity design. This consequently improves the technology that we have today especially in dense wavelength division multiplexing system (DWDM) [1-5] and optical fiber sensors [6-14] by providing a compact laser source with a variety of wavelength options.

The wavelength selective elements, or components employed in a particular experimental set up to select the lasing wavelength, employed in this work include fiber Bragg grating (FBG), tunable bandpass filter (TBF) and arrayed waveguide grating (AWG). The principle functional of all of these three wavelength selective elements will also be discussed in this chapter. Two gain media are used in this chapter, which are EDF and SOA. We shall begin our discussion on tunable fiber lasers with erbium doped fiber lasers before continuing with semiconductor optical amplifier lasers in the next subsection.

3.2 Erbium Doped Fiber Lasers (EDFLs)

As the name suggests, erbium doped fiber lasers are fiber lasers which employ an erbium doped fiber as the gain medium. As erbium exhibit homogenous line broadening, this investigation will be focused on the limits of generation and tunabiliy of EDFLs.

Figure 3.1 shows a simple experimental setup to analyze the cavity lasing spectra of a 5 m erbium doped fiber (EDF). A laser diode with a pumping wavelength of 980 nm is injected to the 5 m EDF with a maximum pump power of 100 mW. The energy absorbs by the erbium ion from the 980 nm laser diode then produces an amplified spontaneous emission (ASE) and is then connected to a 10 dB coupler. 90% power from the cavity portion is looped back to the input of the 5 m EDF through a 980/1550 nm wavelength division multiplexer (WDM). The circulation of the ASE inside the cavity then creates lasing. An isolator is inserted between the WDM and the coupler to ensure a unidirectional propagation of light inside the cavity. The lasing profile is then extracted by the 10 dB coupler through the 10% port to be analyzed by an optical spectrum analyzer (OSA).

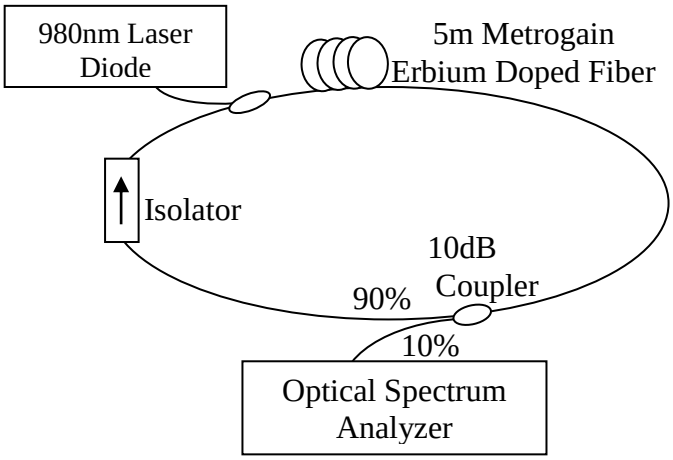

Figure 3.1: Experimental setup of free lasing by using 5 m Metrogain EDF.

Figure 3.2 shows the 5 m EDF lasing spectra for different pump power from 0.027 mW until 98 mW. As expected, increasing the pump power causes an increase in the output power. However lasing is only initiated at 17 mW, with increasing peak power at higher pump powers, reaching its maximum at the maximum pump power of 98 mW. At the maximum pump power, it can be seen that the lasing occurs within a small region with about 1 nm of 10 dB bandwidth and 2 nm of 30 dB bandwidth, centralized at 1563 nm. The output spectrum is considerably narrow, due to homogeneous gain broadening behavior of the EDF. The maximum obtained output peak power is at -12.6 dBm, while the average output power taken from the optical power meter (OPM) is about 3 dBm.

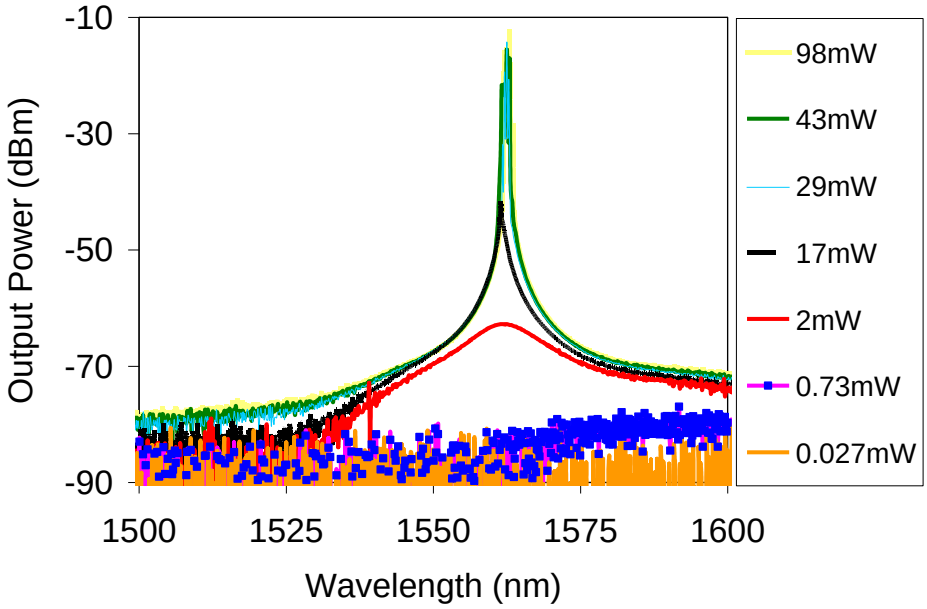

Figure 3.2: The spectra of lasing output power by varying the pump power.

The effect of inserting an isolator is then investigated. Figure 3.3 shows the output of lasing profile taken in two conditions that is when the fiber laser operates with and without the isolator. It can be seen that the peak power is higher by incorporating the isolator inside the setup, with a difference of roughly 10 dB, which is quite significant. It can be concluded that forcing unidirectional propagation inside the laser cavity improves the output power within this C-band spectrum -22.4 dBm to -12.6 dBm and reduces the propagation of back reflected emission. The improvement of the output power is due to the fact that unidirectional propagation leads to the higher stimulated emission in one particular direction, thus improving the production of photons in creating a laser.

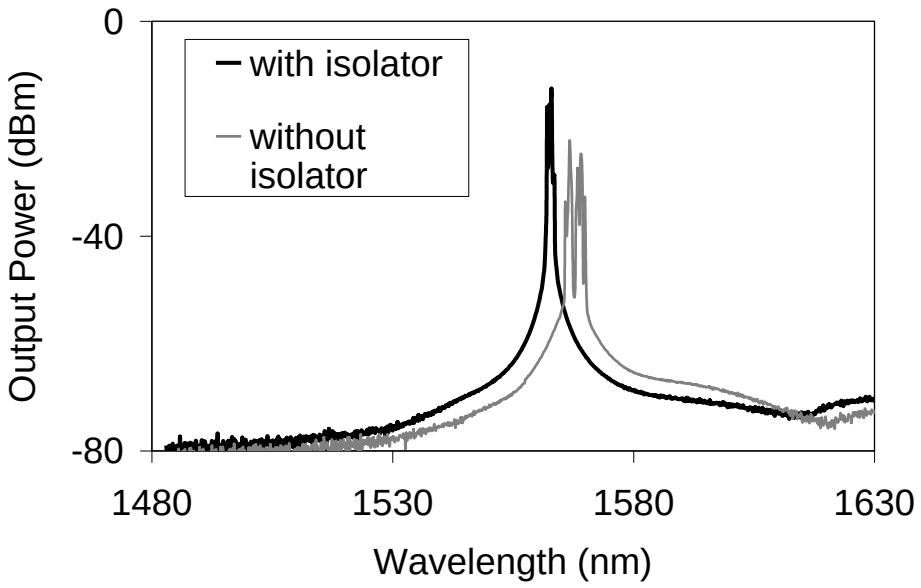

Figure 3.3: Comparison with and without isolator inside the cavity layout by using the same amount of pump power.

3.2.1 Tunable Fiber Laser by Employing Different Wavelength Selective Elements

As can be seen from Figure 3.3, a fiber laser with no wavelength selective element can produce multiple output lasing. This can be attributed to the random selection of the lasing wavelength of any wavelength with an output power higher than the lasing threshold for a configuration without a selective element, and therefore, the lasing wavelength the fiber laser is not fixed at a certain value but shifts to any wavelength with the lowest threshold power. There are two factors which influences the generation of laser at a certain wavelength, namely, the EDF's gain profile and the lower lasing threshold of longer wavelengths. If the gain profile of the EDF is consistent throughout the whole spectrum, the threshold power will be the lowest at the longest wavelength. This can be attributed to the fact that longer wavelengths need a lower accumulation of energy as compared to the shorter wavelength. However, as the homogeneous gain broadening profile in EDF has a highest gain at 1539 nm wavelength, the possibility exists for the shorter wavelength to have a lower lasing. Therefore, a laser cavity without any wavelength selective element will generate laser at any wavelength, depending on the length of the EDF, the pump power and the portion of the coupler as a feedback used in the setup.

In order to generate fiber lasers with an ability to control the wavelength operation, a wavelength selective element has to be inserted inside the cavity design. This will also allow the bandwidth and the wavelength of the fiber laser to be chosen at any desired value. The bandwidth of the fiber laser is dependent on the type of wavelength selective element used in the experiment. In this section, three types of wavelength selective elements are introduced, namely, the tunable bandpass filter, fiber Bragg grating and arrayed waveguide

grating. The working principle of each wavelength selective element is explained as follows.

3.2.1.1 Tunable Bandpass Filter (TBF)

One of the wavelength selective elements used in this thesis is a TBF. The following discussion is set forth to explain the working principle of a TBF.

3.2.1.1.1 Principles of TBF

One of the wavelength selective elements used in this work is a tunable bandpass filter (TBF). The TBF consists of an angled-tuned etalon filter, which operates in the S- and C-band regions. The 3 dB bandwidth of the TBF is about 0.8 nm with 0.05 nm of tuning resolution. The maximum insertion loss of the TBF is about 3 dB with typical insertion loss of 1.5 dB. The back reflection is about -50 dB which make it a reliable wavelength selector. A schematic diagram of the fiber-coupled TBF is shown in Figure 3.4(a). The beam from a single mode fiber (SMF) passes through a collimator, thereby collimating the beam, before travelling through a free space region and encountering a Fabry-Perot etalon, which then acts as the filter. The propagating beam is then recoupled into the second collimator before entering a second SMF. The Fabry-Perot etalon filter is mounted on a rotational stage. This setup allows the selection of particular wavelength by varying the incident angle of the propagating beam by tuning the high precision micrometer, and therefore rotating the Fabry-Perot etalon, to select any desired wavelength within the operation region of the TBF.

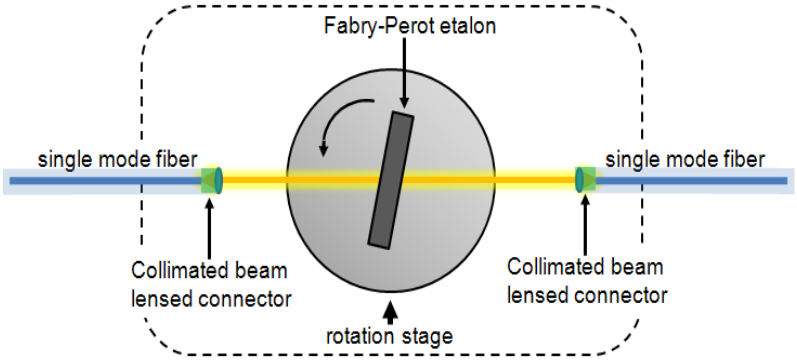

(a)

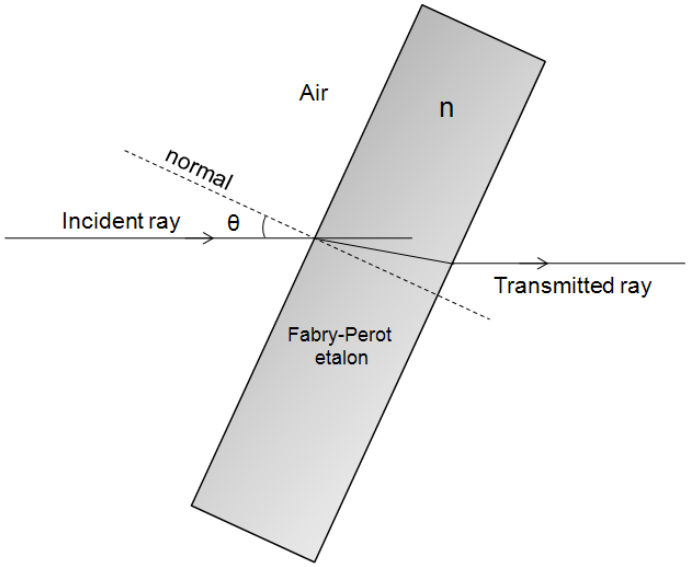

(b)

Figure 3.4: (a) An illustrative layout of the fiber coupled angle-tuned Fabry-Perot etalon and (b) propagation of light through the Fabry-Perot etalon.

Figure 3.4(b) illustrates schematically the propagating light into and out of the Fabry-Perot etalon filter. The TBF uses the Fabry-Perot interferometer theory as explained by Frankel et al. [15]. The wavelength selection can be done by changing the incident angle of the beam. This can be obtained by the following expression [15]:

$$\lambda = \left(\frac{2nL}{m}\right)(\cos\theta) \tag{3.1}$$

where L is the thickness of the etalon filter, m is an integer; n is the refractive index of the etalon, λ is the wavelength of interest and θ is the angle between the incident beam and the normal axis.

3.2.1.1.2 Tunable Fiber Laser by Using TBF

In order to investigate the effect of the TBF, it is then inserted into the experimental configuration shown in Figure 3.5. Similar works about use of TBF have been reported in [16, 17]. By using a tunable bandpass filter (TBF), a single wavelength fiber laser can be produced in any desired wavelength between 1480 nm and 1560 nm, provided that there is ASE within that region. As bandwidth of EDF is only in C-band region, the output fiber laser is only taken within this region. The result of the tunable single wavelength fiber laser is shown in Figure 3.6.

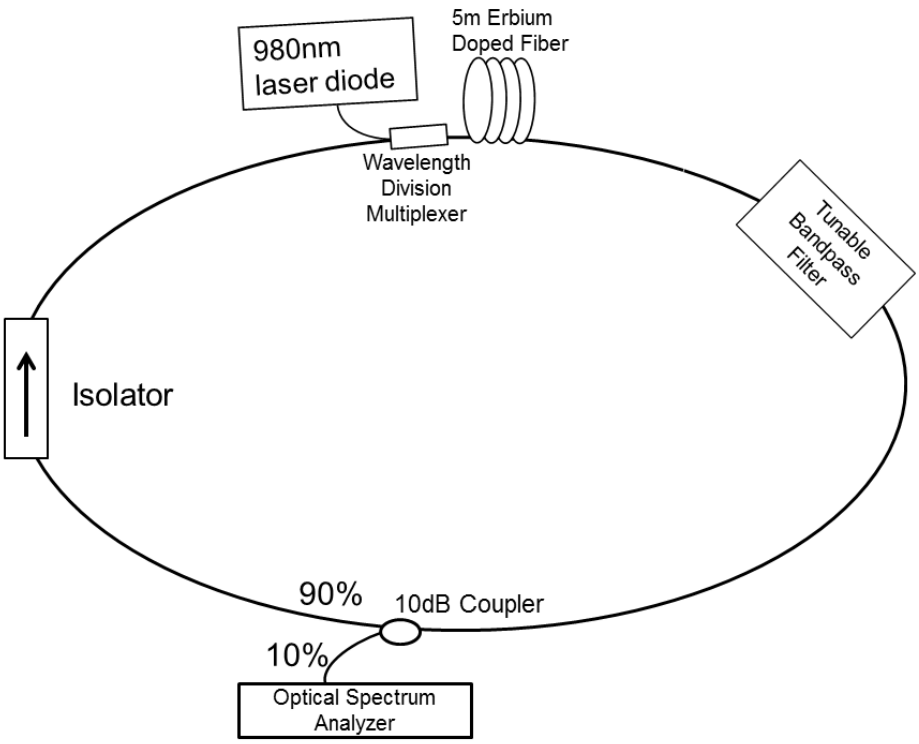

Figure 3.5: Experimental setup for tunable single wavelength fiber laser by using a tunable bandpass filter (TBF).

The graph depicted in Figure 3.6 shows that the tuning range is only in the C-band region that starts from 1522 nm until 1560 nm. It can be seen that the output power of each wavelength is roughly equal, with the difference between maximum to minimum output power being only about 5 dB and an output average power of -8 dBm.

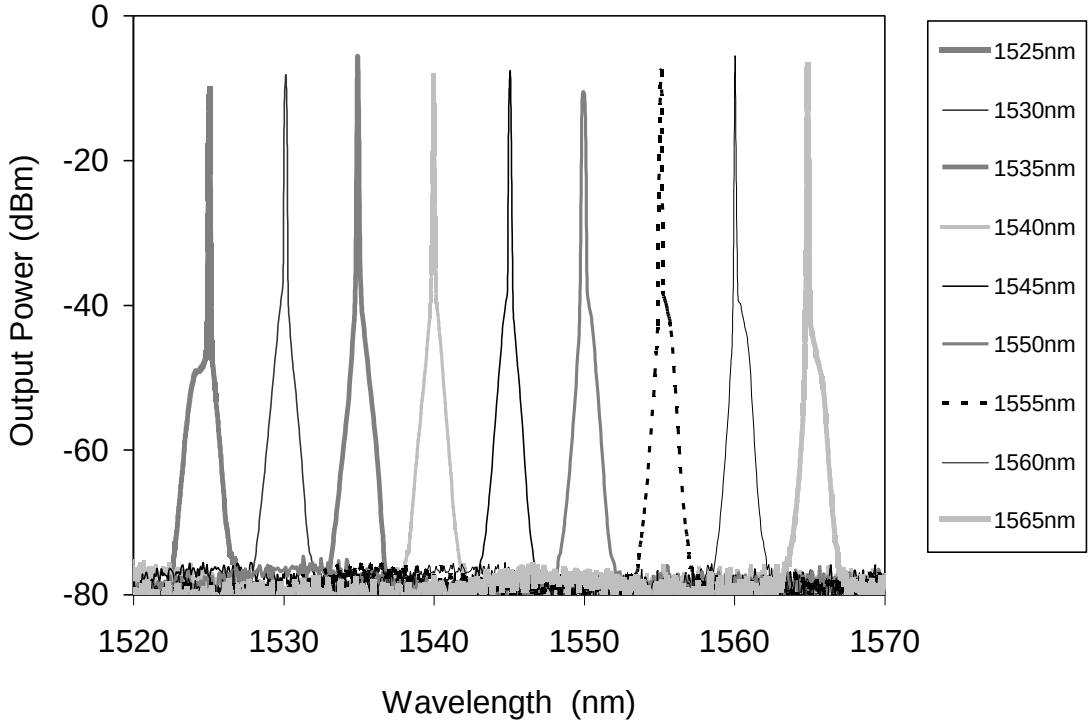

Figure 3.6: Single wavelength tunable operation by using TBF in the C-band region.

Further analysis was done by measuring the output power and the SMSR as depicted in Figure 3.7. The average output power is found to be -7.95 dBm with a maximum value of -5.91 dBm at 1560.01 nm and the minimum value of -10.60 dBm at 1521.1 nm. The maximum difference between the highest and the lowest output power values is 4.69 dB. This indicates the consistency of the tunable fiber laser due to the small change of output power due to change in wavelength. The SMSR value is also quite high with average value of 67.82 dB. The maximum difference between the highest and the lowest SMSR is 4.66 dB.

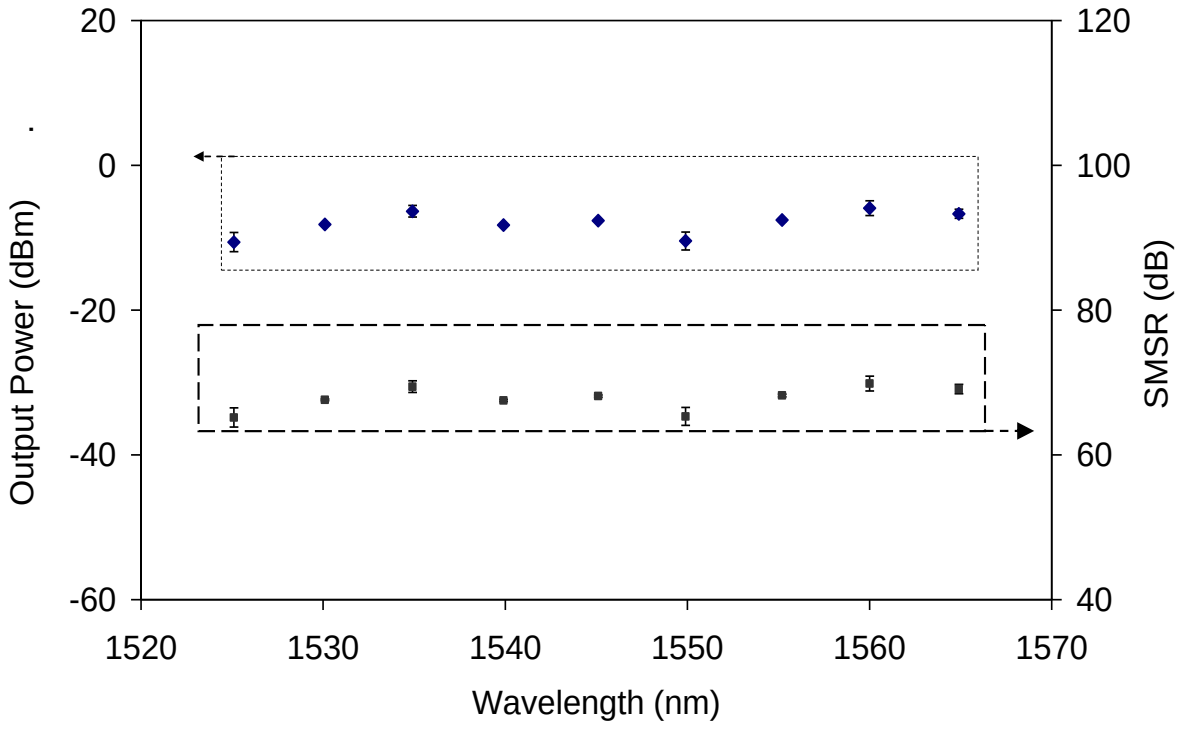

Figure 3.7: The output power and SMSR value of fiber laser by using a tunable bandpass filter (TBF) as the wavelength selective element.

3.2.1.2 Fiber Bragg Grating (FBG)

Another selective method investigated in this work is the fiber Bragg grating, or FBG. An FBG is a fiber based device which utilizes a variation in the refractive index in order to obtain a reflection at a particular wavelength. The operating principle of the FBG will be elaborated in the following subsection.

3.2.1.2.1 Principle of FBG

Fiber Bragg grating (FBG) is another wavelength selector used in this work in order to design fiber lasers in the next section. A fiber Bragg grating is essentially a series of periodic variations of refractive index with length in a fiber, which allows it to act as a filter [18, 19]. The basic equation that yields the characteristic Bragg wavelength, λ_B [20]

$$\lambda_B = 2n_{eff}\,\Lambda \tag{3.2}$$

Here λ_B represent the center wavelength that also called as Bragg wavelength, n_{eff} is the effective refractive index of the fiber core and Λ is the grating period. The FBG works as a filter, with λ_B being the wavelength reflected by the FBG while all other wavelengths are transmitted. It is clear that the center wavelength selected by the FBG is directly dependant on the grating period, Λ, of the FBG. The FBG is a narrow bandwidth low loss passive device which can easily be coupled to any configuration.

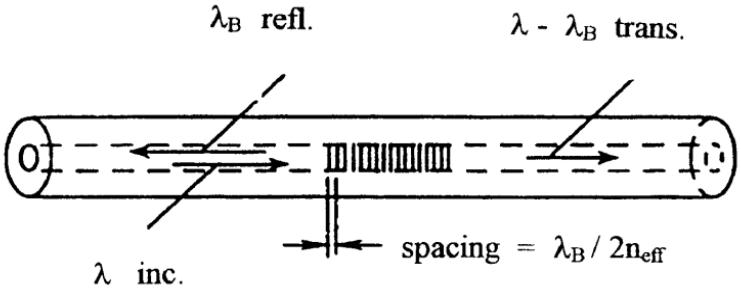

Figure 3.8: An illustration of grating inside an FBG [20].

This makes it one of the most preferable wavelength selectors for fiber-based applications. The 3 dB bandwidth of a FBG is typically 1.0 nm. The reflectivity of the FBG is typically between 80% to 99%, which is depending on the properties provided by the manufacturer. The illustration of the FBG is shown in Figure 3.8.

However, although FBGs are able to serve as a selective element, they cannot be tuned if left unaltered and independent. Tunability requires the addition of additional components or the physical change to the FBG in order to allow the reflected wavelength to be altered. In this work, the former is achieved via the introduction of Sagnac loop mirrors and by employing multiple FBGs, while the latter is accomplished by applying a compressive or tensile force to the grating, which results in the change of the reflected wavelength of the FBG.

3.2.1.2.2 Tunable Fiber Laser by using Sagnac Loop Mirror and FBGs

A Sagnac loop mirror is a device in which two counter propagating beams circulate in one optical path which are then recombined [21, 22]. This then results in the interference of the two beams, which can then be tuned, depending on the particular configuration employed.

In this work, the primary mechanism by which the interference of these two beams are controlled is the state of polarization of both beams. This is accomplished by utilizing a polarization controller in conjuntion with a sufficiently long polarization maintaining fiber (PMF), which allows the control over the state of polarization of the two counter-propagating beams, which is explained in more detail in this subsection. The addition of an isolator, which only allows for unidirectional operation, together with the 3 dB fiber

coupler means that there will be a phase shift of $kz = \frac{\pi}{2}$ and therefore ensures interference in the configuration[23, 24]. The polarization controller then allows for a degree of tunability in the configuration.

Similar work have been undertaken by other researchers [25-28]. In this work, the fiber laser is improved by having six different wavelengths. Several technique have also achieved similar results by cascading multiple FBGs [29-31]. Figure 3.9 shows the experimental setup used by me as the wavelength tuning mechanism. In this configuration a 5 m of erbium doped fiber is used as the active gain medium. EDF is pumped in a forward configuration by using a 980 nm laser diode combined by using a WDM with 180 mW of output power. There are two polarization controllers (PCs) employed in the configuration. Both PC1 and PC2 are used to adjust the state of the polarization (SOP) of the light propagating in the lasing cavity giving a variety of output spectrum patterns [32, 33]. Initially, the ASE produced by the EDF as shown in chapter 2 (which explain the characterization of this gain medium) propagates in all directions. However, the isolator used inside the ring cavity suppressed propagation in the counter clockwise direction, forcing unidirectional propagation, which is in a co-propagation direction. The ASE then passes through the second 980/1550 nm WDM and is then sliced by the 2 m PMF in such a way that spectral hole burning is allowed for certain discrete wavelengths, depending on the selected state of polarization by PC1 and PC2.

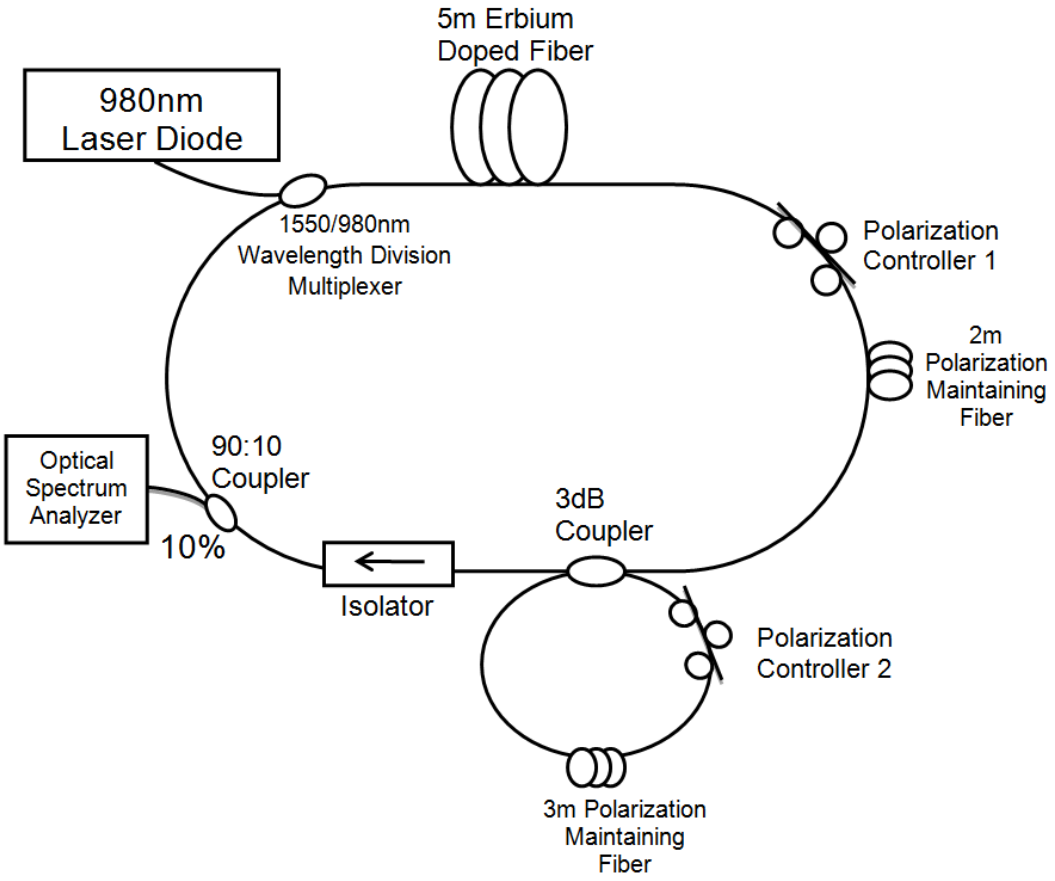

Figure 3.9: Experimental setup used for wavelength tuning of the lasing output through use of a Sagnac loop mirror.

The transmission spectrum (T) of the Sagnac loop mirror can be expressed as [34]

$$T = \left[\sin\left(\frac{\beta L}{\lambda}\right)\cos(\theta_1 + \theta_2)\right]^2 \qquad 3.3$$

where β is the birefringence, defined as $\beta = n_y - n_x$, with n_y and n_x being the refractive indices along the fast and slow axes, respectively, L represents the length, λ represents the wavelength in operation, θ_1 represents the angle between the light at both ends of the fiber and θ_2 is the angle between the fast axis of both end of the fiber.

The wavelength spacing after traversal of the Sagnac loop interferometer can be predicted as the formula given by [34]

$$\Delta\lambda = \frac{\lambda^2}{\beta L} \qquad 3.4$$

The selection of wavelength is made experimentally possible by the adjustment of the polarization controllers, PC1 and PC2 in this case. The results for the ASE selection by using this setup are shown in Figure 3.10 and 3.11.

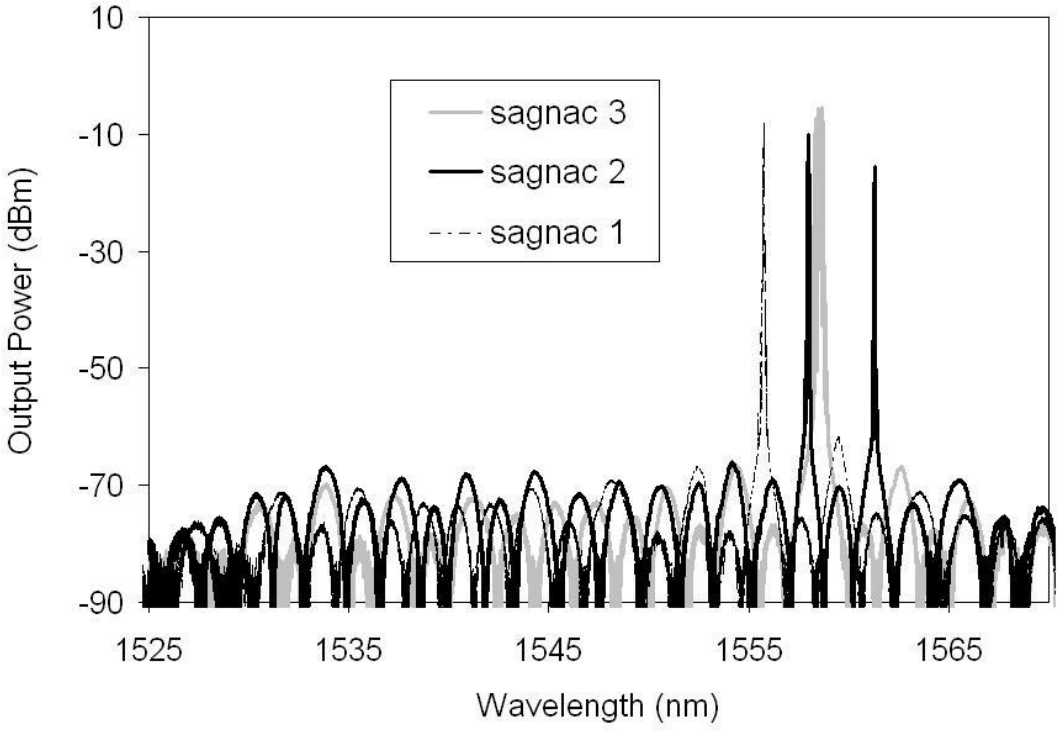

Figure 3.10: The output spectrum after the Sagnac loop interferometer.

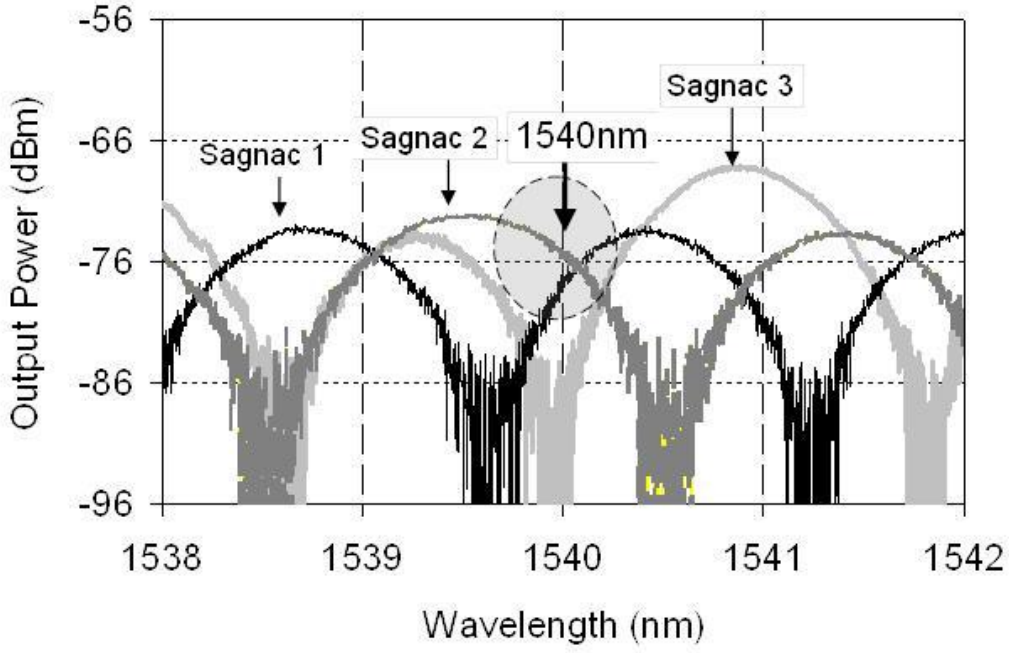

Figure 3.11: The close up of Figure 3.10.

Figure 3.10 and Figure 3.11 show that the slicing region changes by rotating PC1 and PC2. Through rotations of PC1 and PC2, the wavelength selection can be carefully adjusted to obtain the desired wavelength that is reflected by the FBGs.

The Sagnac loop mirror technique is then employed in conjunction with six FBGs, each having a distinctly different Bragg wavelengths (1534 nm, 1540 nm, 1548 nm, 1554 nm, 1555 nm and 1556 nm) that have been spliced all together, as shown in Figure 3.12. In this setup, a circulator is employed between the 2m PMF and the Sagnac loop mirror to allow for the addition of the six FBGs. The combination of these six FBGs with the Sagnac loop mirror allows for the selection of only one wavelength of the six, with the selection made by tuning PC1 and PC2. Figure 3.13 shows the resulting spectra for tuned single wavelength operation. The spacing of the Sagnac loop can be determined by the length of

PMF used while varying the tilt of the two PCs allows for the selection of the desired output wavelength.

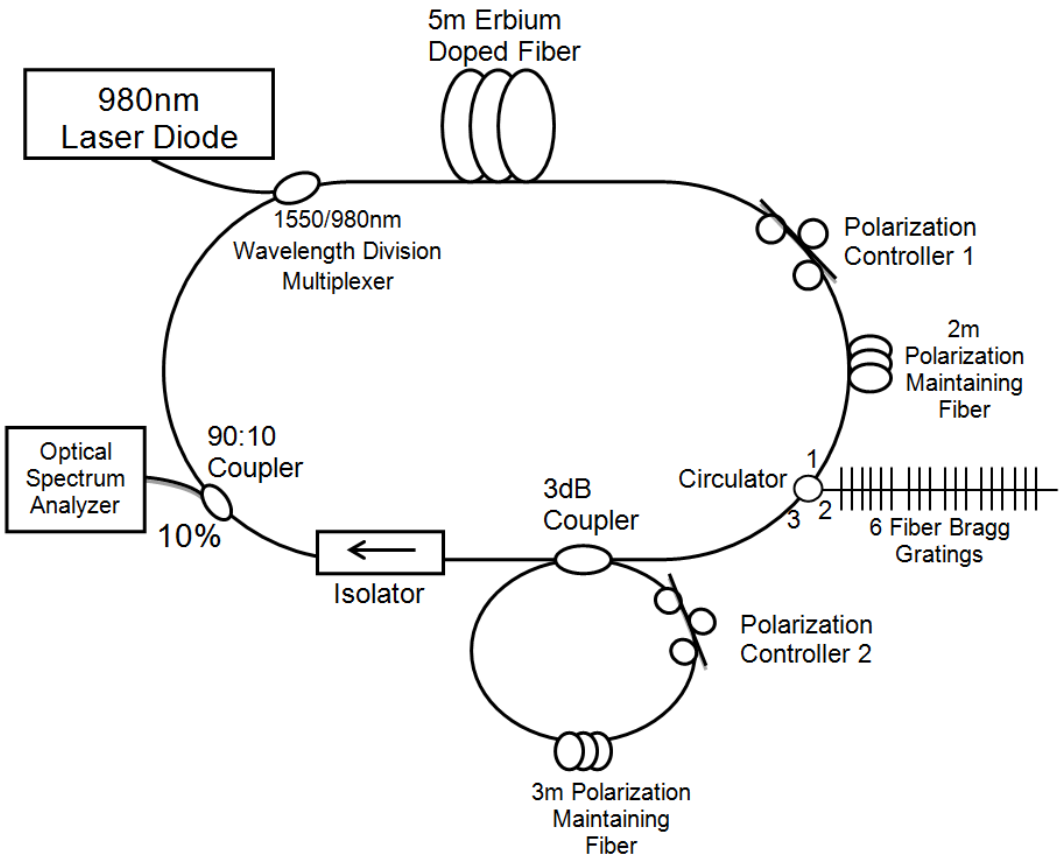

Figure 3.12**:** Experimental setup with six FBGs' different of Bragg wavelengths.

Figure 3.13 shows the final configuration after the six FBGs have been inserted in the setup. The peak power for each wavelength is quite similar with an average power of -10 dBm and a variation of 7 dB between the maximum and minimum values. The average SMSR for this output powers is 58 dB, which is quite high for a single wavelength operation. This setup, however, can only provide six tunable output wavelengths at one particular time, as compared to the previous configuration which allows the output to be tuned to cover the entire C-band region. Nevertheless, this configuration allows for the

precise selection of the six wavelengths due to the fixed value provide by the respective FBGs, with the added advantage of having a narrower bandwidth, and therefore can allow for attaining a better and more precise of fiber lasing wavelength.

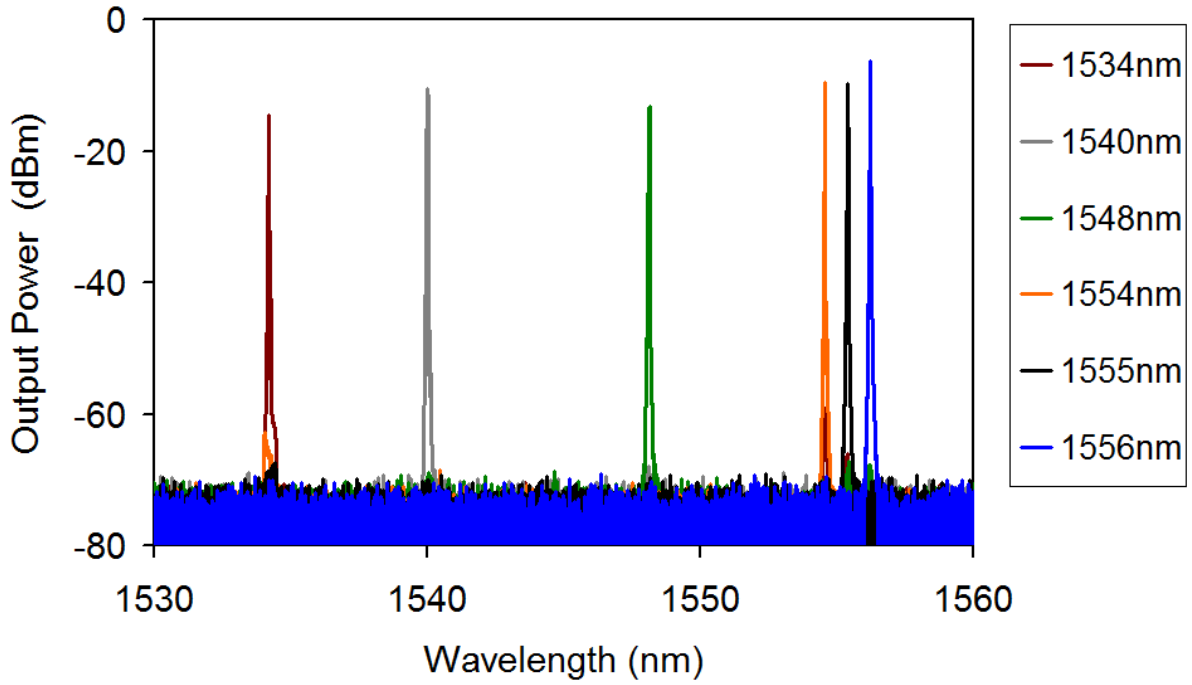

Figure 3.13: single wavelength tuning operation by using Sagnac loop mirror technique.

Figure 3.14 shows the output power and the SMSR for the six selectable single wavelength fiber lasers. The average output power is -10.82 dBm, with the maximum value being -6.39 dBm at 1556.22 nm and the minimum value -14.58 dBm at 1534.19 nm. Therefore, the calculated difference between the maxima and minima is 8.19 dB. The average value of the SMSR was found to be 55.38 dB with a maximum of 63.94 dB at 1556.22 nm and a minimum of 44.51 dB at 1534.19 nm. The difference between the SMSR maxima and minima is therefore 19.44 dB.

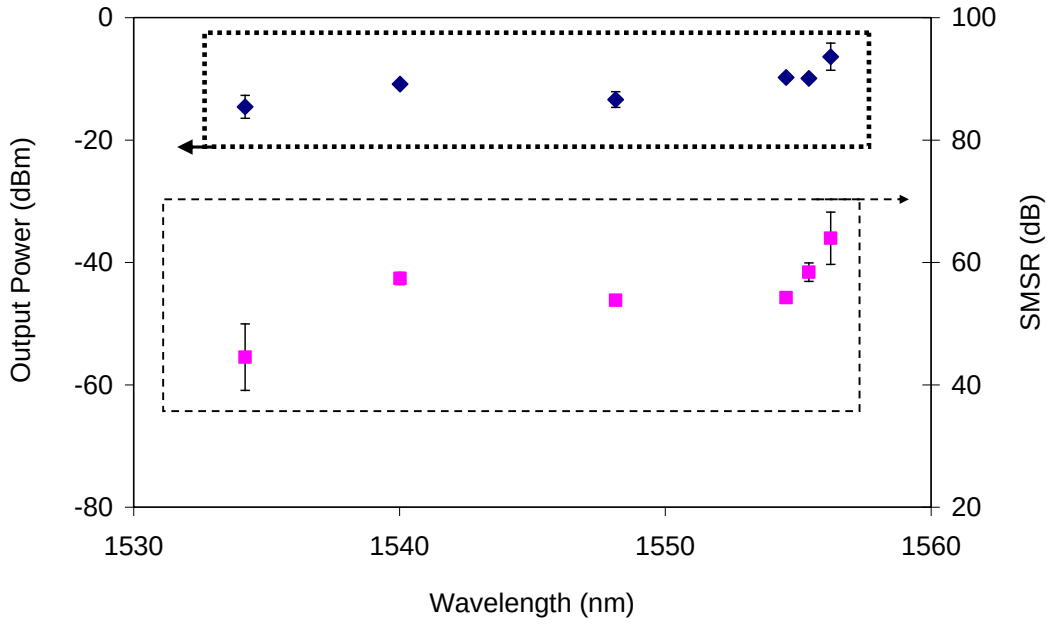

Figure 3.14: Output power and SMSR value for the tunable single wavelength fiber laser by using 6 different FBGs as the wavelength selective element.

3.2.1.3 Compression and Tensile Strain FBGs

FBGs, by virtue of being fibers, can also be bent and compressed. This change in tensile strain results in a change in the spatial period Λ of the FBG, thereby changing the reflected wavelength of the device (see equation 3.2), and thereby conferring tunability to the system.

3.2.1.3.1 Principle of FBG Tunability via Compression and Tensile Strain

As demonstrated previously, a fiber laser with multiple wavelengths can be created by cascading several FBGs with the wavelength selection made through use of a Sagnac loop filter incorporated in the cavity. Alternatively, one can also tune the central reflected

frequency of the FBG by inducing stresses on the fiber, either via compression or contraction. This will then induce a change on the axial strain ε_z across the grating with the shift in the reflected wavelength of the FBG given by [35, 36]

$$\Delta \lambda = (1 - \rho_e)\varepsilon_z \lambda_B \qquad 3.4$$

where ρ_e = 0.22 is the photo-elastic coefficient and λ_B is the Bragg Wavelength without any stress induction.

In order to control the tuning operation, the FBG has to be mounted on a hybrid material, which, in this case, is comprised of Perspex, as the material with a low Young's modulus, and a spring made of steel, as the material with a high Young's modulus materials. This design allows for the increase in the efficiency of the bending moment, as a single solid substrate has a higher bending moment [35]. Therefore, by utilizing materials with two different Young's modulus, we are able to increase the capability of tuning the length between the epicenter axes of the substrate to the FBG. The design is as illustrated in Figure 3.15.

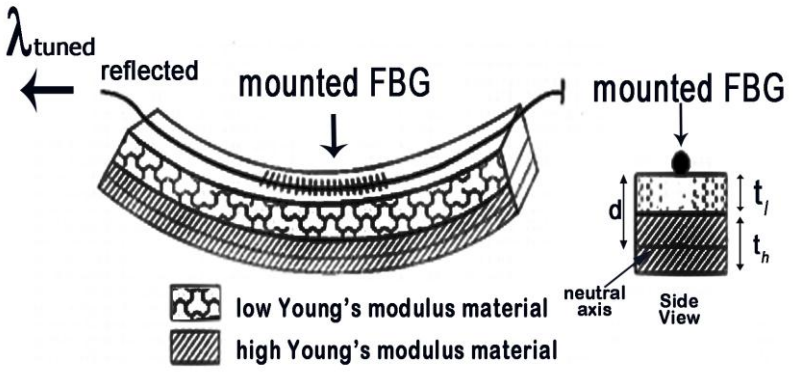

Figure 3.15: A FBG embedded on a Hybrid-material substrate as in ref [35].

The strain given to the FBGs can be predicted by the equation [35]

$$\varepsilon_z(R) = \pm\frac{d}{R} \tag{3.5}$$

where R is the hybrid material bending radius. The negative and positive signs represent the compression and traction mode respectively, while d is the length between the epicenter axes of the substrate to the FBG.

In this thesis, two FBGs of the same wavelength operating in normal conditions (without stress applied) are used. One FBG will experience a compressive strain, while the other will experience a tensile strain by putting the FBGs above and below the Perspex, respectively. This is as illustrated in Figure 3.16.

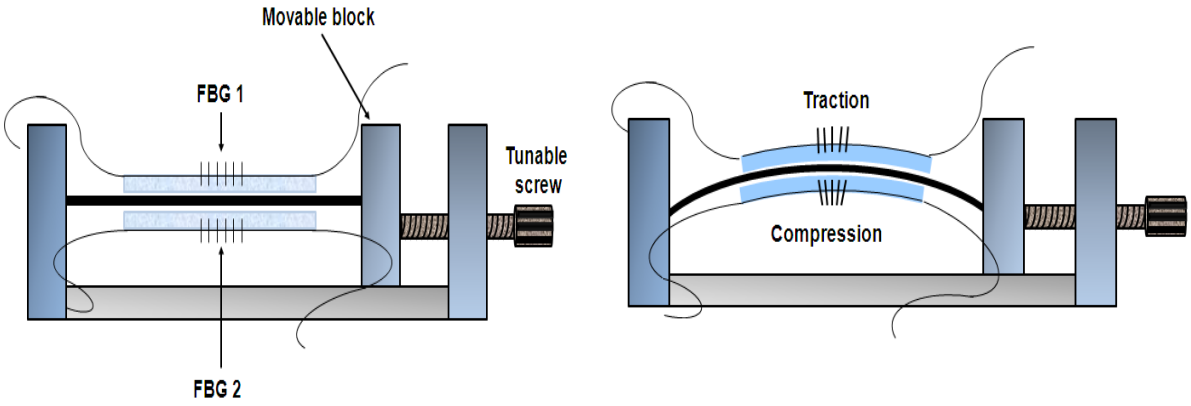

(a) (b)

Figure 3.16: Schematic layout of the tunable FBGs (a) in normal conditions, i.e. without giving stress and, (b) when stress is induced by rotating the screw.

The d-factor for the combination of two Perspex and a spring of steel can be approximated as [35]

$$d = t_l + \frac{E_h t_h^2 - E_l t_l^2}{2(E_h t_h + E_l t_l)} \quad 3.6$$

where E_l is the Young's modulus of the Perspex and E_h is the Young's modulus of the spring steel, t_h and t_l are the thickness of the spring of steel and the Perspex respectively, as depicted in Figure 3.14.The resulted wavelengths shift can be expressed as

$$\Delta\lambda = \pm(1-\rho_e)\frac{d}{R}\lambda_B \quad 3.7$$

where d is the factor given as equation (3.5). This factor, then, is responsible for changes in the value of $\Delta\lambda$ value, indicating an increment of the simultaneous shift in both shorter and longer wavelengths experienced by FBG2 and FBG 1, respectively.

3.2.1.3.2 Tunable Fiber Laser by Using Compression and Tensile Strain of FBGs

Employing this principle, an experimental setup was configured to produce a tunable single wavelength fiber laser, shown in Figure 3.17. The generation of the fiber laser starts with the propagation of the ASE from the 5m EDF when a 980 nm laser diode with a pump power of 98 mW is injected to the EDF through the 980/1550 nm WDM. The ASE emitted by the EDF then propagates through the isolator before entering the port 1 of a three port optical circulator.

From port 1, the ASE then enters port 2, where only one wavelength reflected by the FBG 1 or FBG 2 will be reflected and subsequently being forced to enter port 3 before entering a 10 dB coupler. 90% of the signal is then reinserted to the input of the WDM to complete the circle for the generation of fiber laser, while the remaining 10% is extracted for analysis by using the OSA. The selection of the FBG is done by switching the OCS to select either FBG 1 or FBG 2. The wavelength tuning is done by the C-band Tunable FBGs or also can be called as the Compression and Tensile Strain FBGs. As has been discussed previously, the wavelength tuning is done by turning the rotating screw in Figure3.16. As a result, the wavelength of FBG 1 and FBG 2 will be tuned to a shorter and longer wavelength, respectively. The spectra of tunable outputs recorded by the OSA, shown in Figure 3.17.

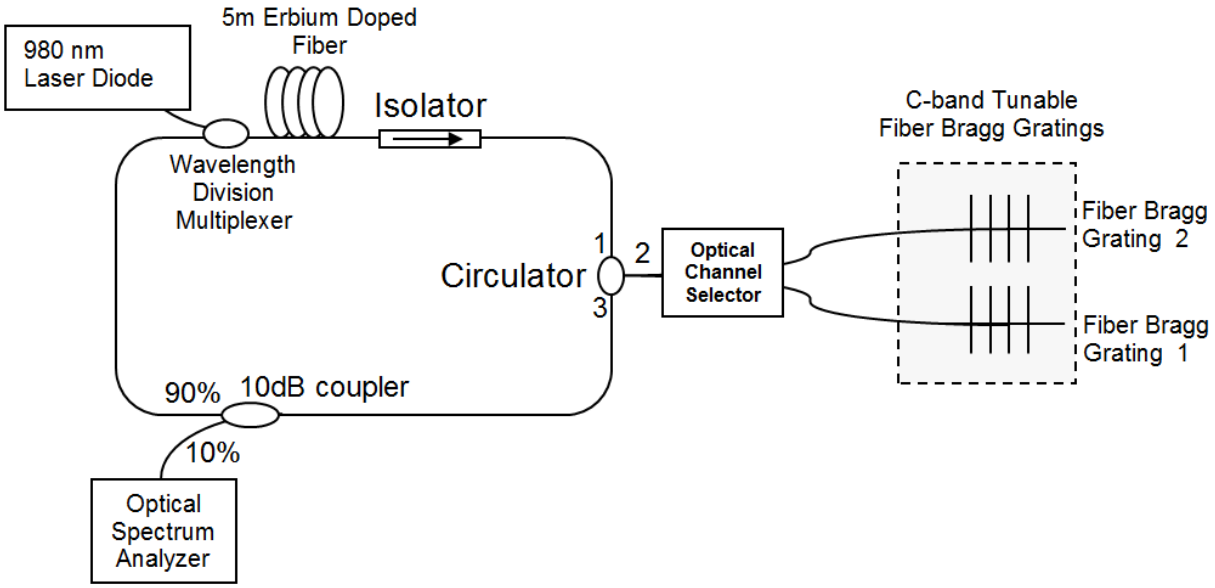

Figure 3.17: Experimental layout of single wavelength fiber laser by using compression and tensile strain FBGs.

The spectrum of the configuration employed in for this setup is depicted in Figure 3.18. The output power is seen to be quite flat in terms of its output power level. The wavelengths between 1546 nm and 1551 nm are attributed to FBG 1 while wavelengths from 1551.1 nm to 1556 nm originate from FBG 2. This design allows for the easy tuning of wavelengths, which only requires the selection of a particular channel and the change of the tensile stress of the two FBGs. The wavelength selection can also be made at any point within the operating range of the design.

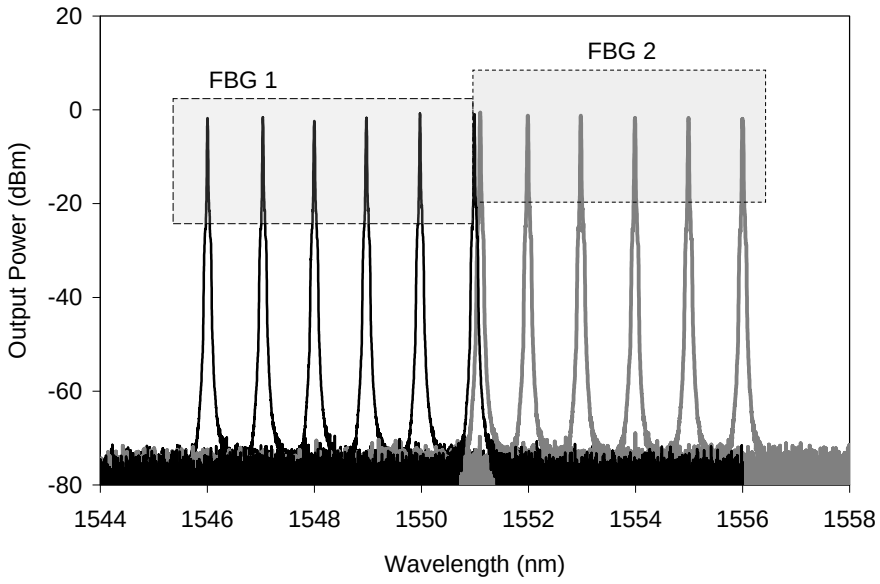

Figure 3.18: The spectrum of single tunable wavelength fiber laser by employing two tunable FBGs.

The data that is taken is further analyzed in terms of its output power and SMSR as in Figure 3.19. The average output power for the configuration is -1.77 dBm, which is quite high compared to the other designs that have been proposed in the thesis. The maximum output power is recorded at 1551.10 nm with an output power value of -0.93 dBm while the

minimum output power is found at 1548.004 nm with a value -3.108 dBm. Therefore, the difference between the maxima and minima is calculated at 2.18 dB. The average value for SMSR is 71.68 dB, indicating that this design performs very well. The maximum SMSR comes from 1511.02 nm with a value of 72.57 dB, while the minimum SMSR is obtained at a wavelength of 1548.00 nm with a value of 70.34 dB. Therefore, the difference between the maximum and minimum SMSR value is calculated to be 2.18 dB.

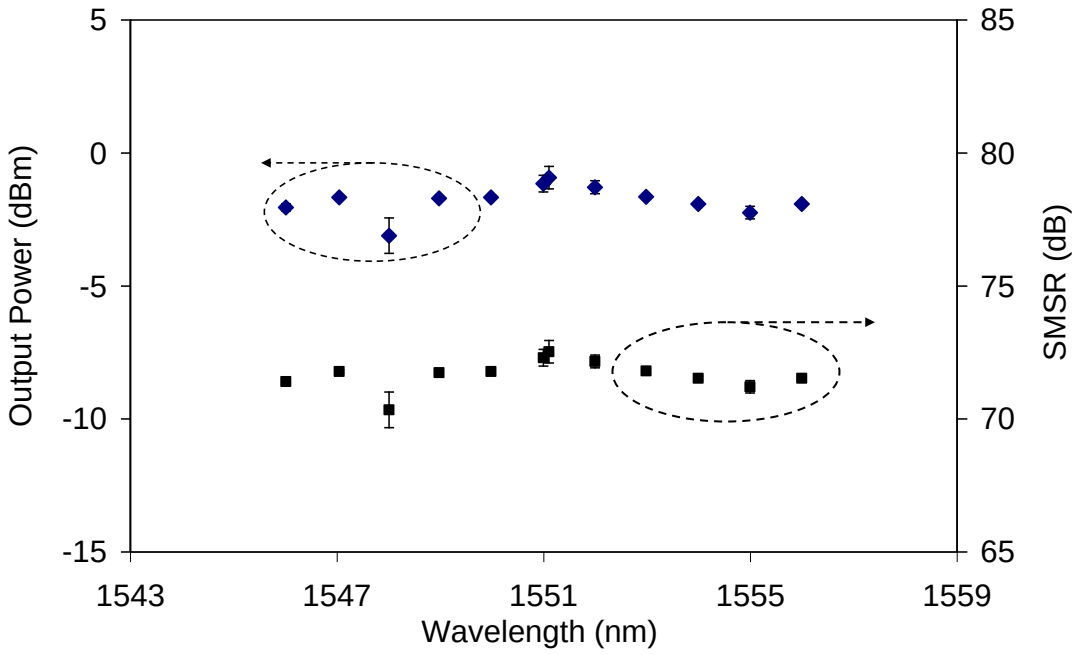

Figure 3.19: The output power and SMSR for a single wavelength fiber laser by using tunable FBGs.

Further works is also being done by our group in the S-band region to expand the range of tunability by using the technique proposed in [37].

3.2.1.4 Arrayed Waveguide Grating (AWG)

3.2.1.4.1 Principle of an AWG

It is also possible to employ an arrayed waveguide grating (AWG), a silica-based waveguide, as a wavelength selective element. As illustrated in Figure 3.20(a), the AWG is used to split the incident beam into different multiple, typically 16 and 24 channels. The insertion loss inside the AWG is about 3 dB. This process of this 'splitting' or 'slicing' of wavelengths begins first with the insertion of a beam into the input of the AWG, that passes through the first slab waveguide, called the transmission waveguide. The beam then passes through the 'object plane' as shown in Figure 3.20(a), and diffracts into multiple wavelengths, similar to a way a prism diffracts incoming visible light. The beam is then coupled to the receiver waveguide via the 'image plane', whose task is to refocus the incoming beams, slightly offsetting each in order to allow each beam to be coupled to a different fiber. Therefore, the arrayed waveguide number of channels is dependent on how many waveguides are fabricated with a constant increase in magnitude of difference in length. The process of constructive interference is then happens where the focal point is dependent of the chosen wavelength, λ_0.

Figure 3.20(b) shows a graphical representation of the process in more detail. The input waveguide separation is denoted as D_i, the arrayed waveguide separation d_i and the curvature radius f_i with $i = 0$ for the first output waveguide and $i = 1$ for the second. Gaussian distribution is used to approximate the amplitude of output from each arrayed waveguide, as the incoming light is assumed to originate from a SMF carrying laser.

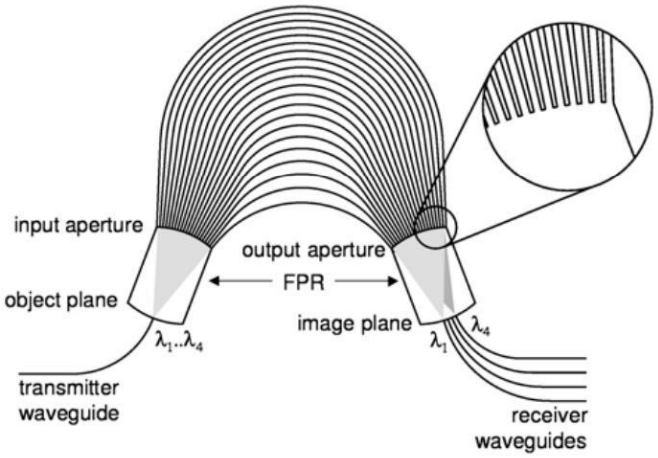

(a)

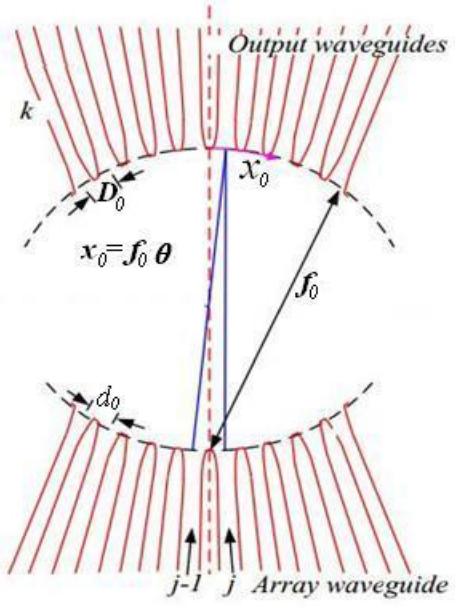

(b)

Figure 3.20: (a) Schematic diagram of an AWG (b) slab waveguide.

The light from the input array travels through the AWG and is split into a number of different 'beams', with the phase retardation between the j^{th} and $(j\pm1)^{th}$ waveguide being a multiple of 2π. When this condition is fulfilled, a constructive interference at x_0 will be

produced, with the next constructive interference occuring at a displacement of D_0 from x_0, as shown in Figure 3.20(b). This portion is taken from Hibino [38], and is put into this thesis for easy reference and completeness.

This interference condition is summarised in equation 3.8 [38],

$$\beta_s(\lambda_o)\frac{d_1 x_1}{f_1} - \beta_s(\lambda_o)\frac{dx}{f} + \beta_c(\lambda_o)\Delta L = 2m\pi \tag{3.8}$$

where $\beta_c = n_c k$ and β_s are the propagation constants in the arrayed waveguide region and the slab region, respectively, $\lambda_o$is the center wavelength, and m is an integer. When $\beta_c(\lambda_o)\Delta L = 2m\pi$, or equivalently

$$\lambda_o = \frac{n_c \Delta L}{m} \tag{3.9}$$

the location of the input light x_1 for the first slab and output location for the second slab x_0 should have the same value, and can be represented as in equation 3.3 below,

$$\frac{d_1 x_1}{f_1} = \frac{d_0 x_0}{f_0} \tag{3.10}$$

The wavelength spacing, $\Delta\lambda$, is then given by,

$$\Delta\lambda = \frac{n_c\, d_0 D_0\, \lambda_o}{N_c\, f_0 \Delta L} \tag{3.11}$$

where N_c is the group index, n_c is the core refractive index inside the arrayed waveguide. From equation 3.11, it is clear that the bigger the length difference, ΔL between each neighboring waveguide, the smaller wavelength spacing can be obtained from the AWG.

3.2.1.4.2 Tunable Fiber Laser by Using an AWG

The AWG can then be employed to produce a tunable fiber laser, as depicted in Figure 3.21. The wavelength selection is made by using the 1 x16 channels of AWG, which slices the ASE into 16 ‘components’, with an inter-channel spacing value of 0.8 nm. Lasing is commenced with the generation of the ASE from the 5 m erbium doped fiber active medium pumped by the 980 nm Laser diode with a maximum power of 98 mW. The ASE then travels from port 1 to port 2 of a circulator, which is connected to optical channels selector (OCS) and subsequently to the AWG and then to a broadband FBG (BB-FBG). The tuning technique is realized by combining the AWG and the OCS with the former functioning as a wavelength ‘slicer’ in the range of 1530 nm to 1540 nm while the latter acts as a channel selector which picks out one of the 16 channel respectively. The selected wavelength is then reflected by the BB-FBG back to the AWG and OCS before travelling to port 3. The output of port 3 then enters the 3 dB coupler with one ‘leg’ acting as the output and connected to the OSA, while the other leg is connected to the input of the 1550 nm WDM, thereby completing the circuit. This setup, by virtue of the circulator, theoretically only allows for unidirectional circulation in the cavity at one time.

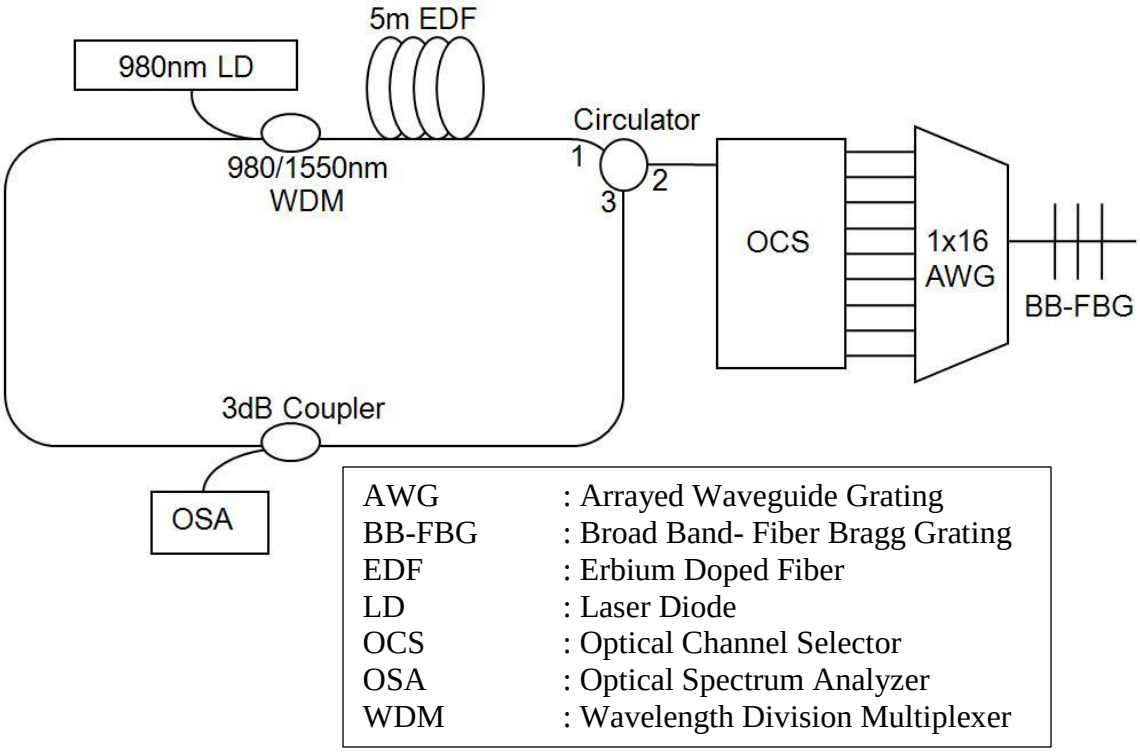

Figure 3.21: Setup for tunable output laser by using AWG and BB-FBG [39].

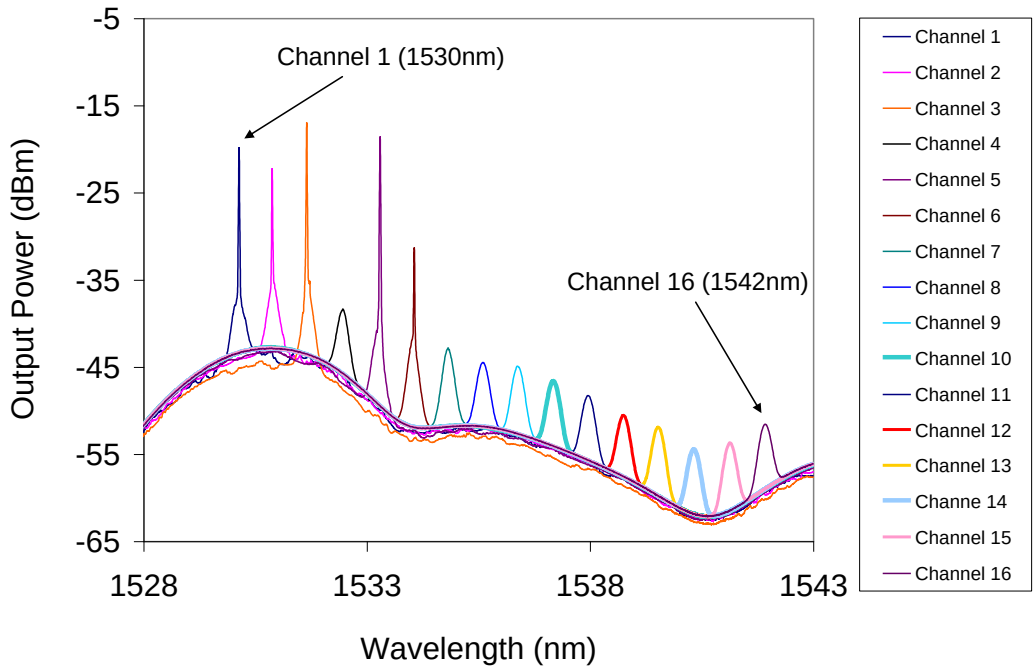

Figure 3.22: Obtained spectrum from the setup for realizing single wavelength fiber laser without BB-FBG [39].

Figure 3.22 shows the spectrum with the BB-FBG removed. The BB-FBG is used to reflect the entire C-band spectrum back to the cavity, with a reflectivity of 99%. The absence of the BB-FBG means that the reflection responsible for the selection of wavelength in the configuration is provided only by air, whose reflectivity is roughly 4.2%, due to Fresnel. It can be seen clearly from the same figure that the amplitude of the output wavelength will follow the general spectral curve of the ASE of the EDFA, with points 1 to 6 having a relatively higher output power as compared to the others.

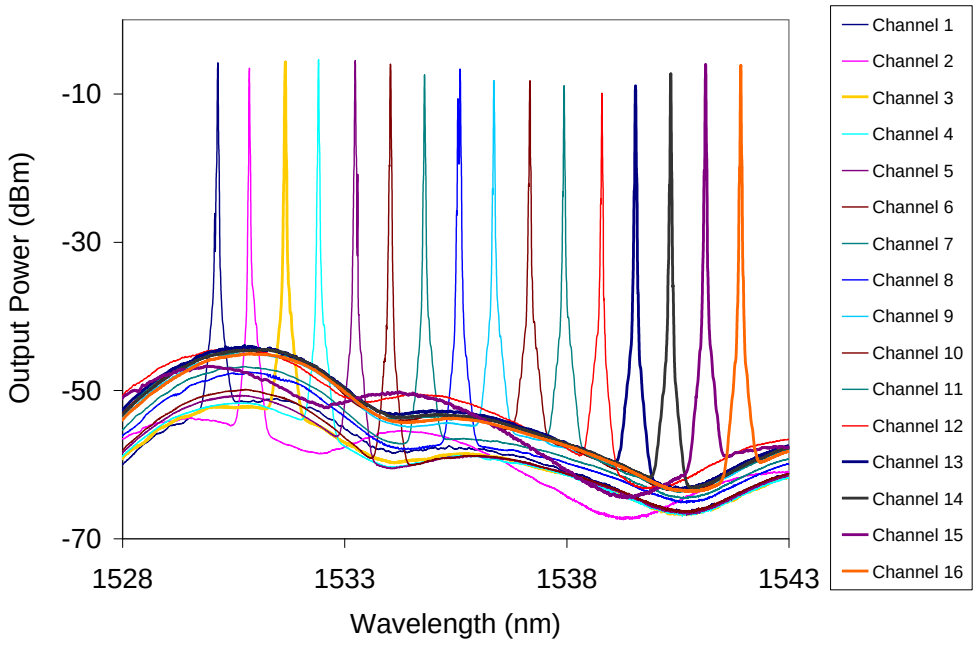

Figure 3.23: Single wavelength tuning operation by AWG and BB-FBG [39].

The laser output can be improved substantially by re-introducing the BB-FGB, as shown in Figure 3.23. From the plot, the introduction of the BB-FBG causes the output power throughout the entire tunable range in the C-band to become flatter, with an average output power of -4 dBm and the difference between the lowest and highest output powers being roughly 5 dB.

Now, theoretically, *caeteris paribus*, lasing can be achieved with relative ease at longer wavelengths, due to the fact that the lasing energies at longer wavelengths are lower than those for longer wavelengths. However, as the EDF has a higher gain curve in the 1530 nm region, the lasing threshold for the gain medium is lowered at this particular region, thus increasing the tendency for lasing.

The comparison of output powers of the configuration with and without the BB-FBG is given in Figure 3.24. Without the BB-FBG, the average output power is -40.21 dBm with a maximum value of -16.92 dBm recorded at 1531.66 nm and a minimum value of -54.86 dBm from 1541.12 nm.

With the BB-FBG, the average output power is recorded to be -7.08 dBm, with a maximum output power of -5.38 dBm from 1531 nm and a minimum of -9.92 dBm at 1538.79 nm. The difference between the highest and the lowest value is 4.69 dB. Therefore, there is a clear improvement in the output power by inserting the BB-FBG in the cavity.

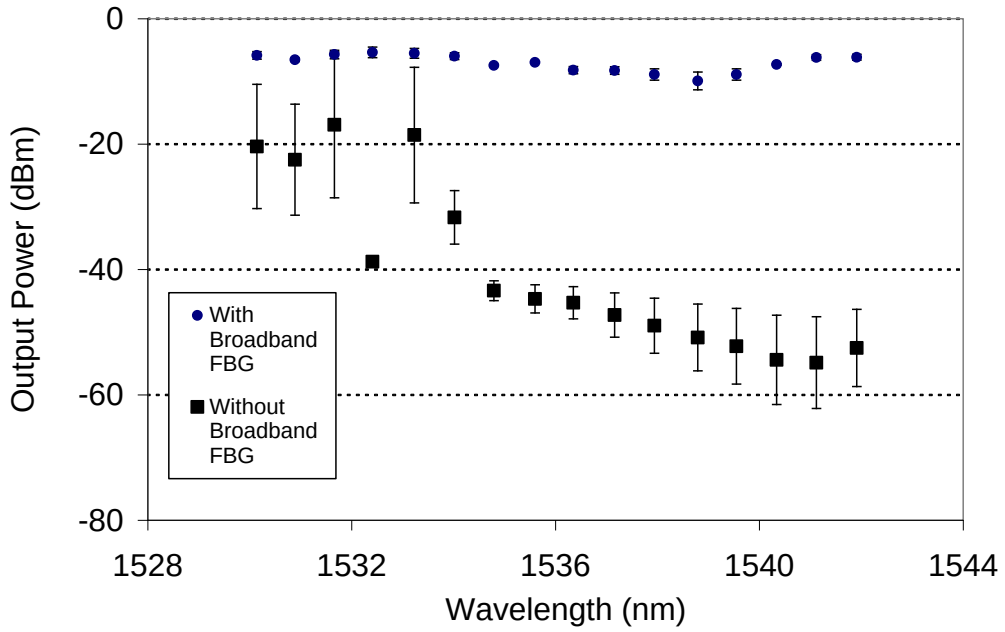

Figure 3.24: Output power measurement with and without the BB-FBG by using the AWG as a wavelength selective element.

The value of the SMSR is then taken and compared in Figure 3.25. By operating the laser without the BB-FBG the average SMSR value is 6.53 dB with a maximum value of 20.54 dB from 1531.66 nm and a minimum value of 1.08 dB from 1536.35 nm. Thus, giving a maximum difference of 19.46 dB between the maxima and minima. As with the output power, the SMSR was significantly improved by inserting the BB-FBG in the setup. This can be seen also in Figure 3.25, which shows that the average SMSR of the configuration with the BB-FBG has a significantly higher value at 36.92 dB, with improved values for the SMSR maxima and minima of 44.13 dB and 31.16 dB, measured at 1532.41 nm and 1539.55 nm, respectively. The different between maxima and minima is 12.97 dB. The SMSR is slightly lower compared to methods which employ different selective elements, and is primarily due to the insufficient isolation of the two output ports (ports 2 and 3) of the circulator, which has an attenuation of 40 dB, as compared to typical values for optical isolators, which is roughly 60 dB. This lack of isolation resulted in a small portion of the ASE counter propagating in the cavity, therefore removing the optimum theoretical condition of unidirectional propagation. This has the effect of reducing the SMSR value since this parameter is defined as the difference between the peak output power and the highest noise level, which, in this case, is provided by a relatively high level of ASE, propagating in the two directions.

This effect can be significantly reduced by inserting an isolator between the 3 dB coupler and the input of 1550 nm WDM, as this prevents the ASE from the backward direction. As can be seen from Figure 3.22 and 3.23, the noise level is quite high at around 1530 nm. As the wavelength is tuned to longer wavelengths the noise level increases, leading to degradation in the SMSR value.

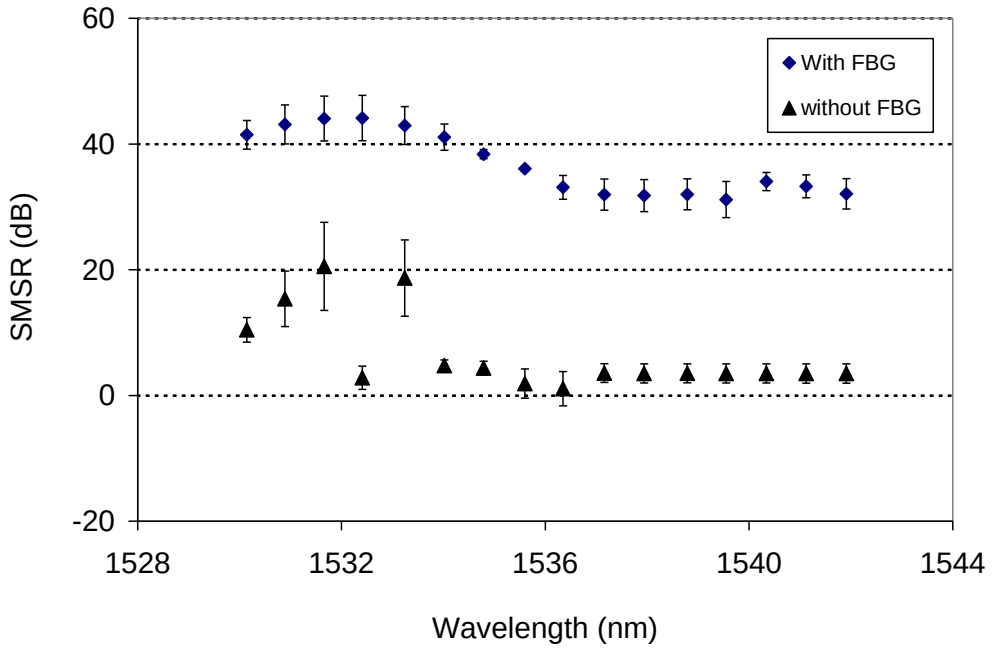

Figure 3.25: The SMSR measurement with and without the BB-FBG by using the AWG as a wavelength selective element.

The tunable single wavelength by using the AWG is also giving a few contributions to high power fiber laser [40] and mode-locked fiber lasers [41] as being done by our group.

3.2.2 Summary of the Various Techniques for a Tunable Fiber Laser

To summarise the data presented above, a few important characteristics of each fiber laser design are compiled in a simple timetable as shown in table 3.1 below:

Table 3.1: Comparison for different design of fiber lasers.

	Tunable Bandpass Filter (TBF)	Sagnac Loop Mirror and FBGs	Compression and Tensile Strain FBGs	Arrayed Waveguide Grating (AWG)
Average output power	-7.95 dBm	-10.82 dBm	-1.77 dBm	-7.08 dBm
Average SMSR value	67.82 dB	55.38 dB	71.68 dB	36.92 dB
Tunability	39.8 nm	21.8 nm	10 nm	11.86 nm
Number of wavelength options	Any wavelength within range	6 wavelengths	Any wavelength within range	16 wavelength with 0.8nm of adjacent channel spacing
3 dB Bandwidth	0.8 nm	1 nm	1 nm	0.44 nm
Precise wavelength selection	Moderate	Difficult	Moderate	Easy

The output power is highest by using the compression and tensile strain FBGs as the wavelength selective element with the average output power of -1.77 dBm. As for the tuning range, the one using the TBF is having the widest tuning capability of 39.8 nm. Even though the fiber laser by the TBF having the widest tuning range and by using the Compression and tensile strain FBGs having the highest output power, the AWGs having an advantage of precise wavelength selection with a gap of 0.8 nm from adjacent channels, giving an advantage of using the AWG by its precise wavelength selection.

The highest SMSR value is coming from Compression and Tensile strain FBG with the average SMSR of 71.68 dB. It is then followed by TBF design with SMSR value of 67.82 dB, the Sagnac loop mirror with FBG design with SMSR value of 55.38 dB and finally the AWG with SMSR value of 36.92 dB. The SMSR for The compression and tensile strain FBGs and TBF are having relatively almost the same value. However the single wavelength fiber laser by using the FBGs with Sagnac loop mirror method and AWG used as the wavelength selective elements shows a significant degradation of SMSR compare to the other two. For the case by using the FBGs with the Sagnac loop mirror, the lower peak output power leads to the lower of SMSR especially at the shortest wavelength of 1534.2 nm wavelength. The peak power of -14.58 dBm leads to a lower SMSR value since by definition, the SMSR is a different between the peak power and the noise level of laser output. The same situation implies to the setup by using the AWG, since the SMSR value is quite low for this design due to the higher noise level that following the ASE shape of the EDF emission.

3.3 Semiconductor Optical Amplifier Fiber Lasers (SOAFLs)

Another method in generating tunable fiber lasers involved employing a semiconductor optical amplifier (SOA) as the gain medium. This principle is depicted in Figure 3.26, whose configuration is identical with the setup in Figure 3.1 except for the gain medium used.

As with the setup for a 5m EDF, the free running design for a tunable SOA fiber laser also contains a 90:10 coupler and an isolator. There is, however, a difference in operating concept as the ASE is dependent on the external bias current supplied to the SOA as compared to the Er-doped fiber which requires optical pumping in order to produce the ASE. The operating current of the SOA used in the design is 300 mA of operating current. The lasing profile of the SOA is can be observed in Figure 3.27.

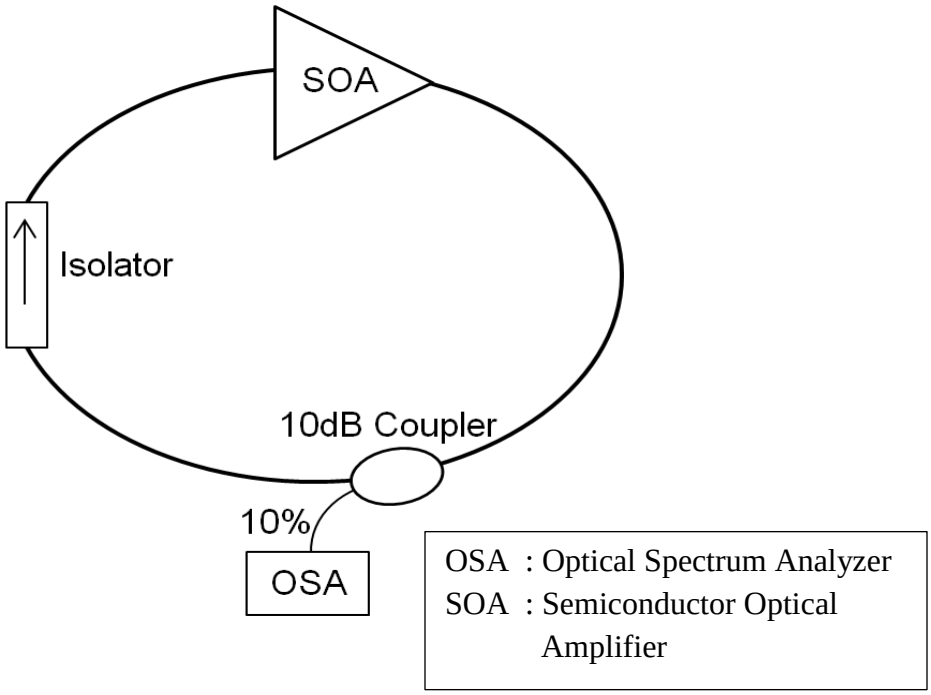

Figure 3.26: Experimental setup for SOA lasing spectral profile.

Figure 3.27 shows the lasing spectrum of the free-running fiber laser configuration of a semiconductor optical amplifier (SOA) at different driving current values. The driving current is varied between 63mA and 320mA, with the output shown in Figure 3.27. From the figure, it can be seen that the cavity lasing spectrum of an SOA fiber laser is quite different when compared to that of an EDFL. By measuring the spectrum bandwidth, the measurement of 10 dB and 30 dB bandwidth is calculated to be about 6.6 nm and 12 nm, respectively. The bandwidth of the SOA's is wider and roughly six times bigger than the EDF's lasing profile. This is due to the fact that the line shape of an SOA is Gaussian, attributed to the random emission process in the SOA, whilst EDFs typically have a Lorentzian line shape, which is the manifestation of the forced vibrations of the molecular electrons. The lasing output peak power of the 5m EDF is also higher with a peak output power of -12.6 dBm, as compared to the peak output power of an SOA, which is recorded to be -27.0 dBm. The average output power measured by the OPM for the SOA is -2.95 dBm. The wavelength of the laser output keep on increasing until its stop at 1560 nm where the SOA is driven by its highest driven current. The shifting of the lasing output to longer wavelengths can be observed as the drive current is increased because the lasing threshold of longer wavelengths reduces as the drive current is increased.

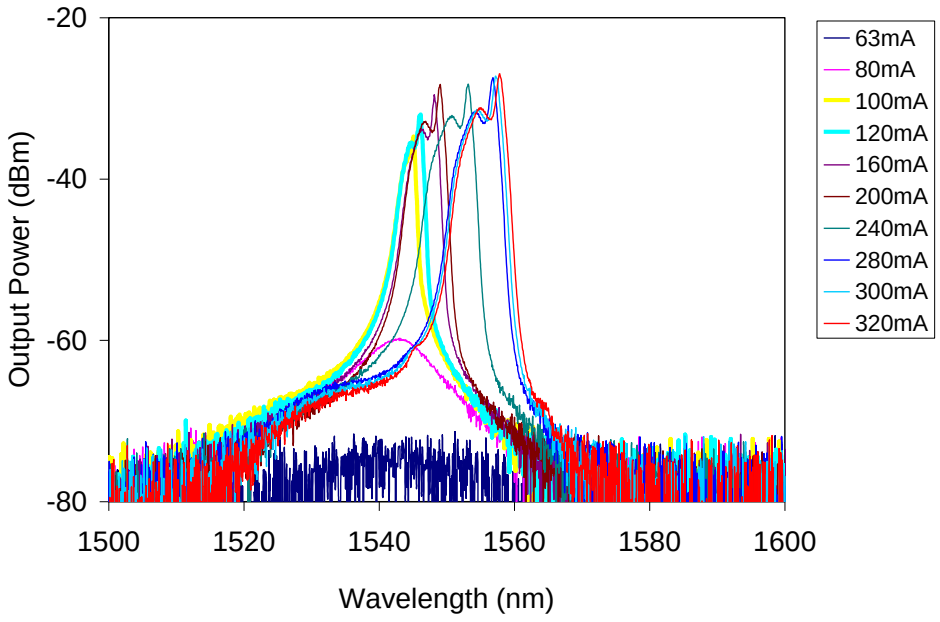

.

Figure 3.27: Cavity lasing spectrum of SOA as the gain medium.

3.3.1 Tunable SOAFLs by using Compression and Tensile Strain FBGs

The same principle for the generation of a tunable fiber laser by employing a tunable FBG can also be employed with an SOA as the gain medium, shown in Figure 3.28. The SOA is driven by the maximum driving current of 320 mA in the proposed configuration. The OCS is used to select the wavelength either from FBG 1 or from FBG 2. The output power spectrum is then analyzed by the OSA.

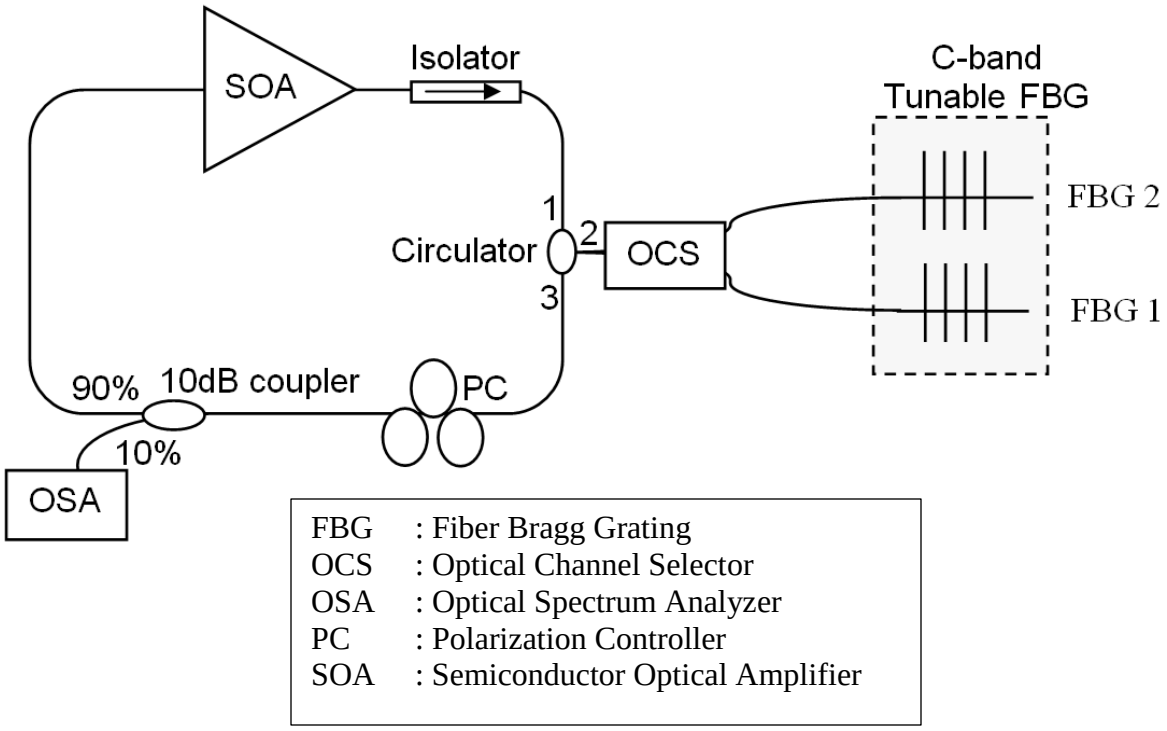

Figure 3.28: The configuration layout of tunable fiber laser by using SOA and the Compression and Tensile Strain FBGs as the wavelength selective element.

The spectrum of the wavelength tuning is depicted in Figure 3.29. The output power can be seen to be quite flat with wavelengths between 1546.55 nm and 1550.9 nm originating from FBG 1 while wavelengths 1551 nm to 1554.76 nm come from FBG 2. The wavelength tunabilty of FBGs 1 and 2 are roughly 4.35 nm and is 3.76 nm, respectively, thereby giving a total tunability of 8.2 nm. This design allows the simple tuning of wavelength easily by applying the tensile and compress force to the FBGs. The wavelength selection can also be made at any point within the operation range of the configuration.

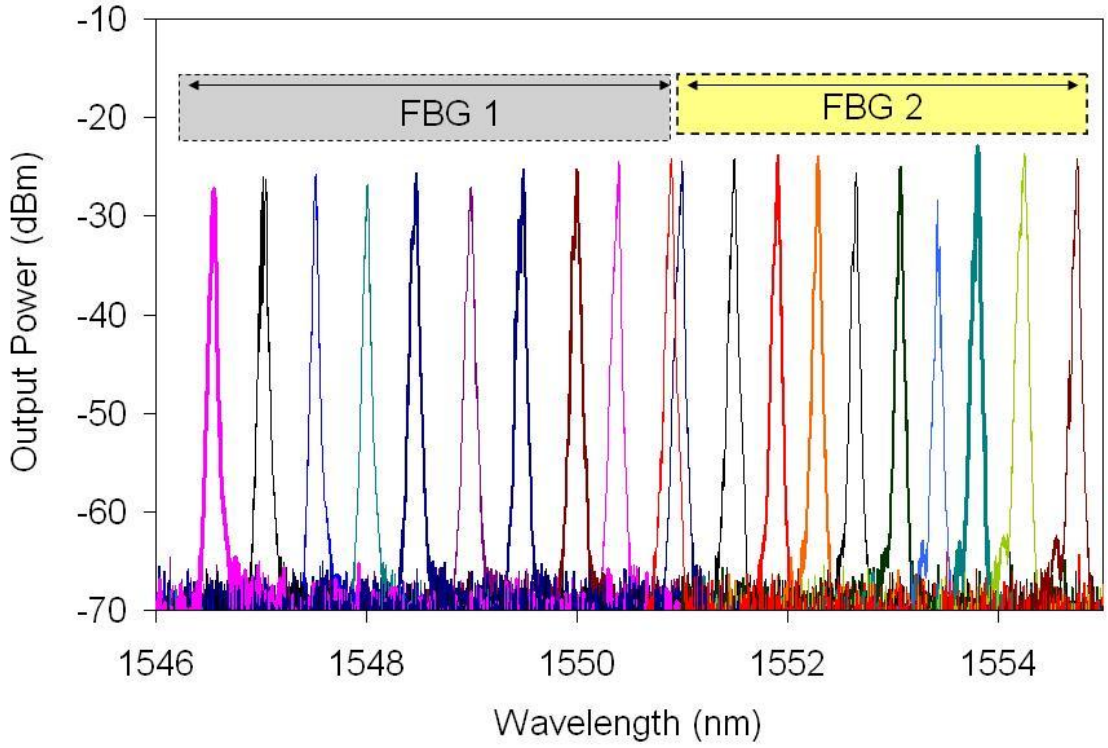

Figure 3.29: The spectra of tunable fiber laser by using SOA and the compression and tensile strain FBGs as the wavelength selective element.

The output power and SMSR of the setup is then taken and analyzed, as shown in Figure 3.30. The average output power achieved for this configuration is -25.41 dBm, which is quite low compared to the other designs that have been proposed. The maximum output power is measured at 1553.82 nm with a value of -23.14 dBm while the minimum power is measured to be -28.38 dBm at1553.43 nm. Therefore, the difference between the maximum and minimum output power is calculated to be 5.24 dB. The average value, on the other hand, for the SMSR is 40.12 dB. The maximum SMSR is recorded at1551.50 nm with a

value of 42.57 dB, while the minimum SMSR is 35.12 dB at 1553.43 nm, and therefore, difference between the SMSR maxima and minima is calculated to be 3.46 dB.

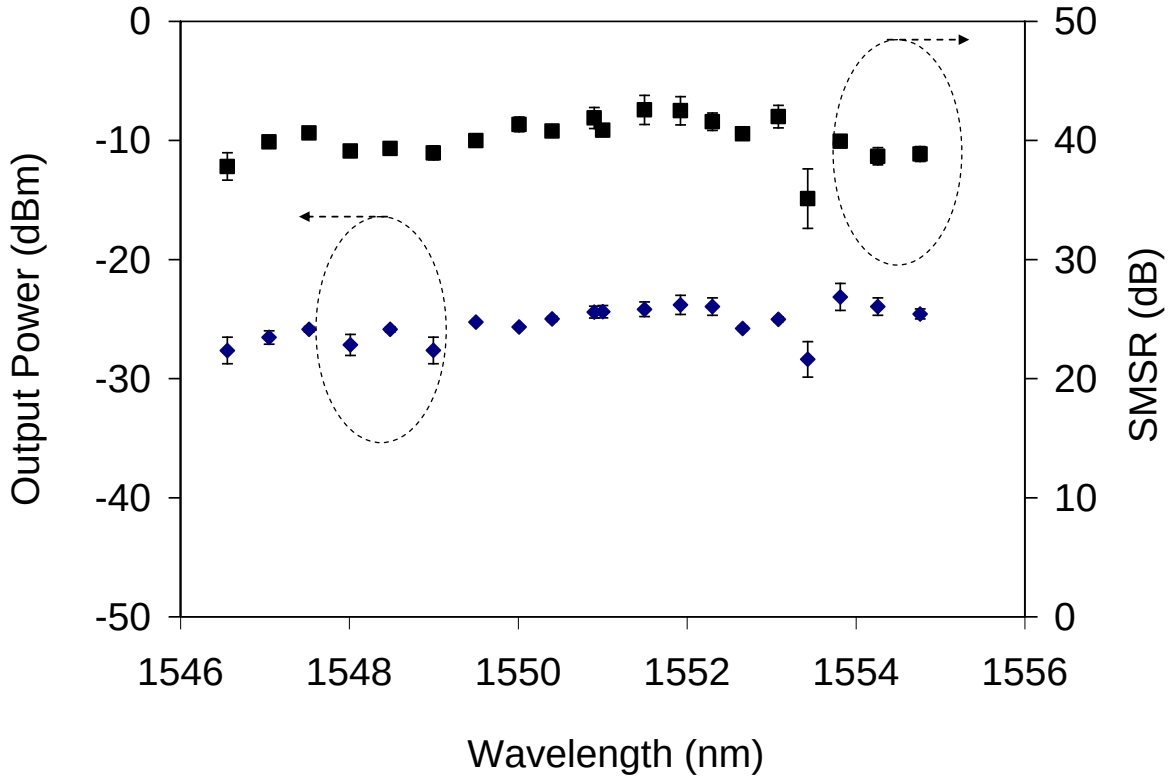

Figure 3.30: Cavity lasing spectral of SOA.

3.3.2 Tunable SOAFLs by Using an AWG

The second wavelength selective element used in the SOA is the 1x16 of AWG. The experiment is identical to the previous experiment which employed an EDF as the gain medium, but with the SOA as the gain medium, as depicted in Figure 3.31. The wavelength selection is also done by controlling the OCS to select different AWG channels. The same

operating current maximum of 320 mA is also used in the design. The output is then analyzed by the SOA as depicted in Figure 3.32.

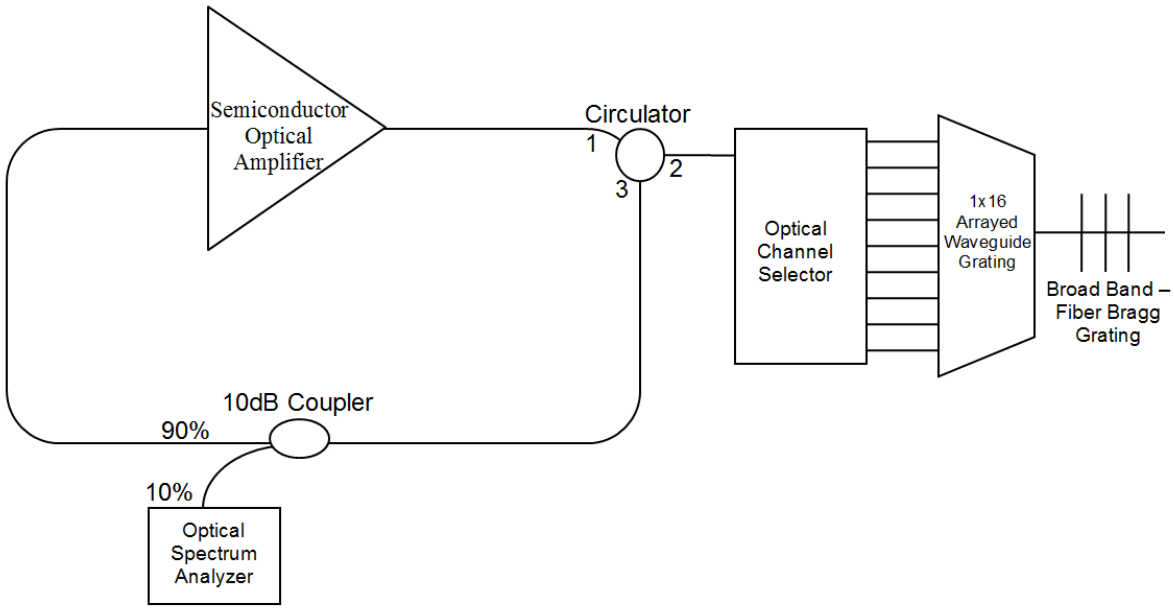

Figure 3.31: Experimental setup of tunable single wavelength SOA fiber laser by using an AWG [42].

The output power of the tunable single wavelength SOA fiber laser by using an AWG is shown in Figure 3.32. The spectra show that the output power level is quite flat from channel 1 to channel 16. The lasing wavelength starts at 1530.24 nm with an output power of -12.17 dBm and ends at 1542.08 nm with an output power of -9.37 dBm. The spacing between the AWG channels is 0.8 nm, identical to the one employed with the EDFA. But, however, unlike the one using the EDFA, the SOA-based fiber laser is having a slightly lower output peak power with 5 dB lower to the same configuration of EDFA. This is due to a lower light power emitted by SOA compared to EDFA. Channel 1 can be seen to have

a higher noise level compared to the other channels, due to the uneven response of losses inside the connectors and different spectral response of the AWG.

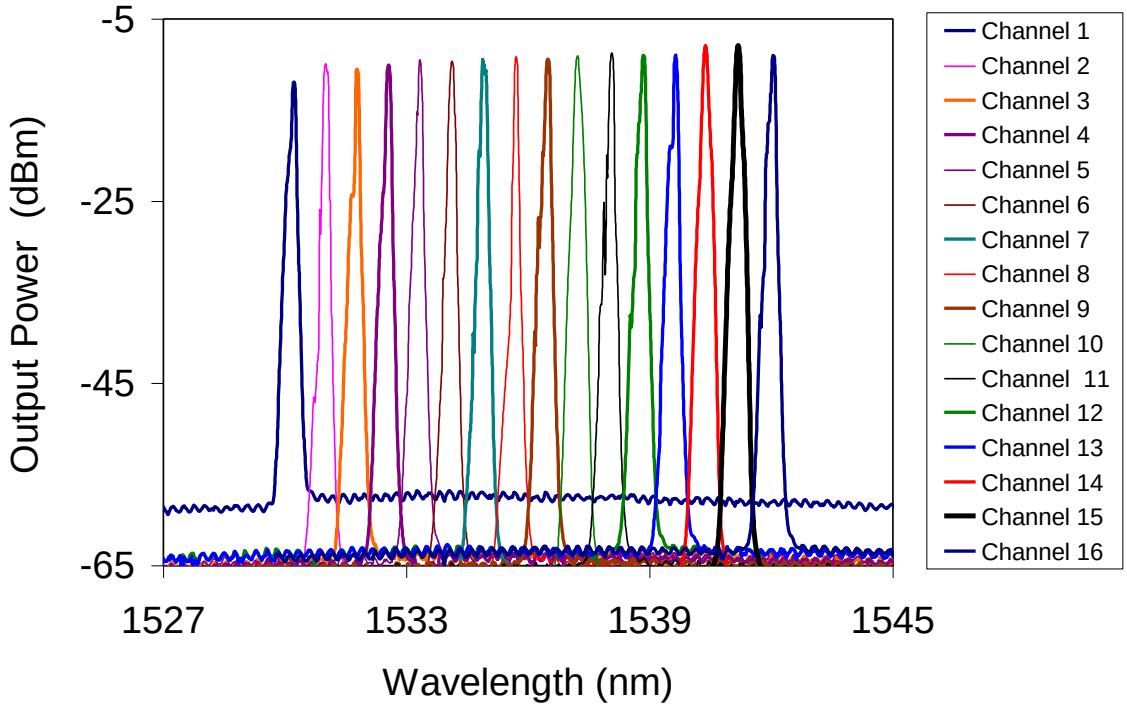

Figure 3.32: Output power spectra by using the AWG[42].

Figure 3.33 shows the average output power for the design with -9.70 dBm of output power. The maximum output power is coming from 1541.18 nm with -7.93 dBm of output power and the minimum is coming from 1530.24 nm with -12.17 dBm of output power. Thus giving a 4.24 dB of maximum different between the highest and the lowest value. The average value for SMSR is 54.66 dB. The maximum comes from 1540.4 nm with 58.78 dB of SMSR, while the minimum comes from 1530.24 nm with 45.57 dB of SMSR. Thus giving a maximum SMSR different of 13.21 dB between the highest and the lowest value.

The same technique but by using a wider gain bandwidth of SOA has also being done by our group to improve the switching tunability [43, 44].

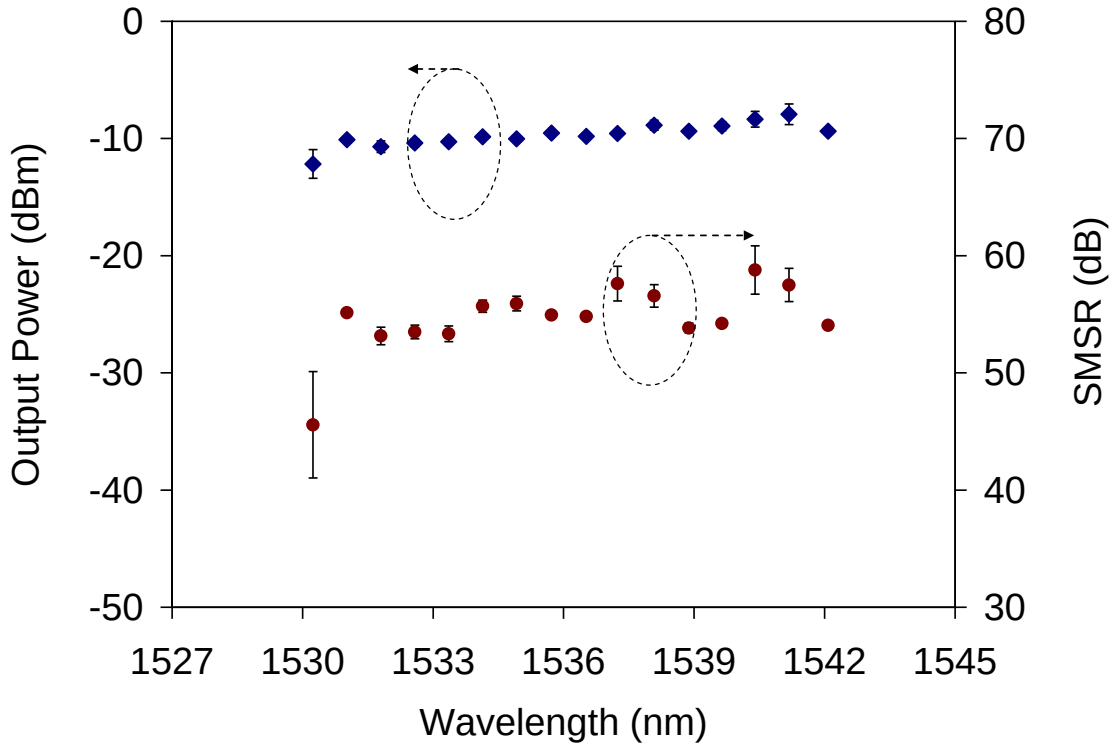

Figure 3.33: Cavity lasing spectral of SOA.

3.3.3 Comparison for Every Technique in SOA-Based Single Wavelength Fiber Lasers

To conclude the data presented above, a few important characteristics of each SOA-based Single Wavelength Fiber Laser designs are compiled in a simple timetable as shown in table 3.2 below:

Table 3.2 : Comparison for different design of fiber lasers.

	Compression and tensile strain FBGs	Arrayed Waveguide Grating (AWG)
Average output power	-25.41 dBm	-9.70 dBm
Average SMSR value	40.12 dB	54.66 dB
Tunability	8.21 nm	11.84nm
Number of wavelength options	Any wavelength within range	16 wavelength with 0.8 nm of adjacent channel spacing
3 dB Bandwidth	1 nm	0.44 nm
Precise wavelength selection	Moderate	Easy

3.4 Summary

In this chapter, the generation of tunable single wavelength fiber laser has been demonstrated. Different wavelength selective elements comprise a TBF, 6 FBGs with Sagnac loop mirror method, compression and tensile strain FBGs; and an AWG. The generation of fiber laser is first demonstrated by using a homogeneous broadening gain media that is by using EDFA as an amplifier. The different output power and SMSR for each design were then discussed.

The second discussion is followed by generation of tunable single wavelength fiber laser by using SOA as the gain medium. This is being demonstrated in order to give another option rather than using the EDF as the gain medium, as SOA having the emission close to the inhomogeneous gain broadening. The wavelength tuning capabilities of the two gain media are almost the same. The different is on the output power, as the EDFA produces a higher output peak power compared to by using the SOA.

In the next chapter, however, it can be seen that the broadening effect emits by the homogeneous and inhomogeneous gain media. This is due to the different properties of those two giving different means to generate tunable dual-wavelength fiber laser.

Reference

1. Bellemare, A., et al., *Room temperature multifrequency erbium-doped fiber lasers anchored on the ITU frequency grid.* Lightwave Technology, Journal of, 2000. **18**(6): p. 825-831.
2. Libatique, N., L. Wang, and R. Jain, *Single-longitudinal-mode tunable WDM-channel-selectable fiber laser.* Opt. Express, 2002. **10**(25): p. 1503-1507.
3. Bellemare, A., et al. *Erbium-doped fiber ring lasers step-tunable to exact multiples of 100 GHz (ITU-grid) using periodic filters*. in *Optical Communication, 1998. 24th European Conference on*. 1998.
4. Liaw, S.K., et al. *Dynamically wavelength-switching, gain-equal, and high-SNR fiber Bragg grating ring lasers*. in *Lasers and Electro-Optics, 1998. CLEO 98. Technical Digest. Summaries of papers presented at the Conference on*. 1998.
5. Libatique, N.J.C. and R.K. Jain, *Precisely and rapidly wavelength-switchable narrow-linewidth 1.5μm laser source for wavelength division multiplexing applications.* Photonics Technology Letters, IEEE, 1999. **11**(12): p. 1584-1586.
6. Tanaka, S., et al. *Wavelength-switchable fiber laser for thermally stabilized fiber Bragg grating vibration sensor array*. in *Sensors, 2004. Proceedings of IEEE*. 2004.
7. Liu, S., et al., *Simple hybrid wire-wireless fiber laser sensor by direct photonic generation of beat signal.* Appl. Opt., 2011. **50**(12): p. 1792-1797.
8. Wei, X., et al., *Nano-structured Pd-long period fiber gratings integrated optical sensor for hydrogen detection.* Sensors and Actuators B: Chemical, 2008. **134**(2): p. 687-693.

9. Chan, C.C., et al., *Investigation of unwanted interferometric signals in a fiber Bragg grating sensor using a tunable laser and a first derivative interrogation technique.* Optics Communications, 2000. **173**(1–6): p. 203-210.

10. Shemshad, J., S.M. Aminossadati, and M.S. Kizil, *A review of developments in near infrared methane detection based on tunable diode laser.* Sensors and Actuators B: Chemical, 2012. **171–172**(0): p. 77-92.

11. Fu, Z., et al., *Widely tunable compact erbium-doped fiber ring laser for fiber-optic sensing applications.* Optics & Laser Technology, 2009. **41**(4): p. 392-396.

12. Yao, C.-L., et al., *Novel tunable laser sources with 1.5-μm and 1.57-μm cascaded DFB reflectors for in situ gas monitoring applications.* Sensors and Actuators B: Chemical, 2009. **140**(2): p. 371-377.

13. Changchun, L., L. Zuhong, and L. Fei, *Measurement of absolute strain based on a tunable cw semiconductor laser.* Sensors and Actuators A: Physical, 2000. **80**(1): p. 31-34.

14. Gladyshev, A.V., et al., *Tunable single-frequency diode laser at wavelength λ=1.65μm for methane concentration measurements.* Spectrochimica Acta Part A: Molecular and Biomolecular Spectroscopy, 2004. **60**(14): p. 3337-3340.

15. Frenkel, A. and C. Lin, *Angle-tuned etalon filters for optical channel selection in high density wavelength division multiplexed systems.* Lightwave Technology, Journal of, 1989. **7**(4): p. 615-624.

16. Hongxin, C., et al., *Widely tunable single-frequency erbium-doped fiber lasers.* Photonics Technology Letters, IEEE, 2003. **15**(2): p. 185-187.

17. Gupta, K.K. and D. Novak, *Millimetre-wave repetition-rate optical pulse train generation in harmonically modelocked fibre ring laser.* Electronics Letters, 1997. **33**(15): p. 1330-1331.

18. Erdogan, T., *Fiber grating spectra.* Lightwave Technology, Journal of, 1997. **15**(8): p. 1277-1294.

19. Chunn-Yenn, L., C. Gia-Wei, and A.W. Lon, *Periodical corrugated structure for forming sampled fiber Bragg grating and long-period fiber grating with tunable coupling strength.* Lightwave Technology, Journal of, 2001. **19**(8): p. 1212-1220.

20. Hill, K.O. and G. Meltz, *Fiber Bragg grating technology fundamentals and overview.* Lightwave Technology, Journal of, 1997. **15**(8): p. 1263-1276.

21. Dong, X.P., et al. *Multiwavelength erbium-doped fiber laser with a high-birefringence fiber loop mirror*. in *Lasers and Electro-Optics, 2000. (CLEO 2000). Conference on*. 2000.

22. Feng, X., et al., *Multiwavelength Erbium-Doped Fiber Laser Based on a Nonlinear Hi-Bi Fiber Loop Mirror.* Optical Communication (ECOC), 2007 33rd European Conference and Ehxibition of, 2007: p. 1-2.

23. Keiser, G., *Optical fiber communications*2000: McGraw-Hill.

24. Ghatak, A. and K. Thyagarajan, *An Introduction to Fiber Optics*1998: Cambridge University Press.

25. Hu, S., et al., *Switchable multiwavelength erbium-doped fiber ring laser with a multisection high-birefringence fiber loop mirror.* Photonics Technology Letters, IEEE, 2005. **17**(7): p. 1387-1389.

26. Guoyong, S., et al., *Broadly Tunable Fiber Laser Based on Merged Sagnac and Intermodal Interferences in Few-Mode High-Birefringence Fiber Loop Mirror.* Photonics Technology Letters, IEEE, 2010. **22**(11): p. 766-768.

27. Chunmei, O., et al., *Wavelength-Tunable High-Energy All-Normal-Dispersion Yb-Doped Mode-Locked All-Fiber Laser With a HiBi Fiber Sagnac Loop Filter.* Quantum Electronics, IEEE Journal of, 2011. **47**(2): p. 198-203.

28. Moon, D.S., et al., *Tunable multi-wavelength SOA fiber laser based on a Sagnac loop mirror using an elliptical core side-hole fiber.* Opt. Express, 2007. **15**(13): p. 8371-8376.

29. Mao, Q. and J.W.Y. Lit, *Switchable multiwavelength erbium-doped fiber laser with cascaded fiber grating cavities.* Photonics Technology Letters, IEEE, 2002. **14**(5): p. 612-614.

30. Yang, Y., et al. *Polarization-Controlled Switchable Multi-Wavelength Erbium-Doped Fiber Laser with Cascaded Fiber Bragg Gratings*. in *Photonics and Optoelectronics (SOPO), 2011 Symposium on*. 2011.

31. Tran, T.V.A., et al., *Switchable multiwavelength erbium doped fiber laser based on a nonlinear optical loop mirror incorporating multiple fiber Bragg gratings.* Opt. Express, 2008. **16**(3): p. 1460-1465.

32. Ummy, M.A., et al. *Dual-output port widely tunable fiber laser based on a SOA dual Sagnac loop mirror configuration*. in *LEOS Annual Meeting Conference Proceedings, 2009. LEOS '09. IEEE*. 2009.

33. Lim, K.S., Pua, C. H., Awang, N. A. , Harun, S. W., and Ahmad, H. , *Fiber Loop Mirror Filter with Two-Stage High Birefringence Fibers* Progress In Electromagnetics Research C, 2009. **9**: p. 101-108.

34. Frazão, O., J. Baptista, and J. Santos, *Recent Advances in High-Birefringence Fiber Loop Mirror Sensors.* Sensors, 2007. **7**(11): p. 2970-2983.

35. Goh, C.S., S.Y. Set, and K. Kikuchi, *Widely tunable optical filters based on fiber Bragg gratings.* Photonics Technology Letters, IEEE, 2002. **14**(9): p. 1306-1308.

36. Chong, S.S., et al., *Synchronous tunable wavelength spacing dual-wavelength SOA fiber ring laser using Fiber Bragg grating pair in a hybrid tuning package.* Optics Communications, 2012. **285**(6): p. 1326-1330.

37. Ahmad, H., et al., *Tunable single longitudinal mode S-band fiber laser using a 3 m length of erbium-doped fiber.* Journal of Modern Optics, 2012. **59**(3): p. 268-273.

38. Hibino, Y., *An array of photonic filtering advantages: arrayed-waveguide-grating multi/demultiplexers for photonic networks.* Circuits and Devices Magazine, IEEE, 2000. **16**(6): p. 21-27.

39. Zulkifli, M.Z., et al., *Flat output and switchable fiber laser using AWG and broadband FBG.* Optics Communications, 2009. **282**(13): p. 2576-2579.

40. Latif, A.A., et al., *Tunable high power fiber laser using an AWG as the tuning element.* Laser Physics, 2011. **21**(4): p. 712-717.

41. Ahmad, H., et al., *Wide-band fanned-out supercontinuum source covering O-, E-, S-, C-, L- and U-bands.* Optics & Laser Technology, 2012. **44**(7): p. 2168-2174.

42. Ahmad, H., et al., *Switchable semiconductor optical fiber laser incorporating AWG and broadband FBG with high SMSR.* Laser Physics Letters, 2009. **6**(7): p. 539-543.

43. Ahmad, H., et al., *120 nm wide band switchable fiber laser.* Optics Communications, 2010. **283**(21): p. 4333-4337.

44. Ahmad, H., et al., *Novel O-band tunable fiber laser using an array waveguide grating.* Laser Physics Letters, 2010. **7**(2): p. 164-167.

CHAPTER 4

THE DESIGN OF DUAL-WAVELENGTH FIBER LASERS

4.1 Introduction

The generation of DWFLs is basically the continuation of single wavelength fiber lasers that is done by adding one more wavelength selective element to ensure only two frequencies oscillating simultaneously on behalf of the two wavelengths inside the cavity. DWFLs have become light sources that are needed especially for certain applications such as an application for sensor [1-4], wavelength converter [5-7] and also for the generation of microwave [8-11] and Terahertz wave [12-14].

As has been mentioned previously, the process in order to obtain a dual-wavelength fiber laser by using an EDF is quite challenging. This is due to the homogenous line broadening effect of rare earth doped fiber as the active gain medium, causing mode competition that hinder the process to get dual-wavelength output power simultaneously [15-18]. Several techniques have been realized to overcome this problem and have been discussed in detail in Chapter 1. This include the cooling of the EDF using liquid nitrogen [19, 20], polarization hole burning process [21, 22], hybrid with inhomogeneous line broadening gain medium [23, 24], by using an elliptical EDF [25], by using a polarization maintaining FBG for wavelength selection [26], by using a frequency shifter in the cavity [27], by using DFB fiber laser source with a separate resonance cavity [9], four wave mixing effect

(FWM) as a stabilizer [28], and last but not least is by using the optical injection Fabry-Perot laser [29]. Even though they seem effective in solving the mode competition issues, most of them are really difficult to handle and needed a complicated setup in order to generate the dual-wavelength outputs. Most of the methods are incapable of generating tunable dual-wavelength output laser source which makes our design a novel architecture as compared to the others.

In this chapter, several new techniques to generate dual-wavelength fiber lasers are presented. The wavelength selectors used are the arrayed waveguide grating (AWG), tunable bandpass filter (TBF) and fibre Bragg grating (FBG) and the gain media used are the EDFs and SOAs which inhibit homogeneous and inhomogeneous profile, respectively. Issues related to mode competition, due to the homogeneous gain medium, are also addressed in discussing these techniques.

4.2 Dual-Wavelength Fiber Lasers by Using EDF

The experimental setup to generate a dual-wavelength fiber laser is shown in Figure 4.1. Two FBGs are used as the wavelength selective elements with 98% reflection at 1535 nm and 1537 nm for FBG1 and FBG2, respectively, corresponding to the two lasers in the cavity. A 5 m EDF is used as an active gain medium and is pumped with a 980 nm laser diode at 120 mW. The isolator, as explained in previous chapters, allow for propagation in only one direction, ‘forcing’ the ASE to propagate in a clockwise direction. The beam

enters the circulator via port 1 to port 2 whereby the two wavelength are selected via the FBGs and are then reflected to the cavity via port 3. The beam then propagates through a 10 dB coupler, where 10% of the beam is extracted and analysed by the OSA, which records the output spectrum.

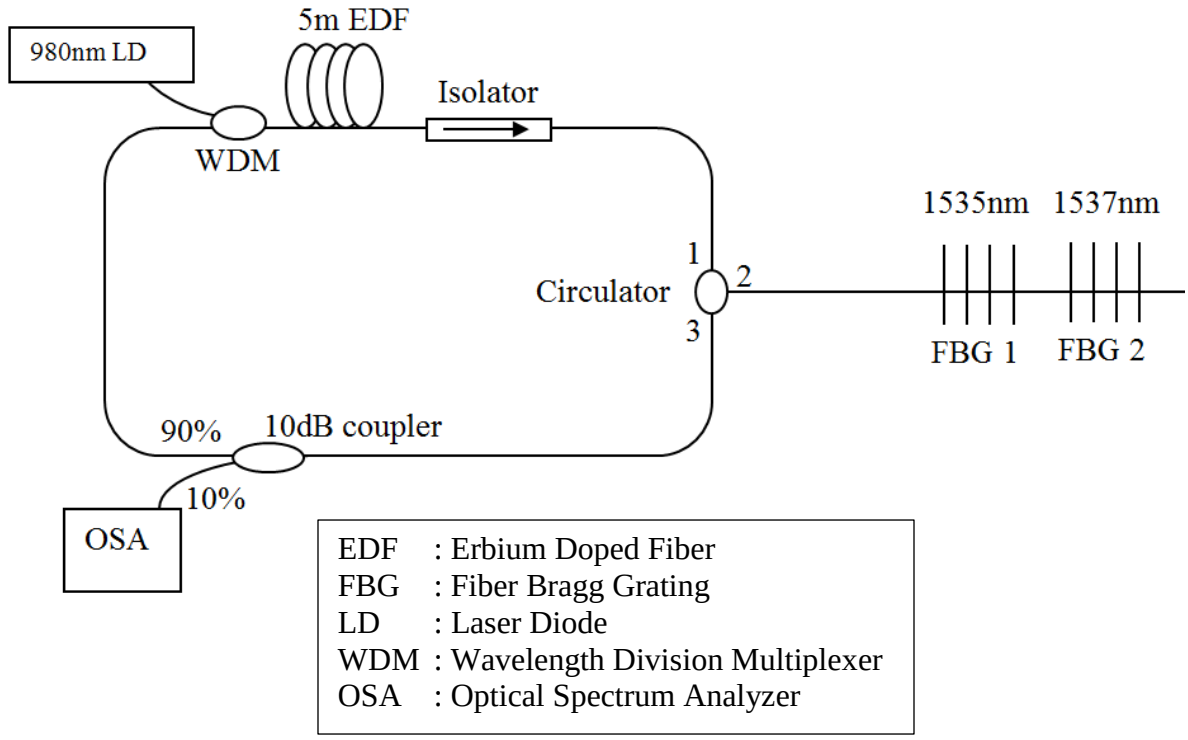

Figure 4.1: An experiment layout of dual-wavelength fiber laser by using EDF.

DWFLs are generally difficult to generate due to homogeneous line broadening and mode competition. This is depicted in Figure 4.2 whereby the imbalanced dual-wavelength output can be observed clearly from the spectrum taken from the OSA. The homogeneous broadening gain profile intrinsic to the EDFs has a gain saturation effect which causes the

mode competition problem, leading to serious problem in the generation of multiwavelength fiber lasers including the dual-wavelength fiber lasers.

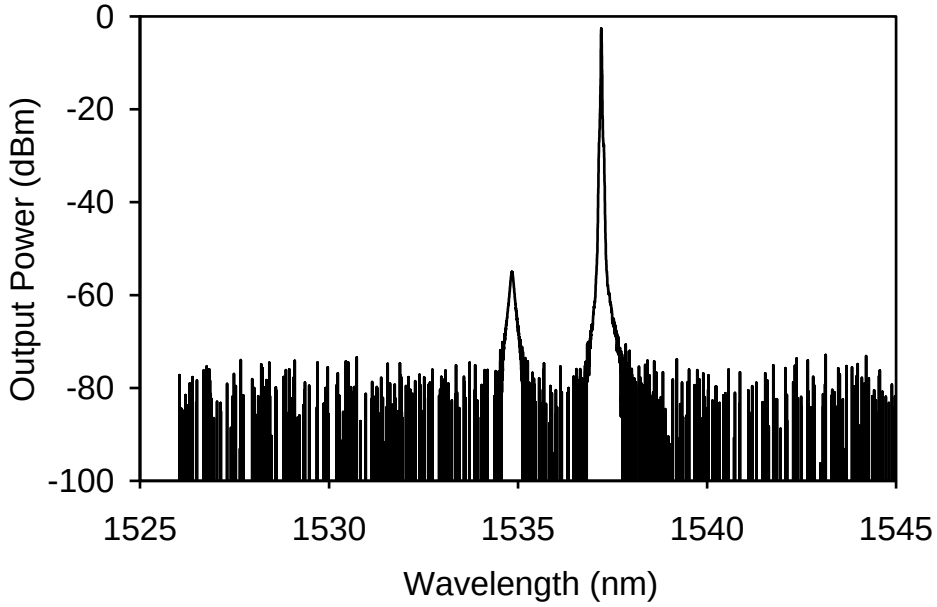

Figure 4.2: Spectrum of dual-wavelength fiber laser with mode competition.

The dual-wavelength fiber laser can easily be generated with a gain medium that exhibit inhomogeneous line broadening. However, the inhomogeneous gain medium such as the semiconductor optical amplifier exhibit higher noise and lower gain profile than homogeneous gain media that makes the EDF lasers more attractive.

In the next section, a new method of generating dual-wavelength fiber lasers is presented. This technique relies on controlling the cavity loss in order to balance the dual-wavelength via a variety of configurations and gain media. The tunability, output power and side mode suppression ratio (SMSR) profile will also be discussed to obtain the best design for all configurations.

4.2.1 DWFL by Using AWG

In this chapter, the generation of the DWFL is done by using the AWG in a ring cavity, linear cavity and finally for the application of high power fiber laser. The tunability of the spectrum is examined through the OSA and will be discussed later in this chapter.

4.2.1.1 DWFL in Ring Cavity Configuration

Figure 4.3 depicts a new and novel configuration to generate a dual-wavelength fiber laser by using a 5 m Metrogain EDF as an active gain medium. This setup consists of two ring cavities with both of them sharing the same gain medium that is the 5 m EDF.

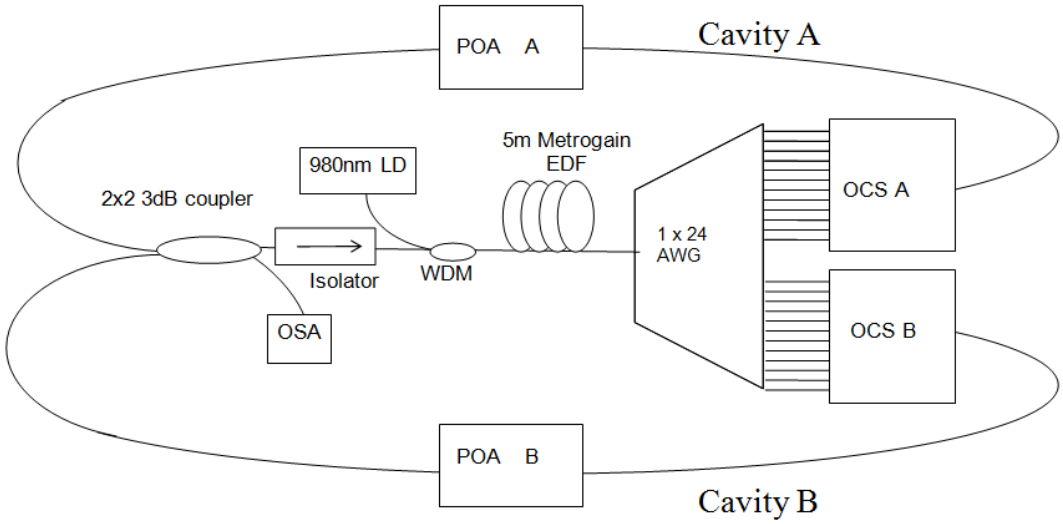

AWG	: Arrayed Waveguide Grating
EDF	: Erbium Doped Fiber
LD	: Laser Diode
WDM	: Wavelength Division Multiplexer
OCS	: Optical Channel Selector
OSA	: Optical Spectrum Analyzer

Figure 4.3: Schematic layout of the dual-wavelength fiber laser by using 1 x 24 AWG [30].

The 5 m EDF is pumped by using a 980 nm laser diode with a pump power of 80 mW to generate the ASE. The ASE then propagates in the anticlockwise direction in cavity A through optical channel selector (OCS) A and programmable optical attenuator (POA) A, and in clockwise direction in Cavity B through OCS B and POA B. The generated ASE passing through the AWG is then sliced to 24 Channels of 0.8 nm spacing between adjacent channels, which is equivalent to a spacing of 100 GHz. Channels 1 through to 12 designated as channel A1 to channel A12 and are connected to OCS A while channels 13 to 24 designated as channel B13 to channel B24 are connected to OCS B. Therefore, the proposed setup only selects two wavelengths a time, one each from OCS A and OCS B, respectively.

This design utilizes two cavities in order to control every single wavelength independently. This will allow the cavity power to be adjusted in such a way that both the output wavelengths will have the same energy. This technique is called cavity loss control. The two wavelengths from OCS A and B then pass through POA A and POA B, respectively, and are then combined via a 2x2 3 dB coupler. The output of the DWFL is measured and analyzed by using an optical spectrum analyzer (OSA) with a resolution of 0.05 nm.

Figure 4.4 shows the DWFL with different POA B attenuation values in order to control the wavelength power. When both of the attenuation of POA A and POA B are at zero value, the output wavelength A at 1530.48 nm has an output power of -60.44 dBm while wavelength B at 1548.91 nm has an output power of 0.91 dBm. The oscillation at 1548.61 nm extracts more energy from the population inversion of the EDF, thus depriving the energy for the output at 1530.48 nm.

As the attenuation of POA B is increased to 3.2 dB, the peak powers of output wavelength A increases to -50.9 dBm, while the power of output wavelength B decreases slightly to -0.66 dBm. Further increase in the attenuation to 4.05 dB will result in a situation whereby the output powers of both wavelengths are at approximately the same power level, i.e. -2.69 dBm for output wavelength A and -3.26 dBm for output wavelength B.

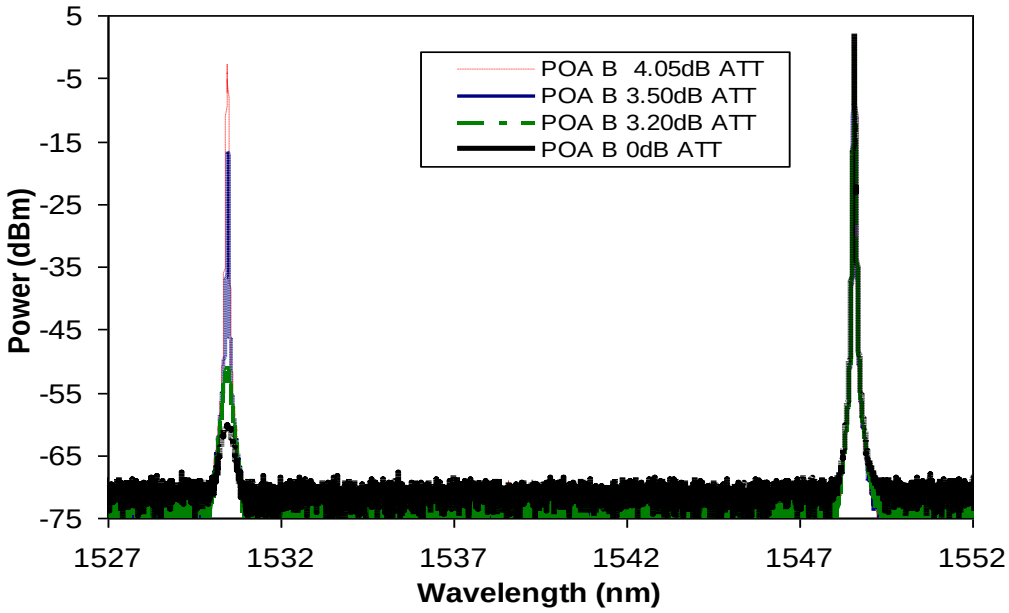

Figure 4.4: The performance of the DWFL with different amount of attenuation applied to Cavity B.

Next, a combination of different wavelengths are probed, with the OCSs being employed as switches which selects different ports on the AWG. This allows for a fast switching time between adjacent channels of the OCS of only roughly 500 ms. Figure 4.5 shows the DWFL with a tunable range of 20 nm in which the spacing was adjusted by changing channels OCS A and OCS B. From the data, the spacing of the dual-wavelength fiber laser

are 18.13 nm spacing for channels A1 and B24 (Figure 4.5(a)), 14.97 nm for channels A3 B22 (Figure 4.5(b)), 11.81 nm for channels A5 and B20 (Figure 4.5(c)), 8.68 nm for channels A7 and B18 (Figure 4.5(d)), 5.52 nm for channels A9 and Channel B16 (Figure 4.5(e)) and finally 0.8 nm for channels A11 and B12 (Figure 4.5(f)). The widest and narrowest channel spacing obtained, therefore, is 18.13 nm and 0.80 nm respectively. The measured output power of the DWFL is roughly 0 dBm as can be seen in the figure.

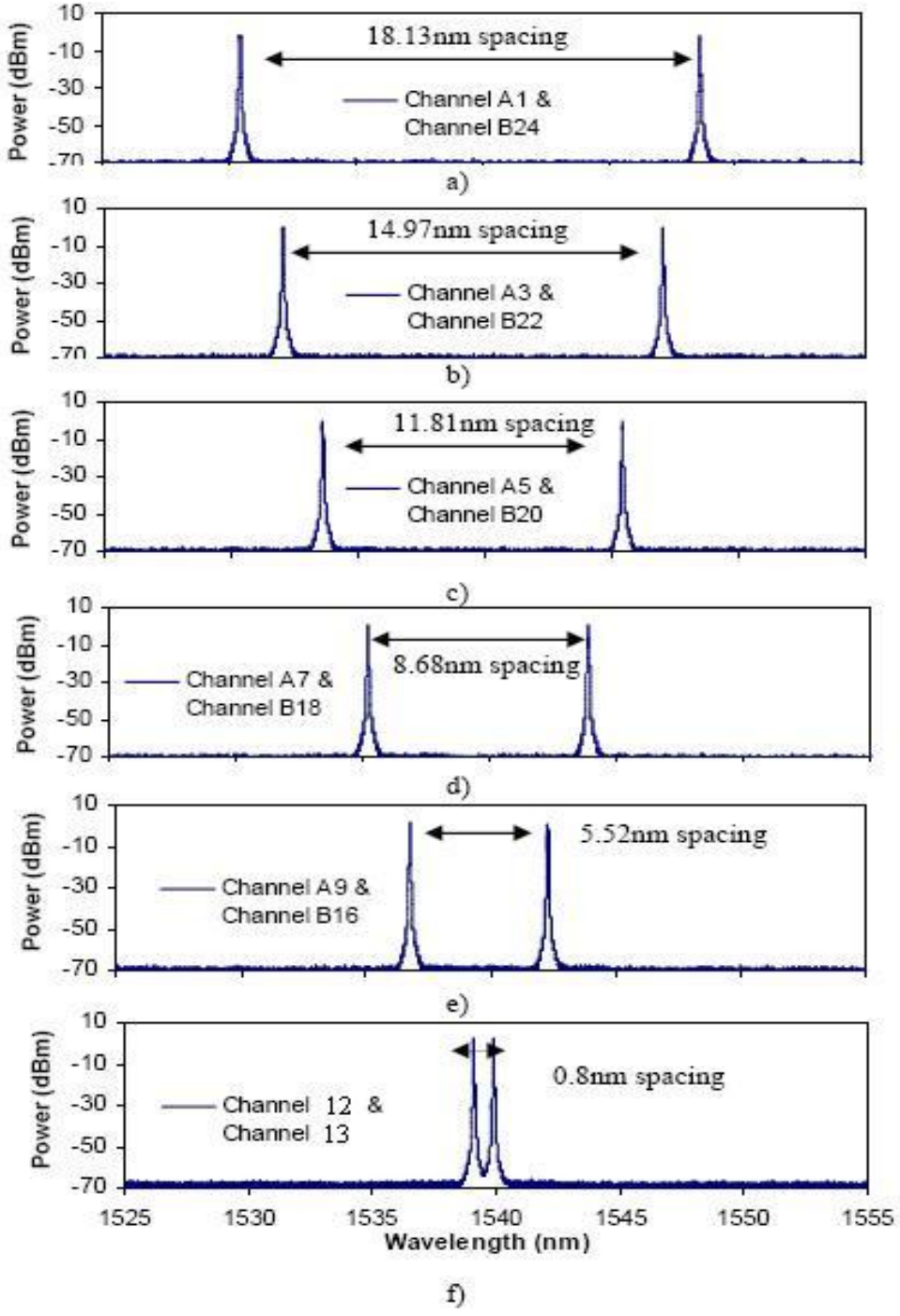

Figure 4.5: The tunable range from (a) the widest to (f) the narrowest spacing of the proposed DWFL [30].

Figure 4.6 shows the spectrum of the dual-wavelength fiber laser outputs that are taken in pairs from Channel 1 and Channel 24, Channel 2 and Channel 23, Channel 3 and Channel 22 until Channel 12 and Channel 13. The superimposed output scan be seen to be quite flat with a relatively minor fluctuation. By virtue of the cavity loss control technique used in this experiment, it is easier to obtain a balanced dual-wavelength output power by just controlling the power inside the cavity to eliminate the domination of one particular wavelength in order to obtain a stable dual-wavelength output.

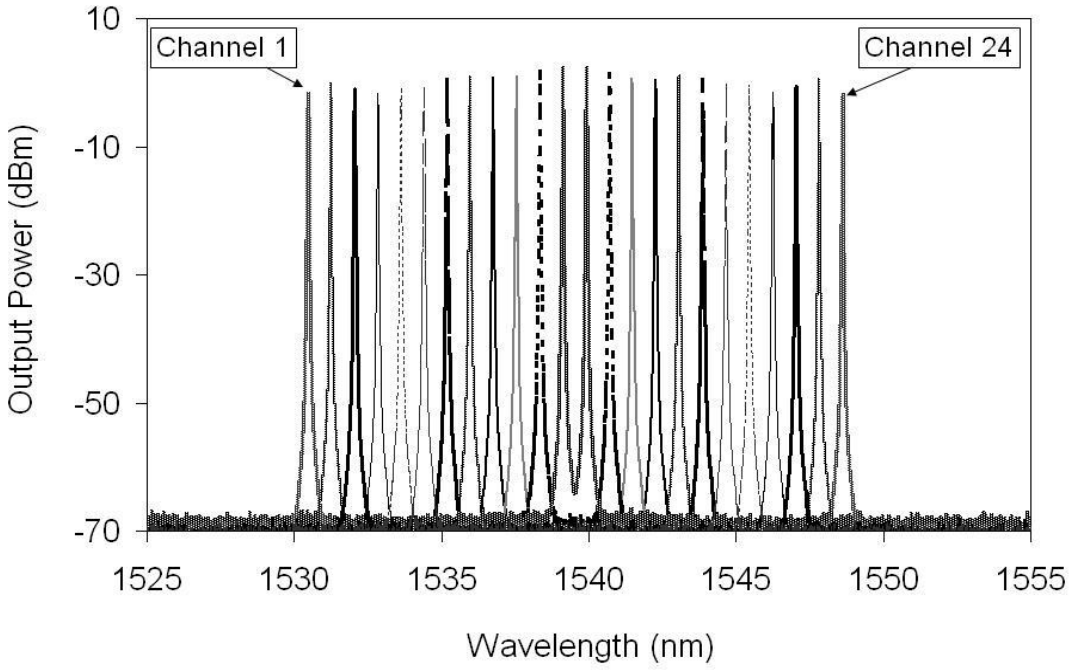

Figure 4.6: Spectrum of the dual-wavelength fiber laser for 12 pairs of dual-wavelength outputs starting from Channel 1 and 24, Channel 2 and Channel23 until Channel 12 and Channel 13.

Figure 4.7 shows the output powers of each of the 24 channels of the AWG with each channels taken in pairs, as with the data presented in Figure 4.6. The output powers for all channels can be seen to be quite flat with each pair having almost the same output power. This is due to the fact that we only measure one pair at a time, and adjust the power of each wavelength in the pair so that they are roughly equivalent. The flatness of the output powers is because the total power used in each pair is almost the same. In this experiment, only twelve channel combinations are being considered even though there are many other ways of selecting the two channels, as the principle does not depend on the combination of particular wavelengths. The average output power obtained in this experiment is 0.12 dBm with a maximum difference between the highest and lowest output powers of 4.51 dB.

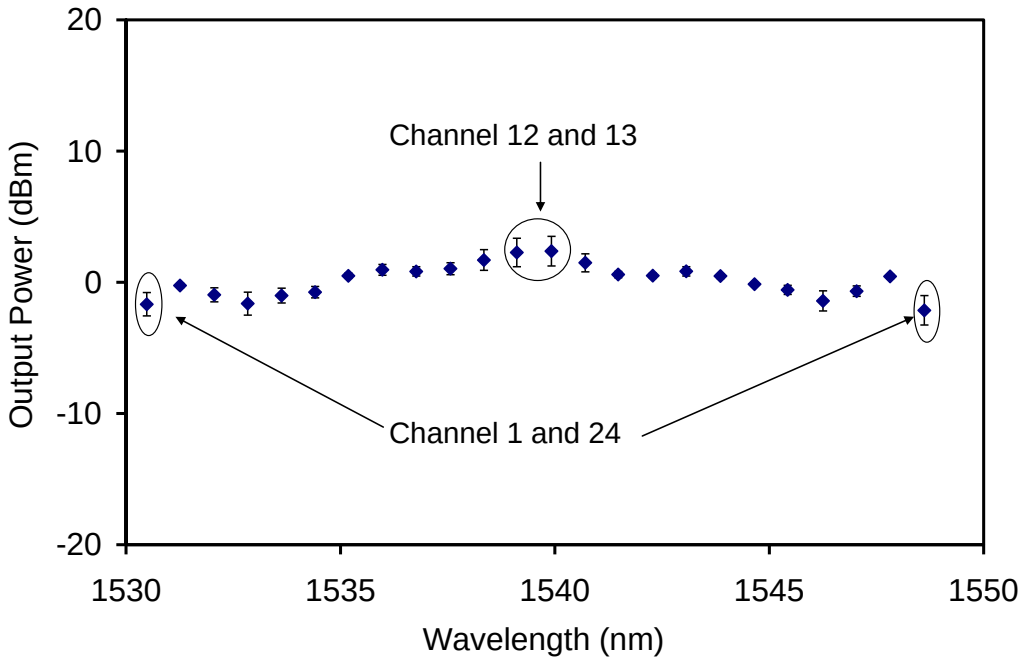

Figure 4.7: The DWFL output that is taken in pairs from Channel 1 and 24 to Channel 12 and 13.

Figure 4.8 shows the SMSR for all 24 channels of the AWG obtained from the proposed setup with an average value of 67.86 dB. The SMSR for all of the wavelengths show only small fluctuations with a maximum difference of 3.46 dB. It can be observed that the SMSR trend is similar to the output power trend. The SMSR is dependent on the peak power of the DWFL, and from Figure 4.8 the stability of the SMSR of the dual-wavelength laser over a wide range of wavelengths implies that it can be used for applications which require a dual-wavelength fiber laser with a switchable stable output power.

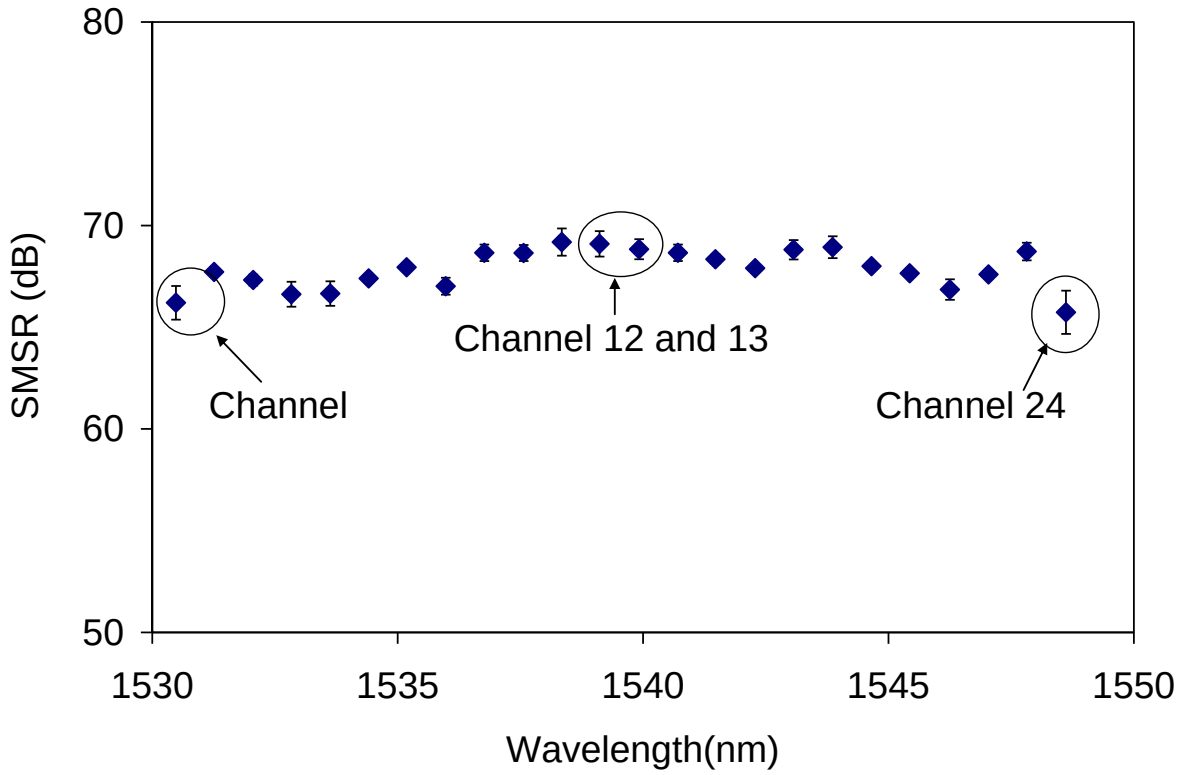

Figure 4.8: SMSR with different wavelength channel which is taken in pairs from Channel1 and 24, Channels 2 and 23 until Channels 12 and 13.

The durability and life expectancy is verified by investigating the temporal stability of the fiber. This is done by monitoring the output of the laser for a continuous operation time intervals of 5 minutes for over an hour. Figure 4.9(a) shows the output spectrum of a DWFL with a spacing of 18.13 nm at different times within a period of one hour. Figure 4.9(b) shows the same DWFL with the narrowest spacing of 0.08 nm over the same duration.

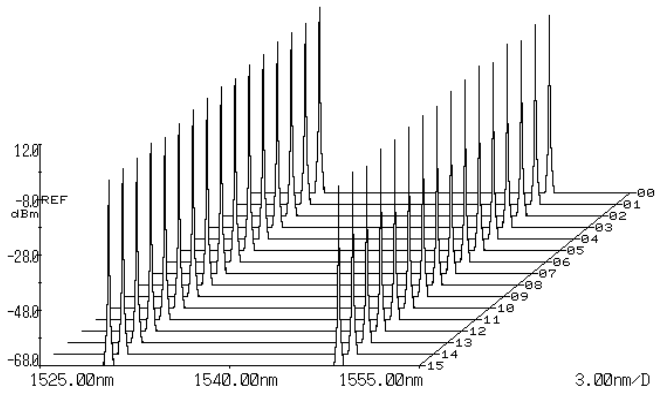

(a)

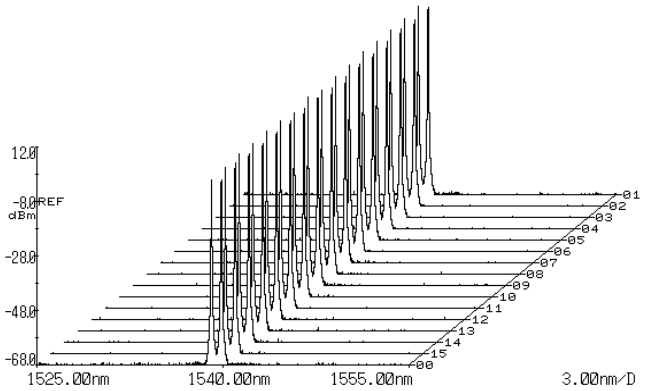

(b)

Figure 4.9: The operational stability of the DWFL for (a) the largest wavelength spacing from channel A1 and B 24and (b) the narrowest tuning range from channel A12 and B13 for a continuous operation time of one hour [30].

It is evident that in both cases, the laser output is generally very stable over the one-hour period. Therefore, this technique is able to overcome the issue of mode competition for long periods of time even with a relatively narrow spacing.

Figure 4.10 shows various wavelength spacings for the dual-wavelength fiber laser. The switching from one wavelength spacing to another is being done by first identifying which of the two cavities is higher in power. Once this cavity is identified, the process of balancing the dual-wavelength fiber laser output power is done by measuring the amount of attenuation needed to get the balance dual-wavelength output. It can be seen from the figure that the power does not vary significantly, thus providing a stable output for wavelength switching of the dual-wavelength fiber laser. The same design was also reported as a further extension of this work, operating in the 1060 nm region by using a ytterbium doped fiber as the active gain medium [31] .

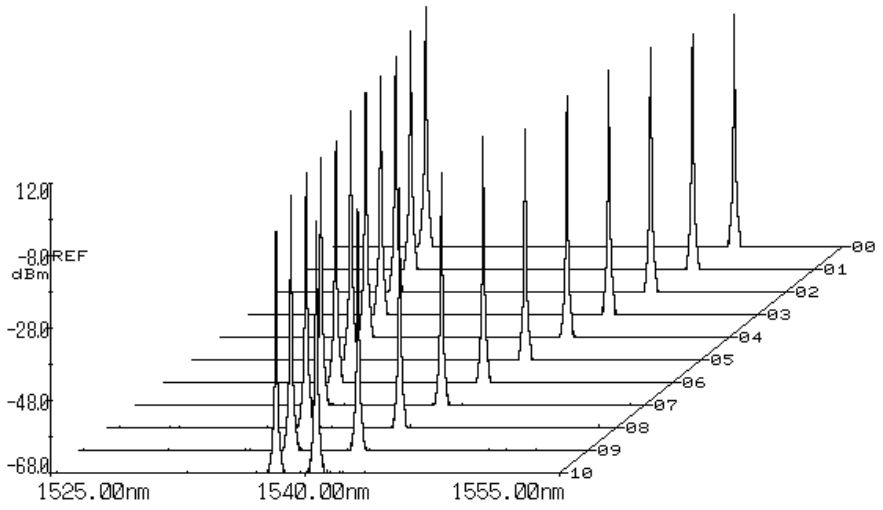

Figure 4.10: The tuning spectrum for all of the tuning spacing from the narrowest tuning range (0.08nm) to the widest tuning range (18.13nm) [30].

4.2.1.2 The DWFL in Linear Cavity Configuration

It is also possible to create a DWFL within a linear cavity using the same principles as that of a dual-ring laser. To accomplish this, an experimental setup as shown in Figure 4.11 comprising of a short length of 5 m EDF with a dopant concentration of 900 ppm (absorption 11.9 dB/m at 980 nm) as the active gain medium is used. The EDF is pumped by a 980 nm laser diode operating at 110 mW through a 980/1550 nm WDM fused biconical coupler. The front reflector in this setup is a composition of a 3-port optical circulator (OC) at 1550 nm with port 1 connected to a 90:10 fused coupler and the other end looping back to the optical circulator. The 10% port of the fused coupler is connected to the OSA with a resolution of 0.02 nm which also acts as the output coupler. Port 2 of the OC is connected to the input port of the WDM coupler. The back reflector consists of a 1 x 16 AWG at 100 GHz inter channel spacing with its output port at two different channels connected to a C-band broadband fiber Bragg grating (BB-FBG).

The ASE from the gain medium emits at both ends of the EDF. The portion of ASE that travels to the 1 x 16 AWG are then sliced into 16 different outputs with interchannel spacings of 0.8 nm which ranges from 1536.7 nm to 1548.6 nm. For generating the DWFL outputs purposes, two output channels of the AWG are connected to a broadband FBG reflector which will be reflected back into the gain medium and travel towards the optical circulator.

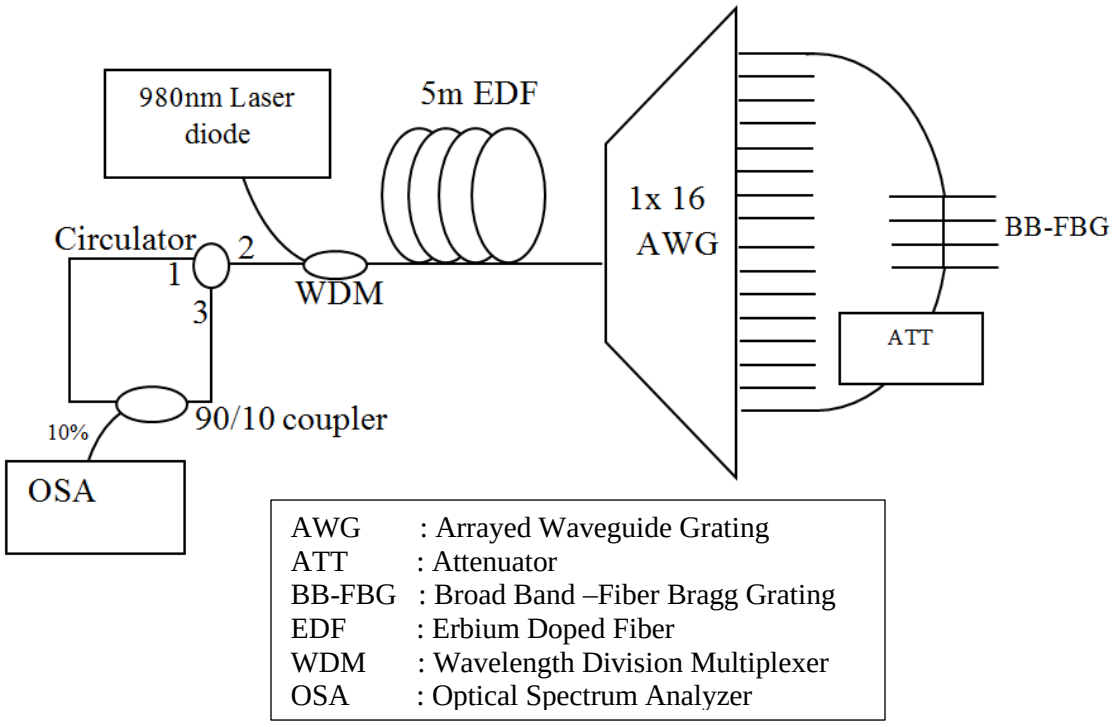

Figure 4.11: Experimental setup of DWFL in a linear cavity configuration [32].

These two wavelengths are then amplified by the EDF gain medium and then reflected by the optical circulator. The dual-wavelength outputs are taken out at the 10% port of the fused coupler. This process is then repeated and the spacing between the two wavelengths can be adjusted by taking outputs at different channels.

As a result of the homogeneous broadening in the EDF, a stable operation of the DWFL is difficult. This is largely due to the fact that the longer wavelengths generally have a lower threshold compared to the shorter wavelength that leads to a lower energy to support the oscillation. Subsequently, the longer wavelengths will become dominant, thereby reducing the amplitude of shorter wavelengths. To overcome this problem, an optical attenuator is placed at the output end of the high numbered channels(Channel 9 to Channel 16) in order to control the power of the longer wavelength, thus generating the dual-wavelength output.

The wavelength selection of this experiment began with the widest spacing, which is 12 nm for channels 1 and 16, followed by 10.4 nm for channels 2 and 15 and so on down to 0.08 nm for channels 8 and 9.

Figure 4.12 shows the spectrum of the dual-wavelength fiber laser outputs that are taken in pairs from Channel 1 and Channel 16, Channel 2 and Channel 15, Channel 3 and Channel 14 until Channel 8 and Channel 9.

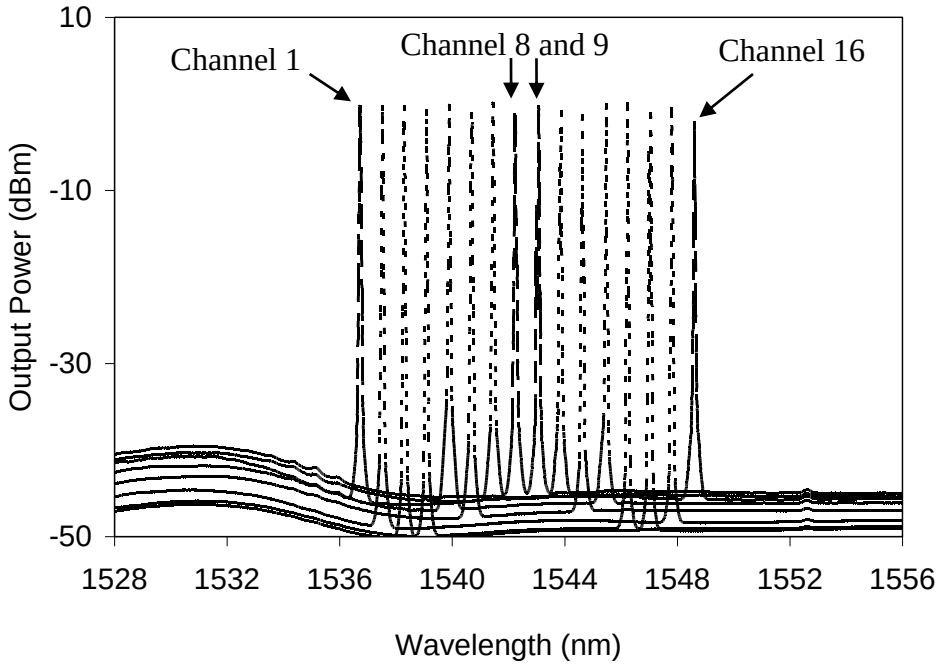

Figure 4.12: The tuning spectrum for all of the tuning spacing from the narrowest tuning range (0.08 nm) to the widest tuning range (12 nm).

The total output of all pairs is quite flat with some minor fluctuations, as can be seen from the graph. As the spacing of the dual-wavelength fiber laser is varied from the widest to the narrowest spacing, the attenuation applied to the longer wavelength of the pair decreases. As an example, the attenuation given to the DWFL for channel 9, the longer of the two

wavelengths between channels 8 and 9, is much smaller compared to the attenuation that is given to channel 16, which is the longer wavelength in the pair of channels 1 and 16. This is expected from the behaviour of the threshold energy of different wavelengths that was discussed previously.

Figure 4.13 shows the output powers of each of the 16 channels of the AWG which each channels taken in pairs starting from Channels 1 and 16, Channels 2 and 15, and so on until Channels 8 and 9. The output powers for all channels are quite flat with each pair having almost the same output power since only one pair of the DWFL is taken at a time, as is the case of the dual-ring cavity DWFL.

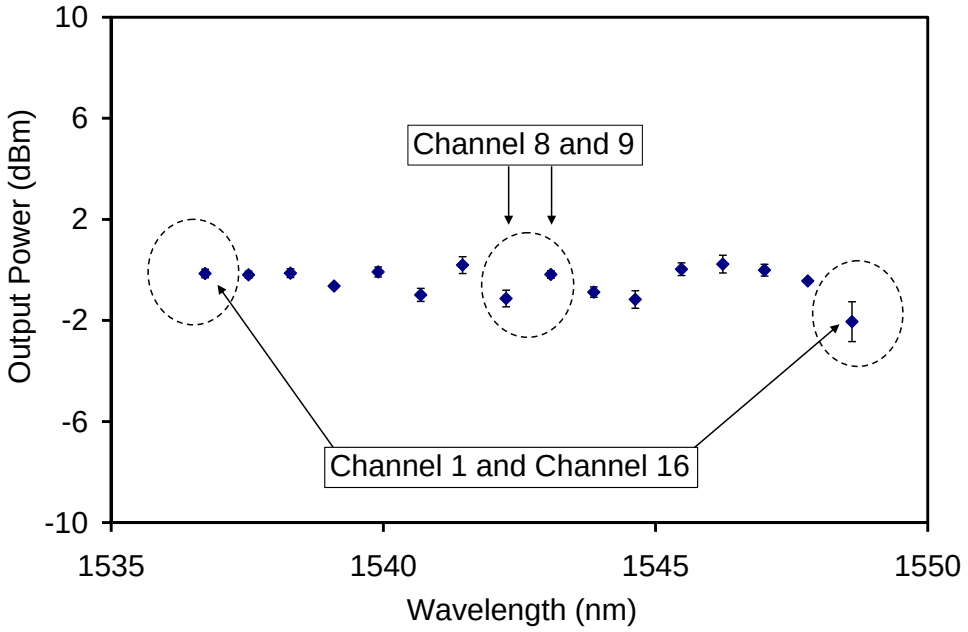

Figure 4.13: Output power value for each channels combination of the DWFL output.

In this experiment, only eight ways of selecting the channel from the AWG from the widest (Channel 1 and 16) to the narrowest spacing (Channel 8 and 9) are considered even though many other ways of selecting the two channels exist. The average output power obtained in

this experiment was -0.47 dBm with a maximum difference between the highest output power and lowest output power was calculated to be 2.28 dB.

Figure 4.14 shows the SMSR of the DWFL of the linear cavity configuration with the same selection of channel pairs. The average of SMSR is 44.32 dB with a maximum difference between the highest output power and lowest output power was 10.74 dB. As depicted in the graph, the SMSR value for the channel with the longer wavelength is slightly higher than that of the shorter wavelength, which is due to the higher ASE around this region because of the emission behaviour of erbium. This can be observed from Figure 4.12 where the ASE level is quite high at around 1532 nm wavelength. It also can be observed that each pair obtained in this experiment has an SMSR which is almost equal, as is expected.

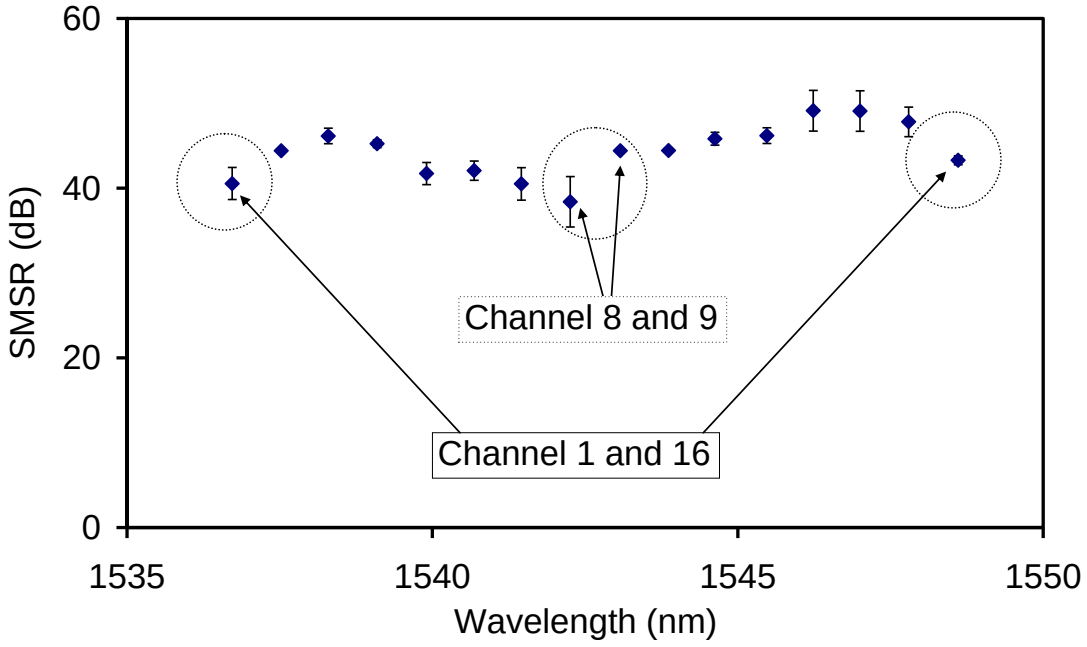

Figure 4.14: SMSR value for each channels of the DWFL output.

The stability of the dual-wavelength output is investigated by plotting a three dimensional graph of the output at 10-minute intervals for a continuous operation of 60 minutes. Figure 4.15 shows the stability of the dual-laser with the widest possible spacing of 12 nm for a continuous operation time of more than an hour. It can be clearly seen that the output is extremely stable over the entire duration of the experiment, as is the case of a dual-ring cavity dual-wavelength fiber laser. Therefore, this can act as an alternative method to create a dual-wavelength laser for the applications in which the previous setup might be inappropriate.

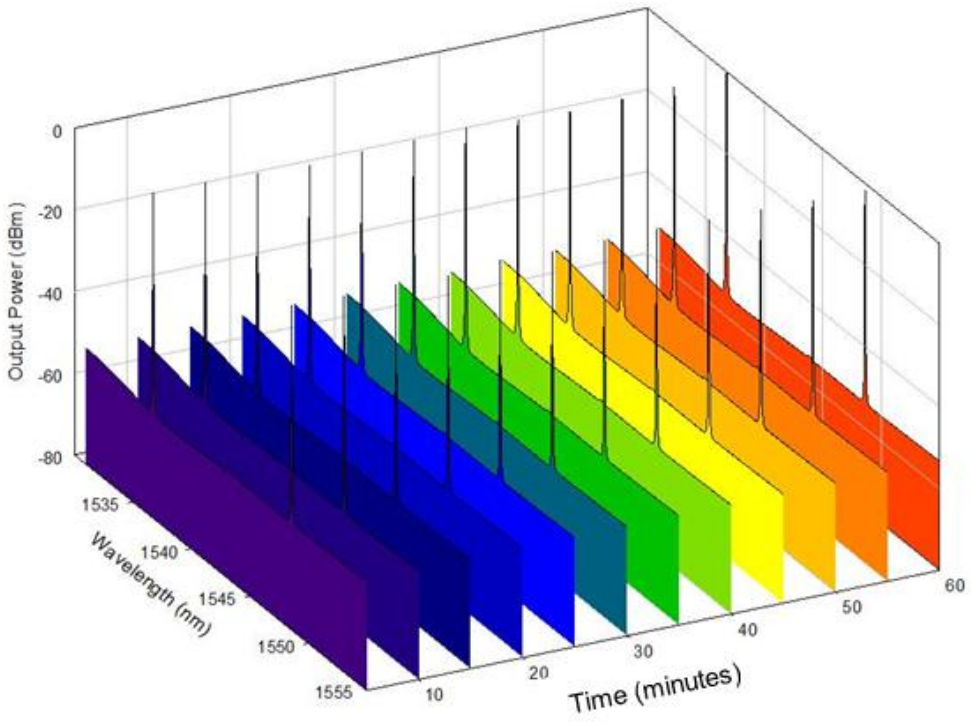

Figure 4.15: The three-dimensional graph of the dual-wavelength output at 10 minute intervals for a continuous operation of 60 minutes for channels 1 and 16.

4.2.1.3 Comparison Between Linear and Ring Cavity Configuration

A comparison between the dual-ring cavity and the linear cavity fiber lasers was made to investigate the difference in performance between these two configurations. However, due to the limitations in the laboratory, the 16 channel AWG, rather than the 24channel AWG, was employed for both setups.

The linear cavity configuration, as shown in Figure 4.16(a), consists of a 5 m Metrogain (Fibercore) EDF with an absorption coefficient of 11.9 dB/m and16 dB/m at 980 nm and 1550 nm, respectively. The EDF is pumped by a 980 nm laser diode at 110 mW via a 980/1550 nm WDM. The Metrogain EDF acts both as a source for the ASE as well as the amplifying medium for the DWTFL. The output ASE will travel in both directions, and the ASE on the right-hand side will be sliced by the 1x16 AWG with an interchannel spacing of 100 GHz (0.8 nm). To generate the dual-wavelength output, any two channels of the AWG can be combined to a BB-FBG which also acts as a ‘mirror’ on the right-hand side of the experimental setup. The ASE will be sliced into 16 different wavelengths, from 1536.7 nm (Channel 1) to 1548.6 nm (Channel 16), and for instance, Channel 1 and Channel 16 can be connected to the input ports of the BB-FBG which will then reflect these two wavelengths back into the AWG. The combined output will then travel into the 5 m EDF to be amplified and will be emitted at the 1550 nm port of the WDM towards Port 2 of the OC. Port 2 is then connected to Port 3 whereby the dual-wavelength output will travel towards the 90:10 coupler with the 10% port connected to the OSA. This dual wavelength will continue to travel to Port 1 and be emitted to Port 2 again to travel into the amplifying

medium for further amplification and moving onwards to the 1x16 AWG, where the whole process repeats until two lasing wavelengths of the desired power are obtained. The tunability of these two wavelengths is accomplished by selectively choosing the combinations of the channels. As was done previously, an optical attenuator is placed at the longer wavelength outputs as a means to balance the dual-wavelength output power, so as to create two lasing wavelengths of equal power.

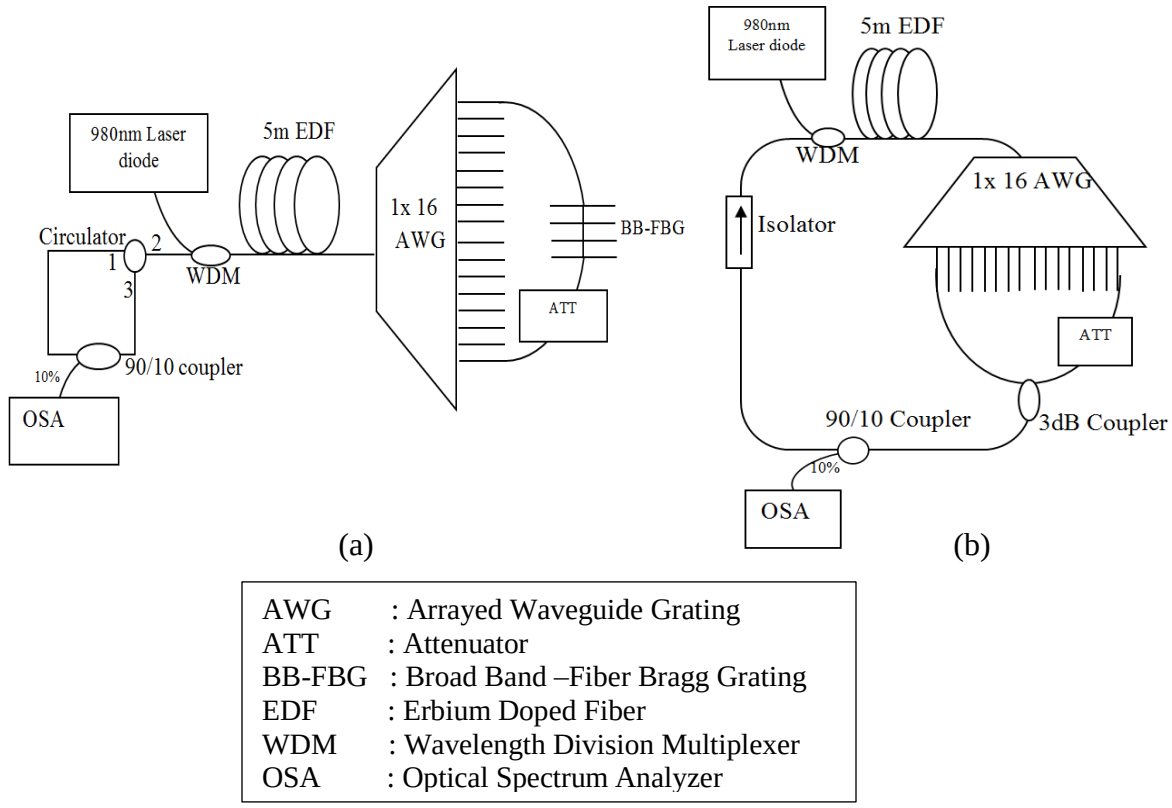

Figure 4.16: Experimental setup of (a) linear cavity and (b) ring cavity configurations [33].

A similar approach is taken for the ring configuration as shown in Figure 4.16(b). In the ring configuration, there is no need for reflecting 'mirrors', instead the ASE generated on the right hand side of the EDF travels to the 1x16 AWG where it is sliced into 16 different wavelengths (channels) similar to the linear cavity. For a dual-wavelength output, two of the channels are combined using a 3 dB fused coupler which is then connected to a 90:10 fused coupler in the ring cavity. As with the linear cavity configuration, the 10 % port is connected to an OSA, while the 90 % port is connected to an isolator (to ensure unidirectional travel) and onward to the 1550 nm port of the WDM. The common port of the WDM is connected to the EDF, which provides amplification and also completes the ring cavity. As with the linear cavity, an attenuator is placed at the longer wavelength channel. Both configurations are analysed for their output spectra, output power, SMSR and stability to determine which of the two designs provides the higher output power as well as good SMSR. The largest channel spacing available in this experiment is 11.9 nm (Channels 1 and 16) and the narrowest spacing is 0.8 nm (Channels 8 and 9). This is not restrictive to these channels; various channel pair configuration can be created to provide a near continuous channel spacing.

The output powers are measured for different pair combinations are shown in Figure 4.17. The pair's wavelengths are given as the abscissa of the graph and the ordinate is the output power. From this figure, the linear cavity has an average power of about 0 dBm with a power variation of 2.3 dB. In the case of the ring cavity, the average power is about –5 dBm with a power variation of 1.1 dB. Although the linear cavity has a higher output power as compared to the ring cavity, it fares badly in terms of the SMSR as given in

Figure 4.18. The slight variation in the power output of Figure 4.17 can be further improved by proper cleaning of the Port channels of the AWG.

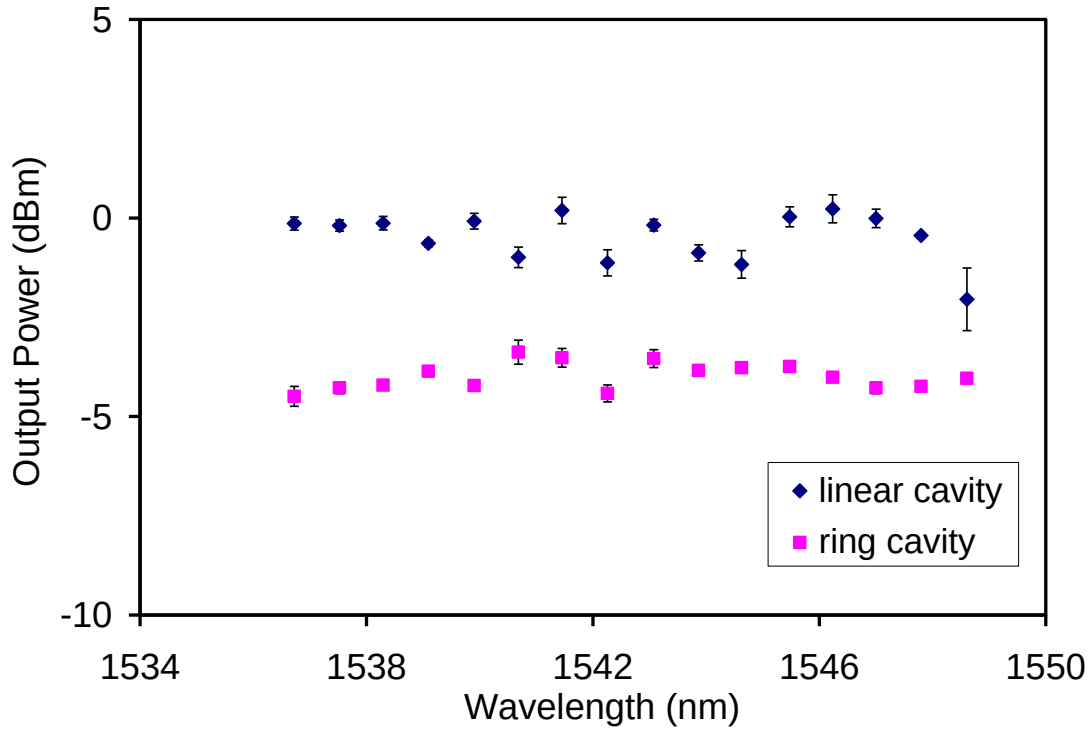

Figure 4.17:DWFL Output Power for the Ring and Linear Cavity Configurations[33].

As shown in Figure 4.18, the SMSR of the ring cavity is superior as compared to that of the linear cavity, with the average SMSR value of 66 dB for the ring cavity compared to an SMSR value of 44 dB for the linear cavity. The SMSR variation between the pair channels is approximately 2.5 dB for the case of the ring cavity, whilst for the linear cavity the variation is about 10.7 dB. This implies that the output power of the dual-wavelength output from the ring cavity is more consistent against the various combinations of the pair channels. In the case of the linear cavity, the large variation of the SMSR in the pair channels makes it unsuitable for applications which require a tunable dual-wavelength

output with constant power. From this, we can infer that the ring cavity configuration will be an important source for a dual-wavelength with a stable and constant power.

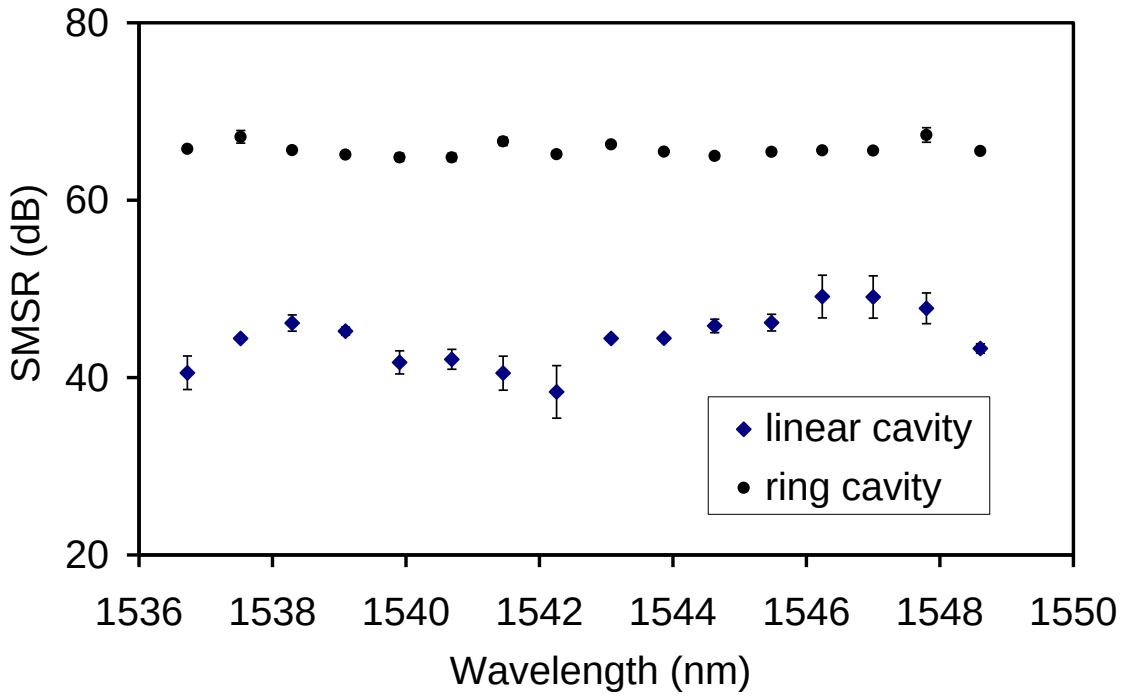

Figure 4.18: The SMSR value for linear and ring cavity configuration [33].

Figure 4.19 shows the spectrum profile for the DWTFL for the linear and ring cavity configurations. Figure 4.19 (a) shows the dual wavelength output taken in pairs from the largest to the smallest channel spacing, i.e. Channel 1 and 16 (largest), Channel 2 and 15 and so forth until Channel 8 and 9 (smallest) which are super-imposed. The peaks ride on the ASE background where the floor is about -45 dBm and the inset indicates the ASE spectrum of the 5 m Metrogain fiber. The maximum power of the dual-wavelength output is about 0 dBm.

In the case of the ring cavity, the maximum power of the dual wavelength output is about – 5 dBm and has a constant value throughout the different dual wavelength pairs. As can be seen from the graph, the dual wavelength pairs do not ride onto the ASE spectrum thereby giving a better SMSR. The tunability of the wavelength spacing can be chose by taking various combinations of the output channels (in addition to the pair scheme as proposed here).

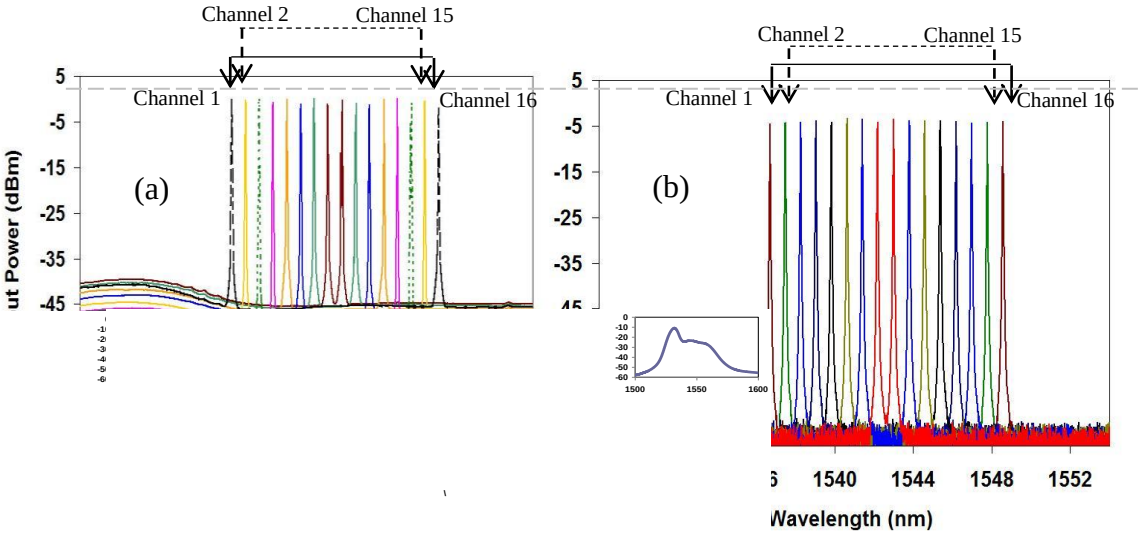

Configuration and (b) Ring
e 5m Metrogain EDF[33].

Figure 4.20 shows the dual-wavelength fiber laser spectrum for the ring cavity and the linear cavity configurations. It can be seen that the noise level for the ring cavity is significantly lower than the linear cavity configuration with the difference calculated to be roughly 15dB. A higher level of noise near 1530nm region for the linear cavity is due to higher ASE level in 1530nm wavelength as compared to the 1550nm wavelength.

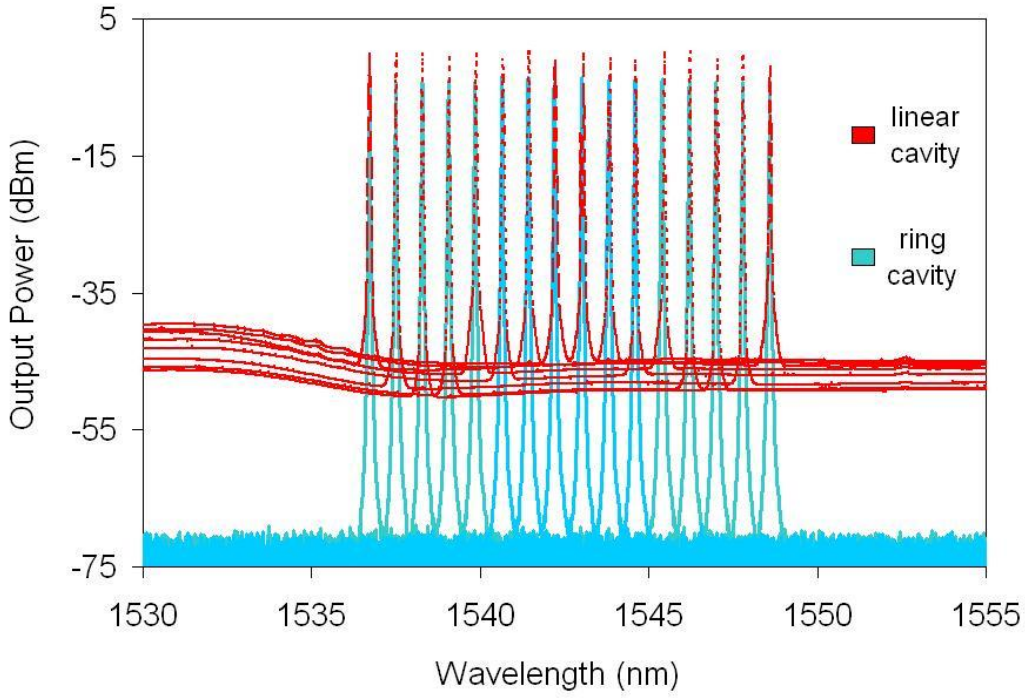

Figure 4.20: The spectrum of dual-wavelength fiber lasers for eight pairs of dual-wavelength outputs.

Figure 4.21 (a) and (b) shows the 3-dimensional time evolution graph of the dual-wavelength fiber laser for channels 1 and 16 in both the ring and linear cavity configurations for a continuous operating time of 60 minutes. Both configurations are very stable with only minor fluctuations observed for the duration of the experiment. However, it can be seen clearly that the noise level of the linear cavity is slightly higher compared to the ring cavity, which contributes to a smaller SMSR value. Therefore, it is more advantageous to use the ring cavity as a seed signal for telecommunications systems as the output is extremely stable over extended periods of time.

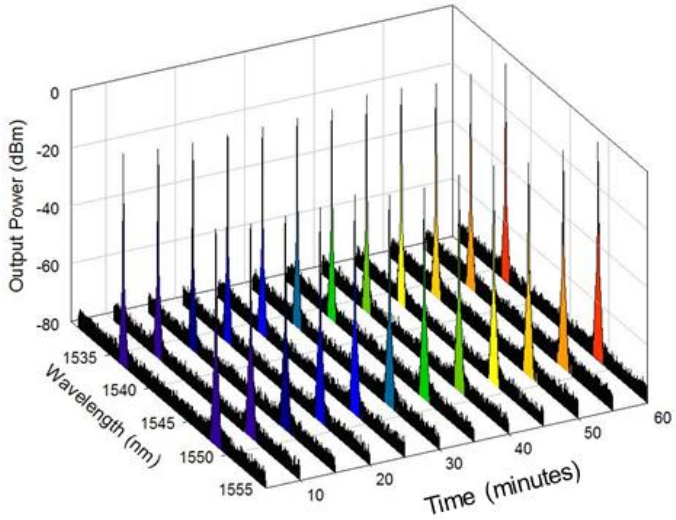

(a)

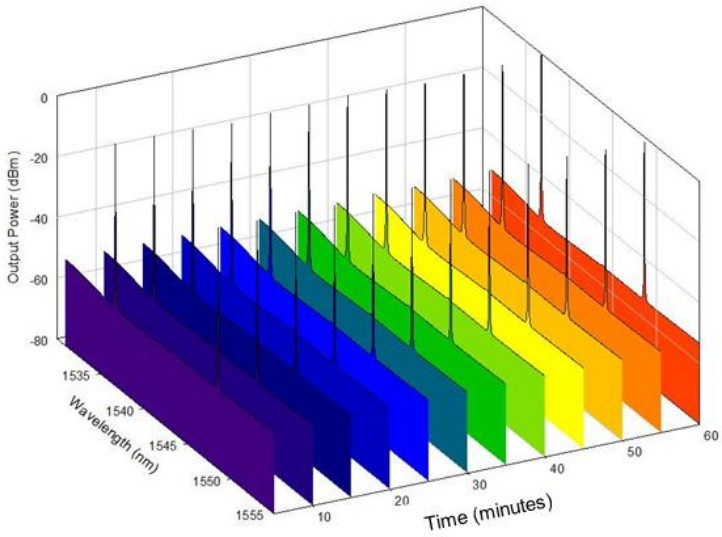

(b)

Figure 4.21: 12nm spacing of dual-wavelength fiber laser stability for (a) ring cavity and (b) linear cavity configuration [33].

4.2.1.4 Dual Wavelength High Power Fiber Laser

In this section, a high power fiber laser is designed by using the ring cavity configuration as the seed signal. The reason the ring cavity was selected, as was explained previously, is that it is more stable and more reliable due to its higher value of SMSR.

The configuration as shown in Figure 4.22 consists of two different parts, namely, a seeding signal and a booster amplifier. The seeding signal in the first section comprises of a ring cavity with the same working principle as the one used previously, employing the 1 x16 AWG. Channels 1 (1536.7 nm) to 8 (1542.3 nm) of the AWG are grouped together and are connected to an 8x1 optical switch denoted as OS1, while channels 9 (1543.1 nm) to 16 (1548.6 nm) are grouped together and connected to second optical switch denoted as OS2. The only difference of this ring cavity configuration is the use of a 2x2 optical variable coupler (OVC). The OVC works by varying the coupling ratio between the two inputs which allows for the balancing of the amplitudes between the two inputs. The OCS1 and OCS2 are connected to the input of the 2x2 OVC. One of the 2X2 OVC output ports is then connected back to the 1550 nm input port of the WDM1 coupler via the optical isolator to complete the cavity.

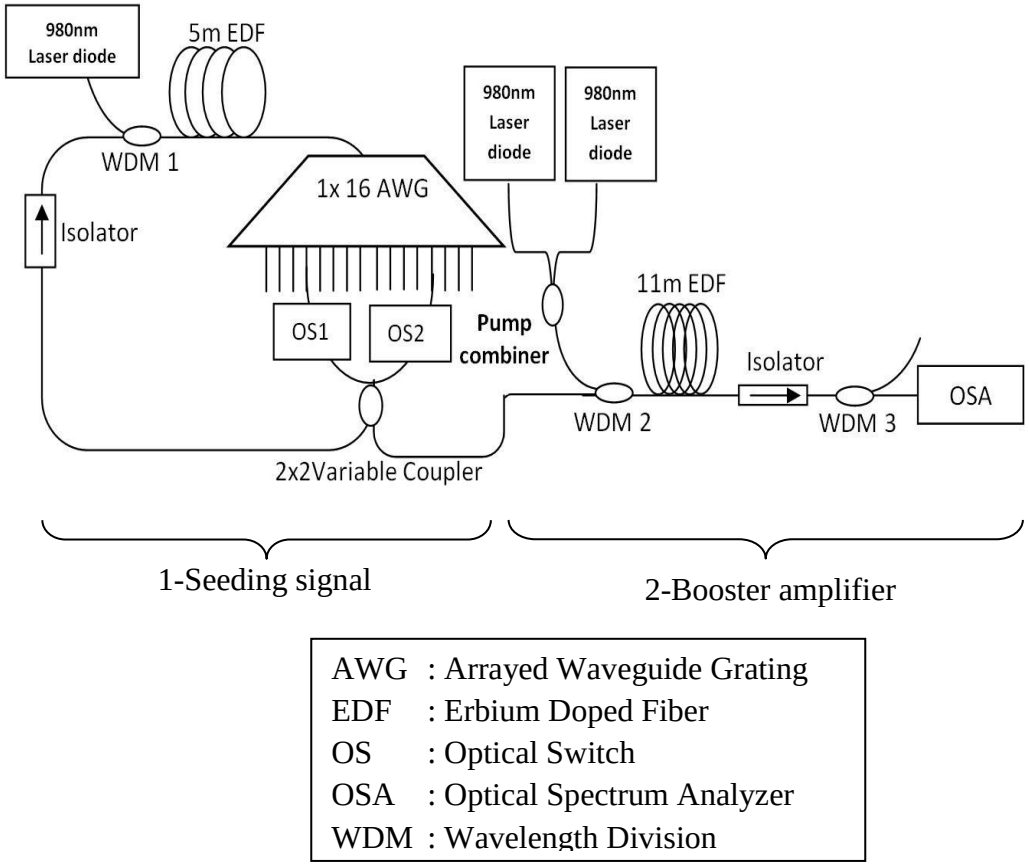

Figure 4.22: Experimental setup showing the various components for generating the HP-DWTFL [34].

The other OVC port is connected to a second EDF with 11 m long via a 980/1550 nm WDM2 coupler. This is where the second section, the booster amplifier, begins. The 11 m Metrogain EDF used has an absorption coefficient of 11.9 dB/m at 979 nm and 16.4 dB/m at 1531 nm, which works as a second gain medium. Optimum amplification of this 11 m EDF requires a high pump power. Therefore a pump combiner is used to connect two individual 980 nm laser diodes to produce a total pump power of 430 mW before it is connected to the fiber via a 980/1550 nm WDM coupler, labelled as WDM 2.

The 11 m EDF is then connected to an isolator and subsequently to another WDM coupler (WDM 3) before being connected to the OSA for spectrum analysis. The WDM 3 coupler inserted before the OSA to act as a filter to ensure that only the 1550 nm output enters the OSA. Therefore, the ring cavity works as a seeding signal (DWFL provider) while the 11 m EDF acts as a second amplifier which further amplifies this DWFL signal to provide a higher output power.

As discussed earlier, the gain media used in the proposed setup are EDFs which is well known for its inherent homogeneous broadening effect. Therefore, the dual-wavelength outputs tend to lase at only the dominant wavelength. In this case, the use of the OVC provides a cavity loss control mechanism to control the input entering the second stage of amplification to ensure the exact peak value of DWFL for the production of a balanced high power DWTFL.

Figure 4.23 shows the ASE spectrum of the 11 m EDF (second EDF) amplifier without the DWFL seeding signal. As depicted in the graph, maximum output power, and therefore the maximum amplification, is centred roughly at 1560 nm. This is due to fact that the EDF gain profile shifts to longer wavelength as its length increases [18]. However, due to the limitation of the AWG, the DWFL is produced only in in the C-band region (between 1530 nm and 1545 nm). If this limitation can be overcome, in principle, wideband lasing from the C-band to the L-band is possible. The uneven distribution of the amplification in the 1530 nm region as can be seen from the graph is later shown to be the reason for the degradation of SMSR at longer wavelengths as reported in the experimental results.

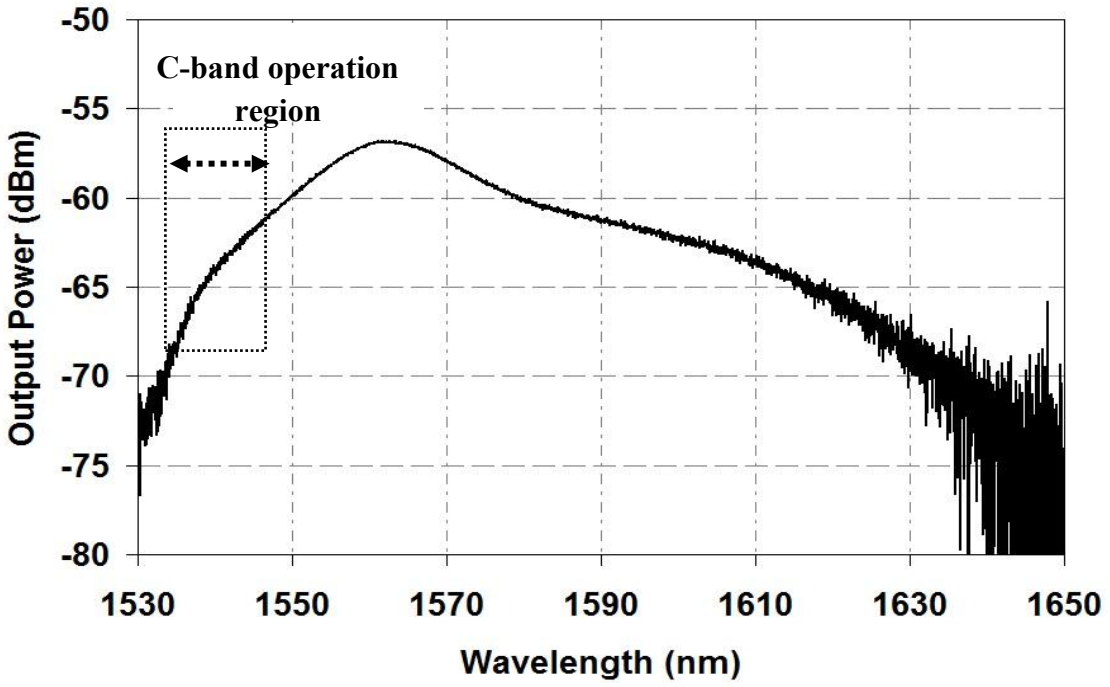

Figure 4.23: The ASE spectrum of the booster amplifier [34].

The proposed experiment actually faces two issues related to mode competition in producing a balanced dual-wavelength fiber laser. The first is mode competition in the seeding signal and this is overcome by adjusting the cavity losses inside the ring cavity. This is done by using the OVC to control the exact amount of power inside the cavity between the two wavelengths. The second and more challenging issue that the booster amplifier will also homogenously broaden only one wavelength. This is also solved by carefully varying the OVC, thereby varying the DWFL output, such that the total output of the booster amplifier is balanced. This method works as the imbalances of the output power of the ring cavity DWFL is compensated by the wavelength dependent gain in the booster amplifier as have been shown in Figure 4.24.

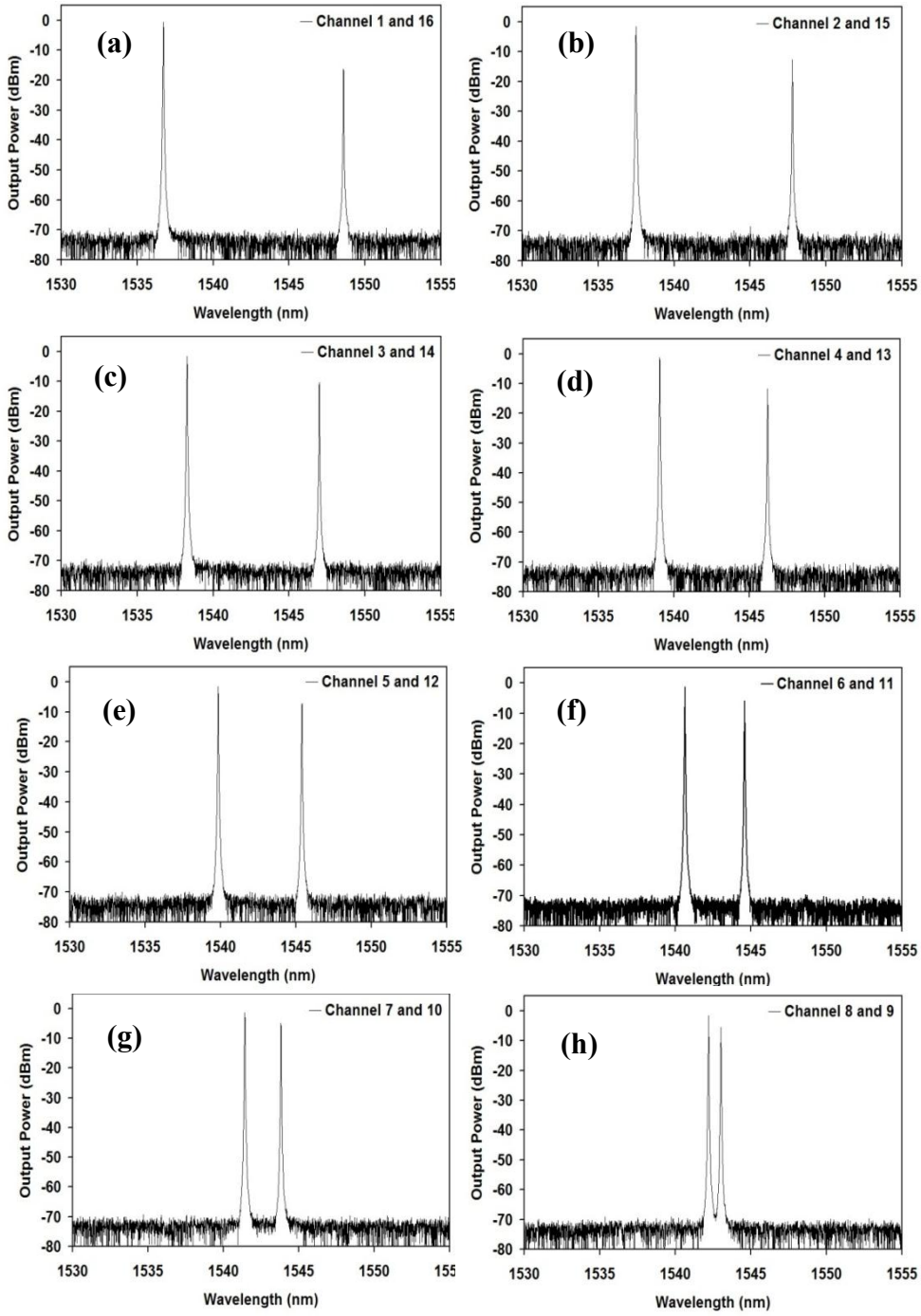

Figure 4.24: DWFL output from ring cavity (a) Channel 1 and 16, (b) Channel 2 and 15, (c) Channel 3 and 14, (d) Channel 4 and 13, (e) Channel 5 and 12, (f) Channel 6 and 11, (g) Channel 7 and 10, and (h) Channel 8 and 9 before connected to the booster amplifier [34].

Figure 4.25 shows the tuning range of high power DWTFL from the widest tuning range of 12 nm in Figure 4.25(a) for channels 1 and 16 at wavelengths 1536.7 nm and 1548.6 nm respectively, until the narrowest tuning range of about 0.8 nm in Figure 4.25(h) channels 8 and 9 at wavelengths 1542.2 nm and 1543.0 nm respectively. The broadest tuning range can be improved by using an AWG with a higher number of channels, as previously discussed. The narrowest tuning range, on the other hand, can be improved by using a lower interchannel spacing of 25 GHz which can allow a spacing of 0.2 nm. Unfortunately, the high power fiber laser produced by the proposed setup leads to four-wave mixing (FWM) inside the booster amplifier, which is triggered when the intensity of the incoming electric field is much higher as compared to the interatomic electric field, causing the generation of third harmonic effects [35]. This FWM effect can be seen to start from channels 6 and 11until channels 8 and 9, as shown in Figures 4.25(f)-(h), with the mode offset of the idler and signal wavelengths having the same spacings as the dual-wavelength spacings. The FWM effect is greater as the spacing of the DWTFL is reduced which causes a decrease in the SMSR value. It is possible to overcome this by inserting PCs to change the shape of the propagating longitudinal wave, thereby reducing the peak of the idler and signal wavelengths, thus improving the value of SMSR. This method should be extremely effective as the FWM effect is polarization state dependent. However, this was not undertaken due to limitations of time and equipment. Due to the high power of the DWFL, the ASE level is higher at longer wavelengths, causing the SMSR to be lower at longer wavelengths.

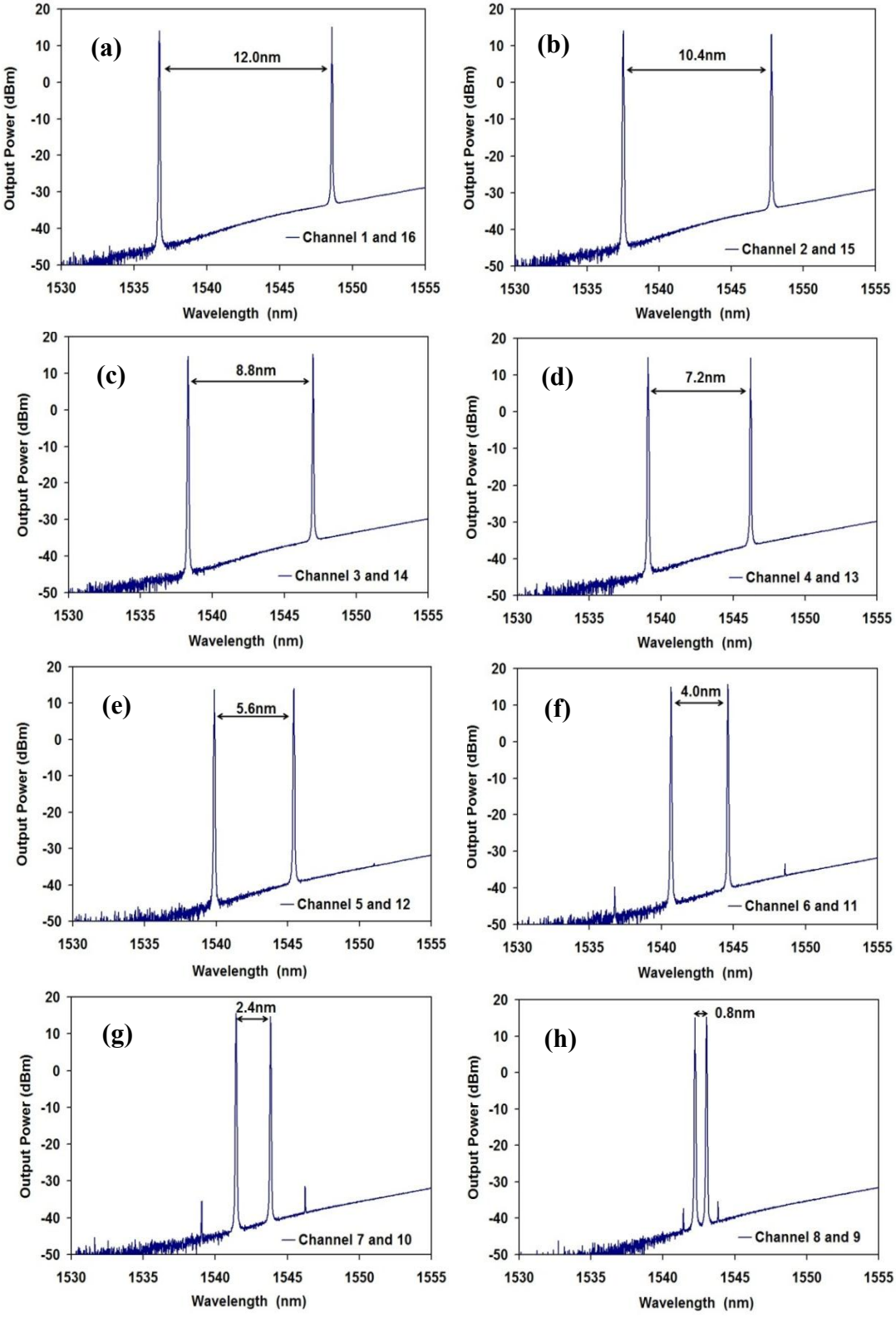

Figure 4.25: The high power DWFL tenability spectrum. (a-h) [34]

Figure 4.26 shows the output power of the high power DWFL from channel 1 (1536.74 nm) to channel 16 (1548.6 nm). The average value of the output power is 15 dBm with the highest output power coming from channel 11 (1544.62 nm) and the lowest from channel 15 (1547.8 nm) with an output power of 13.11 dBm. It can be seen that the output wavelength is distributed evenly with a separation of 0.8 nm between two neighbouring channels.

This DWFL is quite flat in terms of its output power, with a variation in power of only ±1.315 dBm, indicating the consistancy of the output power thoroughout the whole range of the DWFL. The advantage of this setup is the ease with which the laser can be managed as the switching time between two wavelengths is very short due to the use of the two OSs. However, the optical variable coupler have to be adjusted and controlled carefully to ensure that the DWFL output is balanced. The drop of the output power observed at channels 5 and 15 is probably due to higher connection losses at the connecting point of the channel ports with the optical switch. This problem can be prevented by properly cleaning the pigtails of the AWG.

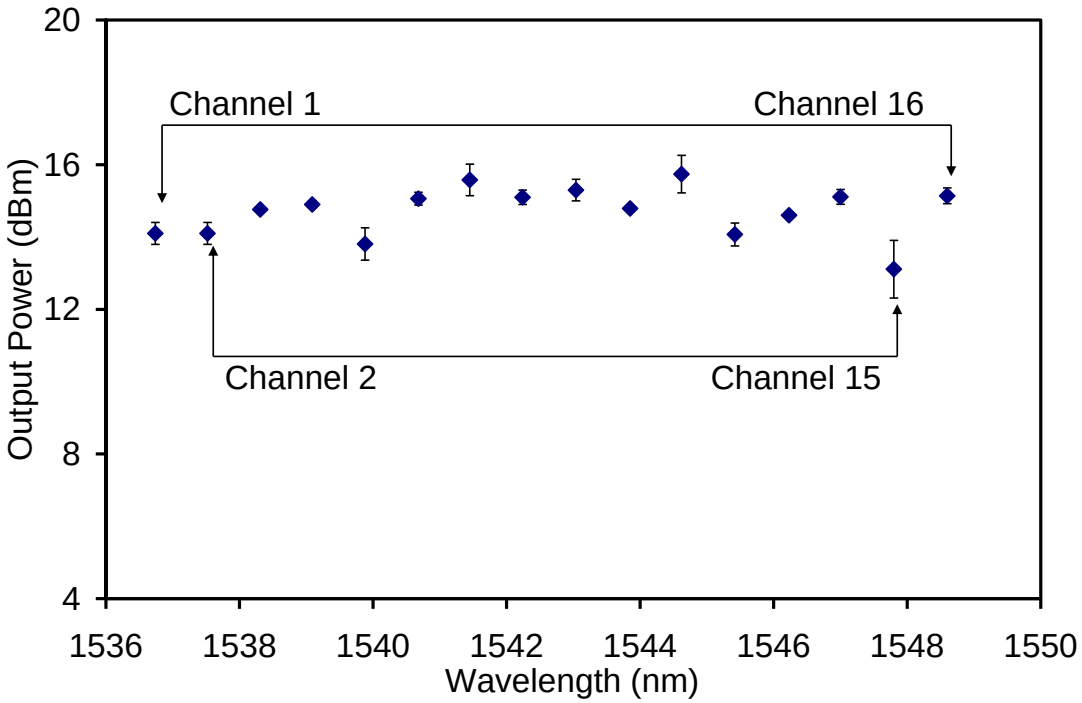

Figure 4.26: Output power of the DWFL.

Figure 4.27 shows the SMSR of the DWFL with the average value calculated to be 52.55 dB, and the maximum difference between the highest and lowest SMSR being 12.4 dB, indicating that the propoposed setup is extremely stable over a wide selection of wavelength. The highest SMSR value achieved is 58.77 dB at channel 1, while the smallest value is comes from channel 10 at 46.38 dB. The relatively high difference of 12.4 dB is due to the difference in the ASE level of the DWFL, as explained previously.

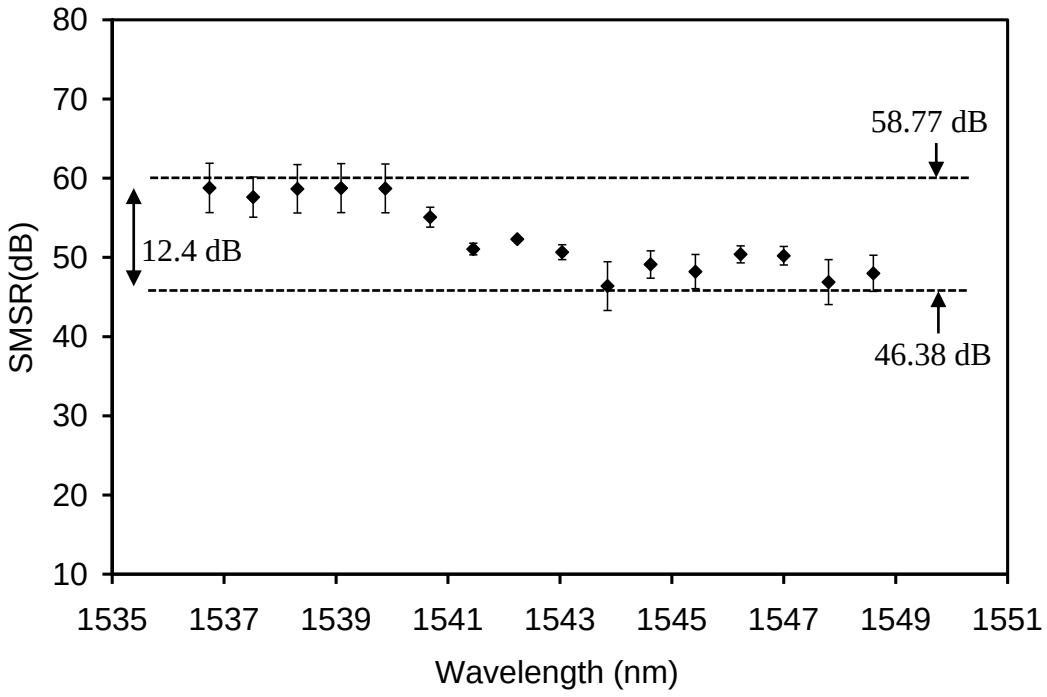

Figure 4.27**:** SMSR of the DWFL output [34].

Figure 4.28 shows the temporal evolution of the DWFL for a continuous operation of over an hour. It is obvious from the graph that the DWFL is extremely stable with only small variations in the output power. However it can be seen that the stability of channel 1and 16 is better compared to channel 8 and 9. This is due to the higher stability of the DWFL at the longer separations, as the homogeneous broadening effect is much stronger for two closely spaced wavelengths. However, this problem can be overcome by proper monitoring of the output of the setup. This is done by taping 1% of its portion to be monitored by the analyzer. Any variation in the output can be quickly adjusted by controlling the cavity loss using the OVC until the output of the DFWL is balanced.

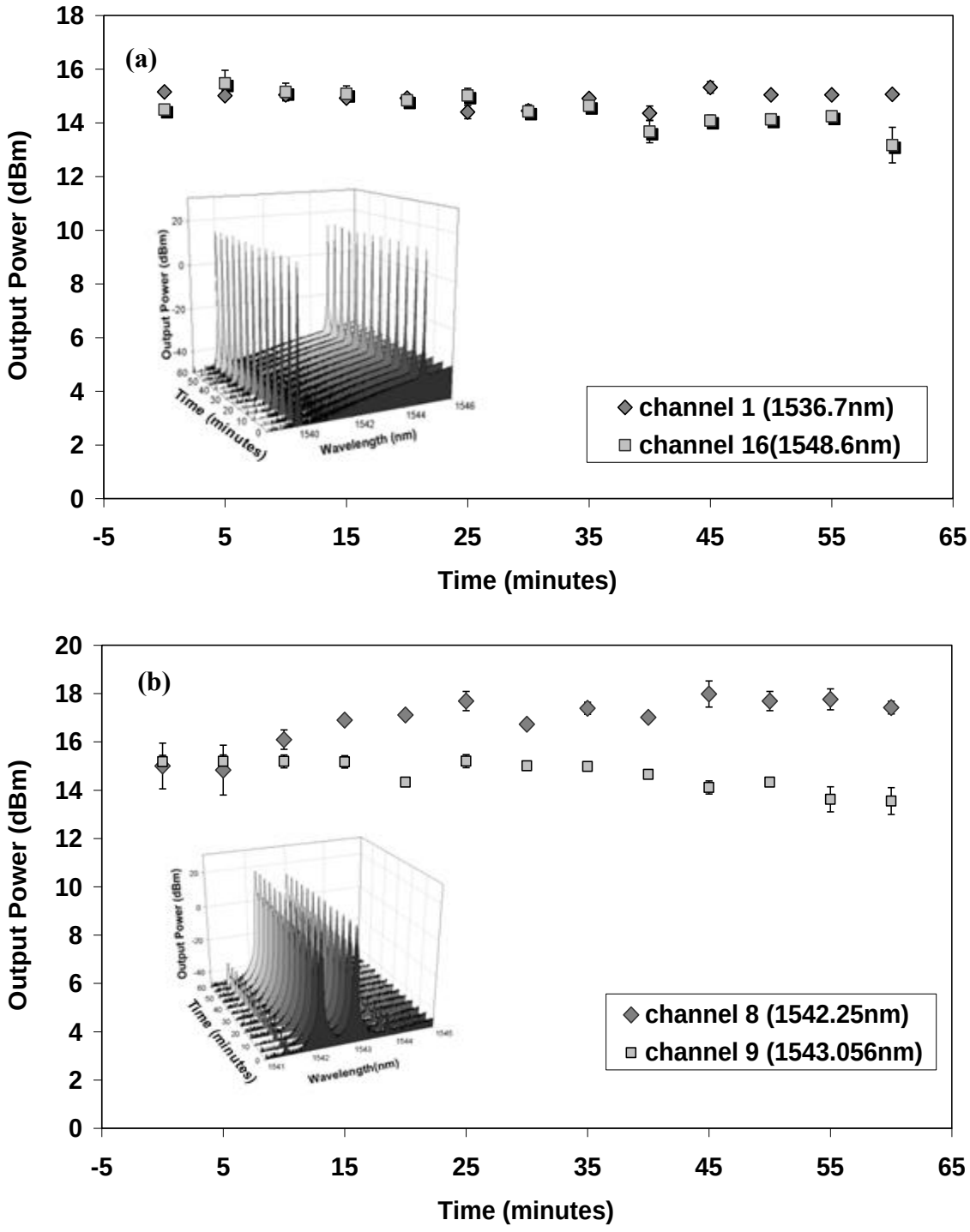

Figure 4.28: Stability of the DWFL with 7(a) the DWFL from the Channel 1 and 16 and (b) from Channel 8 and 9 [34].

4.2.2 Dual-Wavelength Fiber Laser by Using Compression and Tensile Strain FBGs

Figure 4.29 shows the configuration to generate a dual-wavelength fiber laser by using the C-band compression and tensile strain FBGs (CTS-FBGs) as the mirrors for the dual-wavelength laser which works as has been discussed previously in Chapter 3. The other components employed in this setup include a 980nm Laser diode, an isolator, a circulator, a 10dB coupler, a 3dB coupler, 5 m Metrogain EDF gain medium, and an optical variable attenuator.

The propagation of light begins in the 5m EDF which produces an ASE which then passes through an isolator. The ASE then travels through the circulator and exist at port 2, which is connected to the 3dB coupler whereby 50% of the signal travels to the first C-band compression strain FBG denoted as FBG 1 and the other 50% port travels to the C-band tensile strain FBG denoted ad FBG 2 via an optical variable attenuator. The signal is then reflected by the two FBGs and re-enters the optical circulator, exiting at port 3, which is connected to a 10dB coupler with the 10% port being connected to the OSA and the 90% port being connected to the input of the WDM to complete the circulation of the fiber laser.

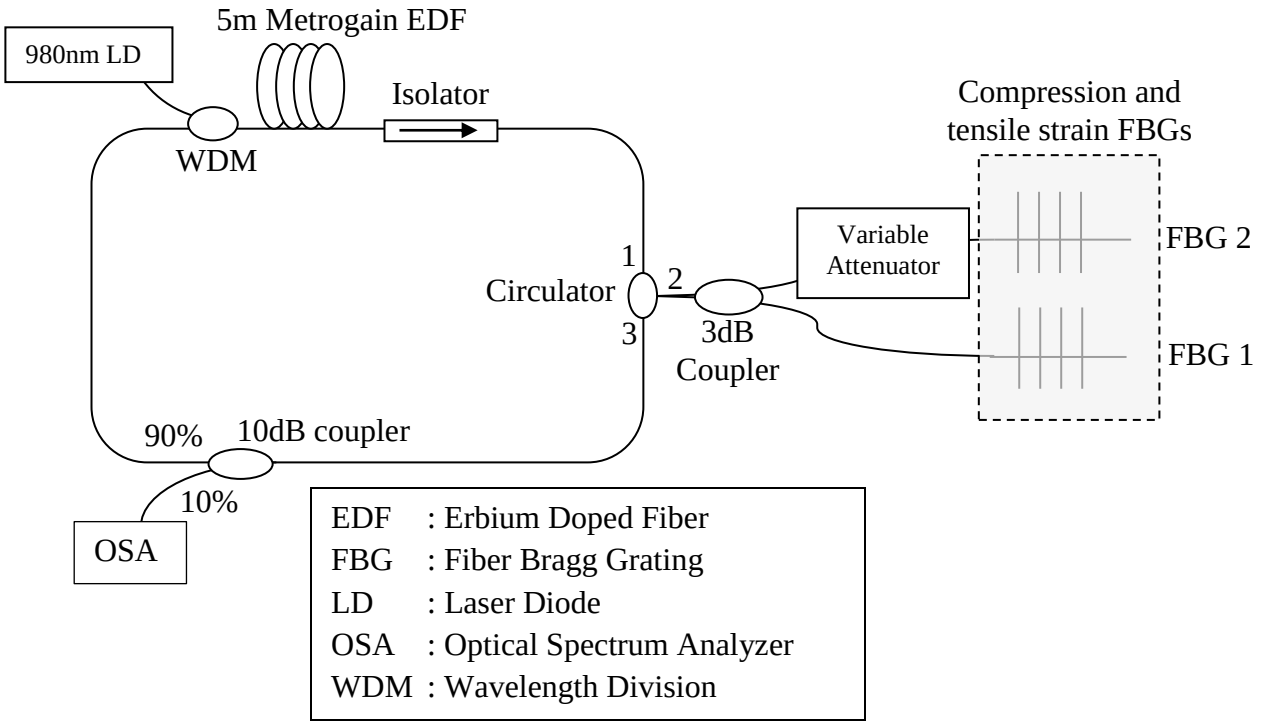

Figure 4.29: Experimental layout of the dual-wavelength EDFL by using FBGs.

The cavity loss control technique is also used in the experiment in order to obtain a balance DWFL. The wavelength selection of the two wavelengths is done by using the compression and tensile technique for FBG 1 and FBG 2 respectively. This leads to the reflection of shorter wavelength by FBG 1 and longer wavelength by FBG 2. The optical variable attenuator is inserted in the optical path of the FBG which reflects the longer wavelength due to the fact that it has a lower threshold for amplification, allowing the output power DWFL to be balanced. The results are then analysed by the OSA.

Figure 4.30 shows the different pair selection of wavelengths of the dual-wavelength spectrum taken one at a time and subsequently superimposed on the same graph. The wavelengths are varied by the two FBGs, FBG 1 and FBG 2, with FBG 1 always selecting the shorter of the two wavelengths. Here, the cavity loss control technique is also employed to control the amplitude of the signal with the longer wavelength as it has a lower lasing threshold as compared to the shorter wavelength. It is clear that the DWFL in this configuration has a relatively wide range of tunability, with the range being 6.07 nm for FBG1 and 4.66 nm for FBG2. FBG2 has a smaller tunable range as compared to FBG 1. This is expected as the FBG 1 is compressed while FBG 2 is pulled, leading to different stresses and therefore slightly different ratios of wavelengths shifts. This problem is exacerbated if we continue to add more tensile or compression force on the FBGs. However, this can be overcome by improving the design of the C-band tunable FBGs in the future.

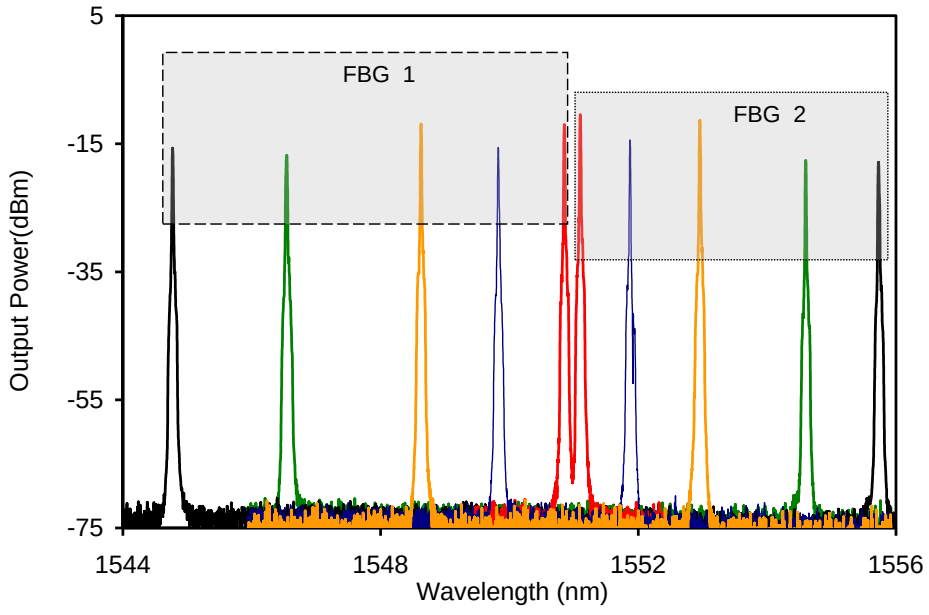

Figure 4.30: The superimposed spectra of the DWFL.

Figure 4.31 is shown to better investigate the spacing of the DWFL, depicting the wavelength tunability from the narrowest spacing of 0.3 nm to the largest spacing of 11 nm.

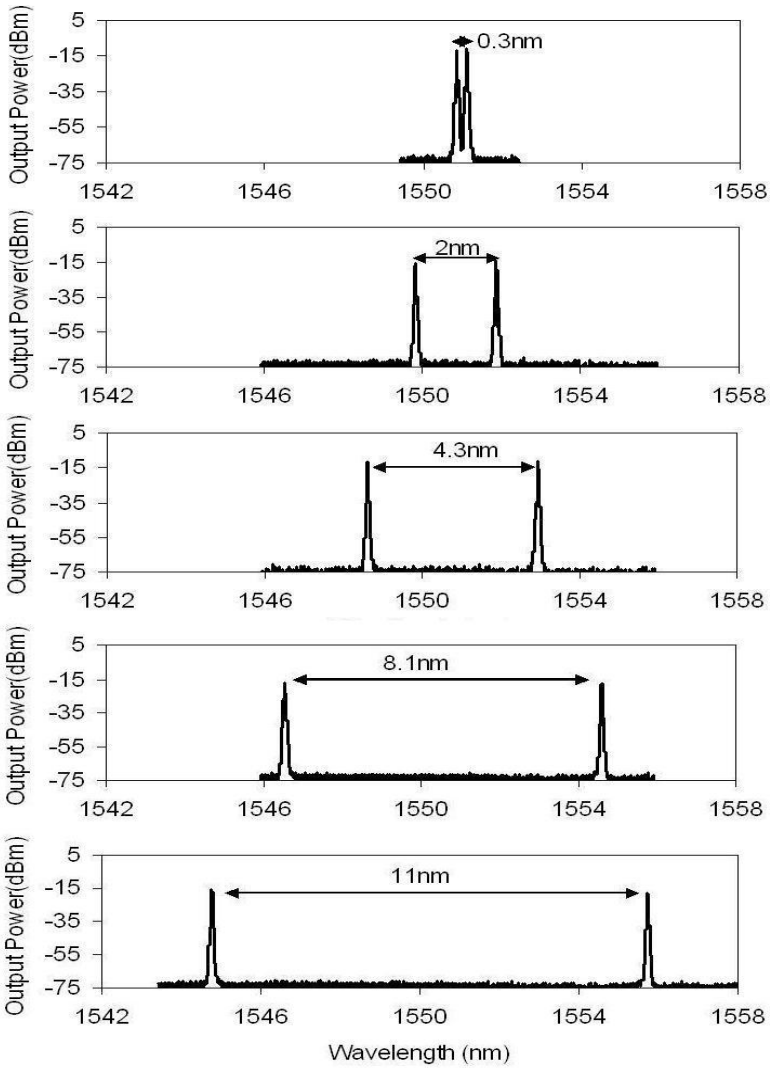

Figure 4.31: The individual spectrum of the DWFL by using two C-band tunable FBGs.

The data in the graph depicts the tunability of the dual-wavelength fiber laser, from 0.3 nm, 2 nm, 4.3 nm, 8.1 nm, until 11 nm, which is the widest range that can be obtained by this design. Thus this design is able to produce a wavelength spacing that is much smaller

compared to the AWG while simultaneously provide a comparable value for the widest wavelength spacing.

The output power of this DWFL configuration is then plotted in Figure 4.32. It can be seen that the output power level coming from each of the dual-wavelength is similar. The minimum output power obtained is -17.9 dBm at 1555.7 nm while the highest recorded output power was obtained at 1551.1 nm with a power of -11.28 dBm. The average output power of this configuration is calculated to be -14.76 dBm with the difference between the maximum and minimum power of 6.62 dB.

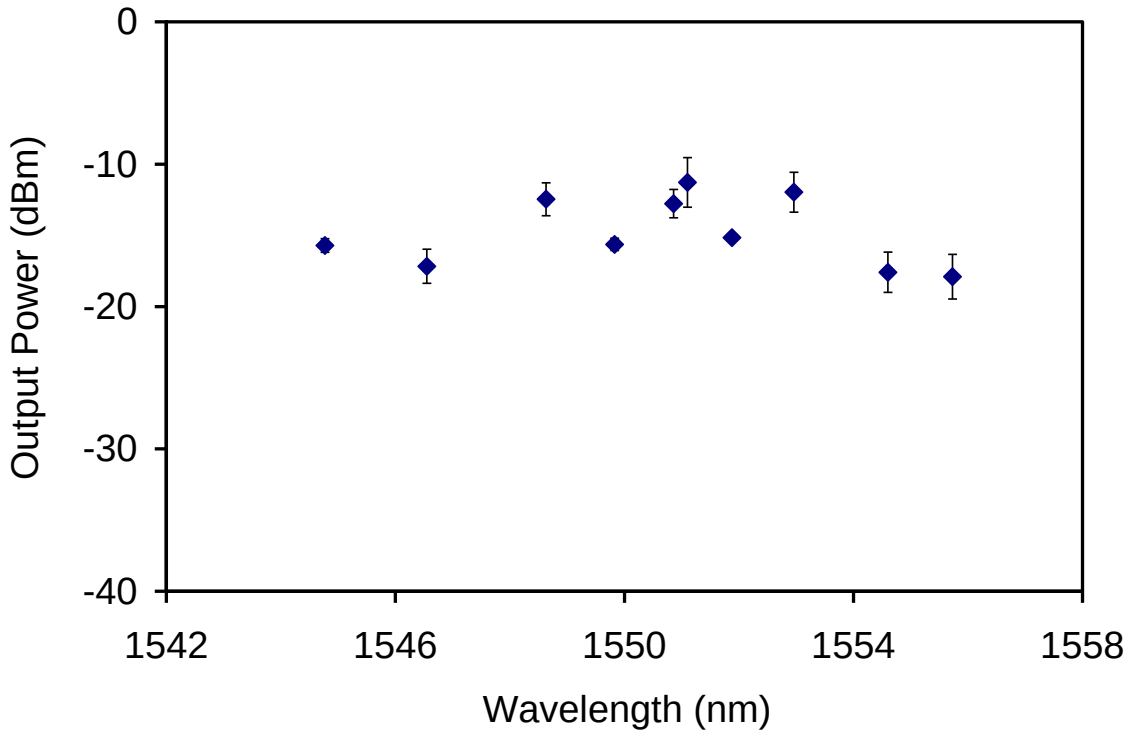

Figure 4.32: The output power value of the proposed DWFL by using FBGs.

Figure 4.33 shows the SMSR value of the DWFL by using the CTS-FBGs. The lowest SMSR value is measured at 1554.6 nm with a value of 56.5 dB while the highest was obtained at 1551.1 nm with a value of 60.5 dB. The average SMSR is calculated to be 53.17 dB with a difference between SMSR maxima and minima of 7.3 dB.

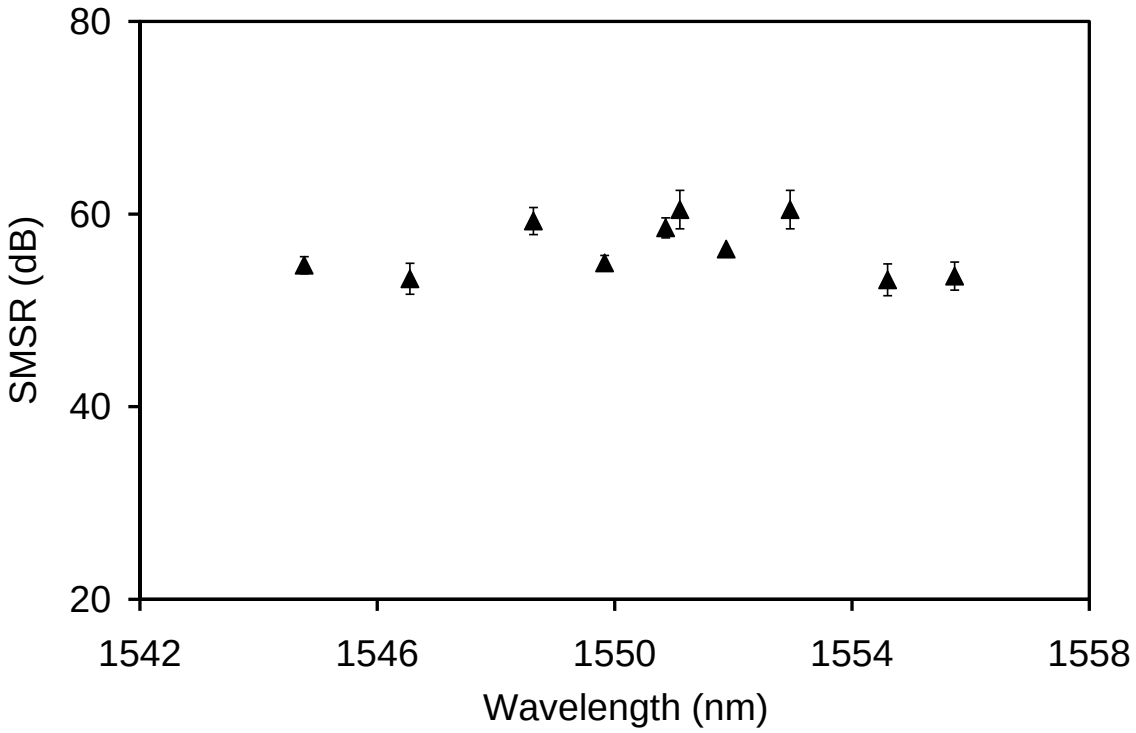

Figure 4.33: The SMSR value of the proposed DWFL by using FBGs.

4.2.3 Dual-Wavelength Fiber Laser by Using TBF

Figure 4.34 shows the configuration to generate a dual-wavelength fiber laser by employing two TBF. The other components include two of S and C multiplexers, WDMs, three 980 nm laser diodes as a pump to the EDF, an isolator, two 3 dB couplers, optical attenuator denoted as ATT, a 10 dB coupler as well as a 5 m Metrogain EDF and a 30 m depressed cladding-EDF (DC-EDF) as gain media.

First, two individual 980 nm is used to pump the two gain media, with the 5m metrogain EDF pumped with a pump power of 80 mW and the 30 m DC-EDF pumped bidirectionally with a total pump power of 300 mW. This will generate two ASE which propagates in all directions. The oscillation is then forced to propagate in a clockwise direction by the isolator. The ASE from both of the EDFs is then combined by using the S and C band multiplexer. The light then enters the 3 dB coupler where the shorter of the two wavelengths is selected by TBF1, while the longer wavelength is selected by TBF 2 and passes through an OVA. The selected wavelength is then recombined by using the 3 dB coupler which then enters the multiplexer through the isolator to complete the oscillation inside the ring cavity. The output is then analyzed by the OSA through a 10 dB coupler which extract 10% of the signal from the cavity.

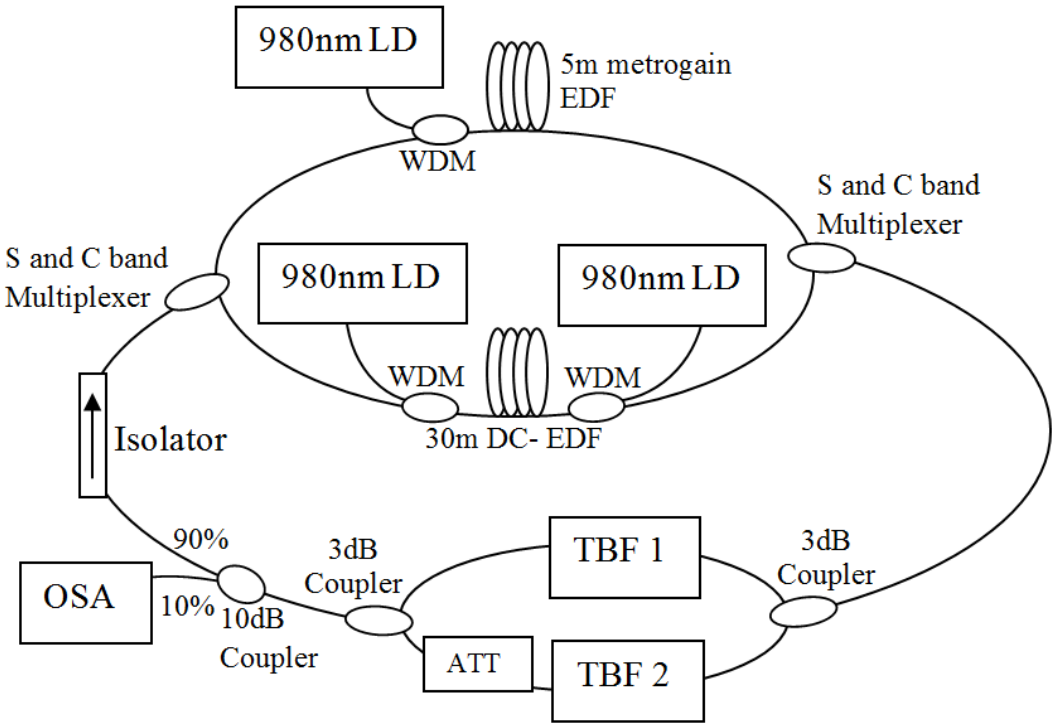

ATT	: Optical Attenuator
DC- EDF	: Depressed Cladding- Erbium Doped Fiber
EDF	: Erbium Doped Fiber
LD	: Laser Diode
OSA	: Optical Spectrum Analyzer
TBF	: Tunable Bandpass Filter

Figure 4.34: Experimental layout of dual-wavelength EDFL by using the TBFs.

Figure 4.35 shows the superimposed spectra of the DWFL by using two TBFs as recorded by the OSA. The wavelength selected by TBF 1 is fixed, while the other wavelength is varied to produce a range of wavelength spacings from the shortest to the longest dual-wavelength spacing. Here, the cavity loss control technique is also used to control the amplitude of the longer wavelength which has a lower lasing threshold than the shorter

wavelength. By inducing loss to the longer wavelength selected by the TBF 2, a balance dual-wavelength output is successfully achieved.

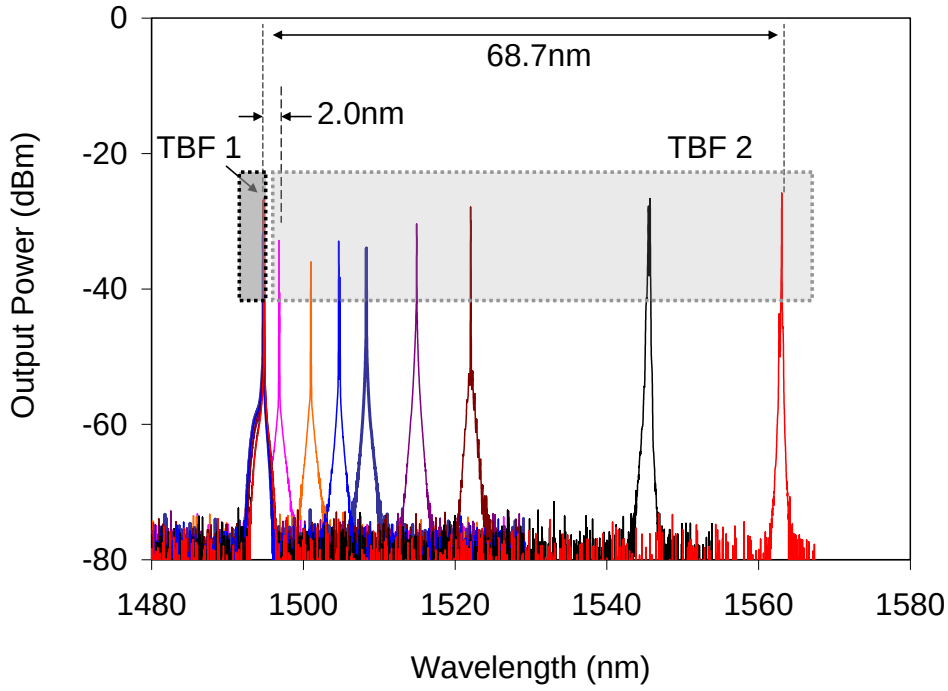

Figure 4.35: The superimposed spectra of the DWFL by using TBFs.

To make the analysis easier, Figure 4.36 is shown for different wavelength tunabilities from the narrowest spacing of 2 nm to the largest spacing of 68.23 nm. The dual-wavelength fiber laser proposed in the thesis can be conveniently adjusted to the desired wavelength within the S-band and C-band region. The spectrum shows the tunability of the dual-wavelength fiber laser, starting from 2 nm, 13.48 nm, 27.23 nm, 50.90 nm, until 68.23 nm, which is the widest range that can be obtained by this design.

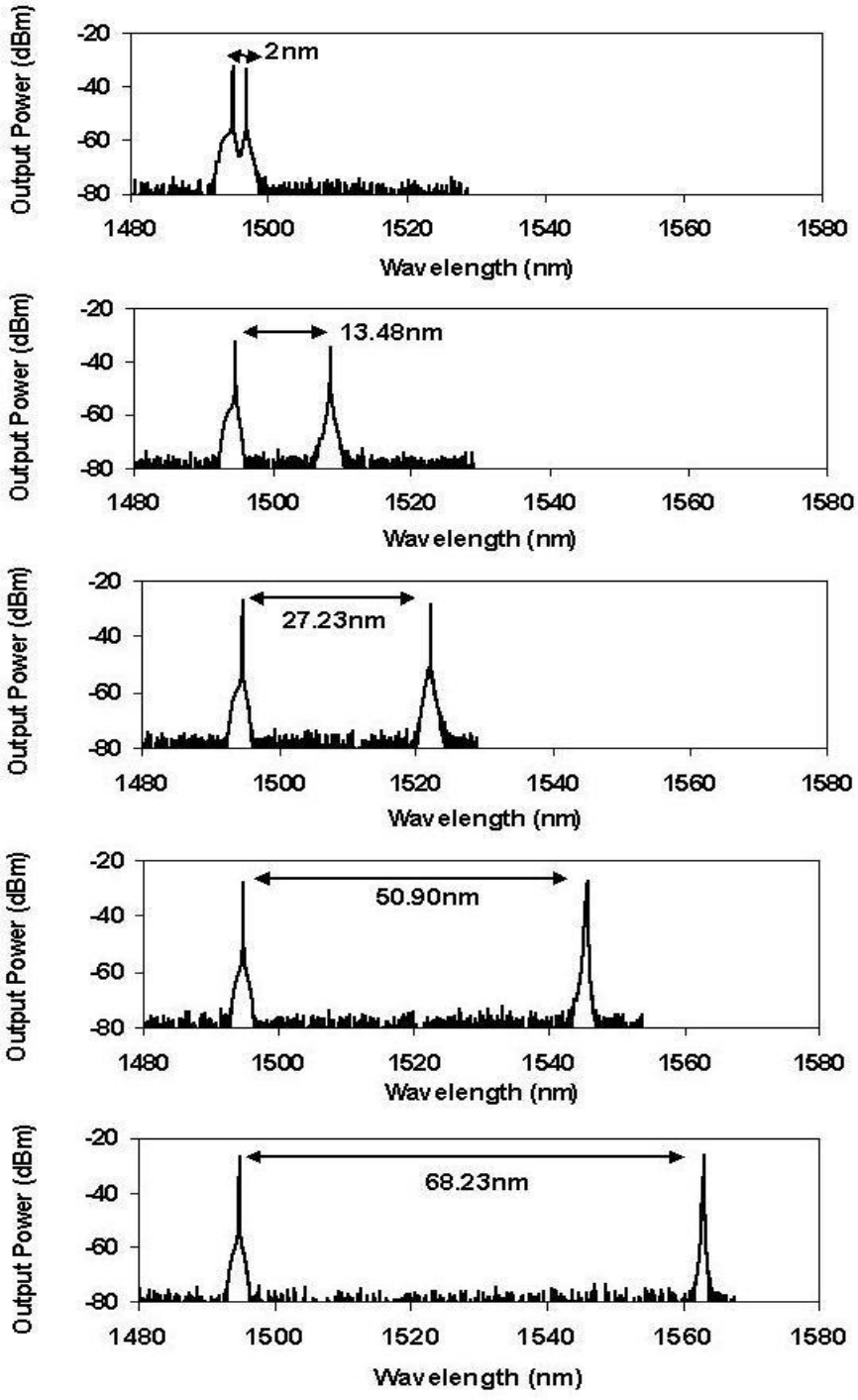

Figure 4.36: The tunability from the narrowest (2 nm) to the widest spacing (68.23 nm).

Figure 4.37 shows the output power of the DWFL in this setup. It can be seen that the output power from the S-band region is lower compared to that of the C-band region, with the minimum output power obtained at 1508.3 nm with an output power of -34.6 dBm while the highest recorded output power was recorded to be -25.9 dBm at 1563.05 nm. The average output power is -30.05 dBm with a maximum difference between the maxima and minima calculated at 8.69 dB.

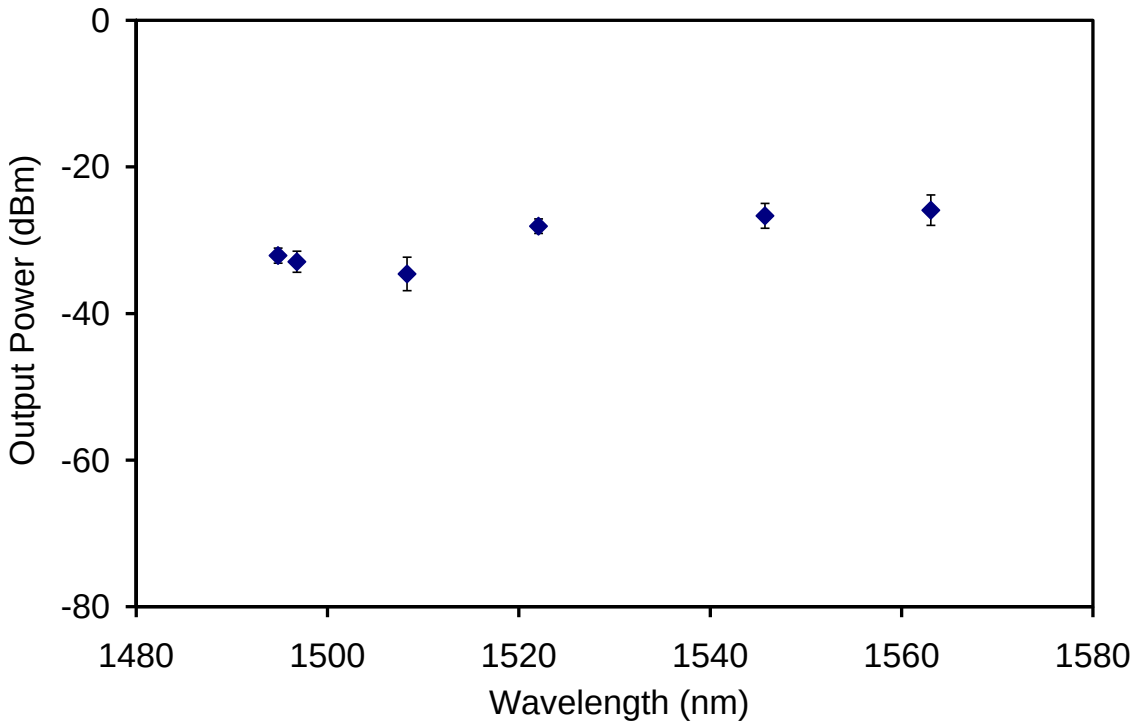

Figure 4.37: The output power value of the proposed DWFL by using TBFs.

Figure 4.38 shows the SMSR value of the DWFL by using TBFs. The SMSR from the S-band region also has the same characteristics of the output power, and therefore has a lower value compared to the C-band region. The minimum SMSR in the data range was obtained at 1508.3 nm with an SMSR value of 39 dB while the highest SMSR was recorded to be 47.4 dB at 1563.05 nm. The average SMSR is 43.62 dB with a maximum difference of maxima and minima of 8.5 dB.

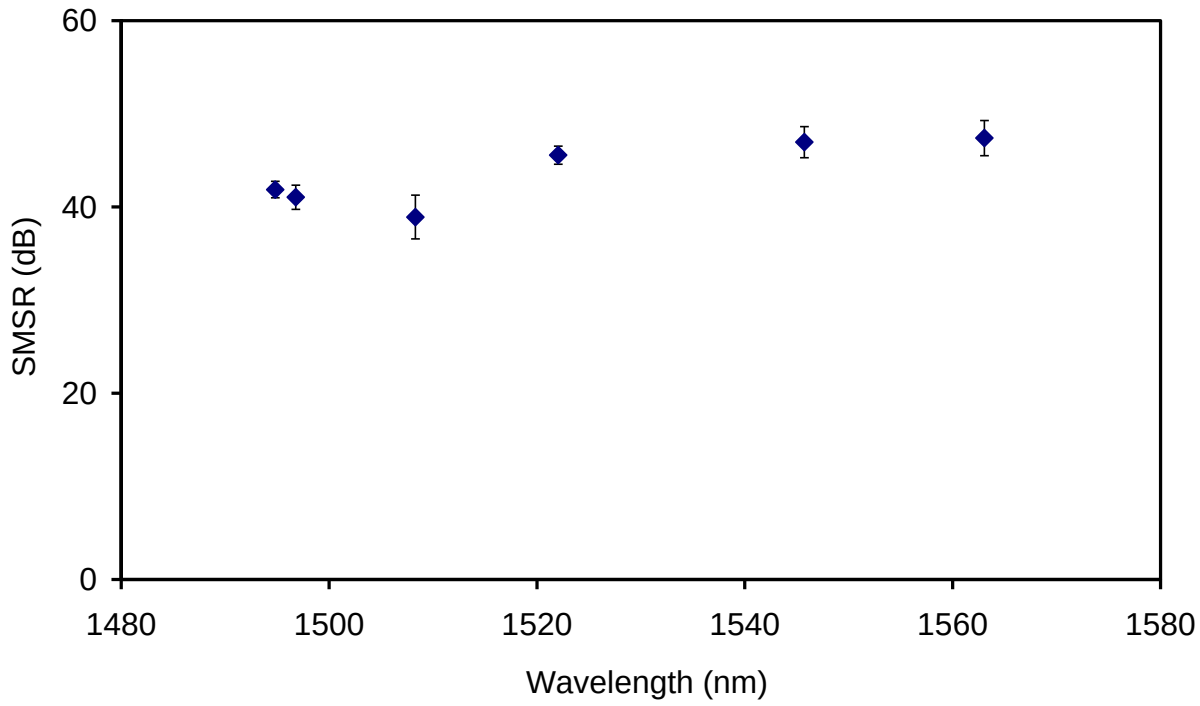

Figure 4.38: The SMSR value of the proposed DWFL by using TBFs.

4.2.4 Summary of the Various Techniques for Tunable Dual-Wavelength Fiber Lasers

To summarize the output performance all of the erbium doped DWFLs designs, all of the data are compiled in a simple timetable as shown in table 4.1 below:

Table 4.1: Comparison for different design of erbium doped DWFLs.

	Arrayed waveguide grating (AWG)	Compression and tensile strain FBGs (CTS-FBGs)	Tunable bandpass filters (TBFs)
Average output power	0.12 dBm	-14.76 dBm	-30.05 dBm
Output power maximum difference	4.51 dB	6.62 dB	8.69 dB
Average SMSR value	67.86 dB	53.17 dB	43.62 dB
Minimum tuning range	0.8 nm	0.3 nm	2 nm
Maximum tuning range	18.13 nm	10 nm	68.70 nm
Number of wavelength options	24 wavelength with 0.8 nm of adjacent channel spacing	Any wavelength within range	Any wavelength within range
Precise wavelength selection	Easy	Moderate	Moderate

From the time table, it can be observed that the output power is the highest by using the AWG as the wavelength selector with the output power of 0.12 dBm. Whilst the CTS-FBGs being the second highest with -14.76 dBm of output power, while by using TBF is the third with -30.05 dBm of output power. The SMSR value of the design with the AWG as the wavelength selector is also having the highest value with 67.86 dB of SMSR value. The other two are 53.17 dB and 43.62 dB for CTS-FBGs and TBFs, respectively. The maximum difference between the highest and the lowest output power are also the best by using the AWG design with the minimum value of 4.51 dB as compared to the two others with 6.62 dB and 8.69 dB of maximum difference for CTS-FBGs and TBFs respectively.

The wavelength selection is also easier by using the AWG as it can be tuned just by using the OCS to select any desired wavelength. The other two however need to be precisely tuned to obtain the desired wavelength, which make the AWG design is more preferable as compared to the others. The compression and tensile strain FBGs and TBF however have their own advantage. The CTS-FBGs design has the narrowest tuning range with 0.3 nm spacing, while the TBF design has the widest tuning range of 68.79 nm spacing tunability. Each of the advantage is important depending on the targeted use.

4.3 Dual-Wavelength Fiber Lasers by Using SOA

Besides EDFs, SOAs are also used in fiber laser applications. As was discussed previously, it is easier to control the output of the DWFL by using an SOA by the virtue of its inhomogeneous broadening profile. In this section, two kinds of wavelength selective elements are used with the SOA which is AWGs and FBGs.

4.3.1 DWFL by Using AWGs

In this section, two configurations for generating DWFL using SOAs by employing AWGs as the wavelength selection element are presented, namely, the figure-of-eight cavity and the ring cavity configurations.

4.3.1.1 Figure-of-Eight Cavity Configuration

Dual-wavelength lasing can be easily generated by using the SOA, which made it a popular alternative to EDFs for the generation of a dual-wavelength fiber laser. The inhomogeneous property that inherent to the SOA allows the generation a balance peak power by careful adjustment of the cavity polarization state, as was discussed in Chapter 2. In this thesis, we propose a unique figure-of-eight configuration to generate a DWFL using a SOA and two AWGs, as shown in Figure 4.39.

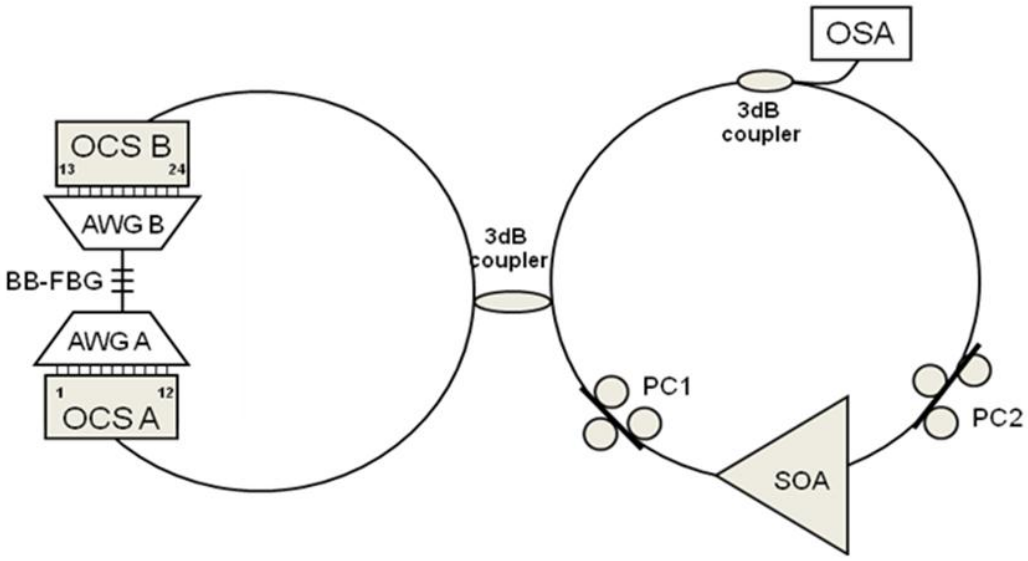

AWG	: Arrayed Waveguide Grating
BB-FBG	: Broad Band – Fiber Bragg Grating
PC	: Polarization Controller
SOA	: Semiconductor Optical Amplifier
OCS	: Optical Channel Selector
OSA	: Optical Spectrum Analyzer

Figure 4.39: Experiment setup of dual-wavelength fiber laser by using a SOA as an inhomogeneous gain medium [36].

First, the SOA is switched on and driven by a current of 340 mA, generating light in all direction whose state of polarisation is adjusted by two PCs denoted as PC1 and PC2 at the back and in front of the SOA. The ASE then propagates through a 2x2 3 dB coupler at both its port, entering the second loop in the figure-of-eight configuration. AWG A and AWG B both have 16 channels each, denoted A1 to A16 and B1 to B16, respectively. The two AWGs, in combination with two OCS, namely, OCS A for AWG A and OCS B for AWG B, act as wavelength selectors two create the DWFL. The selected wavelengths then propagate to the BB-FBG before they are reflected through the AWGs and OCSs,

subsequently recombining at the 3 dB coupler. By choosing a different channel from the two OCSs the two wavelengths can be conveniently selected to obtain the desired wavelength combination before they are recombined at the 3 dB coupler. The dual-wavelength then travels out of the 3 dB coupler and 50% of the resulting radiation is extracted to be analyzed by the OSA.

Figure 4.40 (a) until (h) show the wavelength spectra of the DWFL from the largest to the smallest spacing. The channel spacing can be adjusted by altering the channels selected at OCS A and OCS B. The widest possible wavelength spacing of the DWFL spectrum is approximately 12.21 nm and is obtained by selecting Channels 1 and 16 on OCS A and OCS B, respectively, as shown in Figure 4.40(a), while the narrowest wavelength spacing is approximately 1.16 nm, obtained by selecting Channels 8 and Channel 9 on OCS A on OCS B, respectively, as shown in Figure 4.40(h).

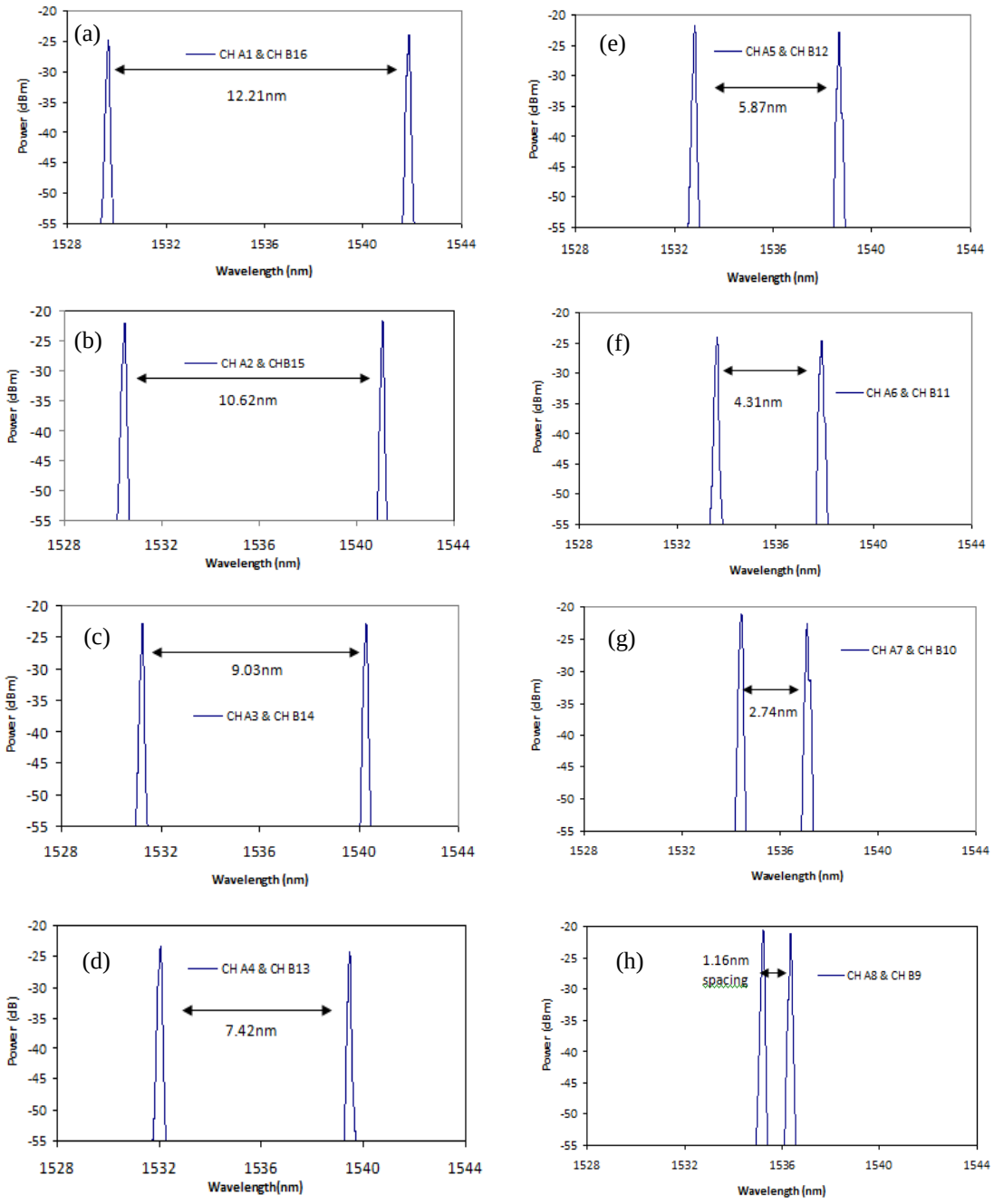

Figure 4.40: Result of the tuning range of dual-wavelength by using SOA from (a) the widest spacing of 12.21 nm to (h) the narrowest spacing of 1.16 nm [36].

Next, the stability of the setup was investigated. Figure 4.41 shows the temporal evolution of the DWFL spectrum for an operation time of more than an hour, with an interval time of 5 minutes between each measurement. Figure 4.41(a) depicts the largest spacing from channels A1 and B16 while figure 4.41(b) shows the narrowest spacing which is the result of choosing channels A8 and B9. As is evident from the graph, the DWFL is quite stable with just minor fluctuation of output power over a relatively long period of continuous operation.

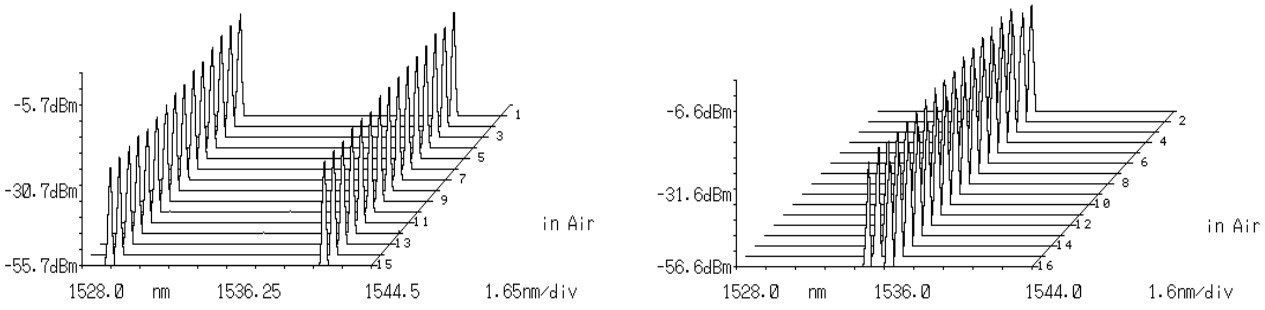

(a) (b)

Figure 4.41: The temporal evolution of the DWFL (a) largest tuning range from channel A1 and B16 and (b) the narrowest spacing of channel A 8 and B 9 [36].

Figure 4.42 shows the output power of the DWFL measured by using the OSA. The average value of the DWFL output power is -23.5 dBm. The maximum difference between the maximum and minimum output powers is 4.4 dB with the maximum and minimum value with an output power of -25.8 dBm and -21.4 dBm, respectively (obtained from Channels 1 and 9). The Channel selection is also done in pairs from channels 1 and 16, Channels 2 and 15 and so on until Channels 8 and 9. The wavelength at channel 1 was

observed at 1529.6 nm with a spacing of 0.8 nm between each channel, and therefore ending at 1541.9 nm. This leads to a tuning range of 12 nm.

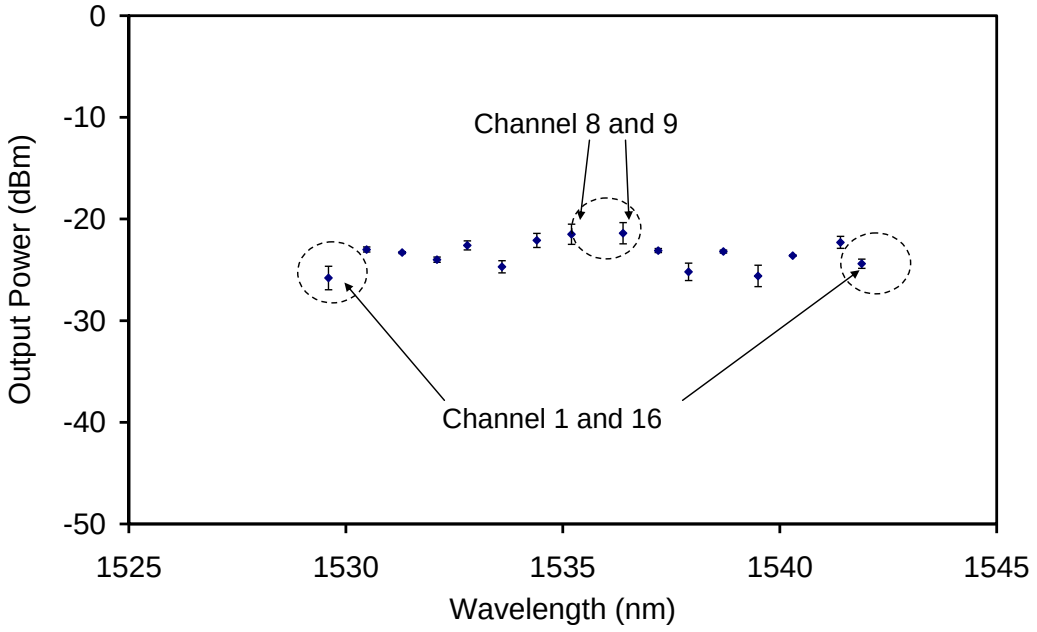

Figure 4.42: Output power value for each channels of the DWFL by using the SOA [36].

The SMSR of the DWFL is depicted in Figure 4.43. The average SMSR value of the DWFL is approximately 38.5 dB with minor fluctuation of not more than 0.5 dB for all wavelengths. This indicates that the use of the SOA as the linear gain medium does not exhibit high SMSR values, even with a presence of a high level of ASE, which is a clear disadvantage when compared to the EDF as the gain medium. Notwithstanding this, a stable DWFL can still be generated with fairly negligible crosstalk.

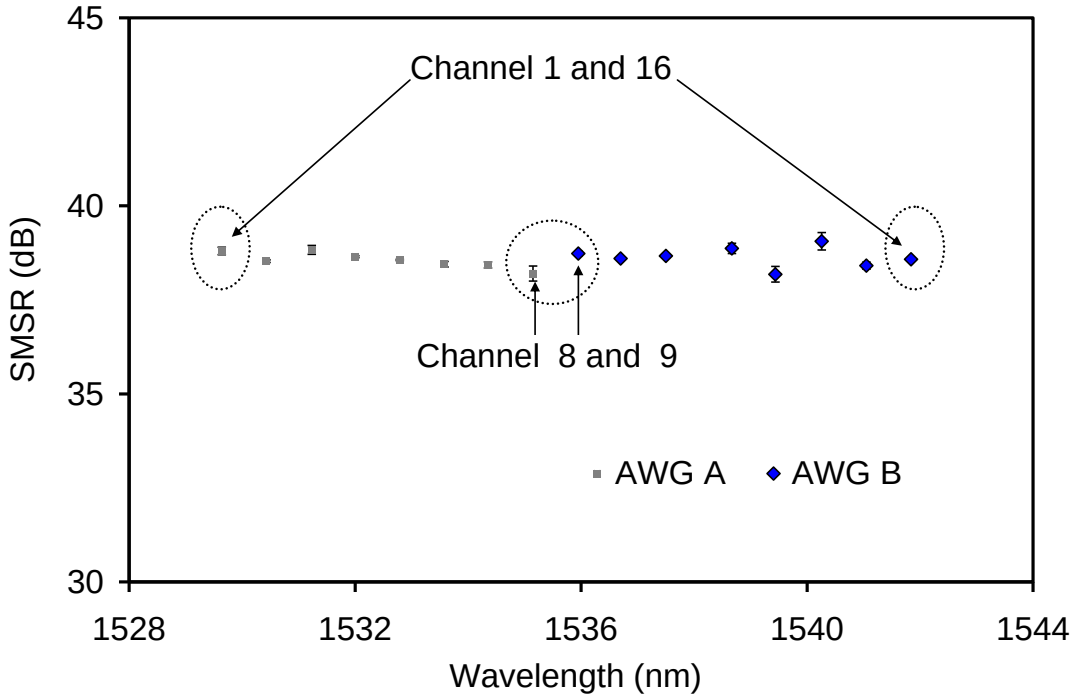

Figure 4.43: SMSR value for each channels of the DWFL output [36].

4.3.1.2 Ring Cavity Configuration

It is also possible to employ a ring design to produce a DWFL using a SOA as the gain medium. Figure 4.44 depicts the proposed experimental configuration of a DWFL which operates in the C-band. The formation of the light begins from the 1550 nm SOA driven by a 340 mA drive current, which acts as the gain medium in this experiment. The ASE produced by the SOA then travels through a PC, before passing through an AWG which splits the beam into 24 choices of channels, from which the two are to be chosen for the laser. One of the legs is connected to one of the channel 1 to 12 and another leg is connected to channel 13 to 24.

Both of the channels from the AWG are then combined at the 2x2 3 dB coupler. One of the 3 dB coupler's output legs is connected to the OSA for analysis while the other output leg is connected to the second PC before passing through an isolator, which ensures unidirectional propagation in the cavity. The output of the isolator is then connected back to the input of the SOA.

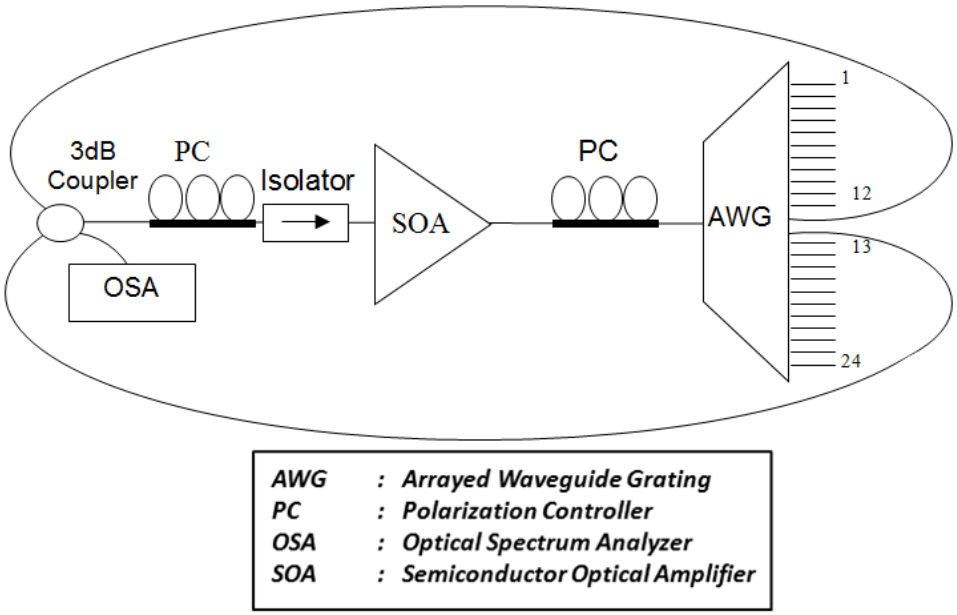

Figure 4.44: Experimental layout of dual-wavelength fiber laser by using SOA.

The inhomogeneous broadening of the SOAs allows the construction of a DWFL with a maximum possible balanced output power by sandwiching the gain medium between two PCs that controls the polarization state of the SOA radiation. The two lasing wavelengths are obtained by dividing the 24 output of the AWG into two parts, with channels 1 to 12 constituting the first output and channels 13 to 24 producing the other output. The desired output peak power of both wavelength is be changed by adjusting the PCs to a certain state of polarization until a balanced DWFL is achieved.

Figure 4.45 shows the DWFL output for different spacings, which are selected by changing the channel numbers. The topmost trace (Figure 4.45(a)) shows the DWFL output with a spacing of 0.8 nm, the smallest spacing obtainable in this experiment, which is the resulting spectrum of selecting channels 12 and 13. The spacing is then increased to 2.4 nm, 4 nm, and up to 18 nm by selecting channels 11 and 14, channels 10 and 15 until channels 1 and 24, respectively as shown in Figure 4.45 (b) to (d). The widest possible spacing for this DWFL configuration was obtained at 18 nm due to the limitation of the AWG used.

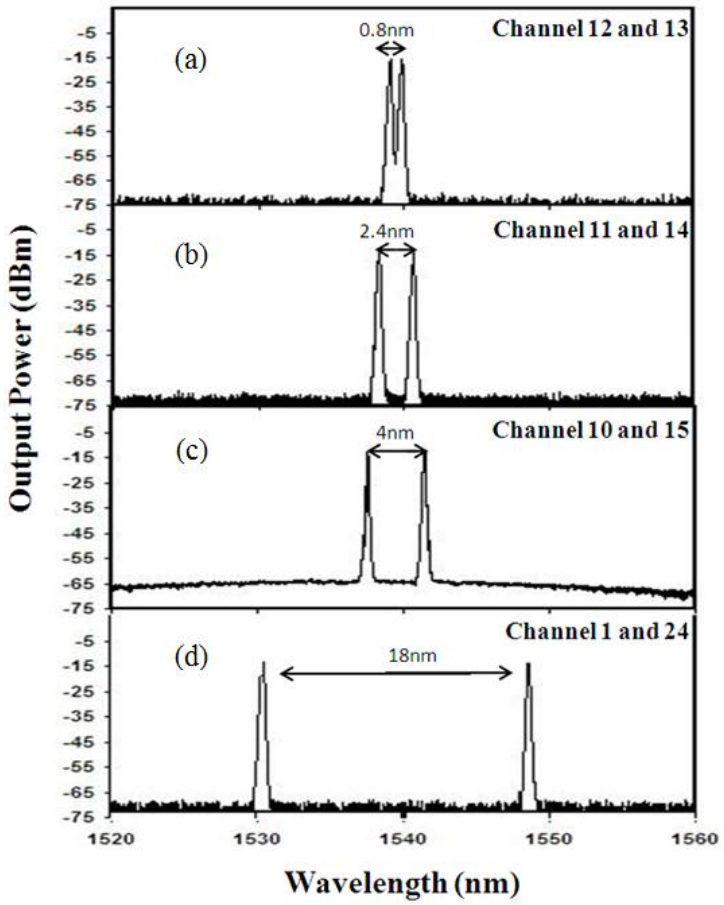

Figure 4.45: The spectrum of the ring cavity DWFL with a SOA as the gain medium.

Figure 4.46 shows the output powers of each of the 24 channels of the AWG which each channels taken in pairs starting from channels 1 and 24, channels 2 and 23, channels 3 and 22, until channels 12 and 13. It can be observed that output powers for all channels are quite flat with each pair having almost the same output power as only the outputs of one pair is taken at one time, and these outputs are adjusted so that they are balanced. In this experiment, only 12 combinations of selecting the channel from the AWG from the widest (Channel 1 and 24) to the narrowest spacing (Channel 12 and 13) are being considered to make the analysis easier. The average output power obtained in this experiment is -13 dBm with a maximum difference of 10 dB between the maximum and minimum output powers.

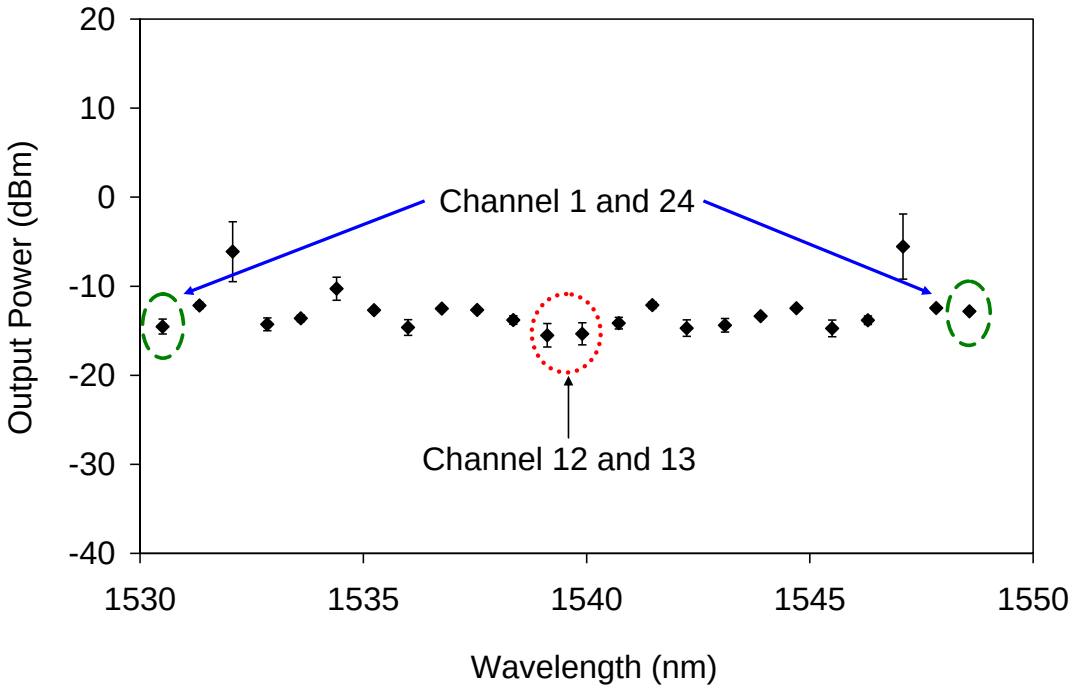

Figure 4.46: The output power for the DWFL by using the SOA as the active gain medium.

Figure 4.47 shows the SMSR value of this configuration. The average value of the SMSR is about 56 dB with a difference between the maximum and minimum SMSR values calculated to be 13 dB, which is substantially higher as compared to configurations which employ EDFs as the gain media. The SMSR value is follows the same trend as the output power curve in Figure 4.46.

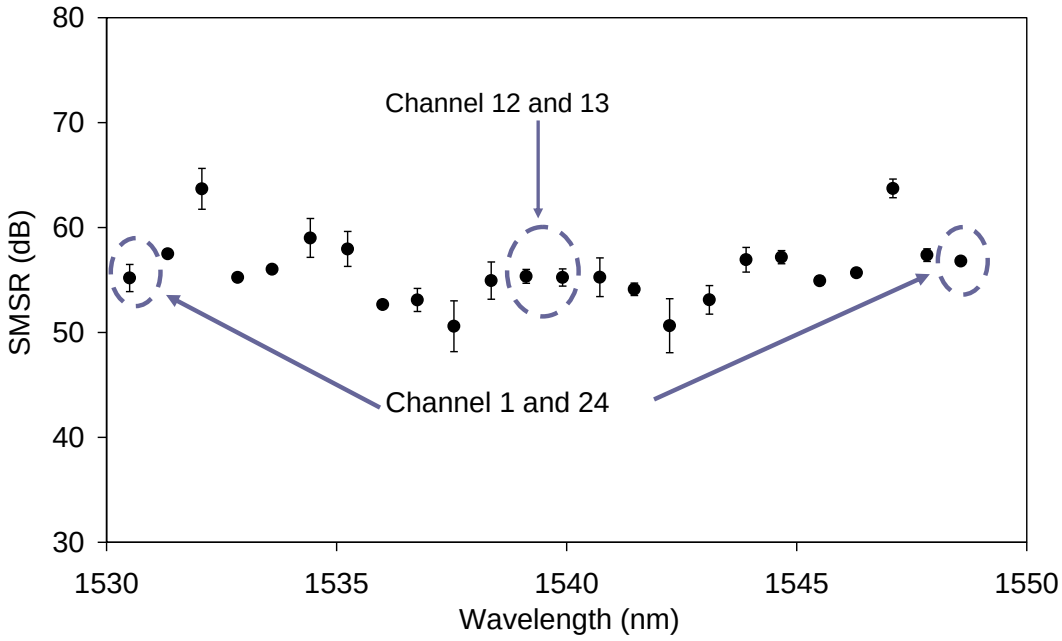

Figure 4.47: The SMSR value of the proposed DWFL by using the SOA.

Figure 4.48 shows the performance of the DWFL at an interval time of 5 minutes for an operation time of over more than half an hour. As depicted in the graph, the DWFL is quite stable with fluctuations of less than 3 dB. Figure 4.48 (a) and (b) shows the DWFL with the widest spacing of 18 nm and the narrowest spacing of 0.8 nm obtained by selecting channels 1 and 24 and channels 12 and 13, respectively. The initial measurement was taken only after the two wavelength of the DWFL output is stable, which is obtained by adjusting

the PCs. The subsequent measurements were taken without any further adjustment of the PCs, which indicates that the proposed setup is highly stable for extended periods of time.

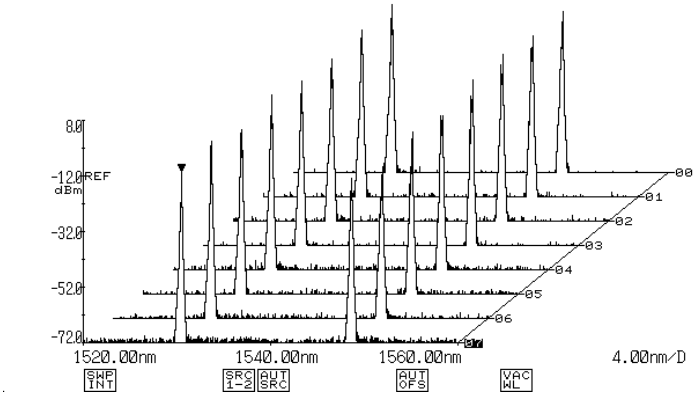

(a)

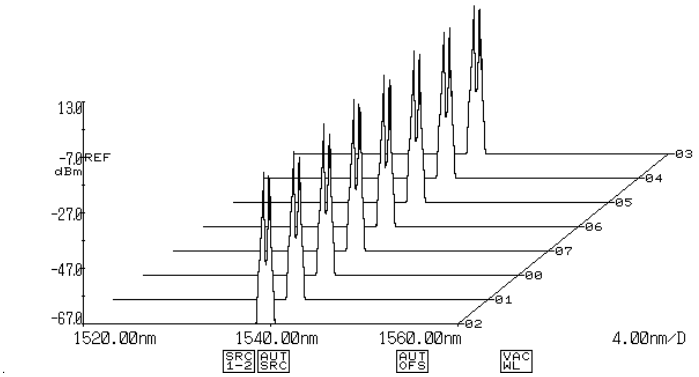

(b)

Figure 4.48: Performance of the proposed DWFL for (a) the widest tuning range (18.13 nm) for Channel 1 and 24 and (b) the narrowest tuning range (0.08 nm) for Channel 12 and 13 for a continuous operation time of more than 30 minutes.

The design was further extend by making a tunable quad wavelength fiber laser generating dual-wavelength fiber laser each in C-band and O-band regions simultaneously [37].

4.3.2 DWFL by Using FBGs

Alternatively, the selection of the two wavelengths can also be done by employing two FBGs. Figure 4.49 shows the experimental setup for the DWFL by using the SOA as the active gain medium with two FBGs as the wavelength selector. As before, the lasing action begins with the ASE from the SOA which is driven by a 350 mA of drive current. Unidirectional operation of the laser was ensured by the isolator. The ASE from the SOA goes to the port 1 of the circulator via the isolator, after which two wavelengths are selected by two C-band tunable FBGs. The two wavelengths are then combined by a 3 dB coupler before entering the cavity via port 2 of the circulator. The dual-wavelength then passes through a 10dB coupler in which 10% of the power is extracted for analysis while the remainder goes to the input of the SOA to complete the laser circulation inside the cavity. The tuning of the FBGs is done with the same method as the one describe in Chapter 3 for a tunable single wavelength fiber laser.

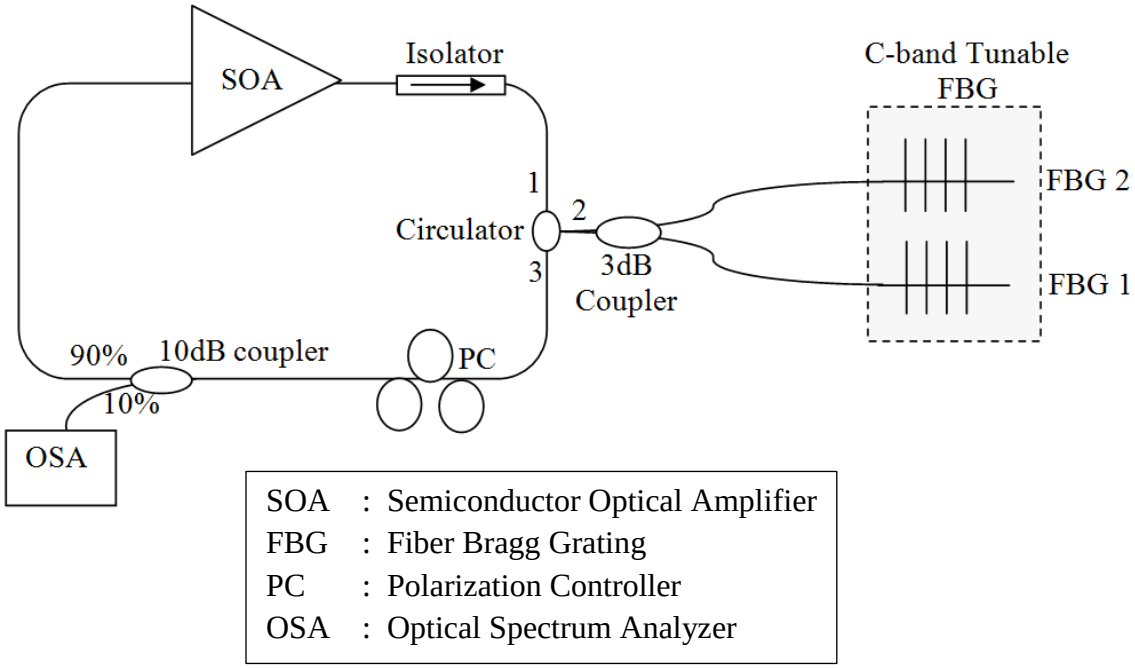

Figure 4.49: Experimental layout of dual-wavelength fiber laser by using SOA [38].

Figure 4.50 depicts the wavelength tunability of the DWFL, showing the DWFL spectrum from the narrowest spacing of 0.12 nm to the largest spacing of 9nm. The measurement taken as in Figure 4.50 (a) to (f) which shows the tunability of the dual-wavelength fiber laser, starting from 0.12 nm, 1 nm, 3 nm, 5 nm, 7 nm to 9 nm which is the widest range that can be obtained by this design. The wavelength can be selected anywhere within the tuning range which can provide a maximum spacing of 9 nm.

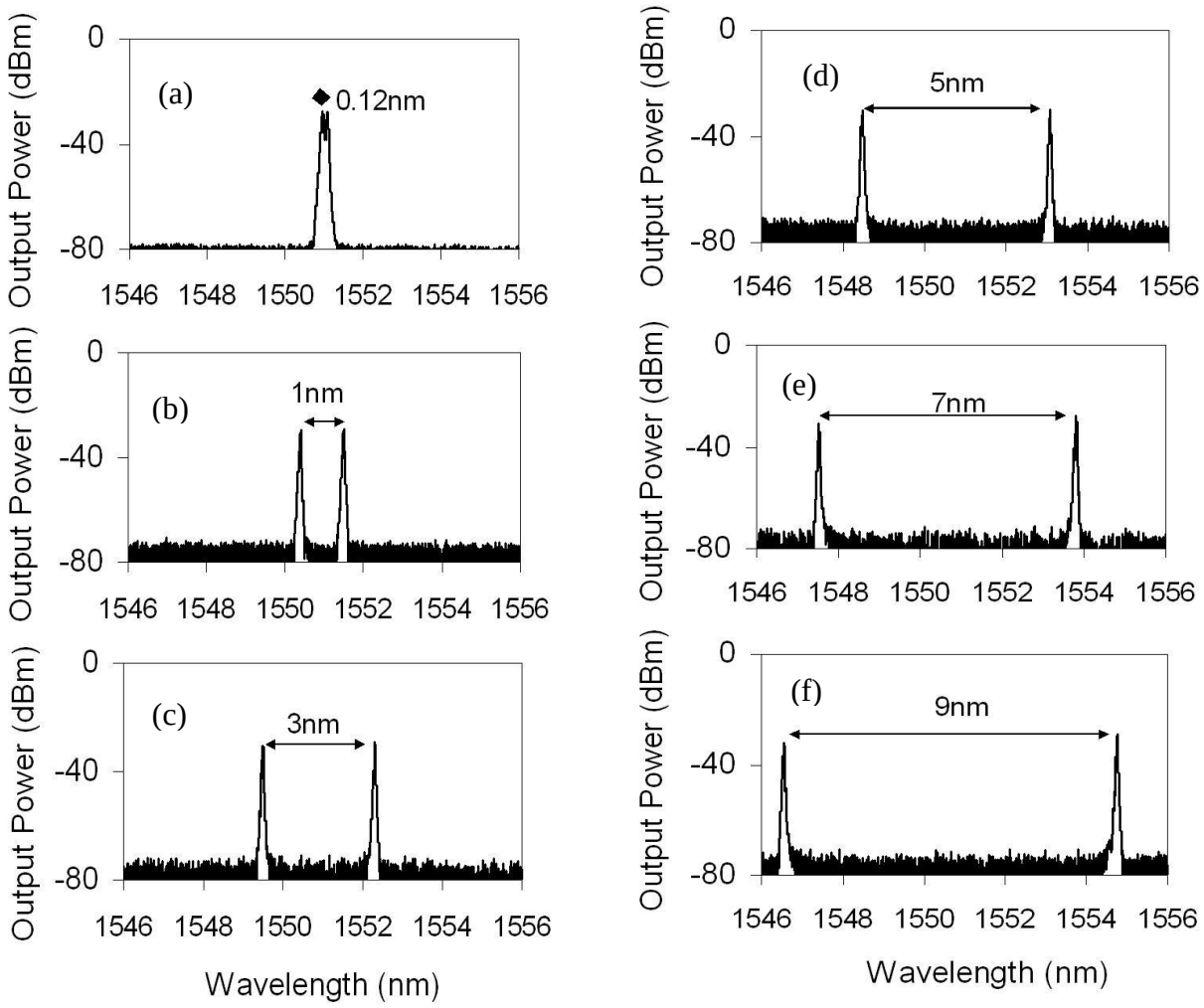

Figure 4.50: The spectrum of the dual-wavelength fiber lasers by using the SOA [38].

Figure 4.51 shows the output power of the DWFL in this configuration. It can be seen that the output power levels from each pair combination of the dual-wavelength is comparable with the exception of the pair which has the closest spacing (0.12 nm). This is due to the fact that each output has a roughly Gaussian distribution, and since the output power of this particular pair is close to one another, the two distributions overlap, causing the peak powers to be relatively high. The minimum output power was obtained at 1546.57 nm with an output power of -33.10 dBm, while the highest output power recorded was -28.15 dBm

at 1550.97 nm. The average output power is –30.28 dBm with the difference between the output power maxima and minima calculated to be 4.95 dB.

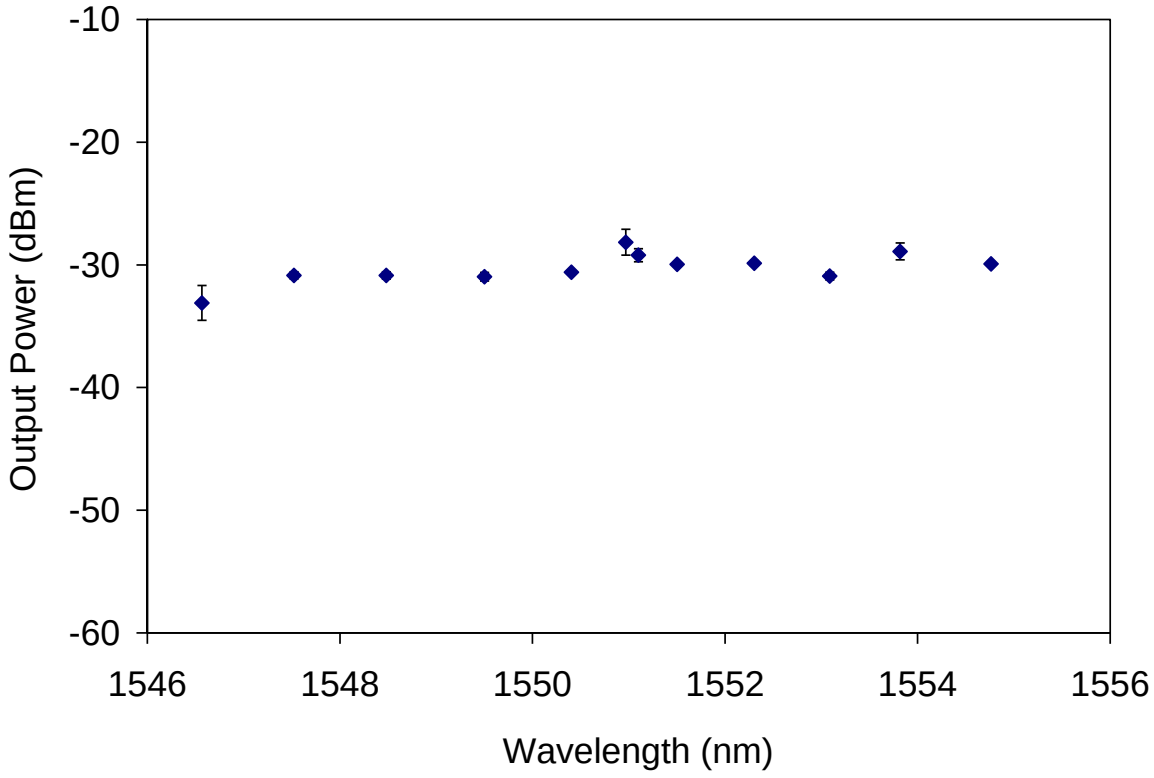

Figure 4.51: The output powers of the DWFL by using the SOA.

Figure 4.52 shows the SMSR of the DWFL in the SOA with the average value of 42.54 dB, with the a maximum difference between the SMSR maximum and minimum values calculated to be 11.02 dB. This value is quite high due to the relatively high value of the maximum SMSR, which is due to the fact that the noise level of this particular pair is relatively small as compared to the peak power. The highest SMSR value is shown to be at 1550.97 nm with 50.45 dB while the smallest is measured at 1546.57 nm with a SMSR value of 39.43 dB.

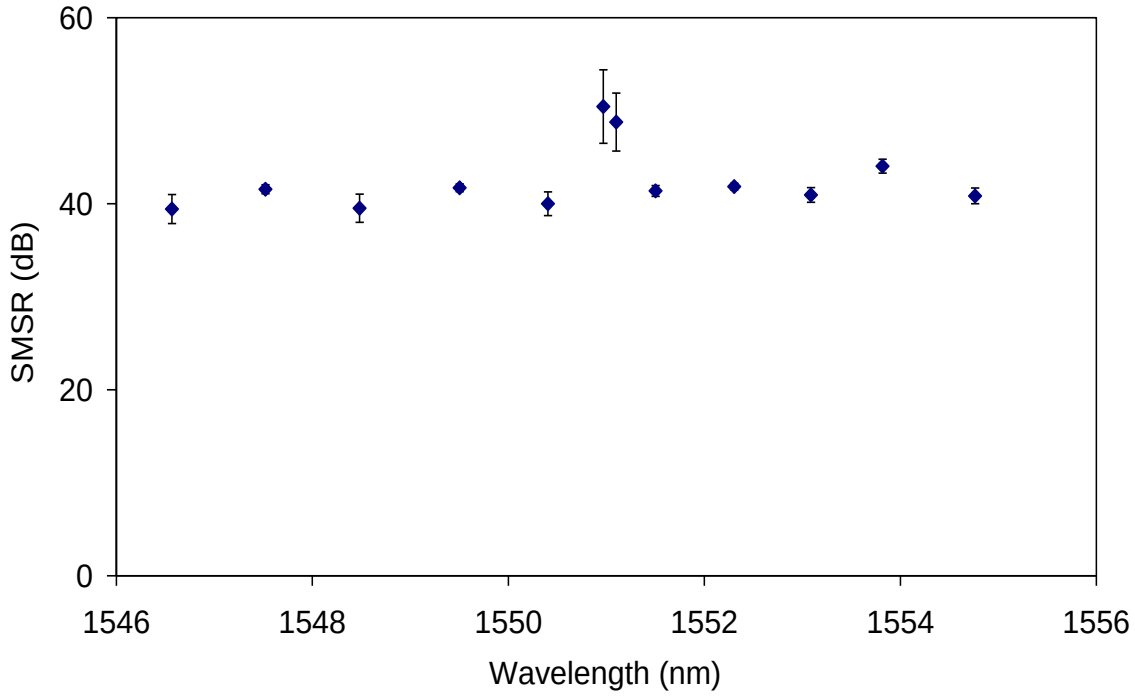

Figure 4.52: The SMSR of the DWFL by using the SOA.

The durability and life expectancy of this setup is investigated by investigating the temporal stability of the DWFL. This is done by measuring the performance of the configuration for more than an hour of continuous operation, shown in Figure 4.53. The DWFL, with a selected spacing of 1 nm, is found to be extremely stable throughout the duration of the experiment, with only minimal variations recorded.

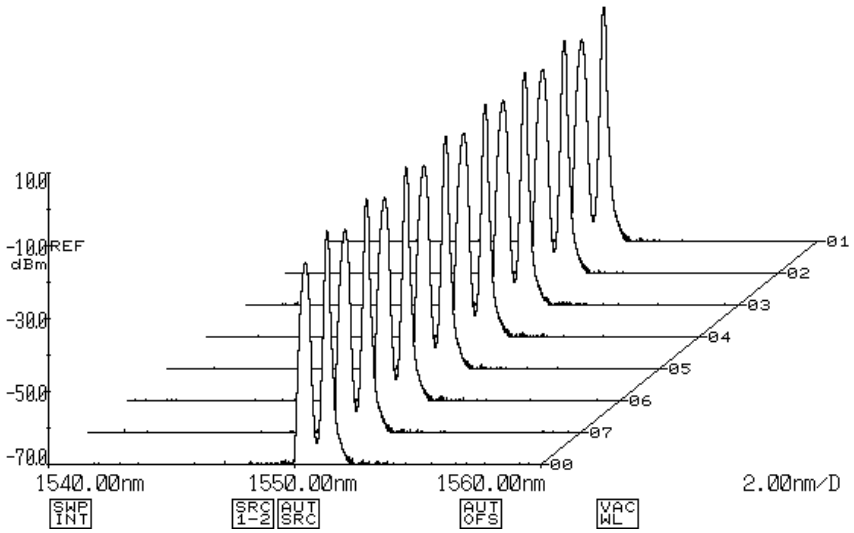

Figure 4.53: The three-dimensional graph of the DWFL output at 10-minute intervals for a continuous operation of more than an hour by using FBG-based configuration with the SOA [38].

4.4 Comparison of DWFLs' Output Performance by Using Homogeneous and Inhomogeneous Gain Media

To observe the difference of output performance by both the homogeneous and inhomogeneous gain media, two setups by using the same wavelength selective element which have been presented previously are being compared as shown in table 4.2:

Table 4.2: Comparison of DWFLs by using AWGs and compression and tensile strain FBGs in EDFA and SOA as the homogeneous and inhomogeneous gain media respectively.

Wavelength Selective Elements	AWG		Compression and Tensile Strain FBGs	
Gain Media	EDFA	SOA	EDFA	SOA
Average output power	0.12 dBm	-13.00 dBm	-14.76 dBm	-30.28 dBm
Output power maximum difference	4.51 dB	10.00 dB	6.62 dB	4.95 dB
Average SMSR value	67.86 dB	56.00 dB	53.17 dB	42.54 dB
SMSR maximum difference	3.46 dB	13.00 dB	7.30 dB	11.02 dB

From the table, it can be conclude that the Erbium Doped DWFLs have better output performance as compared to the SOA-based DWFLs design. This is proved by higher amount of output power and SMSR value by using EDFA than by using the SOA as the gain medium, regardless the type of wavelength selective element used. Most of the maximum difference values for EDFA design are also lower than the SOA design, indicating a better output quality of the DWFLs comes from the EDFA as they provide fiber laser output with a higher level of consistency.

4.5 Summary

In this chapter, the generation of dual-wavelength fiber lasers are set forth by using three different wavelength selective elements namely AWGs, TBFs and FBGs. The gain media used are EDF and SOA with homogeneous and inhomogeneous broadening profile separately.

In the beginning, the dual-wavelength fiber lasers which employed EDF as a gain medium are presented. They are facing mode competition effect problem due to the homogenous broadening exhibited by the EDF material. Therefore, the cavity loss controlled technique has been introduced for the generation of dual-wavelength fiber lasers with two different types of configurations namely the ring cavity and the linear cavity configurations. Three types of wavelength selective elements are used namely the AWG, compression and tensile strained FBGs, and TBF to generate the DWFLs. The output performance of the DWFL by using the AWG having the best quality output with the highest amount of output power and SMSR of 0.12 dBm and 67.86 dB, respectively.The DWFL is then used together with high power amplifier to generate a high power fiber laser.

The SOA is then used as an alternative gain medium that exhibit an inhomogeneous broadening profile without mode competition issue, however, with a lower performance of output power and higher amount of noise. The difference performances of the erbium doped DWFLs and SOA-based DWFLs are then being compared. The result is, the erbium doped DWFLs are better in terms of their quality output. This is proved by higher amount of output power and SMSR value by using EDFA than by using the SOA as the gain

medium, regardless the wavelength selective element that was being used. Thus the EDF is more preferable to the SOA.

The next chapter will describe application of the DWFL by the virtue of new findings that have been explained in this chapter.

References

1. Shimose, Y., et al., *Remote sensing of methane gas by differential absorption measurement using a wavelength tunable DFB LD.* Photonics Technology Letters, IEEE, 1991. **3**(1): p. 86-87.
2. Shengchun, L., et al. *A dual-wavelength DBR fiber laser strain sensor*. in *OptoElectronics and Communications Conference, 2009. OECC 2009. 14th*. 2009.
3. Duan, L., et al., *A Dual-Wavelength Fiber Laser Sensor System for Measurement of Temperature and Strain.* Photonics Technology Letters, IEEE, 2007. **19**(15): p. 1148-1150.
4. Pinto, A.M.R., et al., *Interrogation of a Suspended-Core Fabry-Perot Temperature Sensor Through a Dual Wavelength Raman Fiber Laser.* Lightwave Technology, Journal of, 2010. **28**(21): p. 3149-3155.
5. Qureshi, K.K., et al., *Width-tunable pulse generation using four-wave mixing in bismuth based highly nonlinear fiber.* Optics Communications, 2007. **275**(1): p. 223-229.

6. Uchida, A., et al., *Wide-range all-optical wavelength conversion using dual-wavelength-pumped fiber Raman converter.* Lightwave Technology, Journal of, 1998. **16**(1): p. 92-99.

7. Tomkos, I., et al. *Highly performing wavelength converter based on dual pump wave mixing in semiconductor optical amplifier*. in *Lasers and Electro-Optics Society Annual Meeting, 1998. LEOS '98. IEEE*. 1998.

8. Xiangfei, C., D. Zhichao, and Y. Jianping, *Photonic generation of microwave signal using a dual-wavelength single-longitudinal-mode fiber ring laser.* Microwave Theory and Techniques, IEEE Transactions on, 2006. **54**(2): p. 804-809.

9. Jie, S., et al., *Stable Dual-Wavelength DFB Fiber Laser With Separate Resonant Cavities and Its Application in Tunable Microwave Generation.* Photonics Technology Letters, IEEE, 2006. **18**(24): p. 2587-2589.

10. Fei, W., et al. *A tunable and switchable single-longitudinal-mode dual-wavelength fiber laser for microwave generation*. in *Communications and Photonics Conference and Exhibition (ACP), 2010 Asia*. 2010.

11. Pradhan, S., G.E. Town, and K.J. Grant. *Microwave frequency generation using a dual-wavelength DBR fiber laser*. in *Optical Fibre Technology/Australian Optical Society, 2006. ACOFT/AOS 2006. Australian Conference on*. 2006.

12. Alouini, M., et al., *Dual tunable wavelength Er,Yb:glass laser for terahertz beat frequency generation.* Photonics Technology Letters, IEEE, 1998. **10**(11): p. 1554-1556.

13. Ming, T., et al. *Tunable narrow linewidth THz-wave generation using dual-wavelength fiber ring laser and organic DAST crystal*. in *Infrared Millimeter and Terahertz Waves (IRMMW-THz), 2010 35th International Conference on*. 2010.

14. Gong, Y.D., et al. *Tunable Terahertz Difference Frequency generation with 1550nm fiber laser*. in *Infrared and Millimeter Waves, 2007 and the 2007 15th International Conference on Terahertz Electronics. IRMMW-THz. Joint 32nd International Conference on*. 2007.

15. Pua, C.H., et al., *Study of Dual-Wavelength Mode Competition in an Erbium-Doped Fiber Laser (EDFL) Produced by Acoustic Waves.* Quantum Electronics, IEEE Journal of, 2012. **48**(12): p. 1499-1504.

16. Meng, J., et al. *A stable dual-wavelength single-longitudinal-mode fiber laser with a tunable wavelength spacing based on a chirped phase-shifted grating filter*. in *Communications and Photonics Conference and Exhibition, 2011. ACP. Asia*. 2011.

17. Gong, Y.D., et al., *Dual-wavelength 10-GHz actively mode-locked erbium fiber laser incorporating highly nonlinear fibers.* Photonics Technology Letters, IEEE, 2005. **17**(12): p. 2547-2549.

18. Xueming, L. and C. Lu, *Self-stabilizing effect of four-wave mixing and its applications on multiwavelength erbium-doped fiber lasers.* Photonics Technology Letters, IEEE, 2005. **17**(12): p. 2541-2543.

19. Yamashita, S. and K. Hotate, *Multiwavelength erbium-doped fibre laser using intracavity etalon and cooled by liquid nitrogen.* Electronics Letters, 1996. **32**(14): p. 1298-1299.

20. Park, N. and P.F. Wysocki, *24-line multiwavelength operation of erbium-doped fiber-ring laser.* Photonics Technology Letters, IEEE, 1996. **8**(11): p. 1459-1461.

21. Sun, J., J. Qiu, and D. Huang, *Multiwavelength erbium-doped fiber lasers exploiting polarization hole burning.* Optics Communications, 2000. **182**(1–3): p. 193-197.

22. Feng, S., et al., *Single-polarization, switchable dual-wavelength erbium-doped fiber laser with two polarization-maintaining fiber Bragg gratings.* Opt. Express, 2008. **16**(16): p. 11830-11835.

23. Shilong, P., Z. Xiaofan, and L. Caiyun. *Switchable single-longitudinal-mode dual-wavelength fiber ring laser using hybrid gain medium*. in *Lasers and Electro-Optics, 2008 and 2008 Conference on Quantum Electronics and Laser Science. CLEO/QELS 2008. Conference on*. 2008.

24. Chen, D., S. Qin, and S. He, *Channel-spacing-tunable multi-wavelength fiber ring laser with hybrid Raman and Erbium-doped fiber gains.* Opt. Express, 2007. **15**(3): p. 930-935.

25. Das, G. and J.W.Y. Lit, *L-band multiwavelength fiber laser using an elliptical fiber.* Photonics Technology Letters, IEEE, 2002. **14**(5): p. 606-608.

26. Feng, S., et al., *Switchable single-longitudinal-mode dual-wavelength erbium-doped fiber ring laser based on one polarization-maintaining fiber Bragg grating incorporating saturable absorber and feedback fiber loop.* Optics Communications, 2009. **282**(11): p. 2165-2168.

27. Bellemare, A., et al., *Room temperature multifrequency erbium-doped fiber lasers anchored on the ITU frequency grid.* Lightwave Technology, Journal of, 2000. **18**(6): p. 825-831.

28. Fok, M.P. and C. Shu, *Tunable dual-wavelength erbium-doped fiber laser stabilized by four-wave mixing in a 35-cm highly nonlinear bismuth-oxide fiber.* Opt. Express, 2007. **15**(10): p. 5925-5930.

29. Chien-Hung, Y., et al., *Tunable Dual-Wavelength Fiber Laser Using Optical-Injection Fabry Perot Laser.* Photonics Technology Letters, IEEE, 2008. **20**(24): p. 2093-2095.

30. Ahmad, H., et al., *Tunable dual wavelength fiber laser incorporating AWG and optical channel selector by controlling the cavity loss.* Optics Communications, 2009. **282**(24): p. 4771-4775.

31. Ahmad, H., et al., *Flat and compact switchable dual wavelength output at 1060 nm from ytterbium doped fiber laser with an AWG as a wavelength selector.* Optics and Laser Technology, 2011. **43**(3): p. 550-554.

32. Latif, A.A., et al., *A simple linear cavity dual-wavelength fiber laser using AWG as wavelength selective mechanism.* Laser Physics, 2010. **20**(11): p. 2006-2010.

33. Ahmad, H., et al., *High power dual-wavelength tunable fiber laser in linear and ring cavity configurations.* Chinese Optics Letters, 2012. **10**(1).

34. Latif, A.A., et al., *Dual-wavelength tunable fibre laser with a 15-dBm peak power.* Quantum Electronics, 2011. **41**(8): p. 709-714.

35. Shen, Y.R., *The principles of nonlinear optics*2003: Wiley-Interscience.

36. Ahmad, H., et al., *Dual wavelength fibre laser with tunable channel spacing using an SOA and dual AWGs.* Journal of Modern Optics, 2009. **56**(16): p. 1768-1773.

37. Latif, A.A., et al., *A compact O-plus C-band switchable quad-wavelength fiber laser using arrayed waveguide grating.* Laser Physics Letters, 2010. **7**(8): p. 597-602.

38. Chong, S.S., et al., *Synchronous tunable wavelength spacing dual-wavelength SOA fiber ring laser using Fiber Bragg grating pair in a hybrid tuning package.* Optics Communications, 2012. **285**(6): p. 1326-1330.

CHAPTER 5

APPLICATIONS OF DUAL-WAVELENGTH FIBER LASERS

5.1 Introduction

As has been discussed previously, DWFLs can be used for applications such as sensors and optical instrument testing [1-3] which requires high precision, and therefore normally sophisticated measurement. DWFLs are also applicable for Terahertz generation [4-7], iron concentration measurement [8]; and for microwave and millimeter-wave generation [9-11].

Additionally, dual-wavelength fiber lasers can also be applied in the communication systems as a wavelength converter by employing four waves mixing [12, 13] effects. This is achieved by converting the signal from one communication band to another without the use of any active devices to allow for an optical-electrical-optical conversion, thus effectively fulfilling the communication demand with a low cost borne by the network providers.

This chapter focuses on the potential applications of the DWFLs, and is therefore a continuity of the DWFL designs proposed in Chapter 4. It has to be noted that despite the fact that there are a number of applications for the DWFL, each of the application requires certain changes in the design of the DWFL in order to meet the unique demand of each application. Particularly, the majority of the DWFLs will need to be in single longitudinal

mode (SLM) operations, which is a condition whereby the laser sources are free of noise or mode fluctuations. Therefore, this chapter will also focus on some changes in the DWFL setup in chapter 4 which are required to satisfy the applications.

5.1.1 Single Longitudinal Mode Operation

As the concept of the single longitudinal mode (SLM) shall be very important in this work, it is useful to briefly explain the concept.

The SLM is an operation mode whereby the laser is operating with a narrow bandwidth of up to the KHz regime. Even though a stable cavity laser is operating in a single transverse mode due to the single mode fibers (SMFs), several longitudinal modes can still exist, which is manifested in 'beatings' when measurements are taken by using the spectrum analyzer, thereby increasing the noise of the fiber laser. These longitudinal modes are the result of the conditions within the cavity, which allows for multiple closely spaced longitudinal modes to oscillate inside the cavity [14, 15], and is detected via multiple peaks seen on the radio frequency spectrum analyzer (RFSA).

SLM operation, on the other hand, allows only the operation of one longitudinal mode. This, consequently, enables the forming of a truly stable fiber laser with a high spectral purity and therefore, removes any requirements on the surroundings. The SLM fiber laser design has a number of applications, especially in fiber strain optics sensors, temperature measurement, interferometry sensing, wind speed measurements with Doppler LIDAR, coherent detection in telecommunication, wavelength conversion and atmospheric pollution monitoring. This work will examine a number of these applications.

5.2 Tunable Dual-Wavelength Single-Longitudinal-Modes (DW-SLM) Fiber Laser

In this section, the DWFLs are designed to operate in a Single Longitudinal Mode (SLM). The importance of the design shall be discussed in this section.

5.2.1 Introduction

There are several techniques applicable for the generation of SLM fiber lasers. One such technique is to employ the so-called sub ring cavity technique [16-19], which functions by inserting a sub-ring cavity in the fiber laser design to suppress mode hopping inside cavity. Other techniques for achieving SLM operation rely on using the unpumped EDF technique [20-23], short cavity design [24-26] and an ultra-narrow transmission band FBG [27, 28]. All these design reduces the noise in the lasing system by suppressing the mode fluctuations of densely spaced longitudinal modes around the operating wavelength.

In this section, two techniques, namely, the unpumped EDF and the sub ring cavity design are employed in generating a DW-SLM laser. The setup is as discussed in the proceeding sub-section.

5.2.2 Experimental Setup and Results

The experimental setup of the proposed DW-SLM fiber laser is shown in Figure 5.1 below. This is same design as has been employed in Chapter 4, but with an additional component for the generation of a SLM fiber laser.

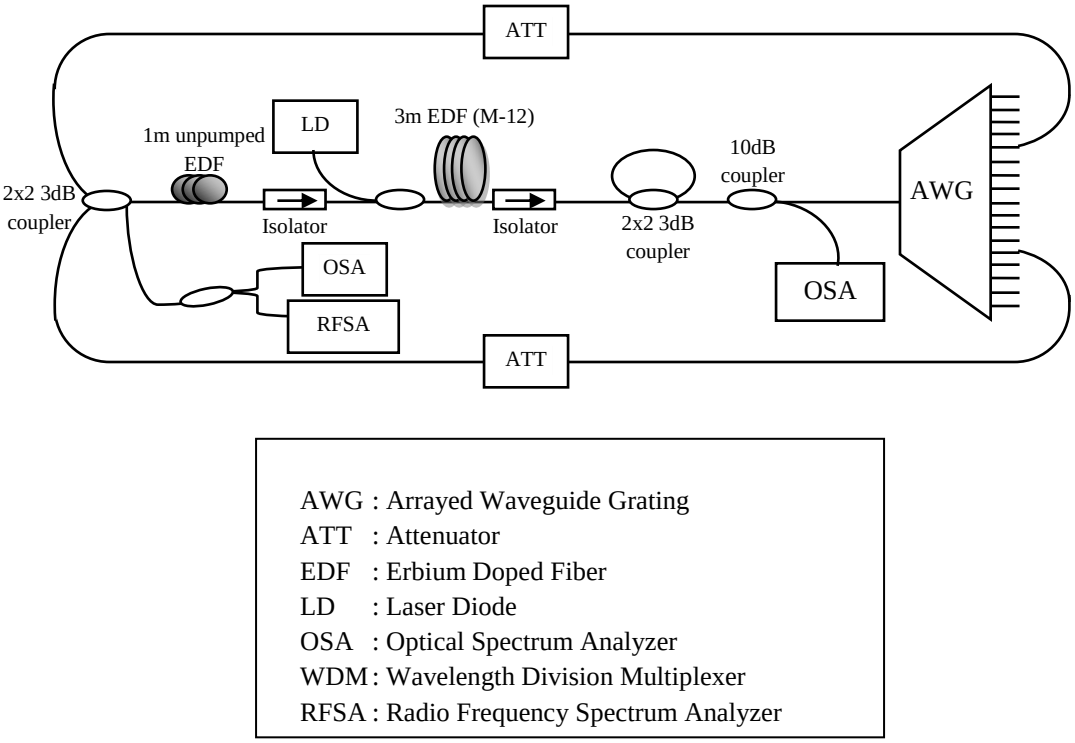

Figure 5.1: Experimental setup showing the various components for generating the DW-SLM.

The proposed system consists of a 3m Metrogain EDF (manufactured by Fibercore Ltd.) with absorption coefficients of 11.9 dB/m at 979 nm and 16.4 dB/m at 1531 nm, which acts as the ring cavity's gain medium. The 3 m EDF is pumped by a 980 nm pump laser operating with an output power of 240 mW through a 980/1550 nm WDM. As mentioned in the previous chapter, the pump laser excites the Erbium ion into higher state before emitting output radiation at both ends of the fiber, and is loosely considered as the ASE.

The difference between this configuration and the one discussed in Chapter 4 is the use of saturable absorbers (SAs) in the cavity. In this experiment, two types of saturable absorbers (SAs) are used to reduce the noise in the system. One SA consist of a sub-ring cavity connected to the cavity via a 2x2 3 dB coupler while the other one is a 1 m unpumped Isogain EDF. They are inserted, respectively, after and before the gain medium.

Figure 5.2 shows the dual-wavelength single-longitudinal-mode (DW-SLM) fiber laser that has been taken from an optical spectrum analyzer (OSA) with 0.02 nm of spectral resolution.

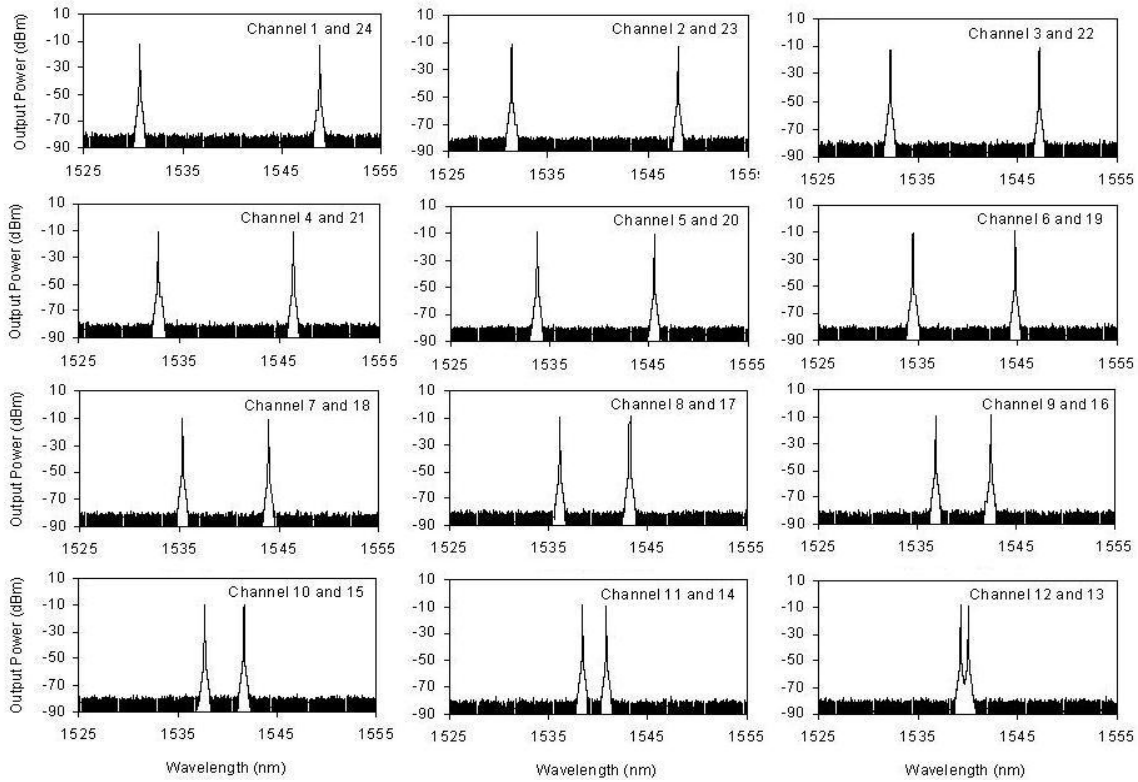

` Figure 5.2: The DW-SLM fiber laser from the widest spacing from Channel 1 and 24 to the narrowest spacing from Channel 12 and 13.

The design has 12 pairs of the DW-SLM fiber laser from 24 channels of the AWG with each taken in pairs from channel 1 and 24, channel 2 and 23 subsequently until channel 12 and 13. The output power is balanced using the cavity loss control method by using the two attenuators to balance the power in both cavity of longer and shorter wavelengths [29]. The average output power of the DW-SLM fiber laser is -10 dBm with a minimum and maximum output powers of -13.18 dBm and -8.12 dBm, respectively. The average of signal

to noise ratio (SNR) is about 70 dB, which indicates that the DW-SLM fiber laser is highly stable.

Figure 5.3 shows spectrum of the DW-SLM fiber laser taken from the RFSA in combination with a 6 GHz bandwidth of photodetector. The dual-wavelength pair measured comes from Channels 6 and 19 with output powers at 1535.4 nm and 1545.65 nm wavelengths, respectively. The wavelength pair chosen yields a 10.3 nm spacing which is equivalent to a wave beating of 1.3 THz.

Figure 5.3(a) shows the frequency domain spectrum analysed by the RFSA from the output power of the DW-SLM fiber laser before any SA is inserted inside the cavity. It can be observed that there are a lot of noise originating from the modes beating, indicating that the fiber laser is unstable. Figure 5.3(b) shows a significant reduction in noise after the sub-ring cavity SA is incorporated in the cavity. However several dominating modes beating still survive, and is finally quenched once the 1m unpumped EDF is inserted in the oscillating cavity. The final dual-wavelength output with the SLM operation is shown in figure 5.3(c).

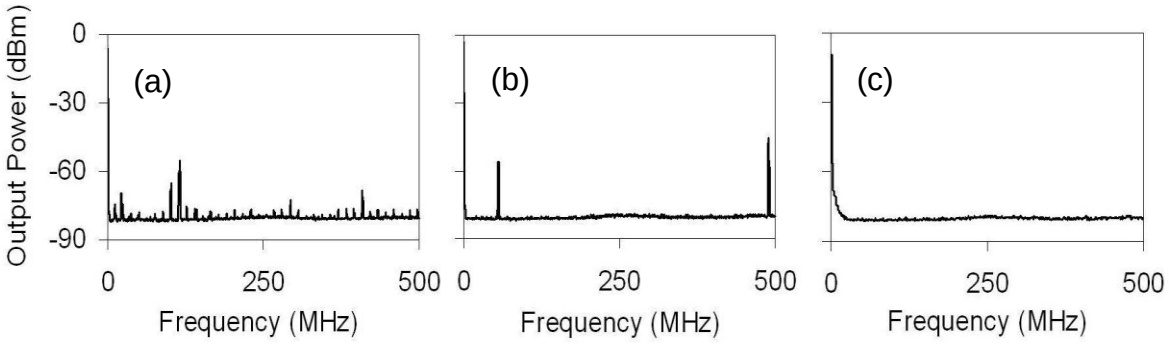

Figure 5.3: Spectrum from the RFSA taken (a) before inserting the SAs, (b) after inserting the sub-ring cavity, and (c) after inserting both SAs, depicting SLM operation.

In this experiment, the sub-ring cavity works in conjunction with the main cavity to only allow for the oscillation of the most dominant frequency, thereby increasing the performance of the fiber laser by reducing the number of longitudinal modes. The insertion of the 1m unpump Isogain EDF (with an absorption coefficient of 40 dB/m at 1530 nm) further suppresses the number of lasing neighbouring mode, consequently generating a SLM fiber laser.

Figure 5.4(a) shows the outputs of the DW-SLM fiber laser that are taken at six-minute intervals for an operation time of an hour. The graph shows that the DW-SLM fiber laser is quite stable as there are only slight changes in the output power. Figure 5.4(b) shows the frequency oscillating inside the cavity, depicted by the noise free curve graph, which spans from 1 to 7.8 GHz. This indicates the SLM operation of the dual-wavelength fiber laser.

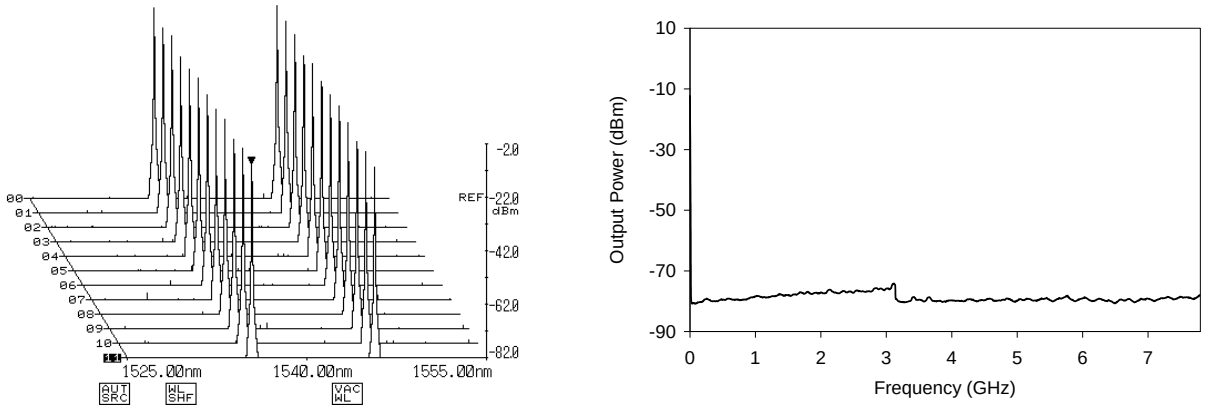

(a) (b)

Figure 5.4: (a) Stability of the DW-SLM fiber laser (b) Spectrum taken from the RFSA indicates a SLM mode operation of the fiber laser.

Figure 5.5(a) shows the spectrum taken from the OSA with two tunable laser sources (TLSs) used as a reference in order to observe the dual-wavelength from channel 6 and channel 19. As can be seen, the TLSs are denoted as TLS1 and TLS2 are inserted together with the dual-wavelength fiber laser in order to get wave beatings which are observable via the RFSA. However, due to the limitation of the RFSA available in our lab, the beatings can only be seen if the wavelengths of the TLSs are selected as close as possible to the wavelength of the DW-SLM fiber laser in order to get beats with frequencies lower than 7 GHz. The two peaks obtained from the beating of the two TLSs with the dual-wavelength fiber laser are observed as in Figure 5.5(b) which is taken from the RFSA.

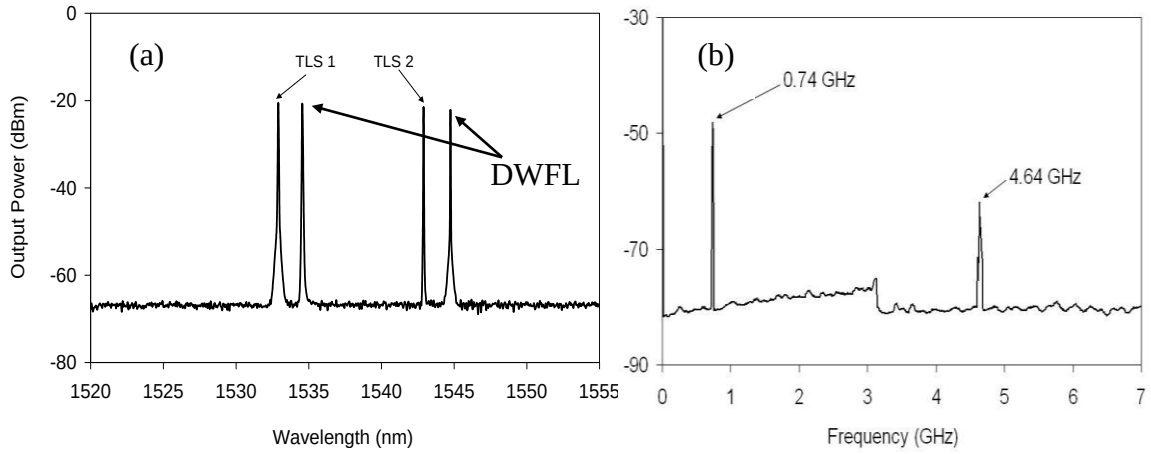

Figure 5.5: (a) The spectrum from OSA with two TLSs and the DW-SLM output are combined together (b) Spectrum from the RFSA.

To differentiate the beats coming from Channels 6 and 19, TLS 1 is operated in a narrow linewidth whilst TLS 2 in a wide linewith operation that is reflected by the two different linewidths of the frequency peaks observed in the RFSA. Only two peaks can be observed during the experiment and suddenly disappeared once the TLS is off indicating that the beats are coming from the beating of both TLSs with the DW-SLM fiber laser.

As the obtained beating of the proposed design is in the THz, this configuration is useful for terahertz generation. This is beyond the scope of this work and will be investigated in the future.

5.3 DWFL Wavelength Converter

Another possible application for the DWFL is for wavelength conversion via the Four-Wave Mixing Effect, as will be explained in this section.

5.3.1 Introduction

Wavelength conversion in communication systems is the process of converting modulated light signals from one wavelength to another. This is important in order to provide a simultaneous conversion of information from one channel to another channel in the DWDM systems. Several designs of wavelength converter have been proposed by other researchers [12, 30-32], and typically comprises a dual-wavelength fiber laser injected into the nonlinear gain media such as a highly nonlinear fiber (HNF) or a SOAs. Further discussion of the wavelength converter design is being discussed in the next sub-section.

5.3.2 Experimental Setup and Results

The setup design for the wavelength conversion application is shown in Figure 5.6. Three gain media are used in the setup, which are EDFA 1, SOA and EDFA 2. EDFA 1 comprises a 48 cm Bismuth EDF (Bi-EDF) that is pumped bidirectionally with pump power of 180 mW each at 1480 nm, whilst EDFA 2 comprises a 14 m EDF that is pumped by a 80 mW of 980 nm laser diode. The SOA is driven by a 300 mA of driven current.

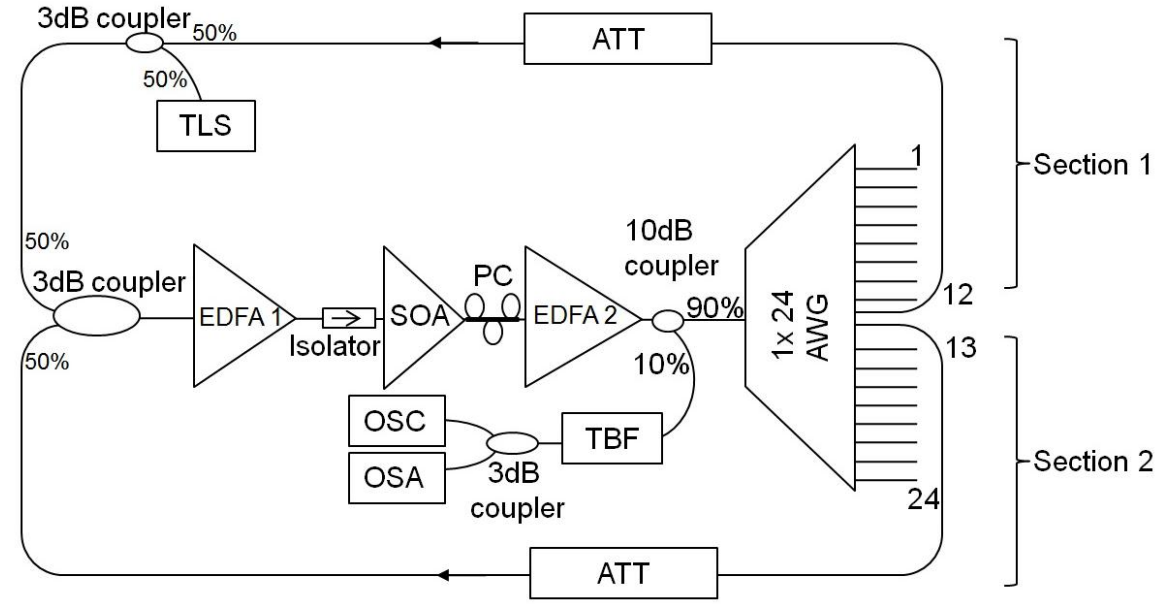

TLS	: Tunable Laser Source	AWG	: Arrayed Waveguide Grating
EDFA	: Erbium Doped Fiber Amplifier	OSC	: Oscilloscope
SOA	: Semiconductor Optical Amplifier	ATT	: Attenuator
TBF	: Tunable Bandpass Filter	PC	: Polarization Controller

Figure 5.6: Experimental setup for wavelength conversion by using DWFL.

The configuration of the wavelength converter design is almost the same as the previous design of DWFL as being described in Chapter 4. The only different is that, a TLS incorporated in the cavity and the SOA used in the setup works as a nonlinear gain medium. This is thus creating a nonlinear phenomenon which is called as a four-wave mixing effect for the wavelength conversion. The PC is used to control the polarization state to maximize the FWM effect.

In the design, Channel 1 until Channel 12 of the AWG ports are grouped as Section 1 while Channel 13 to Channel 24 are grouped as Section 2. The EDFA 1 works as the gain medium to generate the DWFL, at the same time works as a pre-amplifier of the FWM effect that comes from the SOA. The TLS used in the setup is to give the modulation signal to be converted by DWFL design. It is connected to the cavity by using a 50/50 coupler and being inserted in Section 1.

The process of wavelength conversion is firstly done by controlling the ATT in both sections in order to get a balanced dual-wavelength output as depicted in Figure 5.7(a). When the output power of both wavelengths is at the same amplitude, then both the SOA and EDFA 2 are inserted in the cavity as each provides the wavelength conversion and amplification respectively. The spectrum output is shown as in Figure 5.7(b) where λ_{c4} and λ_{c5} are generated from the DWFL denoted as λ_{p1} and λ_{p2} .

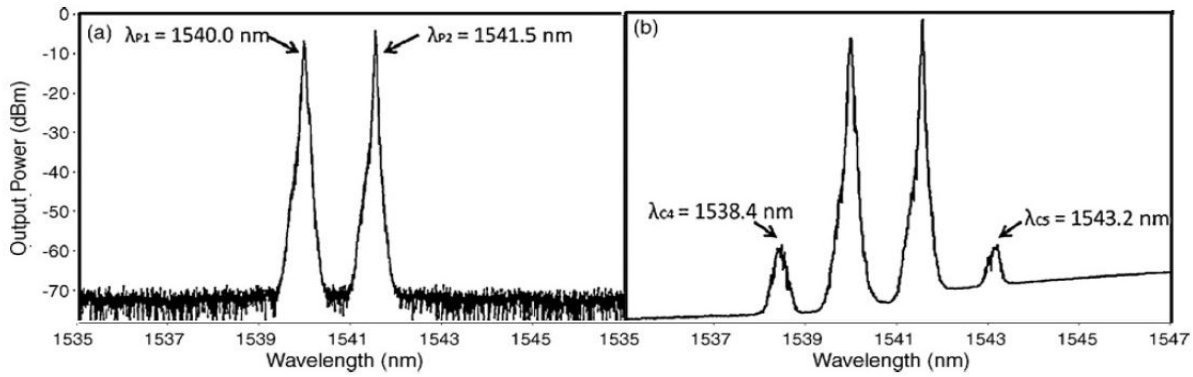

Figure 5.7: The spectrum of DWFL without the modulation from the TLS taken (a) after EDFA 1 and (b) after the SOA where FWM effect can be seen denoted as λ_{c4} and λ_{c5} [33].

The application for wavelength conversion is done by injecting both the pumps λ_{p1} and λ_{p2} and also the modulated signal, denoted as λ_s. As can be seen from Figure 5.8, λ_{p1} and λ_{p2} have two conjugate of FWM which are λ_{c4} and λ_{c5} .

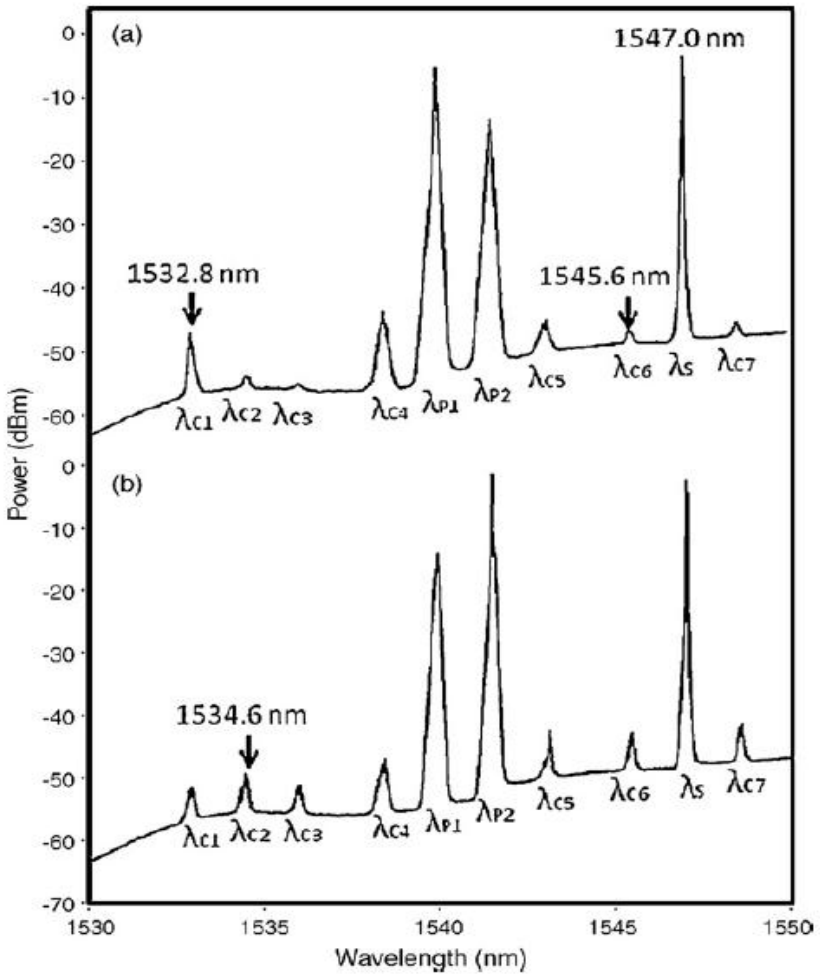

Figure 5.8: The spectrum of four-wave mixing response when two pump which are λ_{p1} and λ_{p2} ; and a modulated signal, λ_s are injected in the cavity, when (a) the power of $\lambda_{p1} > \lambda_{p2}$ and (b) when the power of $\lambda_{p2} > \lambda_{p1}$ [33].

At the same graph, two replicas are also formed called as λ_{c6} and λ_{c7}. The wavelength spacing from the signal, λ_s to each of the replicas are the same as the wavelength spacing between the two pumps, λ_{p1} and λ_{p2} of 1.4 nm. There are also three other conjugates formed at the shorter wavelength side denoted as λ_{c1}, λ_{c2} and λ_{c3}. Each wavelength can be expressed as [33, 34]

$$\begin{aligned}
\lambda_{c1} &= 2 \text{ x } \lambda_{p1} - \lambda_s \\
\lambda_{c2} &= 2 \text{ x } \lambda_{p2} - \lambda_s \\
\lambda_{c3} &= \lambda_{p1} + \lambda_{p2} - \lambda_s \\
\lambda_{c4} &= \lambda_{p1} - (\lambda_{p2} - \lambda_{p1}) \\
\lambda_{c5} &= \lambda_{p2} - (\lambda_{p1} - \lambda_{p2}) \\
\lambda_{c6} &= \lambda_s - (\lambda_{p2} - \lambda_{p1}) \\
\lambda_{c7} &= \lambda_s + (\lambda_{p2} - \lambda_{p1})
\end{aligned} \tag{5.1}$$

Figure 5.8 (a) shows the spectrum, where the output power of λ_{p1} is higher than λ_{p2}, giving a higher amplitude of output power at λ_{c1}, whilst Figure 5.8 (b) shows that λ_{p2} is higher than λ_{p1} which gives a higher amplitude of output power at λ_{c2}. The spectra also implies that both of the conjugates with λ_{c1} at 1532 nm wavelength and λ_{c2} at 1534.6 nm wavelength are generated by the interaction of each pumps with the modulated signal, giving a modulated signal transfer from 1547 nm of λ_s to both of the 1532 nm and 1534.6 nm wavelength of λ_{c1} and λ_{c2} respectively. This is the reason for the name 'wavelength conversion'.

To prove that the modulated signal from λ_s is being transferred to λ_{c1} and λ_{c2}, three modulated signals of 0.5 kHz, 1.5 kHz and 2.0 kHz are given through an internal modulator from λ_s. The converted signal at λ_{c1} and λ_{c2} are then filtered by using a TBF. The output that only has the transferred signal at λ_{c1} or λ_{c2} are then analyzed by using an oscilloscope through a 6 GHz photodetector. The output modulation taken at λ_{c1} is as illustrated in Figure 5.9. The same pattern is also observed by taking the output from λ_{c2} after being filtered by the TBF.

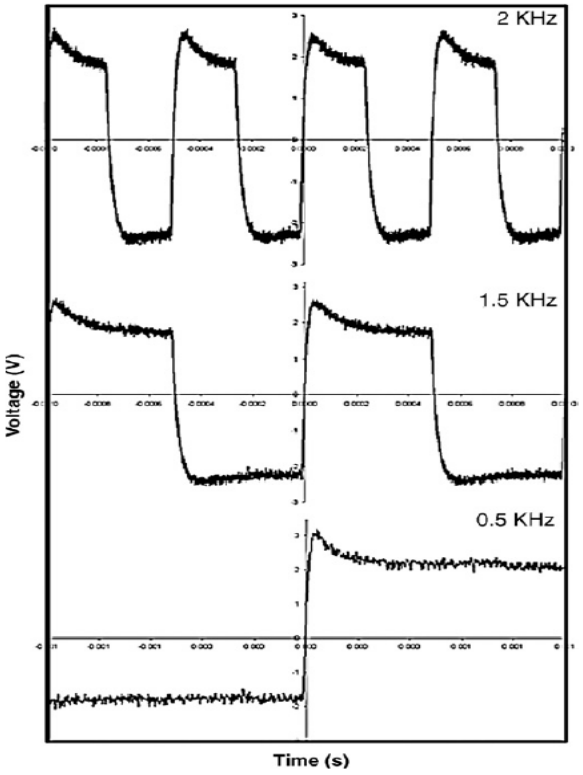

Figure 5.9: A transferred signal from λ_s at 1547.0 nm to λ_{c1} at 1532.8 nm after passing the SOA at 0.5 kHz, 1.5 kHz and 2.0 kHz of modulation signal [33].

5.4 Dual-Wavelength Temperature Sensor

In this section, the DWFL is being designed for the application of temperature sensor. A brief discussion on the importance of the design is being mentioned in the preceding sub-section.

5.4.1 Introduction

There has been significant interest in the development of high resolution temperature sensors capable of detecting and measuring minute shifts in for a wide variety of application recently. This includes the application in nano-biotechnology [35], microfluidic mechanics[36], thermal drift measurement in electronic equipment [37] and also temperature changes from catalysis reactions [38, 39]. Traditionally, such temperature measurements can be done by conventional technologies such as thermistors, thermocouples, resistance temperature detectors (RTDs) and platinum resistance temperature (PRT) sensors, which have resolutions ranging from 0.1^{o}C to 0.001 ^{o}C [40-42]. However, these sensors work on the electrical and mechanical responses to heat stimuli, and as a result very costly and fragile. They are also extremely sensitive to electromagnetic and environmental interference [43].

In this regards, fiber-based sensors are becoming highly potential alternatives with several designs that have been invented [44-49]. In order to increase the resolution of fiber Bragg grating (FBG) based sensors, frequency beating technique by using the dual-wavelength fiber lasers is being set forth in the study with a resolution of 0.0023 ^{o}C [50]. The experimental setup will be discussed in the next sub-section.

5.4.2 Experimental Setup and Results

The experimental setup in this section is being separated into two parts, namely the generation of the (single longitudinal mode) SLM operation in the ring cavity and the beating of two frequencies, from the SLM-FL and the TLS for temperature sensing.

5.4.2.1 SLM-FL Operation

As a means to generate a very stable SLM output with a low noise capability, the cavity length has to be short, in this case approximately 5.2 m. The experimental setup is shown in Figure 5.10, which consists of a single longitudinal mode fiber laser (SLM-FL) capable of generating a stable dual-wavelength output to be used in the development of the dual-wavelength beating measurement system. The design of the SLM-FL for temperature detection consists of a 0.5 m long zirconia-based erbium-doped fiber (Zr-EDF) with an erbium ion concentration of 3000 ppm.

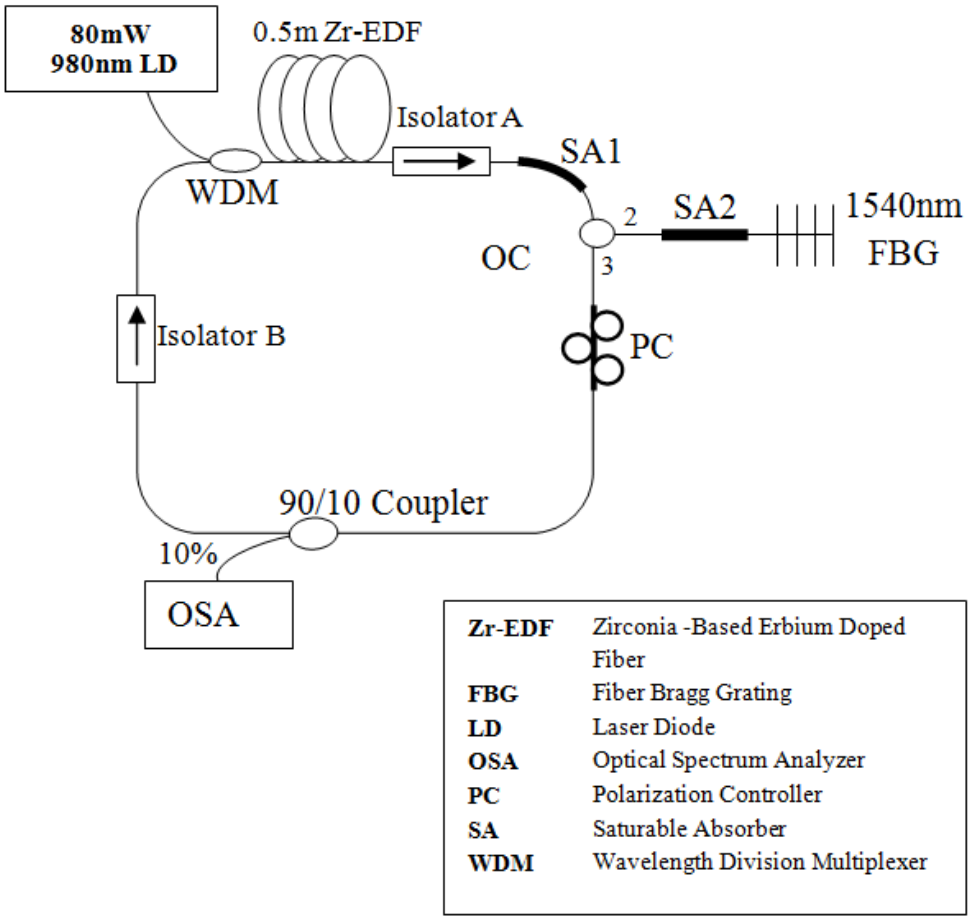

Figure 5.10: Experimental setup of Single Longitudinal Mode Fiber Laser (SLM-FL)[50].

This fiber is pumped by an 80 mW 980 nm laser diode through a 980/1550 nm WDM with a peak absorption coefficient of 18.3 dB/m at 978 nm. The ASE are generated at both ends of the Zr-EDF and made to oscillate in a clockwise direction by having two Optical Isolators, Isolator A and B in the cavity. After passing Isolator A, the ASE then enters the first saturable absorber, designated SA1.The output of SA1 then enters Port 1 of the OC and will then be emitted at Port 2. This will then travel towards a 1540 nm FBG which acts as the temperature sensor via SA2, the second saturable absorber. SAs with different lengths (3 cm for SA1, and 6 cm for SA2) are used to suppress the mode hoping effect, and

allowing only SLM propagation inside the cavity, and also to reduce the noise in the system.

At different temperatures, the reflected wavelengths will be different, corresponding to the expansion or contraction of the FBG as has been discussed in Chapter 2. The reflected beam will then travel back into Port 2 and will be emitted through Port 3 of the OC. It is then travels through a Polarization Controller (PC) towards a 90:10 coupler, with the 90% output travelling to Isolator B. It is finally reconnected to the WDM to complete the ring cavity. The 10% output leg is connected to an Optical Spectrum Analyzer for observing the single longitudinal mode (SLM) oscillation. The SLM operation is verified using a radio frequency-spectrum analyzer (RF-SA, Anritsu MS 2683A, 9 kHz to 3.8 GHz) together with a 6 GHz photodetector.

One of the most important requirements in this study is to get the ring fiber laser to operate in the SLM mode. This can be achieved by using a ring cavity with a short-cavity length. In normal approaches, the active fiber component on standard erbium dopant concentrations will have a length of 15 m or longer. To recall, the length that has been used in this thesis is 5m which is also relatively long. This length limits the shortest length achievable by the cavity, which in turn affects the generation of the SLM output. In this chapter, a new type of fiber based on Zirconia as one of the dopant materials in a silica host allows the accommodation of high erbium concentrations, and in this case is about 3000 ppm giving an active length of only 0.5 m. Although the overall length of the cavity is about 5.2 m, by having shorter fiber lengths on all the components, a very compact cavity can be realized and therefore allowing easy and stable SLM operation.

The roles of the SAs are important in achieving SLM operation as shown in Figure 5.11 and Figure 5.12. Figure 5.11 shows the operation without the SA in a ring cavity. In this measurement, the OSA in Figure 5.10 is replaced by a 6 GHz photodetector together with the RF-SA. From the trace of Figure 5.11, multiple peaks can be observed, indicating multiple longitudinal modes of oscillation.

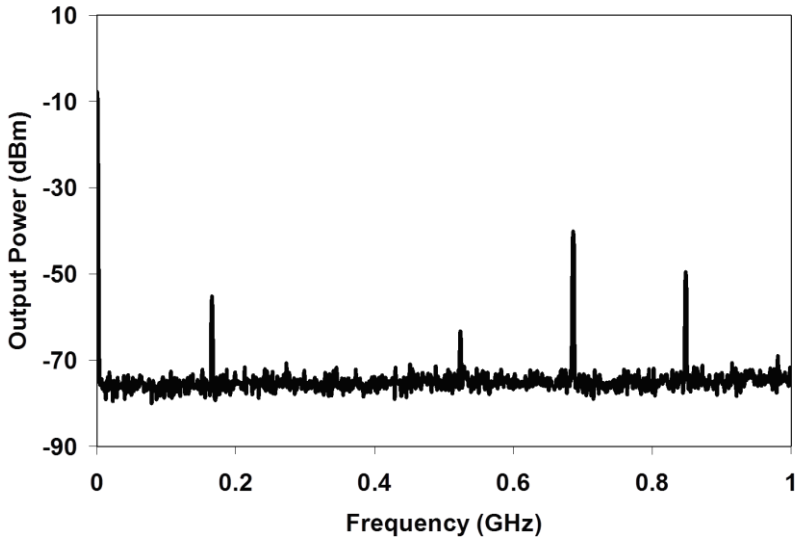

Figure 5.11: Frequency spectrums that have been taken from SLM-FL (a) before adding the saturation absorber [50]

However, when the SAs are placed within the ring cavity as mentioned earlier, the traced obtained indicates only a single longitudinal mode oscillating, as shown in Figure 5.12.

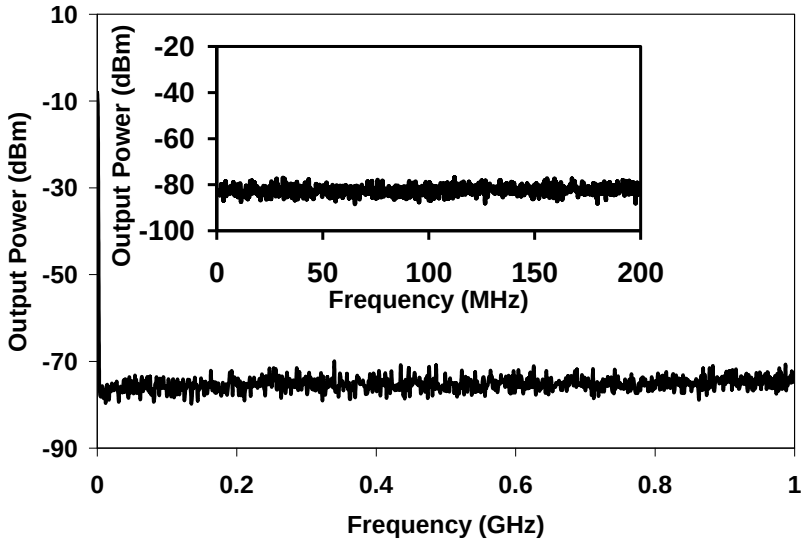

Figure 5.12: Frequency spectrums that have been taken from SLM-FL incorporating saturation absorber (the inset is on the expanded time-scale) [50]

Figure 5.13 shows the stability performance of the SLM-FL as measured using an OSA with a span of 10 minutes between every repetition.

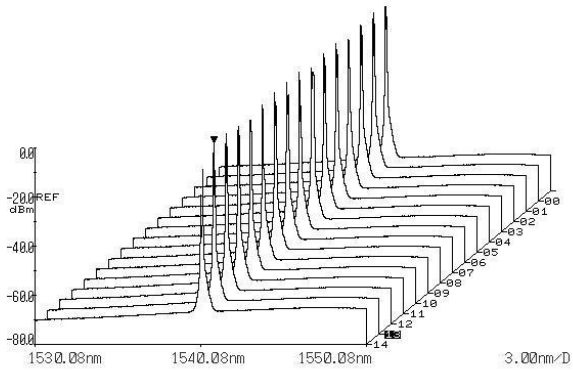

Figure 5.13: Stability performance of the SLM-FL taken from the OSA

Further verification of the SLM behavior is demonstrated using the setup as shown in Figure 5.14 using the delayed self-heterodyning technique as to provide the line-width measurement of the SLM-FL. This confirms that the operation of the ring cavity is in the

single-longitudinal mode only. The line-width measurement consists of the output for the SLM-FL being connected to the input of the first 3 dB fused coupler, with one of the output ports connected to a 500 m long SMF-28 which is then connected to a PC. The other port of the first 3 dB fused optical coupler is connected to an acousto-optic modulator (AOM) operating at 80 MHz. The output ports of the both ends are then recombined using another 3 dB fused optical coupler, with the output port connected to the RF-SA.

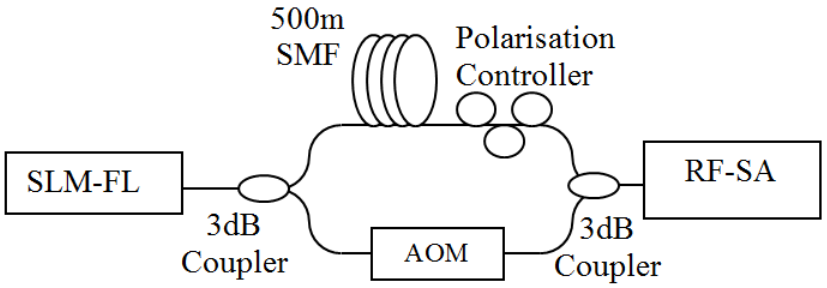

AOM	: Acousto – Optic Modulator
SLM-FL	: Single Longitudinal Mode –Fiber Laser
SMF	: Single Mode Fiber
RF-SA	: Radio Frequency – Spectrum Analyzer

Figure 5.14: Delayed self-heterodyne line-width measurement [50].

The line-width is measured by having the AOM in the off state, to observe the spectrum at the RF-SA, which gives a line at 0 Hz. Once the AOM is turned on, the beating of the two signals will give a spectrum at the same spot as the applied frequency of the AOM. From the Figure 5.15, the line-width is measured to be about 0.2 MHz at 3 dB bandwidth.

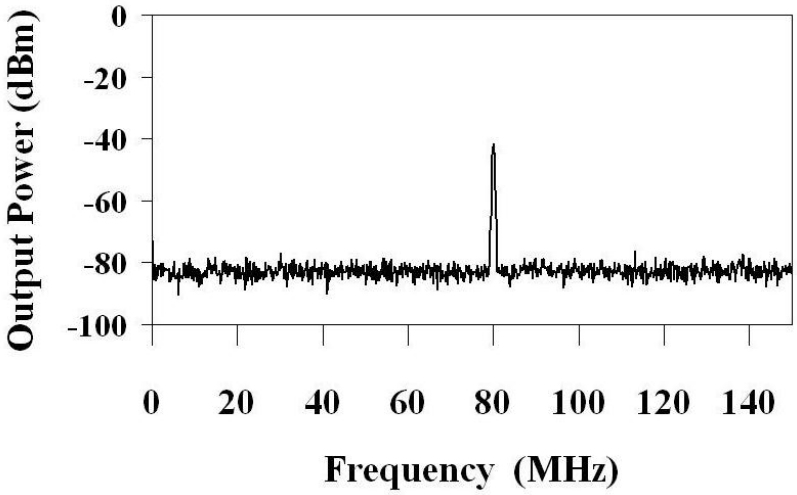

Figure 5.15: Signal at 80MHz of the Acousto-Optic Modulator (AOM) [50].

The above measurements clearly indicate that the fiber laser operates in the SLM mode.

5.4.2.2 Temperature Sensing Using the Beating Technique

The temperature sensor, which is shown in Figure 5.16, consists of a 1540 nm FBG on a hotplate with one end connected to the SLM-FL. The temperature is tuned by adjusting the current flow into the hotplate. A calibrated thermometer (Fluke 53 II) that is placed next to the FBG provides the measured temperature. The hotplate used is a very simple laboratory hotplate, and thus may not be able to provide stable temperatures over time as can be seen from the measurements in the following section.

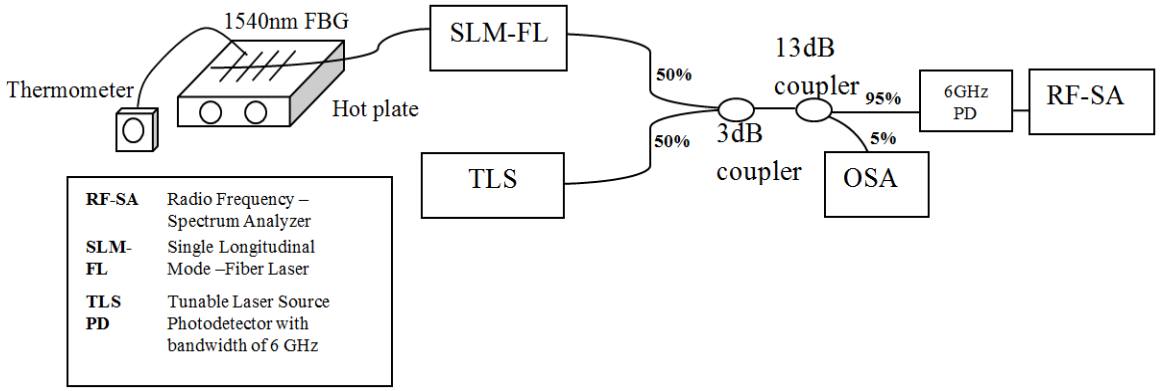

Figure 5.16: Experimental setup of dual-wavelength beating measurement [50].

The output of the SLM-FL, corresponding to any temperature change, giving a particular wavelength or frequency oscillation in the ring cavity that is then mixed with the output from a Tunable Laser Source (TLS, Anritsu MG9638A, range: 1500 to 1580 nm and a linewidth of 700 kHz). The wavelength output of the TLS is chosen to be around 1540 nm, as close as possible to the oscillating wavelength of the SLM-FL, which is mixed with the output of the SLM-FL using a 3 dB fused optical coupler. The output port of the 3 dB fused optical coupler is then connected to the input port of a 13 dB coupler with the 95% output port connected to an RF-SA, while the 5% port is connected to an OSA. The function of the PC in the SLM-FL is to adjust the polarization state of the oscillating signal in the ring cavity as to provide the best beating. The RF-SA provides the signal analysis in terms of obtaining SLM operation in the ring cavity, as well as the analysis of the beating from the two signals. The OSA provides the necessary information for the spacing between the two wavelengths.

In the temperature sensing application, the SLM-FL is used as one of the sources for the beating technique, with the other source being the TLS. One end of the SLM-FL is

connected to the FBG as explained earlier in Figure 5.16, which is placed on top of a hotplate. As the temperature increases from the hotplate (which is being monitored by the thermometer), the reflected wavelength from the FBG will be made to oscillate in the ring cavity, giving an SLM output which is then mixed with the signal from the TLS. The output wavelength of the TLS is adjusted to be as close as possible to that of the SLM-FL, giving a combined output in the OSA as shown in Figure 5.17(a). At 26 ^{o}C, the two traces combine to give a single trace due to the limited resolution of the OSA. As the temperature increases to 27 ^{o}C, the shift of the SLM-FL wavelength is more pronounced as shown in the figure, and continues to increase as the temperature rises, giving the measured displacements of the two peaks. Figure 5.17 (b) shows the measurement from the RF-SA for the same temperature changes. Since the hotplate is not of the precision type, and the measurement of the temperature uses a thermometer, there will be some possibility of error in the temperature measurement.

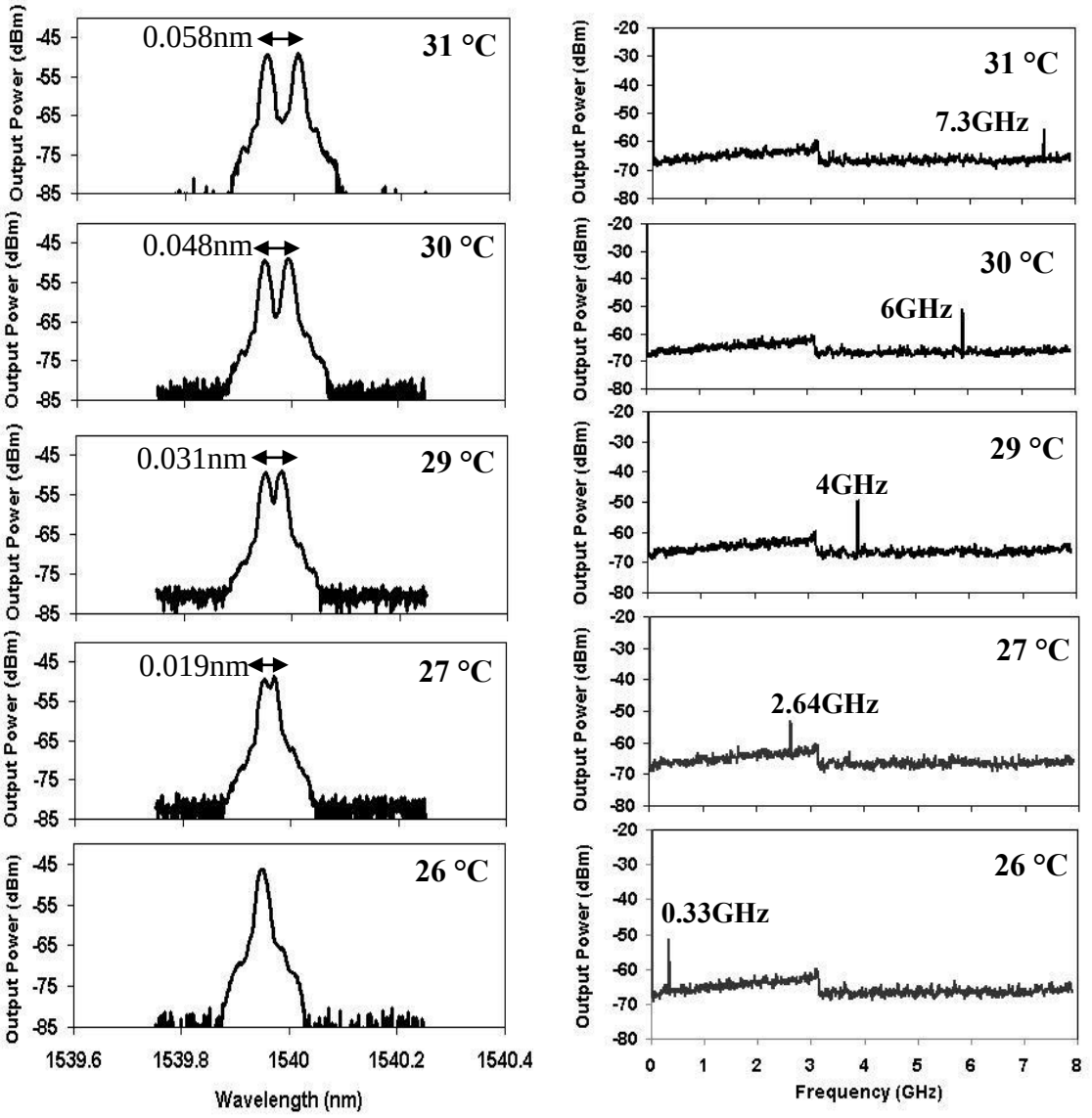

(a) (b)

Figure 5.17: Frequency and wavelength spectrum that have been taken by using (a) OSA and (b)RF-SA respectively [50].

The results from Figure 5.17(b) are tabulated and plotted in Figure 5.18, giving a linear relationship between the rise in the temperature and the increase in the frequency obtained. A linear graph with a gradient of approximately 1.3 GHz/^{o}C is obtained. The linear

regression, R^2 is equals to 0.97. From the values obtained in Figure 5.17(b) and Figure 5.18, an error of ± 0.4 ^{0}C is obtained.

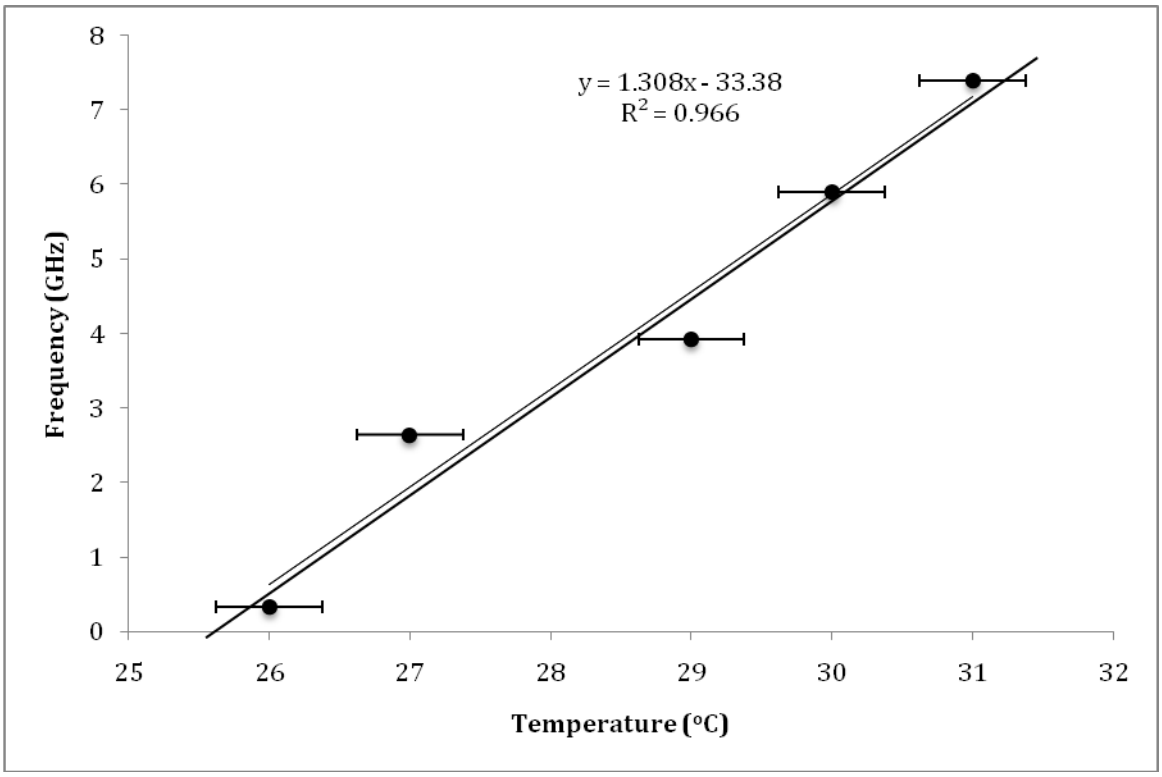

Figure 5.18: Graph of frequency response versus temperature[50].

Taking into account the resolution bandwidth of the RF-SA to be of 20 MHz for the GHz range, the nominal temperature resolution that can be measured with this system is about 0.015 ^{o}C.

From the above demonstration, this is the first report to the knowledge of the author of using the beating frequency technique for temperature sensing. This approach can be further improved to give a better temperature. The current limitation is the usage of the standard laboratory hotplate, as the heating element is not precise and the use of the low

resolution thermocouple to measure the temperature. It is difficult in the current setup to precisely measure the temperature of the hotplate.

5.5 The Generation of Microwave Signals by Using DWFL

Another application of the DWFL is the microwaves generation for the communication systems purposes. This section is set forth to discuss about the microwaves generation deeper by explaining the propose configuration layout in order to generate the microwave signal. Here, the generation of dual-wavelength closely spacing single longitudinal mode fiber laser is done by using two different wavelength selective element which are by using Fiber Bragg Gratings (FBGs) and Arrayed Waveguide Gratings (AWGs) inside the cavity. The technique used is basically using the modulator and polarization controller (PC) as the modulation can produce sidebands that can stabilize the dual-wavelength fiber laser in the optical spectrum. This is suitable especially for the microwave application. The frequency generated varies from 1.4 GHz to 43.4 GHz and can be observed from the RFSA.

5.5.1 Introduction

The generation of microwave and millimeter-wave need the dual-wavelength to be emitted around a close longitudinal mode spacing to produce the microwave or millimeter-wave beats signals. This becomes a vital problem to be solved when the EDFs are used. A few techniques have been done to generate the dual-wavelength close spacing SLM fiber laser in order to obtain the microwave beating [10, 11, 51-53]. The frequency generated is varying, from 3.0 GHz to 60.0 GHz. The normal operation of dual-wavelength fiber laser

usually needs two FBGs to generate dual-wavelength fiber laser. One of an advance technology is a technique proposed by X. Chen et.al. [10] that uses an ultra-narrow transmission band fiber Bragg gratings (UNTB-FBGs) which is yet quite difficult to be fabricated. The work proposed in this chapter is to suggest a new technique for dual-wavelength fiber laser operation with 43.4 GHz of beating frequency by using only a single typical Fiber Bragg Grating; 1.4 GHz, 2.5 GHz and 3.2 GHz by using two AWGs. The designs proposed in this section use a modulation technique which comprises PCs and the modulator. They are used to control the polarization state of the cavity thus, helps in stabilizing the dual-wavelength close spacing fiber laser.

5.5.2 By Using a Single FBG

In this sub-section, a single FBG is used as the wavelength selective element to generate the DWFL with a beating signal that can be detected by using the RFSA as will be discussed in this preceding sub-section.

5.5.2.1 Experimental Setup and Results

The experimental setup of the proposed dual-wavelength closely spaced single longitudinal mode fiber laser, by using an FBG is shown in Figure 5.19 below:

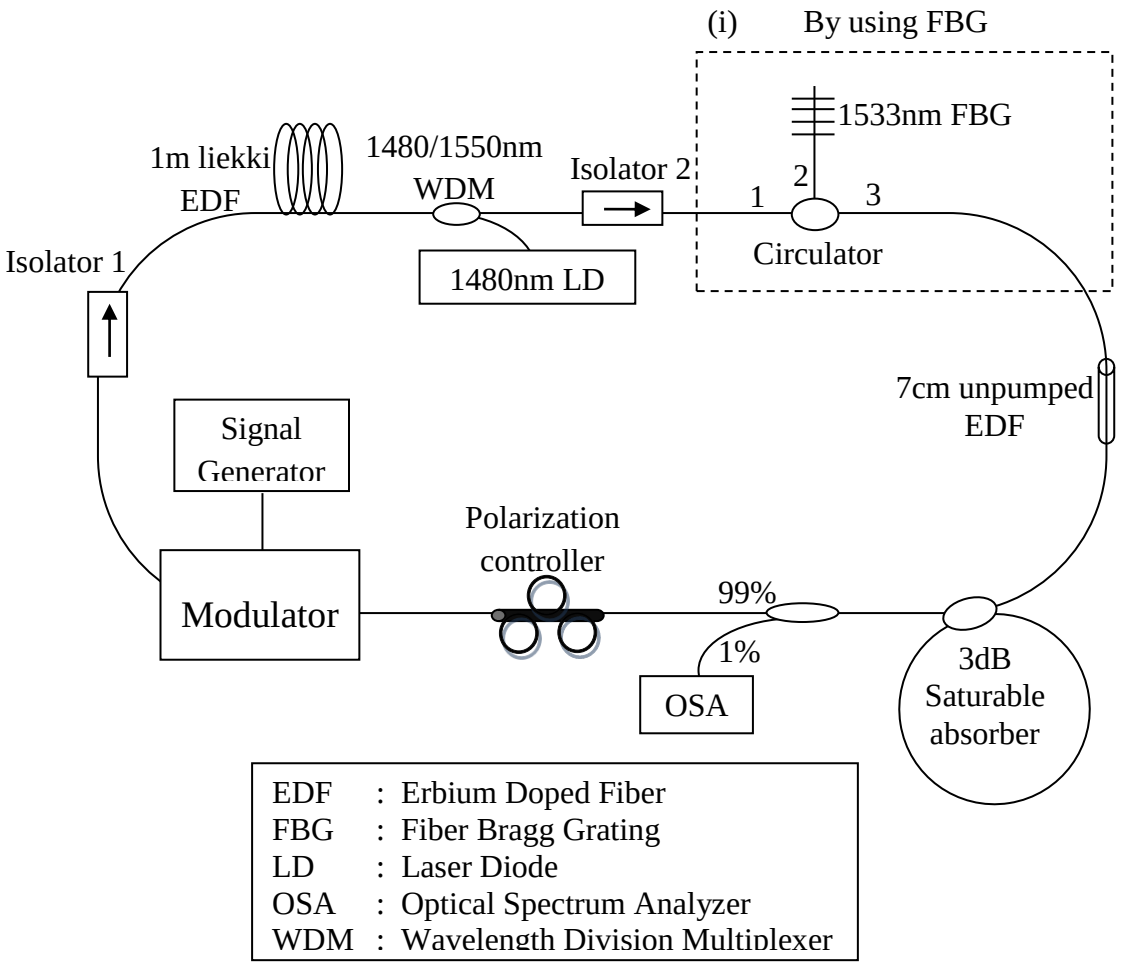

Figure 5.19: Experimental setup showing the various components for generating the DW-close spacing SLM fiber laser by using a single FBG.

The dual-wavelength closely spaced SLM fiber laser is constucted by using a ring cavity configuration. The active gain medium used in the setup is a 1m highly doped EDF from Liekki (Er80-8/125) with absorption of 45 and 80 dB/m for 1400 and 1530 nm respectively, giving some advantages compared to others such that only short fiber length is needed, as well as having low splicing loss and large mode area, which are suitable for medium power fiber laser application.

A 1480 nm LD is used to pump the EDF through a 1480/1550 nm WDM at 340 mW pump power. The backward pumping technique is used in the proposed setup, as suggested by L. Xiao et.al. [54] in order to optimize the usage of the high power laser diode in the experimental setup. The propagation of 1480 nm light through the WDM leads to the creation of the ASE from the EDF that finally propagates in the clock-wise direction by virtue of the 1550 nm isolator which is denoted as Isolator 2. The ASE then travels through a circulator that works together with the 1553 nm FBG connected to port 2 which serves as the wavelength reflector before being connected to a 7 cm unpumped highly doped Liekki EDF (Er80-8/125).

The other end of the 7cm umpumed EDF is connected to a 3dB Saturable Absorber (SA) before connected to a 99:1 coupler. At this point, the 99% port is then connected to the input of a Mach–Zehnder modulator (JDS Uniphase OC-192) to modulate the laser driven by a 130 kHz transmission using a synthesized signal generator (SSG) from Anritsu. The output port of the modulator is then connected to another isolator denoted as Isolator 1 before being looped back to the 1m highly doped EDF to complete the cycle of the fiber laser. Both of the isolators serve to let a unidirectinal circulation in a clock-wise direction

inside the cavity. The 1% port of a 99:1 coupler is connected to an SOA (YOKOGAWA AQ6370B) with a 0.02 nm resolution and to an oscilloscope (LeCroy with 500MHz bandwith and 2Gs/s) to analyze the lasing profile of the proposed fiber laser.

In this setup, two types of saturable absorbers are used in order to obtain a stable single longitudinal mode (SLM) fiber laser which comprises of a sub-ring cavity (from a 2x2 3 dB coupler) and a highly doped umpumed EDF. As explained before, the sub-ring cavity works in conjunction with the main cavity to oscillate the most dominion frequency giving a higher ability to perform a fiber laser with a single-longitudinal-mode operation. By inserting the 7 cm highly doped umpumped EDF, more neighbouring mode lasing can be suppressed, which consequently helps in generating single-longitudinal-mode fiber laser. The use of the PC in the setup is vital as it serves as a stabilizer to control the polarization state of the fiber laser during the operation.

Figure 5.20 shows the dual-wavelength fiber laser with a close-spacing of 0.34 nm which equals to 43.4 GHz spacing coming from a single 1533 nm FBG. The splitting of the dual-wavelength is observed when the fiber laser is modulated with 130 kHz sinusoidal pulse by the synthesized signal generator. The dual-wavelength close-spacing fiber laser is obtained by rotating the PC which gives a certain way of controlling the polarization state of the fiber laser hence stabilizing the dual-wavelength fiber laser output.

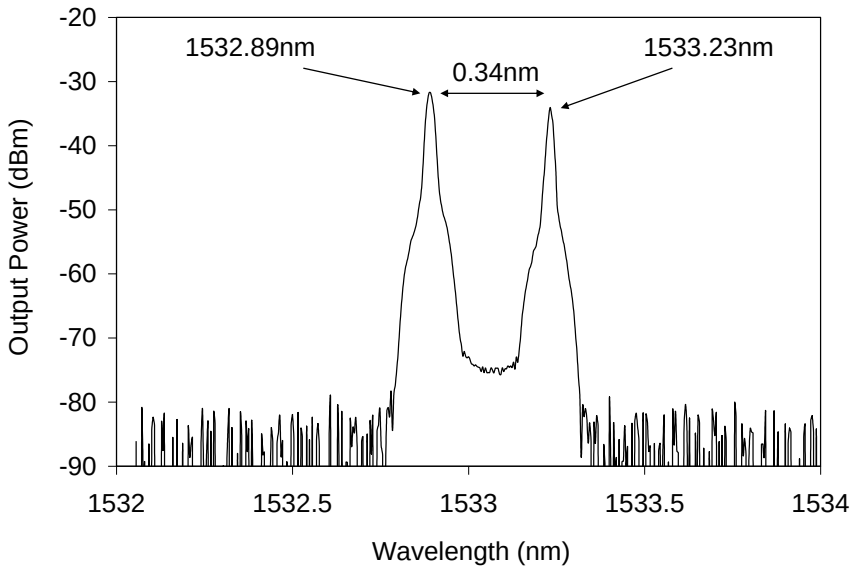

Figure 5.20: The spectrum of the fiber laser with the modulation technique observed from the OSA

The RF modulation given works to split the dual-wavelength output by producing sideband in the optical spectrum [55]. The use of the modulator and PC is greatly improves the dual-wavelength fiber laser performance as compared to the operation without the modulator. This is shown in Figure 5.21, in which the modulator is removed from the setup that leads to the erratic dual-wavelength output even though the PC is used to stabilize the output of the fiber laser.

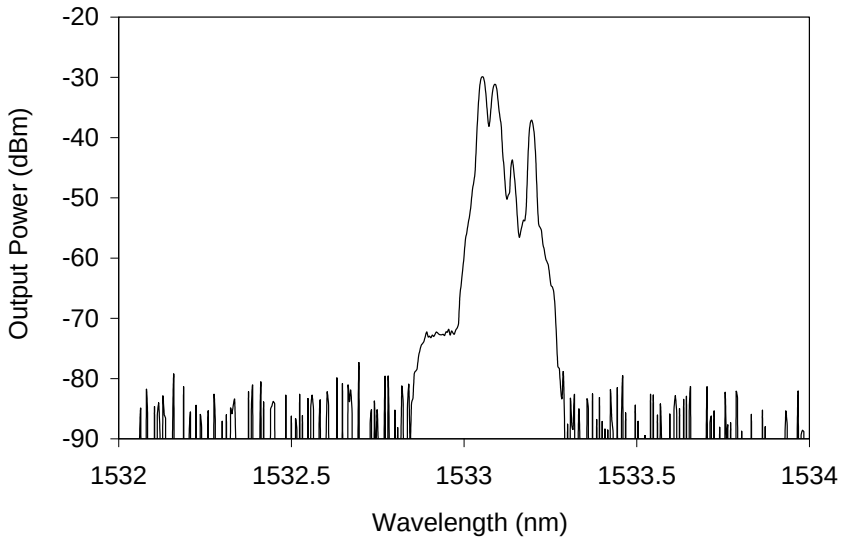

Figure 5.21: The spectrum of fiber laser without the modulation technique, observed from the OSA

Figure 5.22 shows the pulse train from the dual-wavelength fiber laser output with 62.5 kHz repetition rate. The pulse train is generated from a combination of the dual-wavelength output of both shorter and longer wavelength of 1532.89 nm and 1533.23 nm respectively.

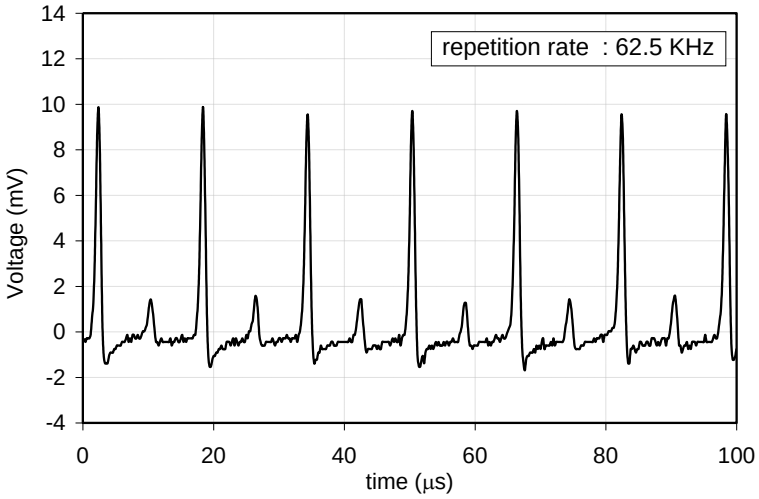

Figure 5.22: The pulse train observed from the oscilloscope for the dual-wavelength close-spacing output.

Figure 5.23 shows the spectrum for each single wavelength from the dual-wavelength close-spacing fiber laser. The seperation of the dual-wavelength is done by adjusting the PC in such a way that only single wavelength output can be observed at a time. Figure 5.23 and 5.24 shows the spectrum taken from the OSA and from the oscilloscope, respectively. It can be observed from Figure 5.23 that the dual-wavelength fiber laser is succesfully being separated into two single wavelength outputs by controlling the PC provided that the modulation is being applied to the fiber laser. As the measurement taken before, both the shorter and longer wavelength are 1532.89 nm and 1533.23 nm respectively.

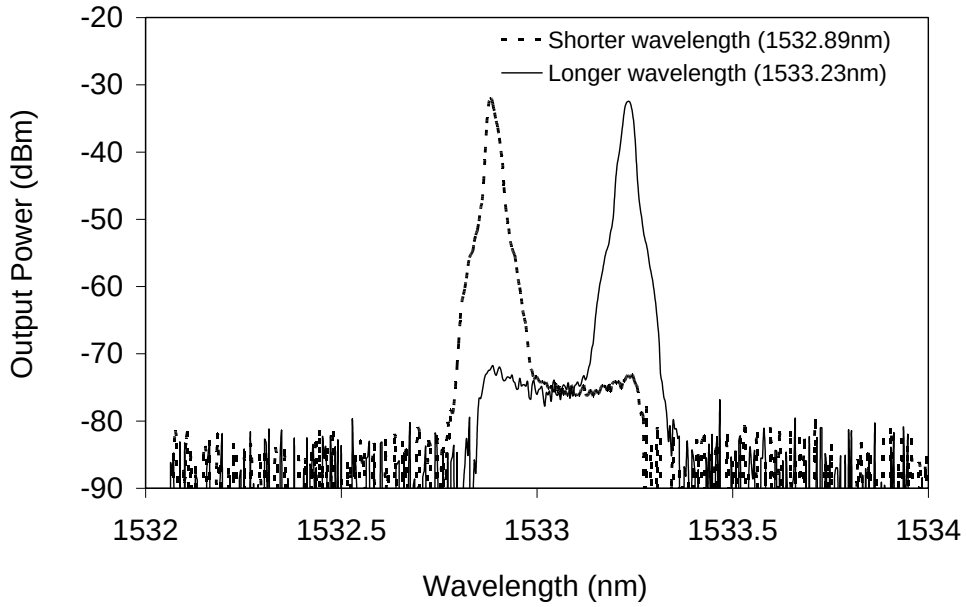

Figure 5.23: The single wavelength output that has been taken separately from the dual-wavelength closed spacing spectrum by adjusting the PC.

Figure 5.24 shows the pulse train for both the shorter and the longer wavelength output. The repetition rate for both the shorter wavelength and the longer wavelength are 62.5 kHz with the pulse of the longer wavelength have a higher amplitude compared to the pulse of the shorter wavelength.

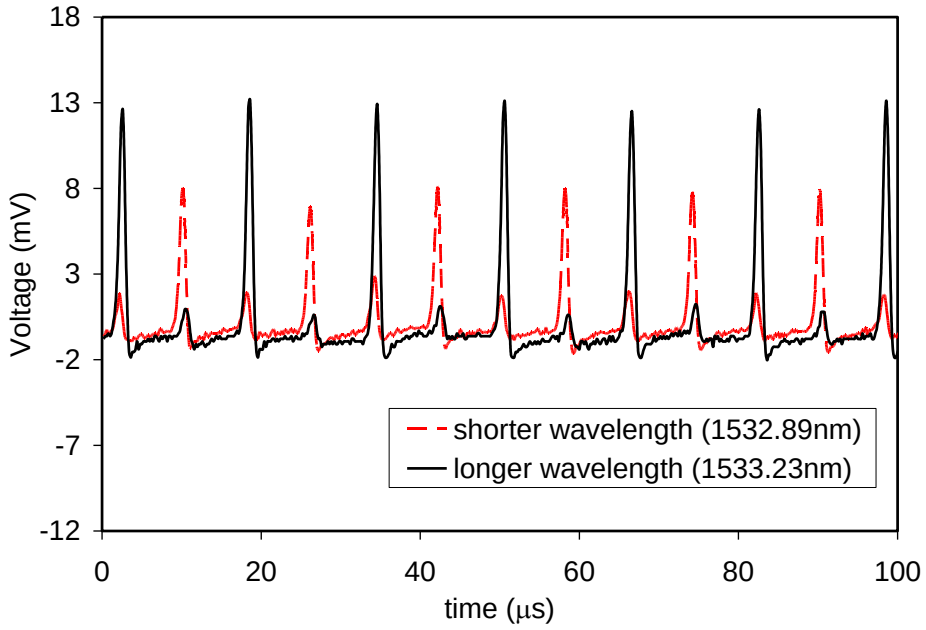

Figure 5.24: The pulse train observed from the oscilloscope for each individual laser.

Figure 5.25(a) shows the spectrum evolution of the DW-close spaced SLM fiber laser that has been taken for an hour of operation within 5 minutes of interval time. The graph depicts that the DW-close spaced SLM fiber laser is quite stable with a slight change of the output power. Figure 5.25(b) shows the spectrum of the DW-close spacing SLM fiber laser in the frequency domain taken from an RFSA which shows the single-longitudinal-mode operation indicated by the flawless spectrum without the mode beating from the noises oscillating inside the cavity. The measurement is taken using the RFSA together with a 6GHz photo detector (HP 83400B Lightwave Detector) giving a high resolution measurement with 3 MHz of resolution bandwidth (RBW) and 1 kHz of video bandwidth (VBW).

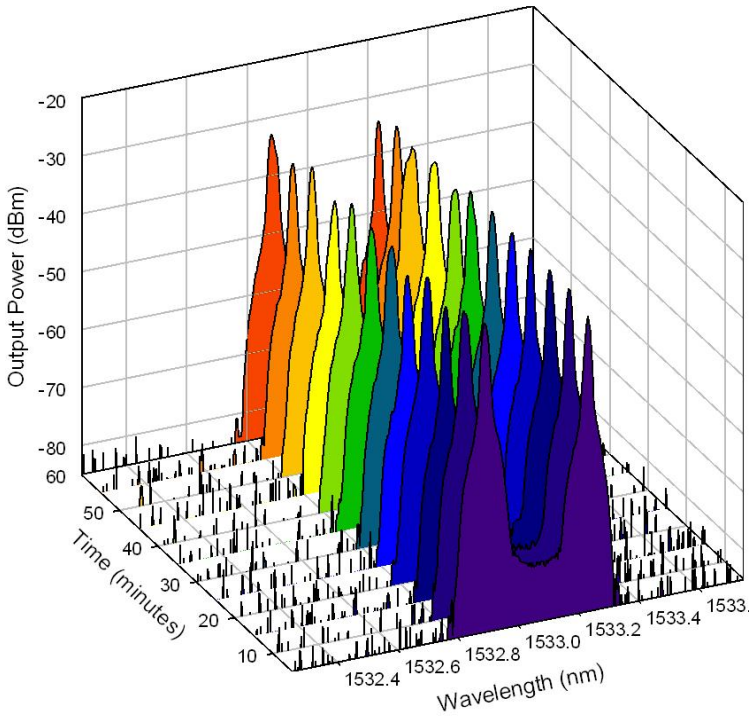

(a)

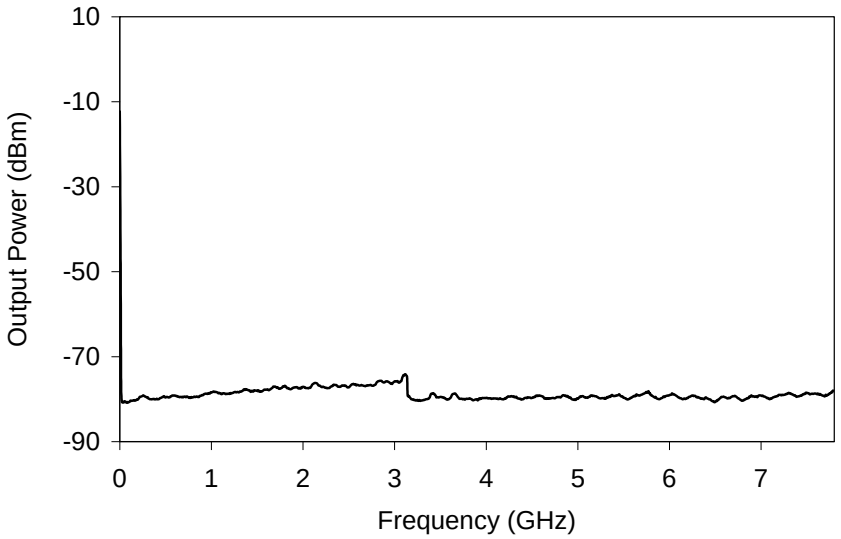

(b)

Figure 5.25: Stability of the DW-close spacing SLM fiber laser with (a) the stability taken from OSA and (b) the spectrum of single longitudinal mode operation taken from the RFSA.

5.5.3 By Using an AWG

In this sub-section, two AWGs are used as the wavelength selective elements with each one connected to the channels which have almost the same wavelength. This is important in order to generate the close spacing DWFL with a beating signal that can be detected by using the RFSA as to provide a microwave source that can be detected at a low radio frequency range.

5.5.3.1 Experimental Setup and Results

In order to improve the spacing limitation of the dual-wavelength closely spaced single longitudinal mode fiber laser, two AWGs are used in this setup as shown in Figure 5.26 below:

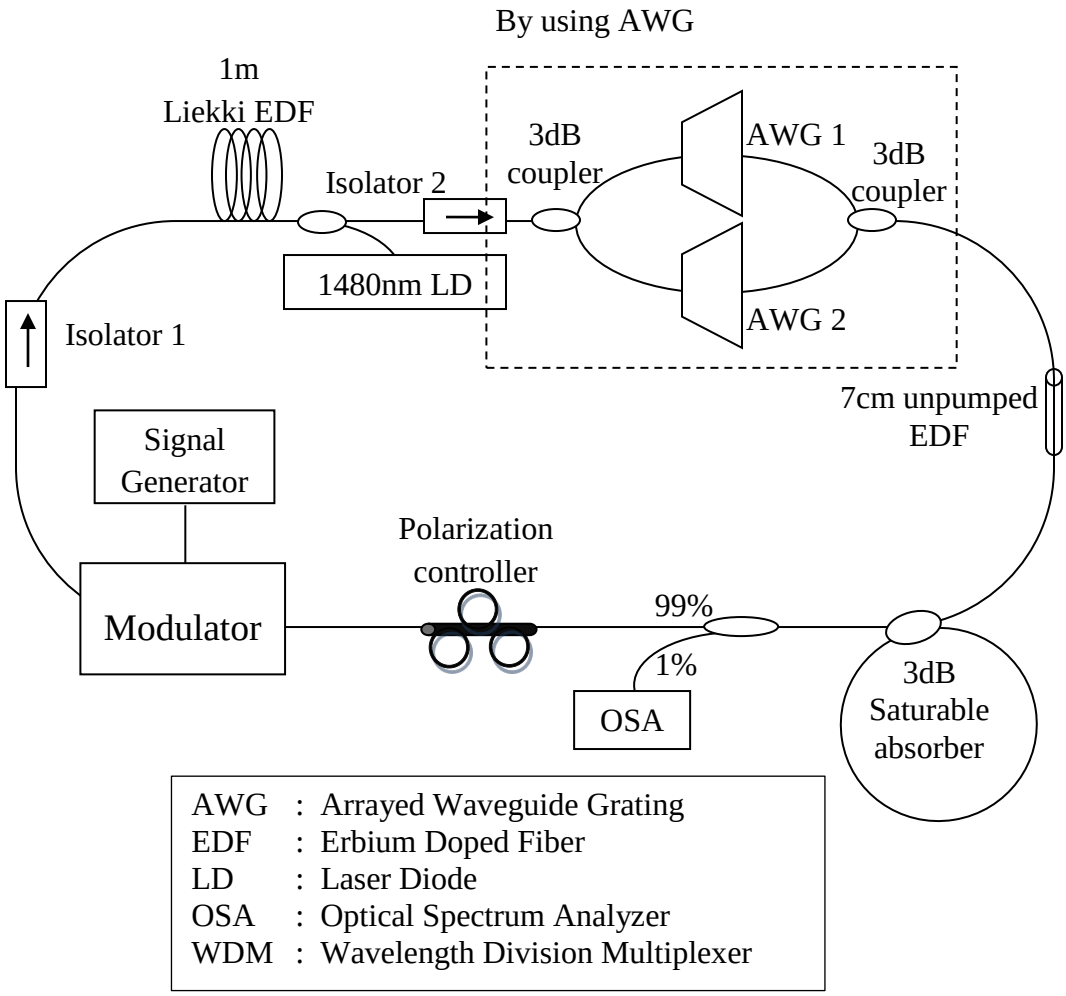

Figure 5.26: Schematic configuration showing the various components for generating the DW-close spacing SLM fiber laser by using AWGs.

The only difference is at the wavelength selection part which uses two AWGs and two 3 dB couplers for the dual-wavelength selection. In this setup, 2 channels from two different AWGs which are selected comprise of Channel 1 and Channel 20 with wavelength of 1530.44 nm and 1530.45 nm respectively. The two channels are selected in order to get the closest spacing of dual-wavelength from the fiber laser whivh gives possibility to obtain 0.01 nm dual-wavelength spacing. In this experiment, the modulator used is driven by a 180 kHz transmission by the same synthesized signal generator (SSG).

Figure 5.27 shows the dual-wavelength fiber laser with a close-spacing of 0.03 nm which is equal to 1.5 GHz spacing coming from the two AWGs. The splitting of the dual-wavelength is observed when the fiber laser is modulated with 180 kHz sinusoidal pulse by the synthesized signal generator. By carefully controlling the PC, dual-wavelength 0.03 nm spacing is obtained.

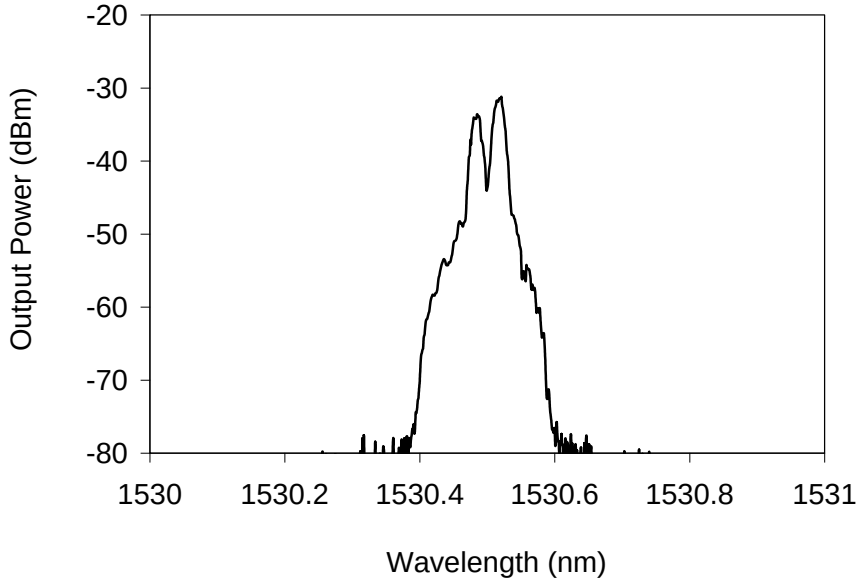

Figure 5.27: The spectrum of the DW-close spacing SLM fiber laser by using two AWGs.

Figure 5.28 shows the pulse train from the dual-wavelength fiber laser output with 192 kHz repetition rate. The pulse train is a combination of the dual-wavelength output at both shorter and longer wavelength of 1530.48 nm and 1530.51 nm respectively.

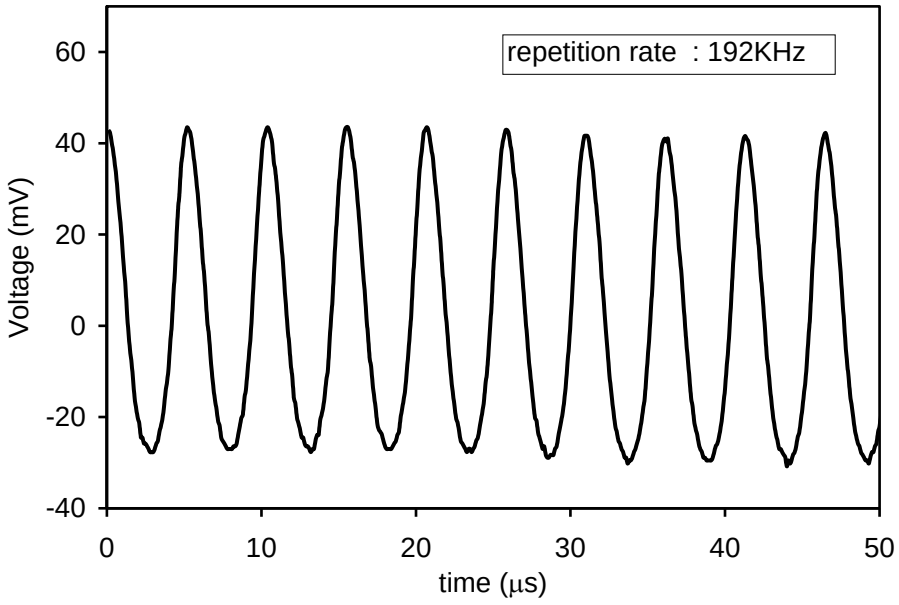

Figure 5.28: The pulse train observed from the oscilloscope for the dual-wavelength close-spacing output.

Figure 5.29 shows the spectrum for each wavelength from the dual-wavelength close-spacing fiber laser by using AWGs taken from the OSA. The PC is used as before, which is for selecting one wavelength out of the two by controlling the polarization state of the laser inside the cavity. It can be observed from Figure 7(a) that the dual-wavelength fiber laser is succesfully being separated by controlling the PC provided that the modulation is being applied to the fiber laser eventhough the spacing is as close as 0.03 nm. Both the shorter and longer wavelengths are 1530.49 nm and 1530.52 nm respectively.

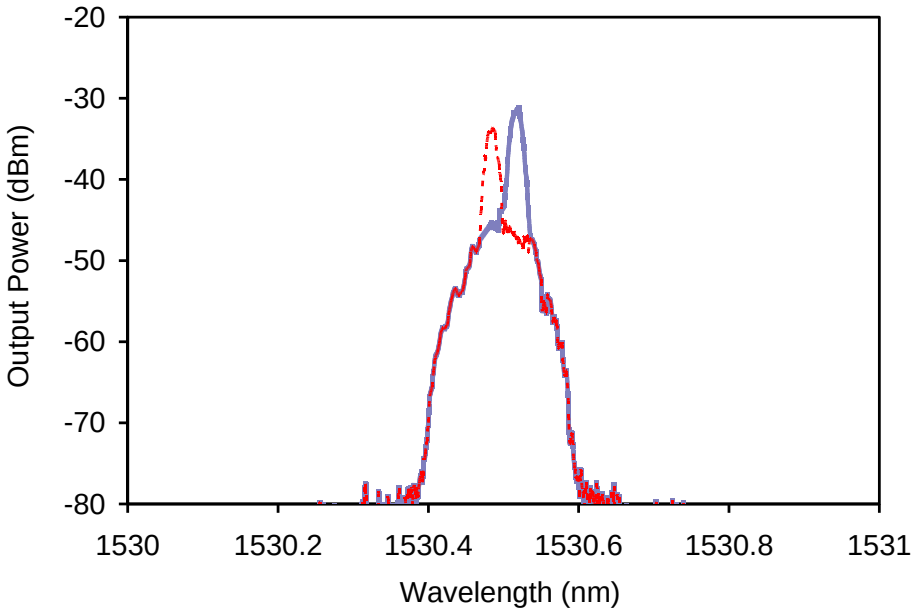

Figure 5.29: The spectrum taken from OSA for each wavelength from the dual-wavelength close-spacing output by adjusting the PC.

The pulse train in the time domain for both the shorter and longer wavelength output is taken from the oscilloscope as depicted in Figure 5.30. The repetition rate for both the shorter wavelength and longer wavelength are 180 kHz with the pulse of the longer wavelength having a higher amplitude compared to the pulse of the shorter wavelength.

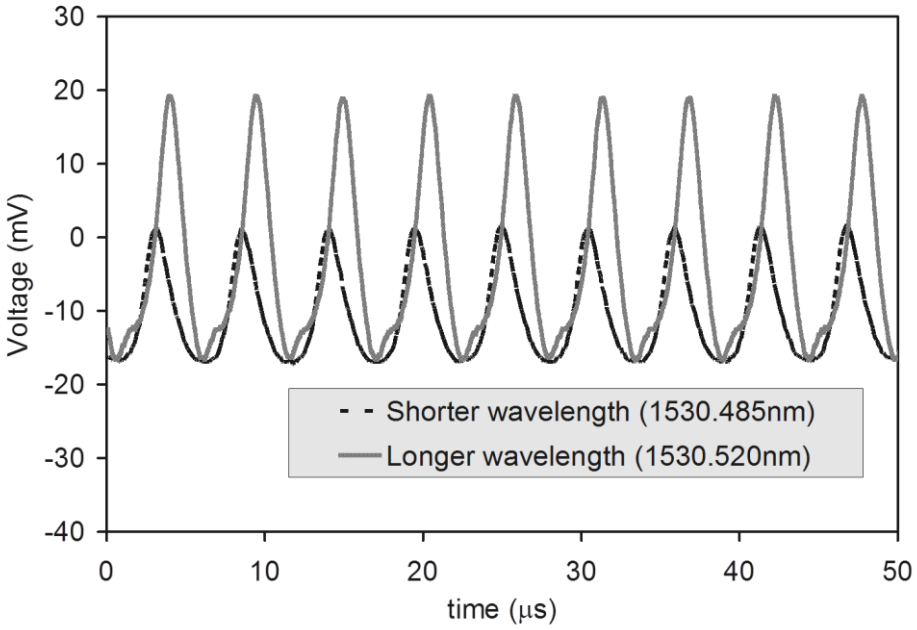

Figure 5.30: The pulse train observed from the oscilloscope for the dual-wavelength close-spacing output from the second configuration layout.

The frequency of the dual-wavelength close-spacing outputs taken from RFSA are shown in Figure 5.31 (a), (c) and (e) .On the other hand, Figure 5.31 (b), (d) and (f) are the corresponding dual-wavelength spacing spectrum taken from the OSA. The central wavelength of channel 1 and 20 are 1530.44 nm and 1530.45 nm respectively. This gives the dual-wavelength spacing of 0.01 nm, the most dominant beating frequency that can be observed.

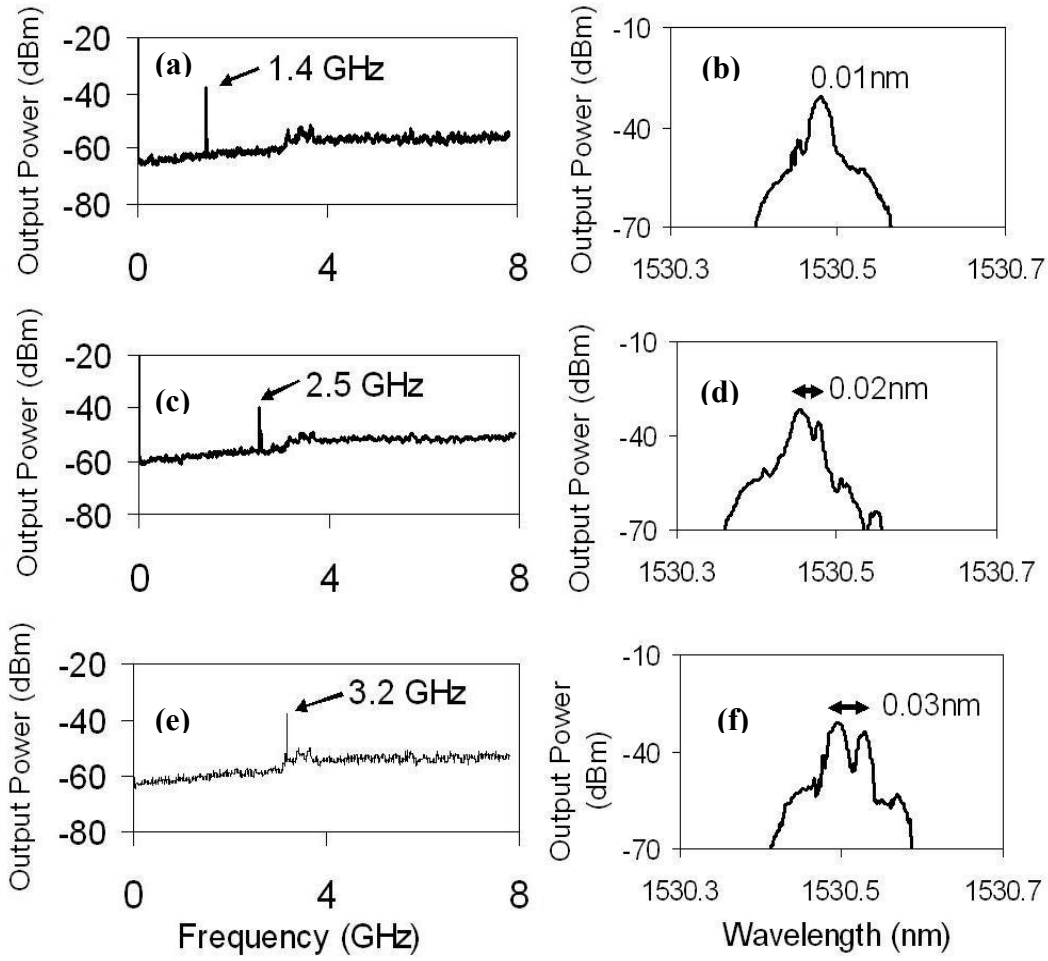

Figure 5.31: (a)-(f) The frequency of the dual-wavelength beating (Figure (a), (c) and (e)) and the corresponding spectrum output (Figure (b),(d) and (f)).

By controlling the PC the output spacing of the dual-wavelength can be adjusted as shown in Figure 5.31. As in Figure 5.31(a) 1.4 GHz beating can be observed from the RFSA with 0.01 nm spacing. However the spectrum is detected as a single wavelength at the OSA as shown in Figure 5.31(b) due to the 0.02 nm resolution limit of the OSA. Figure 5.31(c) shows the frequency beating of 2.5 GHz observed from the RFSA that corresponds to 0.02 nm spacing observed from the OSA as shown in Figure 5.31(d). Figure 5.31(e) shows the 3.2 GHz beating which corresponds to 0.03 nm spacing in the OSA spectrum.

Figure 5.32 shows the baseband data coming from the modulation given to the modulator by the SSG. The modulation can only be observed when it is taken in a small range which is from 0 to 2 MHz. By giving such frequency modulation, the dual-wavelength output can be stabilized due to the phenomenon that is called 'pulse splitting' inside the cavity. The graph shows a constant gap of 180 kHz between each adjacent peak which proves that the modulation comes from the SSG before the noise suppression.

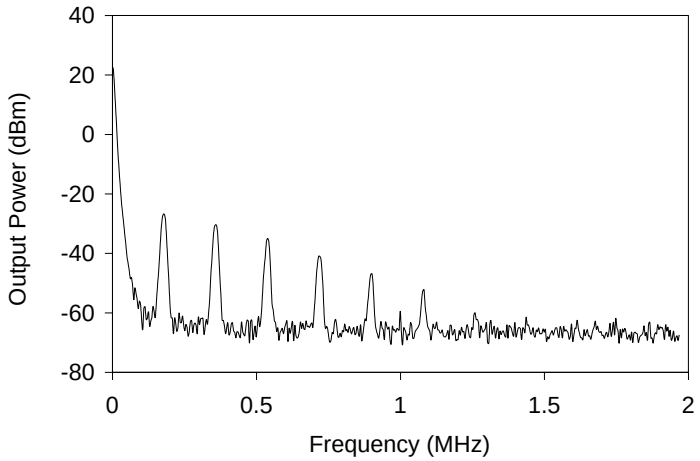

Figure 5.32: Baseband frequency taken from the RFSA.

Figure 5.33 shows the stability of the DW-closely spaced SLM fiber laser taken for an hour of operation within 5 minutes of time interval. The graph reflects the DW-closely spaced SLM fiber laser stability performance with only slight output power changes during the measurement of 0.03 nm spacing which equals to 1.5 GHz beating frequency. By using the AWG many channels can be chosen in order to get the dual-wavelength close spacing output

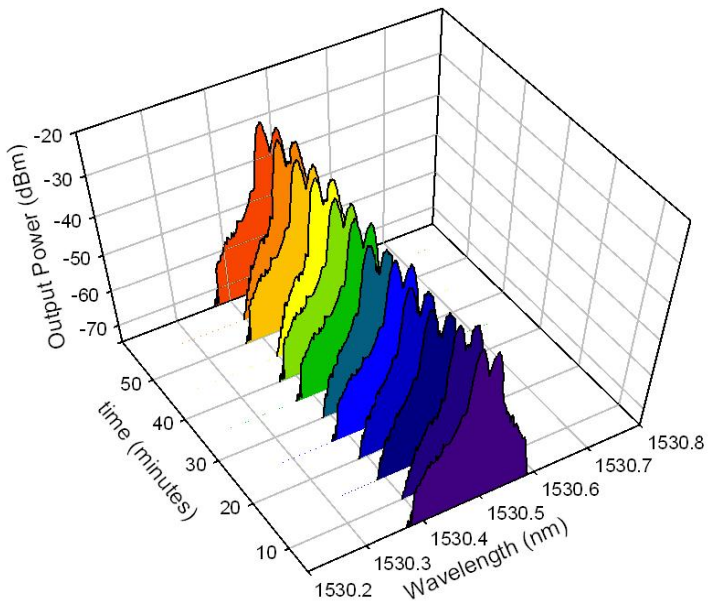

Figure 5.33: The stability performance of the DW-close spacing SLM fiber laser by using two AWGs configuration.

5.6 Summary

In this chapter, the applications of dual-wavelength fiber lasers are being presented. Firstly, in the first part, the generation of tunable dual-wavelength single longitudinal mode fiber laser is presented. The improvement is being made by using two types of saturable absorber to generate a high quality and narrow bandwidth fiber laser. The setup is capable of generating the terahertz wave by selecting the dual-wavelength pair which comes from Channel 6 and 19 with the output power at 1535.4 nm and 1545.65 nm wavelength respectively. The wavelength pair chosen gives a 10.3 nm spacing which is equivalent to a wave beating of 1.3 THz.

The next application is for wavelength conversion to transfer one modulated signal from one wavelength to the other. This is important in order to provide a simultaneous conversion of information from one channel to another channel in the DWDM systems. To

achieve this purpose, the dual-wavelength fiber laser works as the pump power for generating the four-wave-mixing effect by using the SOA as the nonlinear gain medium. By using the TLS as the modulated signal which is injected to the setup design, the data is successfully transferred from the wavelength of 1547 nm to 1532.8 nm. This is proved by the output observed from the oscilloscope after being filtered by the TBF, whereby 0.5 kHz, 1.5 kHz and 2.0 kHz signals are effectively being transferred from the wavelength of 1547 nm to 1532.8 nm.

There has been significant interest in the development of high resolution temperature sensors capable of detecting and measuring minute shifts for a wide variety of applications recently. In this regards, the DWFL presented here is operated by using the beating technique to serve its purpose. In this research work, we successfully design a novel temperature sensor with a resolution of as low as 0.0023 ^{o}C to measure even a slight temperature change. The wavelength selective element used in the setup is the FBG and output is observed by using the RFSA. The single longitudinal mode operation is vital for this application in order to produce a temperature sensor with low noise.

Another application of the DWFL is on microwaves generation for the communication systems purposes. The research work of producing the microwaves signals is found to be novel to the best of our knowledge as our design can provide the spacing as narrow as 1.4 GHz, 2.5 GHz and 3.2 GHz by incorporating two AWGs of the same channels to provide wavelength spacing as small as possible. This is quite difficult and challenging task due to the well-known mode competition issue faced by the gain medium. To record, the narrow spacing fiber laser is typically provided by the Brillouin fiber laser with a spacing of 10 GHz, which is much more higher as compared to the one achieved by using our technique.

The microwaves frequency of 43.4 GHz is also presented in this research work by using a single FBG as the wavelength selective element.

References

1. Shimose, Y., et al., *Remote sensing of methane gas by differential absorption measurement using a wavelength tunable DFB LD.* Photonics Technology Letters, IEEE, 1991. **3**(1): p. 86-87.
2. Shengchun, L., et al. *A dual-wavelength DBR fiber laser strain sensor*. in *OptoElectronics and Communications Conference, 2009. OECC 2009. 14th*. 2009.
3. Duan, L., et al., *A Dual-Wavelength Fiber Laser Sensor System for Measurement of Temperature and Strain.* Photonics Technology Letters, IEEE, 2007. **19**(15): p. 1148-1150.
4. Min Yong, J., et al. *Continuous terahertz wave emission using tunable dual-wavelength erbium-doped fiber laser*. in *Infrared Millimeter and Terahertz Waves (IRMMW-THz), 2010 35th International Conference on*. 2010.
5. Ming, T., et al. *Tunable narrow linewidth THz-wave generation using dual-wavelength fiber ring laser and organic DAST crystal*. in *Infrared Millimeter and Terahertz Waves (IRMMW-THz), 2010 35th International Conference on*. 2010.
6. Jeon, M.Y., et al., *Widely tunable dual-wavelength Er3+-doped fiber laser for tunable continuous-wave terahertz radiation.* Opt. Express, 2010. **18**(12): p. 12291-12297.
7. Taniuchi, T., J. Shikata, and H. Ito, *Tunable terahertz-wave generation in DAST crystal with dual-wavelength KTP optical parametric oscillator.* Electronics Letters, 2000. **36**(16): p. 1414-1416.

8. Lu, G.N., *A dual-wavelength method using the BDJ detector and its application to iron concentration measurement.* Measurement Science & Technology, 1999. **10**(4): p. 312-315.

9. Villanueva, G.E., et al. *Tunable microwave signal generation using dual-wavelength DFB erbium-doped fiber laser*. in *Microwave Photonics, 2009. MWP '09. International Topical Meeting on*. 2009.

10. Xiangfei, C., D. Zhichao, and Y. Jianping, *Photonic generation of microwave signal using a dual-wavelength single-longitudinal-mode fiber ring laser.* Microwave Theory and Techniques, IEEE Transactions on, 2006. **54**(2): p. 804-809.

11. Yu, Y., et al., *Dual-wavelength erbium-doped fiber laser with a simple linear cavity and its application in microwave generation.* Photonics Technology Letters, IEEE, 2006. **18**(1): p. 187-189.

12. Chow, K.K., et al. *Widely tunable wavelength converter using a double-ring fiber laser incorporating a semiconductor optical amplifier*. in *Lasers and Electro-Optics Society, 2001. LEOS 2001. The 14th Annual Meeting of the IEEE*. 2001.

13. Dar-Zu, H., et al. *High-efficiency and wideband SOA-based wavelength converters by using four-wave-mixing with orthogonal pumps and an assisted beam*. in *Lasers and Electro-Optics, 2003. CLEO/Pacific Rim 2003. The 5th Pacific Rim Conference on*. 2003.

14. Saleh, B.E.A. and M.C. Teich, *Fundamentals of photonics*2007: Wiley-Interscience.

15. Siegman, A.E., *Lasers*1986: University Science Books.

16. Jianluo, Z., et al., *Stable single-mode compound-ring erbium-doped fiber laser.* Lightwave Technology, Journal of, 1996. **14**(1): p. 104-109.

17. Lee, C.-C., Y.-K. Chen, and S.-K. Liaw, *Single-longitudinal-mode fiber laser with a passive multiple-ring cavity and its application for video transmission.* Opt. Lett., 1998. **23**(5): p. 358-360.

18. Shilong, P., Z. Xiaofan, and L. Caiyun. *Switchable single-longitudinal-mode dual-wavelength fiber ring laser using hybrid gain medium*. in *Lasers and Electro-Optics, 2008 and 2008 Conference on Quantum Electronics and Laser Science. CLEO/QELS 2008. Conference on*. 2008.

19. Tang, J. and J. Sun, *Stable and widely tunable wavelength-spacing single longitudinal mode dual-wavelength erbium-doped fiber laser.* Optical Fiber Technology, 2010. **16**(5): p. 299-303.

20. Moore, P.J., Z.J. Chaboyer, and G. Das, *Tunable dual-wavelength fiber laser.* Optical Fiber Technology, 2009. **15**(4): p. 377-379.

21. Pan, S. and J. Yao, *A wavelength-switchable single-longitudinal-mode dual-wavelength erbium-doped fiber laser for switchable microwave generation.* Opt. Express, 2009. **17**(7): p. 5414-5419.

22. Yang, X.X., et al., *High-Power Single-Longitudinal-Mode Fiber Laser With a Ring Fabry Perrot Resonator and a Saturable Absorber.* Photonics Technology Letters, IEEE, 2008. **20**(11): p. 879-881.

23. Hongxin, C., et al., *Widely tunable single-frequency erbium-doped fiber lasers.* Photonics Technology Letters, IEEE, 2003. **15**(2): p. 185-187.

24. Jiang, M., et al., *Investigation of Axial Strain Effects on Microwave Signals from a PM-EDF Short Cavity DBR Laser for Sensing Applications.* Photonics Journal, IEEE, 2012. **4**(5): p. 1530-1535.

25. Chinlon, L., C. Burrus, and L. Coldren, *Characteristics of single-longitudinal-mode selection in short-coupled-cavity (SCC) injection lasers.* Lightwave Technology, Journal of, 1984. **2**(4): p. 544-549.

26. Basnayaka, U., X. Fernando, and G. Xijia, *Single Step Generation of Micro and Radio Wave Signals in a Short Cavity Fiber Laser.* Photonics Technology Letters, IEEE, 2011. **23**(20): p. 1445-1447.

27. Liu, X., *A novel ultra-narrow transmission-band fiber Bragg grating and its application in a single-longitudinal-mode fiber laser with improved efficiency.* Optics Communications, 2007. **280**(1): p. 147-152.

28. Xiangfei, C., et al., *Single-longitudinal-mode fiber ring laser employing an equivalent phase-shifted fiber Bragg grating.* Photonics Technology Letters, IEEE, 2005. **17**(7): p. 1390-1392.

29. Ahmad, H., et al., *Tunable dual wavelength fiber laser incorporating AWG and optical channel selector by controlling the cavity loss.* Optics Communications, 2009. **282**(24): p. 4771-4775.

30. Gosset, C. and D. Guang-Hua. *Multi-wavelength conversion and resynchronization of wavelength division multiplexed signals by use of four-wave mixing in a semiconductor optical amplifier*. in *Optical Fiber Communication Conference and Exhibit, 2002. OFC 2002*. 2002.

31. Hsiao-Yun, Y., et al., *Optimization of the frequency response of a semiconductor optical amplifier wavelength converter using a fiber Bragg grating.* Lightwave Technology, Journal of, 1999. **17**(2): p. 308-315.

32. Ligong, C., et al. *40 Gb/s optical wavelength converter converting the same wavelength using a single semiconductor optical amplifier*. in *Communications, 2009. APCC 2009. 15th Asia-Pacific Conference on*. 2009.

33. Awang, N.A., et al., *Four-wave mixing in dual wavelength fiber laser utilizing SOA for wavelength conversion.* Optik, 2011. **122**(9): p. 754-757.

34. Hyoung-Jun, K., S. Ho-Jin, and S. Jong-In. *All-optical Frequency Up-conversion Technique using Four-wave Mixing in Semiconductor Optical Amplifiers for Radio-over-fiber Applications*. in *Microwave Symposium, 2007. IEEE/MTT-S International*. 2007.

35. Collin, E., et al., *Nonlinear parametric amplification in a triport nanoelectromechanical device.* Physical Review B, 2011. **84**(5): p. 054108.

36. Ho, C.M. and Y.C. Tai, *Micro-electro-mechanical-systems (MEMS) and fluid flows.* Annual Review of Fluid Mechanics, 1998. **30**: p. 579-612.

37. Cortés, R., et al., *Interferometric fiber-optic temperature sensor with spiral polarization couplers.* Optics Communications, 1998. **154**(5–6): p. 268-272.

38. Khomenko, A.V., et al., *High-resolution fast response fiber-optic laser calorimeter using a twin interferometric temperature sensor.* Optics Communications, 2001. **198**(1–3): p. 29-35.

39. Zhang, Y.Y. and S. Tadigadapa, *Calorimetric biosensors with integrated microfluidic channels.* Biosensors & Bioelectronics, 2004. **19**(12): p. 1733-1743.

40. Kamat, R.K. and G.M. Naik, *Thermistors – in search of new applications, manufacturers cultivate advanced NTC techniques.* Sensor Review, 2002. **22**(4): p. 334-340.

41. Tong, A., *Improving the accuracy of temperature measurements.* Sensor Review, 2001. **21**(3): p. 193-198.

42. Reeder, T.M. and D.E. Cullen, *Surface-acoustic-wave pressure and temperature sensors.* Proceedings of the IEEE, 1976. **64**(5): p. 754-756.

43. Liu, Y. and L. Wei, *Low-cost high-sensitivity strain and temperature sensing using graded-index multimode fibers.* Appl. Opt., 2007. **46**(13): p. 2516-2519.

44. Yun-Jiang, R., et al., *In-fiber Bragg-grating temperature sensor system for medical applications.* Lightwave Technology, Journal of, 1997. **15**(5): p. 779-785.

45. Lian Shan, Y., et al., *A Simple Demodulation Method for FBG Temperature Sensors Using a Narrow Band Wavelength Tunable DFB Laser.* Photonics Technology Letters, IEEE, 2010. **22**(18): p. 1391-1393.

46. Rao, Y.J., et al., *Simultaneous measurement of displacement and temperature using in-fibre-Bragg-grating-based extrinsic Fizeau sensor.* Electronics Letters, 2000. **36**(19): p. 1610-1612.

47. Melle, S.M., K. Liu, and R.M. Measures, *A passive wavelength demodulation system for guided-wave Bragg grating sensors.* Photonics Technology Letters, IEEE, 1992. **4**(5): p. 516-518.

48. Kersey, A.D., T.A. Berkoff, and W.W. Morey, *Multiplexed fiber Bragg grating strain-sensor system with a fiber Fabry?Perot wavelength filter.* Opt. Lett., 1993. **18**(16): p. 1370-1372.

49. Koo, K.P. and A.D. Kersey, *Bragg grating-based laser sensors systems with interferometric interrogation and wavelength division multiplexing.* Lightwave Technology, Journal of, 1995. **13**(7): p. 1243-1249.

50. Ahmad, H., et al., *Temperature Sensing Using Frequency Beating Technique From Single-Longitudinal Mode Fiber Laser.* Sensors Journal, IEEE, 2012. **12**(7): p. 2496-2500.

51. Jie, S., et al., *Stable Dual-Wavelength DFB Fiber Laser With Separate Resonant Cavities and Its Application in Tunable Microwave Generation.* Photonics Technology Letters, IEEE, 2006. **18**(24): p. 2587-2589.

52. Pan, S. and J. Yao, *Frequency-switchable microwave generation based on a dual-wavelength single-longitudinal-mode fiber laser incorporating a high-finesse ring filter*. Opt. Express, 2009. **17**(14): p. 12167-12173.

53. Weisheng, L., et al., *Dual-Wavelength Single-Longitudinal-Mode Polarization-Maintaining Fiber Laser and Its Application in Microwave Generation.* Lightwave Technology, Journal of, 2009. **27**(20): p. 4455-4459.

54. Xiao, L., et al., *An approximate analytic solution of strongly pumped Yb-doped double-clad fiber lasers without neglecting the scattering loss.* Optics Communications, 2004. **230**(4–6): p. 401-410.

55. Batagelj, B. and M. Vidmar. *Fiber nonlinear coefficient measurement scheme based on four-wave mixing method with externally modulated laser source*. in *Transparent Optical Networks, 2002. Proceedings of the 2002 4th International Conference on*. 2002.

CHAPTER 6

CONCLUSIONS AND FUTURE WORKS

6.1 Conclusions

In conclusion, all the three objectives set in this research work were achieved. The first objective is to generate and characterize tunable single wavelength fiber lasers. It is then followed by the second objective that is to generate DWFLs by using the homogeneous and inhomogeneous broadening gain media. It was solved successfully by using the mode competition issues emit by the EDF as the gain medium. Applications for the DWFL design form the third objective. The three objectives are briefly presented in this chapter.

6.1.1 Generation of Tunable Single-Wavelength Fiber Lasers

The first motivation of the thesis is to generate a tunable fiber laser design as they can be used for various applications especially in sensors and telecommunications systems. A lot of designs are proposed to generate tunable single wavelength fiber lasers. In this thesis, a tunable single wavelength fiber laser was successfully generated by using CTS-FBGs, TBF and AWG as the wavelength selective elements. The novelty of the design presented in this thesis is the generation of a single wavelength by using a design that comprises an AWG, a

Broadband FBG and an OCS working together for the wavelength tunable and selectable device. This is the first design with all of the three devices working together to give a tunable wavelength selection with the speed of 100ms between adjacent channels. Another Wavelength selective element discussed in the thesis is carried out by using 6 FBGs with Sagnac loop mirror method, compression and tensile strain FBGs, and using a TBF. The working principle of each wavelength selective elements is being discussed in Chapter 3. The demonstration of the fiber lasers generation is completed by using a near-homogeneous broadening and inhomogeneous broadening of EDFA and SOA respectively. The different output power and SMSR for each design is then simplified in a table as shown in Table 3.1. These are important characteristics that can provide a few options to be utilized in the DWDM system depending on specific interest such as the range of the wavelength that can be tuned or the amount of loss the system can tolerate.

To summarize the data presented in this thesis, a few important characteristics of each fiber laser design are compiled and shown in Table 6.1 below:

Table 6.1: Comparison of different designs of fiber lasers.

	Tunable Bandpass Filter (TBF)	Sagnac Loop Mirror and FBGs	Compression and Tensile Strain FBGs	Arrayed Waveguide Grating (AWG)
Average output power	-7.95 dBm	-10.82 dBm	-1.77 dBm	-7.08 dBm
Tunability	39.8 nm	21.8 nm	10 nm	11.86 nm
Precise wavelength selection	Moderate	Difficult	Moderate	Easy

The output power is highest by using the compression and tensile strain FBGs as the wavelength selective element with the average output power of -1.77 dBm. As for the tuning range, the one using the TBF is having the widest tuning capability of 39.8 nm. Even though the fiber laser by the TBF having the widest tuning range and by using the Compression and tensile strain FBGs having the highest output power, the AWGs having an advantage of precise wavelength selection with a gap of 0.8 nm from adjacent channels, giving an advantage of using the AWG by its precise wavelength selection.

6.1.2 The Generation of Dual-Wavelength Fiber Lasers

The second motivation of the thesis is to design the tunable dual-wavelength fiber lasers which have been successfully done in the research work. It is known that EDF is a suitable amplifier in the C-band region of a communication window. However, it has its own limitation of difficulty to provide dual-wavelength or multiwavelength output due to near-homogeneous broadening effects emit by the EDF, mentioned previously. A novel approach of using the cavity loss control is reported in this thesis as an alternative way to solve the mode competition issue. The design is effective to overcome the limitation of mode competition inherit in the EDF to provide a balance dual-wavelength output power source. In this thesis, the generation of dual-wavelength fiber lasers are set forth by using three different wavelength selective elements namely AWGs, TBFs and FBGs. The output performance of the DWFL by using the AWG has the best quality output with the highest amount of output power and SMSR of 0.12 dBm and 67.86 dB respectively as shown in table 6.2.

Table 6.2 : Comparison of different designs of Erbium Doped DWFLs.

	Arrayed Waveguide Grating (AWG)	Compression and Tensile Strain FBGs	Tunable Bandpass Filter (TBF)
Average output power	0.12 dBm	-14.76 dBm	-30.05 dBm
Output power maximum difference	4.51 dB	6.62 dB	8.69 dB
Average SMSR value	67.86 dB	53.17 dB	43.62 dB
Minimum tuning range	0.8 nm	0.3 nm	2 nm
Maximum tuning range	18.13 nm	10 nm	68.70 nm
Number of wavelength options	24 wavelength with 0.8 nm of adjacent channel spacing	Any wavelength within range	Any wavelength within range
Precise wavelength selection	Easy	Moderate	Moderate

Another one will be the inhomogeneous broadening gain medium. SOA is used in this research and its performance is compared with that of EDFA. The SOA is then used as an alternative gain medium that exhibit inhomogeneous broadening profile without mode competition issue, however, it exhibits a lower performance of output power and higher amount of noise power. The difference performances of the Erbium Doped DWFLs and

SOA-based DWFLs are then compared. It is shown that Erbium Doped DWFLs are better in terms of their quality output. This is proven by a higher amount of output power and SMSR value in EDFA instead of using SOA as the gain medium, regardless of the wavelength selective element used. Thus as mentioned above, EDF is the preferable medium compared to SOA. Table 6.3 compares the output power performance between the two gain media.

Table 6.3 : Comparison of DWFL by using AWG and compression and tensile strain FBGs in EDFA and SOA as the homogeneous and inhomogeneous gain media respectively.

Wavelength Selective Elements	AWG		Compression and Tensile Strain FBGs	
Gain Media	EDFA	SOA	EDFA	SOA
Average output power	0.12 dBm	-13.00 dBm	-14.76 dBm	-30.28 dBm
Output power maximum difference	4.51 dB	10.00 dB	6.62 dB	4.95 dB
Average SMSR value	67.86 dB	56.00 dB	53.17 dB	42.54 dB
SMSR maximum difference	3.46 dB	13 dB	7.3 dB	11.02 dB

6.1.3 The Applications of Dual-Wavelength Fiber Lasers

The third motivation of the thesis is on the application of DWFL by the virtue of new findings that have been successfully done and explained in Chapter 5. A few applications demonstrated in this research are considered as new and novel, since it is developed using the new and innovative design of the DWFL. They are tunable dual-wavelength single longitudinal mode fiber laser, dual-wavelength as a pump source for wavelength converter application, the DWFL as a temperature sensor and finally, the DWFL application for the generation of microwaves signals.

In this chapter, the applications of dual-wavelength fiber lasers are being presented. Initially, the generation of tunable dual-wavelength single longitudinal mode fiber laser is presented. It was then improved by using two types of saturable absorber to generate a high quality and narrow bandwidth fiber laser. This setup is capable of generating the terahertz range by selecting the dual-wavelength pair that comes from Channel 6 and 19 with output power at 1535.4 nm and 1545.65 nm wavelength respectively. The wavelength pair chosen gives a 10.3 nm spacing which is equivalent to a wave beating of 1.3 THz.

The next application is for wavelength conversion that transfers one modulated signal from one wavelength to another. Its significance is to provide a simultaneous conversion of information from one channel to another channel in the DWDM systems. To achieve this objective, the dual-wavelength fiber laser works as the pump power in generating the four-wave-mixing effect by using the SOA as the nonlinear gain medium. With TLS as the modulated signal injected to the setup design, the data is successfully transferred from 1547 nm to 1532.8 nm wavelength. This is verified by the output observed from the oscilloscope after being filtered by the TBF. Hence, the signals at 0.5 kHz, 1.5 kHz and 2.0 kHz are effectively transferred from 1547 nm to 1532.8 nm wavelength.

Recently, there has been a significant interest in the development of high-resolution temperature sensors. For a wide variety of applications, these sensors are capable of detecting and measuring minute frequency shifts. In this regard, the DWFL presented in this work operates by using the beating technique to serve its purpose. In this research, a novel temperature sensor is successfully designed with a resolution as low as 0.0023 ^{o}C to measure even the slightest temperature change. The wavelength selective element used is the FBG and the output is observed on the RFSA. The single longitudinal mode operation is vital for this application to produce a temperature sensor with low noise as shown by the analyzer.

Another significant application of the DWFL is on microwaves generation in communication systems. To the best of our knowledge, this research in producing the microwaves signals is considered our novelty as our design provides narrow spacings in the values of 1.4 GHz, 2.5 GHz and 3.2 GHz, which is generated by incorporating two AWGs of the same channels to provide as the small wavelength. This is the most difficult and tedious step due to the well-known mode competition issue faced by the gain medium. For the record, the narrow spacing fiber laser is typically provided by the Brillouin fiber laser with a spacing of 10 GHz, which is much more higher as compared to the one achieved by using our technique. The microwaves frequency of 43.4 GHz is also presented in this work by using a single FBG as the wavelength selective element.

6.2 Future Works

Up to this point in time, the objective of producing tunable single wavelength and dual-wavelength fiber lasers have been fulfilled. However, many other avenues in which this research could be continued and explored. One of them is to generate a high quality output beam, in terms of its output power, as most of the design presented in the research works operating in the -30 dBm until 0 dBm of output power which is quite good especially to be used as a seeding signal for further amplification. Another factor to be considered is in the SMSR values. They can be improved by solving the noise level problem inside the laser cavity. Another area of future work is in the tunability range characteristic for the DWFL and single wavelength fiber laser as the tunability represents the capability of the design to be used for many kinds of applications without having any wavelength range limitation problem. All of the suggested improvements are important for the output laser in order to match the ITU and IEEE standards.

The other key focus for future research is to improve the output wavelengths by generating multiwavelength fiber lasers. In this research outline, the DWFL was successfully presented by using a homogeneous gain medium. Subsequently, this study can be extended to find an alternative way to improve the current design to generate multiwavelength fiber lasers. These multiwavelength fiber laser using the cavity loss control method is not applicable in this matter, as the design would be complicated since power for each wavelength has to be controlled to obtain multiwavelength fiber laser with a balance output power. This subsequently leads to the construction of a complicated setup and may be found to be challenging in real applications, hence the need for a further design improvement.

A thorough study for the different types of gain media with homogeneous and inhomogeneous broadening effects can also be considered as a further theoretical research. This study is essential as both effects presents a significant difference in providing a fiber laser's output performance. The knowledge of the differences can help in improving the laser output power level and also the SMSR value. It can assist in the generation of DWFL and multiwavelength fiber laser outputs with a better understanding and prediction condition.

Despite the improvements in the design to produce better laser output, DWFL has still greater potential applications in Terahertz and microwaves generations. Further research should include the Terahertz generation for the applications into the field of sensors, gyroscope and interferometry. However, the terahertz generation is challenging as it needs a high quality beam source to be injected to the crystal as the output power is extremely low that is within the micro range. A few techniques such as by using the saturable absorbers are required to improve the performance of a single longitudinal mode laser operation with a simpler cavity design. The same contention also applies for the microwaves generations.

The DWFL for wireless temperature sensor is also one of the promising research works that could be done in the future in addition of the temperature sensor by using frequency beating technique proposed in Chapter 5 of this thesis. The design capable to detect up to 0.0023 °C of temperature change and at the same time can be translated to the microwave region. These two fields can be merged together for a thorough experimental investigation for wireless temperature sensors that can be used for much kind of purposes in the future.

APPENDIX A:

REPRINT OF SELECTED PAPERS PUBLISHED RELATED TO THE RESEARCH WORK

CHAPTER 3

1. Ahmad H, Zulkifli MZ, **Latif AA**, Hassan NA, Ghani ZA, Harun SW. 120 nm wide band switchable fiber laser. Optics Communications. 2010;283(21):4333-7.

2. Ahmad H, Zulkifli MZ, **Latif AA**, Harun SW. Novel O-band tunable fiber laser using an array waveguide grating. Laser Physics Letters. 2010;7(2):164-7.

3. **Latif AA**, Ahmad H, Awang NA, Zulkifli MZ, Pua CH, Ghani ZA, et al. Tunable high power fiber laser using an AWG as the tuning element. Laser Physics. 2011;21(4):712-7.

4. Zulkifli MZ, Tamchek N**, Latif AA**, Harun SW, Ahmad H. Flat output and switchable fiber laser using AWG and broadband FBG. Optics Communications. 2009;282(13):2576-9.

Optics Communications 283 (2010) 4333–4337

Contents lists available at ScienceDirect

Optics Communications

journal homepage: www.elsevier.com/locate/optcom

120 nm wide band switchable fiber laser

H. Ahmad [a,*], M.Z. Zulkifli [a], A.A. Latif [a], N.A. Hassan [a], Z.A. Ghani [c], S.W. Harun [b,1]

[a] Photonics Laboratory, Department of Physics, University of Malaya, 50603 Kuala Lumpur, Malaysia
[b] Department of Electrical Engineering, Faculty of Engineering, University of Malaya, 50603 Kuala Lumpur, Malaysia
[c] Faculty of Applied Sciences, MARA University of Technology, 40450 Shah Alam, Malaysia

ARTICLE INFO

Article history:
Received 10 March 2010
Received in revised form 9 June 2010
Accepted 10 June 2010

ABSTRACT

A novel method of producing switchable tunable output that spans the S-, C- and L-bands is presented. The achievable tuning range is about 120 nm. The design consists of a wide band SOA, 1 × 16 AWG and an optical selectable switch in a ring configuration. The measured average output powers for S-, C- and L-bands for different output wavelengths are −7.0 dBm, −6 dBm and −6.5 dBm respectively. The SMSR for these wavelengths is about 72 dB.

1. Introduction

Currently there is a need for Switchable Multiwavelength Fiber Laser (SMWFL) to support the Dense Wavelength Division Multiplexing (DWDM) network as a replacement part for the optical source. The advantages of the switchable multiwavelength laser are its ability to select a single channel from a multiwavelength comb [1] and its generally stable output with narrow linewidth emission line which is compatible with existing optical network systems. Besides its application in the telecommunication, the SMWFL can be a source for spectroscopy and for use in the fiber sensor. This flexibility spurs intense research in developing a stable switchable wavelength that can have a wide tuning range. There are various methods of realizing switchable outputs such as that based on polarization dependent device in the cavity [2], the use of high-birefringence fiber loop mirror (HiBi-FLM), cascaded Fiber Bragg Grating (FBG) cavities and cavities with birefringence FBG or cascaded Birefringence FBGs [3–6]. The development of the SMWFL using Sagnac Loop Mirrors (SLM) [7] and compression strain FBG for tunable wavelength has also been demonstrated [8,9]. This system is capable of generating a wide range of tunability specification within the C-band and C- plus L-band. However, the usage of SLMs requires a fixed length of fiber for a particular wavelength which has to be manually adjusted.

As a result of this shortcoming in SLMs based system, use of Arrayed Waveguide Grating (AWG) provides a switchable alternative. The use of the AWG as a wavelength slicing mechanism has generated new interests in developing the Multiwavelength Fiber Laser (MWFL, operating at fixed spacing of 50 GHz, 100 GHz or 200 GHz) that fits well with the DWDM network. This technique has been demonstrated using Amplified Spontaneous Emission (ASE) output of a Semiconductor Optical Amplifier (SOA) or Erbium Doped Fiber Amplifier (EDFA) into AWG [10–14].

Most of the reported works are concentrated within the C- plus L-band and it would be interesting to extend this coverage to include the S-band. Recent migration into the metro-network based or Coarse Wavelength Division Multiplexing (CWDM) would require a switchable fiber laser that can be tuned from the S- to L-band. Recent works to cover all the three bands have been done using thulium doped fiber together with erbium doped fiber in a hybrid configuration [15]. It consists of two components of 20 m in length thulium doped fiber connected in parallel with 12 nm of erbium doped fiber pumped by numerous laser diodes. Although the tunability range is wide, reaching as large as 145 nm, the complexity and usage of many laser diodes can be a hindrance to realizing a commercial unit. A similar approach is also being undertaken by Foroni et al. [16] to achieve a tuning range of 120 nm using three components of erbium doped fibers connected in parallel and multiplexed to generate the tunability range. The tuning for the entire range is not clearly stated but a tunable C-band filter is used in the C-band. The approach in the design is based on a double pass technique as reported in an earlier paper by Harun et al. [17].

As an alternative approach in generating a wide tuning range, a single semiconductor optical amplifier (SOA) is used in place of the many pump lasers and it provides a tuning range of 120 nm covering the S-, C- and L-bands as proposed in this paper. The tunability is performed using an arrayed waveguide grating (AWG) in conjunction with optical channel selector (OCS) providing electronically tuned selectable output. This is illustrated and demonstrated in the following section.

* Corresponding author.
E-mail address: harith@um.edu.my (H. Ahmad).
[1] Tel.: +603 79674290; fax: +603 79676770.

0030-4018/$ – see front matter © 2010 Elsevier B.V. All rights reserved.
doi:10.1016/j.optcom.2010.06.040

Optics Communications 282 (2009) 2576–2579

Contents lists available at ScienceDirect

Optics Communications

journal homepage: www.elsevier.com/locate/optcom

Flat output and switchable fiber laser using AWG and broadband FBG

M.Z. Zulkifli [a,*], N. Tamchek [a], A.A. Latif [a], S.W. Harun [b], H. Ahmad [a]

[a] Photonics Laboratory, Department of Physics, University of Malaya, 50603 Kuala Lumpur, Wilayah Persekutuan, Malaysia
[b] Department of Electrical Engineering, Faculty of Engineering, University of Malaya, 50603 Kuala Lumpur, Malaysia

ARTICLE INFO

Article history:
Received 11 December 2008
Received in revised form 20 March 2009
Accepted 20 March 2009

ABSTRACT

The switchable multiwavelength fiber laser (SMWLSs) using AWG and broadband FBG with tuning range 11.7 nm and 0.75 nm spacing are demonstrated. The switchable lasers for every channel shows flatness output power with variation 3.7 dBm and peak power around −6.1 dBm. The side mode suppression ratio (SMSR) of the laser is significantly improved for every channel when using broadband FBG. The improvement is about 27.7 dBm. The laser for every channel also shows the good stability within the 2 h operation.

1. Introduction

Switchable multiwavelength lasers (SMWLs) are transmission sources with very good potentials to be applied in optical Dense Wavelength Division Multiplexing (DWDM) network systems. This potential arises due to their ability to select a single channel from a multiwavelength comb [1], and as a result of this significant research has been put forward in the development of SMWLs. Initially, the development of SMWLs involved the use of spectral polarization-dependent loss element cavities [2], High-Birefringence Fiber Loop Mirrors (HiBi-FLMs) [3], cascaded fiber Bragg grating (FBG) cavities [4] and cavities with a birefringence FBG or cascaded birefringence FBGs [5,6]. More recently, the development of SMWFLs using Sagnac Loop Mirrors (SLMs) [7], and compression strain FBG for obtaining tunable wavelengths [8,9] have also been reported. These systems are capable of generating a wide range of switchable wavelengths, especially those based on the SLM, but practical use of SMWLs based on the SLM are prevented by certain limitations. These limitations comes in the form of the SLM optimum cavity length; because of the fiber based nature of the SLM, the optimum SLM cavity length for each SMWL must be acquired manually. As a result, a new wavelength slicing mechanism had to be found for the SMWL, and the Arrayed Waveguide Grating (AWG) is the most suitable candidate.

The use of the AWG as a wavelength slicing mechanism has renewed interest in the development of multiwavelength fiber lasers (MWFLs) operating at 50 GHz, 100 GHz and 200 GHz channel spacings which comply to current DWDM networks. Therefore, an AWG can be used in conjunction with an ASE source such as an Erbium Doped Fiber Amplifier (EDFA) or a Semiconductor Optical Amplifier (SOA) to obtain a sliced ASE multiwavelength spectrum, which is then rerouted onto itself to form the MWFL [10,11]. Tunable Fiber Lasers using AWGs have also been explored whereby special input/output mechanisms or integrated Planar Lightwave Circuit (PLC) switches [12,13] are used to obtain switchable wavelengths, although these systems can prove to be very complex to develop. In this letter, we propose a new SMWL design based on the AWG used in conjunction with a broadband FBG. The proposed design uses the AWG to slice the EDFA generated ASE spectrum while the FBG acts as a broadband reflector to provide a flat laser spectrum. An Optical Channel Selector (OCS) is used as a selective wavelength device to provide tunability.

2. Experiment setup

The configuration of the proposed SMWFL is shown in Fig. 1. The setup consists of a 980/1550 Wavelength Selective Coupler (WSC) and a 5 m long highly doped Erbium Doped Fiber (EDF) pumped by a 980 nm laser diode. The EDF is used both to provide the initial ASE spectrum as well as act as the gain medium for the proposed laser. The EDF has a nominal Er^{3+} ion concentration of 1000 ppm and is pumped at 80 mW in a forward pumping scheme. The WSC is used to combine the pump signal with the lasing signal that will be generated from the EDF and AWG. An OCS provides tunability while a 1×16 AWG is used together with a broadband FBG as the spectrum slicing mechanism of the proposed SMWL.

The operation of the SMWL is as follows; the ASE generated from the EDFA travels through Port 1 to Port 2 of the OC. Subsequently, the ASE spectrum will enter the OCS where it directed to one of the 16 output channels that are connected with the corresponding channel on the 1×16 AWG (i.e. output Channel 1 of the OCS is connected to Channel 1 of the AWG, output Channel 2 of the OCS is connected to Channel 2 of the AWG and so on for all 16 channels). The ASE will then travel along the selected channel of the AWG and onward to the single output of the AWG where

* Corresponding author. Tel.: +60 603 79674290; fax: +60 603 79676770.
E-mail address: mohdzamani@um.edu.my (M.Z. Zulkifli).

0030-4018/$ - see front matter © 2009 Elsevier B.V. All rights reserved.
doi:10.1016/j.optcom.2009.03.048

Laser Phys. Lett. **7**, No. 2, 164–167 (2010) / **DOI** 10.1002/lapl.200910118

Abstract: A novel tunable fibre laser (TFL) operating in the ordinary band (O-band) of 1310 nm is proposed and demonstrated. The proposed TFL is developed using a 1×16 arrayed waveguide grating (AWG) as a slicing mechanism for the broadband amplified spontaneous emission (ASE) source and an optical channel selector (OCS) to provide the tunability. A semiconductor optical amplifier (SOA) with a centre wavelength of 1310 nm serves as the compact gain medium for the TFL and also as a broadband ASE source. The TFL has a tuning range of 1301.26 nm to 1311.18 nm with 9.92 nm span and a channel spacing of 0.7 nm. The measured output power is about –4 and –8 dBm and with a side node suppression ratio (SMSR) of 29 to 33 dB.

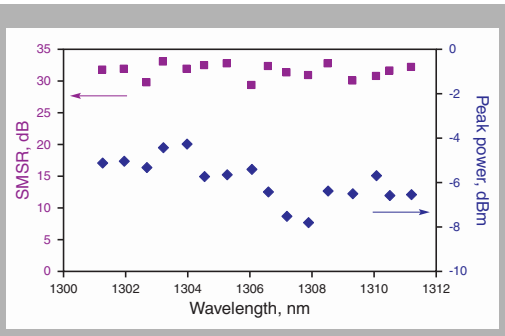

SMSR and peak power performance for every wavelength

Novel O-band tunable fiber laser using an array waveguide grating

H. Ahmad, [1,*] *M.Z. Zulkifli,* [1] *A.A. Latif,* [1] *and S.W. Harun* [2]

[1] Photonics Laboratory, Department of Physics, University of Malaya, Kuala Lumpur 50603, Malaysia
[2] Department of Electrical Engineering, Faculty of Engineering, University of Malaya, Kuala Lumpur 50603, Malaysia

Received: 24 September 2009, Revised: 1 October 2009, Accepted: 4 October 2009
Published online: 12 January 2010

Key words: fiber laser; tunable fiber laser; AWG; O-band source

PACS: 42.55.Wd

1. Introduction

Course wavelength division multiplexing (CWDM) systems in passive optical networks (PONs) gives network providers a very cost-effective method to deploy wavelength division multiplexing (WDM) together with time-division multiplexing (TDM) technologies for access networks [1]. Although implementing CWDM in PON systems saves significant cost in terms of the transmission lines and other in-line components, the system still suffers a drawback from the extensive use of laser diodes required as signal sources for transmission. This already costly requirement is typically made more expensive due to the need for cooled laser diodes with stabilized outputs to ensure uninterrupted signal generation. As a result of this, the cost-effectiveness of the CWDM system is negated by the need to deploy many cooled laser diode, which is especially not-effective in low-density bit data transfers.

A viable alternative to the use of both cooled and uncooled laser diodes is the use of fiber laser sources. Fiber lasers have very good potential to act as transmission sources for application in optical CWDM network systems due to their ability to select a single channel from a multiwavelength comb [2]. This makes the fiber laser a very versatile component which provides a high degree of flexibility to the CWDM system, whereby the fiber lasers can be manufactured from the same template en-mass and then tuned to the required frequency (as opposed to laser diodes which must be manufactured to the desired frequency). This provides significant cost savings using existing ex-stock components, which are readily available to the system.

Furthermore, fiber lasers have many advantages over conventional laser diodes such as lower noise output, higher power output and high side mode suppression ra-

* Corresponding author: e-mail: harith@um.edu.my

ISSN 1054-660X, Laser Physics, 2011, Vol. 21, No. 4, pp. 712–717.

Tunable High Power Fiber Laser Using an AWG as the Tuning Element[1]

A. A. Latif[a], H. Ahmad[a], N. A. Awang[a], M. Z. Zulkifli[a, *], C. H. Pua[a], Z. A. Ghani[b], and S. W. Harun[c]

[a] *Photonics Laboratory, Department of Physics, University of Malaya, 50603 Kuala Lumpur, Malaysia*
[b] *Faculty of Applied Sciences, MARA University of Technology, 40450 Shah Alam, Selangor, Malaysia*
[c] *Department of Electrical Engineering, Faculty of Engineering, University of Malaya, 50603 Kuala Lumpur, Malaysia*
*e-mail: mohdzamani82@yahoo.com

Received October 27, 2010; in final form November 4, 2010; published online March 4, 2011

Abstract—In this paper, a design of a High Power Tunable Fiber Laser (HP-TFL) in C-band region from 1536.7 to 1548.6 nm is set forth with Erbium Doped Fibers (EDFs) being used as a seeding signal and a booster amplifier. With a 1 × 16 channels Arrayed Waveguide Grating (AWG), this setup is capable of generating 16 different wavelengths with an average output power of 20.7 dBm.

DOI: 10.1134/S1054660X11070152

INTRODUCTION

High power fiber lasers have attracted much attention due to their applications in Dense Wavelength Division Multiplexing System (DWDM), cutting, drilling and welding [1, 2] for material processing, gravitational wave detection [3, 4] and also marking. Even though applications in the communication systems involve high power fiber lasers, they are however, not as high powered and are just enough for signal transfers of less than several watts. Several different methods have been used to generate high power fiber lasers such as by using a cladding pumping in Ytterbium, but even though they produced a few hundred until thousands of miliwatts of output power which are quite high, the amplification range is only in the 1060 nm region [5–7]. To shift this gain region to a higher wavelength of about 1550 nm region, which is the region that is gaining a lot of interests due to the infrared eye-safe wavelength laser source with high manipulation for use in the communication systems, co-doped fibers called Ytterbium–Erbium doped fibers are used [8–11] with Ytterbium as a pump absorber that transfers energy non-radiatively to Erbium ion. Here the amplification in 1550 nm range is improved by having higher inversion in this region [12]. Due to problems faced in normal silica-based Erbium-doped fibers, high output power fiber lasers cannot be realized. However, there has been a remarkable growth in the use of optical fiber for communication systems especially in providing more efficient laser diode pumps for use in Erbium-doped Fiber Amplifier (EDFA). There are also more devices to provide higher efficiency in amplification including high pump power laser diodes [13, 14] (more specifically for 980 and 1480 nm laser diode pumps) and efficiently coupled pump combiner of certain particular wavelength. Due to this significant improvement, the use of a normal EDF for high power application can now be realized.

A switchable high power fiber laser also has an added advantage due to the selectable wavelength choices. Even though there have been a lot of researches done in tunable fiber lasers [15–20], most of them operate within a low power regime with just a few providing high power switchable fiber lasers [21]. In this paper, we propose a new design of a high power switchable fiber laser using a seeding signal and booster amplifier to provide 20–21 dBm output power by using an AWG and Optical Switch (OS) as a selective element.

EXPERIMENTAL SETUP

Figure 1 illustrates the experimental setup of the high power tunable fiber laser (HP-TFL). It consists of two sections, Sections 1 and 2. Section 1 acts as the seeding signal which serves as an input power for further amplification at booster amplifier in Section 2. The seeding signal uses a 5 m Metrogain Erbium-doped Fiber (EDF) with absorption coefficients of 11.9 dB/m at 979 nm and 16.4 dB/m at 1531 nm as a gain medium. A 980 nm laser diode with 110 mW pump power is connected to the EDF via a 1550/980 wavelength division multiplexer (WDM) coupler. The propagation of 980 nm pump light through WDM coupler to the EDF creates an Amplified Spontaneous Emission (ASE) which then circulates inside the cavity in a clockwise direction. This ASE is then filtered when it enters an Arrayed Waveguide Grating (AWG) which works as a multiplexer that slices the ASE source into 16 different channels in the C-band region. The AWG has been optimized for use in the C-

[1] The article is published in the original.

CHAPTER 4

1. Ahmad H, Zulkifli MZ, **Latif AA**, Harun SW. Tunable dual wavelength fiber laser incorporating AWG and optical channel selector by controlling the cavity loss. Optics Communications. 2009;282(24):4771-5.

2. **Latif AA**, Zulkifli MZ, Awang NA, Harun SW, Ahmad H. A simple linear cavity dual-wavelength fiber laser using AWG as wavelength selective mechanism. Laser Physics. 2010;20(11):2006-10.

3. Ahmad H, **Latif AA**, Zulkifli MZ, Awang NA, Harun SW. High power dual-wavelength tunable fiber laser in linear and ring cavity configurations. Chinese Optics Letters. 2012;10(1).

4. **Latif AA**, Awang NA, Zulkifli MZ, Harun SW, Ghani ZA, Ahmad H. Dual-wavelength tunable fibre laser with a 15-dBm peak power. Quantum Electronics. 2011;41(8):709-14.

5. Ahmad H, Zulkifli MZ, **Latif AA**, Thambiratnam K, Harun SW. Dual wavelength fibre laser with tunable channel spacing using an SOA and dual AWGs. Journal of Modern Optics. 2009;56(16):1768-73.

6. **Latif AA**, Zulkifli MZ, Hassan NA, Harun SW, Ghani ZA, Ahmad H. A compact O-plus C-band switchable quad-wavelength fiber laser using arrayed waveguide grating. Laser Physics Letters. 2010;7(8):597-602.

7. Ahmad H, **Latif AA**, Norizan SF, Zulkifli MZ, Harun SW. Flat and compact switchable dual wavelength output at 1060 nm from ytterbium doped fiber laser with an AWG as a wavelength selector. Optics and Laser Technology. 2011;43(3):550-4.

8. Chong SS, Ahmad H, Zulkifli MZ, **Latif AA**, Chong WY, Harun SW. Synchronous tunable wavelength spacing dual-wavelength SOA fiber ring laser using Fiber Bragg grating pair in a hybrid tuning package . Optics Communications. 2012;285:1326-1330.

Optics Communications 282 (2009) 4771–4775

Contents lists available at ScienceDirect

Optics Communications

journal homepage: www.elsevier.com/locate/optcom

Tunable dual wavelength fiber laser incorporating AWG and optical channel selector by controlling the cavity loss

H. Ahmad [a,*], M.Z. Zulkifli [a,b], A.A. Latif [a], S.W. Harun [b]

[a] Photonics Laboratory, Department of Physics, University of Malaya, 50603 Kuala Lumpur, Malaysia
[b] Department of Electrical Engineering, Faculty of Engineering, University of Malaya, 50603 Kuala Lumpur, Malaysia

ARTICLE INFO

Article history:
Received 18 April 2009
Received in revised form 31 August 2009
Accepted 31 August 2009

Keywords:
Dual wavelength
Ring erbium doped fiber laser
AWG

ABSTRACT

In this paper, we propose and demonstrated a dual wavelength fiber laser (DWFL) based on the use of an erbium doped fiber (EDF) gain medium as well as an 1 × 24 Arrayed Waveguide Grating (AWG) together with two optical channel selectors (OCS) to provide channel spacing tunability. The output power of the two wavelengths is equalized by controlling the cavity loss in the DWFL using two Programmable Optical Attenuators (POAs). The widest spacing obtained from the DWFL is 18.13 nm while the narrowest spacing is 0.8 nm. The DWFL has good stability with only minor power fluctuations of less than 1.5 dB and a Side Mode Suppression Ratio (SMSR) of approximately 69.1 dB with peak fluctuations of less than 2.3 dB.

1. Introduction

Multi-Wavelength Fiber Lasers (MWFLs) and Switchable Wavelength Fibre Lasers (SWFLs) are fast becoming widely popular choices for replacing conventional single wavelength laser diodes in a multitude of applications. As a result of their compact size and their good cost-per-wavelength ratio, MWFLs and SWFLs have many potential applications in Dense Wavelength Division Multiplexing (DWDM) [1,2], optical sensing [3] and also optical spectroscopy [4]. Recently however, there has been increased focus on the development of dual wavelength laser sources (DWFLs), especially DWFLs with tunable channel spacing. DWFLs are essentially modified SWFL systems with a high potential for generating Terahertz radiation from the reaction of the dual wavelength output with an external crystal. Terahertz radiation has a wide number of applications, most notable in new industrial process quality controls and for security monitoring applications [5].

A key concern in the development of DWFLs, and for that matter MWFLs would be the issue of homogenous broadening in the gain medium. Most MWFL configurations employ the Erbium Doped Fibre (EDF) as a linear gain medium. However, the EDF suffers from a homogeneous broadening effect at room temperature, leading strong mode competition and wavelength suppression as well as a loss of stability in the output power level. Many techniques have been put forward to overcome this problem, including cooling the EDF in liquid nitrogen [6] or using specialized twin-core EDFs [7], or even by utilising spatial mode-beating techniques in multimode fibers [8]. However, these methods are complex and not suitable for practical applications. On the other hand, a gain medium with an inhomogeneous broadening characteristic can be employed, such as the Semiconductor Optical Amplifier (SOA) [9].

Currently, the challenge in developing DWFL systems is in providing tunability characteristics to the DWFL. In this sense, the channel spacing between the two lasing wavelengths can be controlled, as well as the wavelengths themselves. Various methods have been put forward to realize tunabilty such as using FBGs [9], polarization dependent loss elements [10] and other similar methods. The FBG is typically the preferred choice for enabling wavelength tunability, but because it is sensitive to temperature changes it has the tendency to be affected by perturbations by the external temperature, thus affecting the wavelength stability of FBG. Therefore, an alternative method should be found to provide easy channel spacing tunability while at the same time is more stable and not affected by variations in the external temperature.

In this paper we propose and demonstrate a very stable DWFL using a 1 × 24 (1 input channel to 24 output channels) Arrayed Waveguide Grating (AWG) located in an Erbium Doped Fibre Laser (EDFL) in a ring cavity. The system uses two optical channel selector (OCS) to provide the tuning capabilities of the DWFL, and the DWFL output wavelengths can be tuned between a spacing range of 18.1 nm (widest) to 0.8 nm (narrowest) with the output power in the region of 0 dB m. One of the issues that arise in the generation of dual wavelengths in an erbium gain medium is the suppression of one of the wavelengths as a result of the homogeneous broadening in the gain medium. In our system, we are able to generate a stable dual wavelength output by controlling the

* Corresponding author. Tel.: +60 3 79674290; fax: +60 3 79676770.
E-mail address: harith@um.edu.my (H. Ahmad).

0030-4018/$ - see front matter © 2009 Elsevier B.V. All rights reserved.
doi:10.1016/j.optcom.2009.08.066

ISSN 1054-660X, Laser Physics, 2010, Vol. 20, No. 11, pp. 2006–2010.

A Simple Linear Cavity Dual-Wavelength Fiber Laser Using AWG as Wavelength Selective Mechanism[1]

A. A. Latif[a], M. Z. Zulkifli[a], N. A. Awang[a], S. W. Harun[b], and H. Ahmad[a]

[a] *Photonics Laboratory, Department of Physics, University of Malaya, Kuala Lumpur, 50603 Malaysia*

[b] *Department of Electrical Engineering, Faculty of Engineering, University of Malaya, Kuala Lumpur, 50603 Malaysia*

e-mail: mohdzamani82@yahoo.com

Received June 8, 2010; in final form, June 22, 2010; published online October 3, 2010

Abstract—In this paper, a simple design of linear cavity dual-wavelength fiber laser (DWFL) is proposed. Operating in the C-band region stretching from 1538.3 nm to 1548.6 nm, an arrayed waveguide grating (AWG) is used to generate the dual-wavelengths output together with a broadband fiber Bragg grating as a back reflector and an optical circulator with a 10% output coupling ratio which acts as a front mirror. The measured average output power of the DWFL is about −5.66 dBm and with a side mode suppression ratio (SMSR) of 53.1 dB. The spacing between the two output wavelengths can be varied from 0.8 nm to 10.3 nm with a stable output and minimum power fluctuations.

DOI: 10.1134/S1054660X10210061

INTRODUCTION

Multiwavelength fiber lasers have attracted numerous interests especially for possible application as alternative laser sources for wavelength division-multiplexing (network), for terahertz generation and also in high resolution spectroscopy. Generally, these lasers are operated with erbium doped fiber (EDF) as an active gain medium. Interest in the erbium doped fiber is primarily due to its compatibility, compact size and simplicity. There is an issue in generating multiwavelength outputs from EDF which is largely due to the homogeneous broadening exhibited by this material. This inhibits operation of more than one wavelength due to the gain competition. To overcome this, many methods have been used such as cooling the EDF in liquid nitrogen [1, 2], using hybrid gain medium and sagnac loop mirror [3–7], elliptical EDF [8, 9], cavity loss controlled [10, 11] and self-injected laser diode [12, 13] among others [14–17]. These methods are commonly applied to ring resonators, but due to the long length of the cavity they lead to many longitudinal modes oscillating around the central oscillating mode. Many techniques have been utilized to limit these possible large number of modes by incorporating ultra-narrow band fiber Bragg grating (FBG) filter or unpumped erbium doped fiber based saturable absorber [18–22]. As opposed to ring configuration [23–25], a linear cavity will be an attractive approach due to its short length which can limit the number of longitudinal modes [26]. As an example, using an all-polarization maintaining linear cavity which comprises of polarization maintaining fiber Bragg grating and polarization maintaining linearly chirped fiber Bragg grating is able to generate a dual-wavelength output which can be tuned from 0.22 to 0.05 nm [27]. Another approach is to use FBG based Fabry–Perot filter in a ring configuration which is then connected linearly to a section of unpumped erbium doped fiber which is terminated by a narrow band FBG. Wavelength selection and switching are achieved by tuning the FBG to provide a variable spacing between the two wavelengths from 0.20 to 0.54 nm [28, 29]. These two methods have limited tuning range and the system designs are complex and involved.

In this paper, a simple method in generating dual-wavelength output from a linear cavity by using an AWG as a wavelength selector, a broadband FBG and loop back optical as cavity reflectors, is proposed. This design is capable of generating 14 different wavelengths to provide seven ways of dual-wavelength output that can have spacings between them from 0.8 nm to 10.3 nm, which is largely set upon by 100 GHz interchannel spacing of the AWG.

EXPERIMENTAL SETUP

The experimental setup is shown in Fig. 1 which comprises a short length of 5 m erbium doped fiber with a dopant concentration of 900 ppm (absorption 11.9 dB/m at 979 nm) as a gain medium. This erbium doped fiber is pumped by a 980 nm laser diode operating at 110 mW through a 980/1550 nm Wavelength Division Multiplexer (WDM) fused biconical coupler. The front reflector is a composition of a 3-port optical circulator (OC) at 1550 nm with port 1 connected to a 90/10 fused coupler and the other end looping back to

[1] The article is published in the original.

High power dual-wavelength tunable fiber laser in linear and ring cavity configurations

H. Ahmad[1*], A. A. Latif[1], M. Z. Zulkifli[1], N. A. Awang[1], and S. W. Harun[2]

[1]*Photonics Laboratory, Department of Physics, University of Malaya, 50603 Kuala Lumpur, Malaysia*

[2]*Department of Electrical Engineering, Faculty of Engineering, University of Malaya, 50603 Kuala Lumpur, Malaysia*

[*]*Corresponding author: harith@um.edu.my*

Received May 3, 2011; accepted June 10, 2011; posted online August 30, 2011

We describe and compare the performances of two crucial configurations for a tunable dual-wavelength fiber laser, namely, the linear and ring configurations. The performances of these two cavities and the tunability in the dual-wavelength output varied from 0.8 to 11.9 nm are characterized. The ring cavity provides a better performance, achieving an average output power of 0.5 dBm, with a power fluctuation of only 1.1 dB and a signal-to-noise ratio (SNR) of 66 dB. Moreover, the ring cavity has minimal or no background amplified spontaneous emission (ASE).

OCIS codes: 060.2320, 060.2410, 060.3510.

doi: 10.3788/COL201210.010603.

Dual-wavelength tunable fiber lasers (DWTFLs) are relevant to the provision of a stable and tunable dual wavelength output that can be used in many applications, such as the study of high-bit-rate soliton pulses[1], differential absorption measurement of trace gases[2], photonic generation of microwave carriers[3], and microwave photonic filters[4].

Initial research into the development of dual-wavelength fiber lasers has been limited by the inability to generate a high power lasing output. This limitation was caused by the effect of mode competition between the closely spaced wavelengths; resulting in the domination of the longer wavelength over the shorter wavelength. The mode competition itself is largely caused by the homogenous broadening effect in erbium-doped fibers (EDFs), which are normally used as the gain media for fiber-based dual-wavelength sources. To overcome the effect of the homogenous broadening in EDF-based dual-wavelength fiber laser sources, various methods have been proposed, including the cooling of the EDF in liquid nitrogen[5,6] by using elliptical EDFs[7] or by incorporating polarization maintaining fiber Bragg gratings (FBGs) for wavelength selection[8], utilizing frequency shifter in the cavity[9], and many other methods[10−13].

The key ability which is sought after in the development of a DWFTL is repeatability. Generally, multi-wavelength output generated using FBGs as filters to select specific wavelengths provide tunabilty by adjusting the strain or compression that the FBG contends with because of the repeatability issue. The reason is the difficulty to revert to the original position to produce the previous wavelength once the FBG has been modified to select a new wavelength. This problem can be overcome using a filter mechanism with a series of pre-determined wavelengths, such as an arrayed waveguide grating (AWG), as proposed in this letter.

In addition, the cavity configuration plays an important role in the generation of a high-powered output with a good signal-to-noise ratio (SNR). Numerous configurations have been proposed to generate DWFLs, such as linear cavities[14,15], ring cavities[16,17], and sigma cavity configuration[18]. This is in line with the growing research interest in the generation of high-powered DWFLs for applications such as wavelength conversion using four wave mixing (FWM)[19], generation of microwave signals[20], and generation of terahertz waves[21].

We propose the use of AWG as a tuning element because of its repeatability and also compare the two main configurations of DWTFLs, namely, the linear and ring configurations, to determine which can provide a better SNR performance.

Figure 1(a) shows the experimental setup for the linear cavity DWTFL, whereas Fig. 1(b) shows the ring configuration. The linear cavity configuration, as shown in Fig. 1(a), consists of a 5-m MetroGain (fibrecore) erbium-doped fiber with absorption coefficients of 980 and 1 550 nm at 11 and at approximately 13 dB/m, respectively. The length is chosen to meet the requirement of the pumping power of the 980-nm laser diode operating at 110 mW. The EDF is subsequently connected to a 980/1 550-nm wavelength division multiplexer (WDM). The MetroGain EDF acts both as a source for the amplified spontaneous emission (ASE) and as an amplifying medium for the DWTFL. The output ASE will travel in both directions, and the ASE on the right-hand side will be sliced by the 1×16 AWG with an interchannel spacing of 100 GHz (0.8 nm).

To generate the dual wavelength output, any two channels of the AWG can be combined into a broad-band fiber Bragg grating (BB-FBG) that also acts as a "mirror" on the right-hand side of the experimental setup. The ASE will be sliced into 16 different wavelengths, ranging from 1 536.7 (channel 1) to 1 548.6 nm (channel 16). Channel 1 and channel 16 can be connected to the input ports of the BB-FBG that will subsequently reflect these two wavelengths back into the AWG. The broadband reflection spectrum is shown in Fig. 1(c). The tunable wavelength range is approximately 11.9 nm.

Consequently, the combined output will travel to the 5-m EDF for amplification and will be emitted at the 1 550-nm port of the WDM toward port 2 of the optical

PACS numbers: 42.55.Wd; 42.62.–b
DOI: 10.1070/QE2011v041n08ABEH014547

Dual-wavelength tunable fibre laser with a 15-dBm peak power

A.A. Latif, N.A. Awang, M.Z. Zulkifli, S.W. Harun, Z.A. Ghani, H. Ahmad

Abstract. **A high-power dual-wavelength tunable fibre laser (HP-DWTFL) operating in the C-band at wavelengths from 1536.7 nm to 1548.6 nm is proposed and demonstrated. The HP-DWTFL utilises an arrayed waveguide grating (AWG) (1×16 channels) and is capable of generating eight different dual-wavelength pairs with eight possible wavelength spacings ranging from 0.8 nm (the narrowest spacing) to 12.0 nm (the widest spacing). The average output power and side mode suppression ratio (SMSR) of the HP-DWTFL are measured to be 15 dBm and 52.55 dB, respectively. The proposed HP-DWTFL is highly stable with no variations in the chosen output wavelengths and has minimal changes in the output power. Such a laser has good potential for use in measurements, communications, spectroscopy and terahertz applications.**

Keywords: *erbium-doped fibre, arrayed waveguide grating, dual wavelength fibre lasers .*

1. Introduction

Generation of multiple wavelength outputs from fibre lasers has become the focus of increased interest for a number of significant applications including absorption measurements of trace gases and pH measurements, generation of high bit rate soliton pulses, high-resolution spectroscopy, and for fabrication of transmission sources in dense wavelength division multiplexing (DWDM) communication systems. Besides these applications, multiple-wavelength lasers are also used in generating microwave radiation for broadband wireless communication systems and also in sensor networks due to their narrow linewidth of the obtained microwave radiation.

Although there are many types of multi-wavelength fibre configurations, of particular interest to researchers is the dual-wavelength fibre laser (DWFL). It is widely used in applications requiring two or more closely spaced lasing wavelengths that are generated in the erbium-doped fibre amplifier (EDFA) employed as the gain medium for fibre lasers. However, use of the EDFA incurs a limitation due to its homogeneous line broadening, which causes low output powers as well as mode competition. There are, however, attempts to overcome these problems by cooling the EDFA with liquid nitrogen [1, 2], using an elliptical core in the erbium-doped fibre (EDF) [3], by using a polarisation-maintaining fibre Bragg gratings (FBGs) for specific wavelength selection and filtering [4], utilising a frequency shifter in the cavity [5], employing a distributed fibre Bragg (DFB) fibre laser source [6], using the four-wave mixing (FWM) effect as a stabiliser [7], optical injection Fabry–Perot lasers in the DWFL [8], and even dual-ring fibre lasers [9], etc. While these methods are successful to a certain extent in alleviating the problem of mode competition, their complexity and high cost still render them highly prohibitive. Using semiconductor optical amplifiers (SOAs), on the other hand, provides a viable solution to this issue, as the SOA is an inhomogeneous gain medium and thus can be used in the DWFL without causing significant mode competition via cross-gain saturation and strong homogeneous line broadening as in the case of the EDFA. However, SOAs themselves suffer from certain limitations, including a low power output and significant polarisation-dependent loss.

Recently of interest is the fabrication of high-power dual-wavelength laser sources (HP-DWFL) that can be applied in the areas of wavelength conversion using FWM effect [10]. Other applications are the generation of microwave signals [11] and generation of terahertz waves [12], which also require high power dual-wavelength fibre lasers. Existing erbium-doped fibres with high absorption coefficients at 980 nm and 1550 nm offer realisation of a high power dual-wavelength fibre laser, which is due to the ready availability of high pump diode lasers at 980 nm and also the low-loss coupler. There are reported works in this area where ytterbium is used to generate a high power dual-wavelength output at 1060 nm [13, 14] and a codoped Yb/Er was employed for generation at 1550 nm [15–17].

In this paper, we propose a continuous wave high-power dual-wavelength tunable fibre laser (HP-DWTFL) based on a ring cavity coupled to a booster amplifier, which can generate an output power of 15 dBm. The dual-wavelength output is produced by using an arrayed waveguide grating (AWG) together with optical switches (OSs) acting as the selecting element to provide a switchable fibre laser capable of generating wavelength spacings that can be tuned from 0.8 nm to 12.0 nm, which is the first of its kind to be reported.

2. Experimental setup

The experimental setup of the proposed HP-DWTFL is shown in Fig. 1. The system consists of a 5-m-long Metrogain EDF (Fibercore Ltd.) with absorption coefficients of 11.9 dB m^{-1} at 979 nm and 16.4 dB m^{-1} at 1531 nm which acts as the gain

A.A. Latif, N.A. Awang, M.Z. Zulkifli, H. Ahmad Photonics Research Centre (Department of Physics), University of Malaya, 50603 Kuala Lumpur, Malaysia; e-mail: mohdzamani82@yahoo.com;
S.W. Harun Department of Electrical Engineering, Faculty of Engineering, University of Malaya, 50603 Kuala Lumpur, Malaysia;
Z.A. Ghani Faculty of Applied Sciences, MARA University of Technology, 40450 Selangor, Malaysia

Received 21 January 2011; revision received 13 April 2011
Kvantovaya Elektronika **41** (8) 709–714 (2011)
Submitted in English

Journal of Modern Optics
Vol. 56, No. 16, 20 September 2009, 1768–1773

Taylor & Francis
Taylor & Francis Group

Dual wavelength fibre laser with tunable channel spacing using an SOA and dual AWGs

H. Ahmad[a]*, M.Z. Zulkifli[a], A.A. Latif[a], K. Thambiratnam[a] and S.W. Harun[b]

[a]*Photonics Laboratory, Department of Physics, University of Malaya, 50603 Kuala Lumpur, Malaysia;*
[b]*Department of Electrical Engineering, Faculty of Engineering, University of Malaya, 50603 Kuala Lumpur, Malaysia*

(*Received 2 June 2009; final version received 25 August 2009*)

In this paper, we propose and demonstrate a dual wavelength fibre laser (DWFL) based on the use of an inhomogeneously-broadened semiconductor optical amplifier (SOA) gain medium as well as two arrayed waveguide gratings (AWGs) together with two optical channel selectors (OCSs) and a broadband fibre Bragg grating (FBG) to generate dual wavelength output at variable channel spacings. The widest spacing obtained from the DWFL is 12.21 nm, while the narrowest spacing is 1.16 nm. The DWFL has good stability with only minor power fluctuations of less than 2 dB and a side mode suppression ratio (SMSR) of approximately 38.5 dB with fluctuations of less than 0.5 dB.

Keywords: fibre laser; DWDM; SOA; AWG

1. Introduction

Multi-wavelength fibre lasers (MWFLs) are becoming a widely popular choice for replacing conventional single wavelength laser diodes in dense wavelength division multiplexing (DWDM), sensing and characterisation applications. MWFL sources are attractive alternatives to conventional laser diodes because of their simple design as well as their cost effectiveness due to the low cost-per-wavelength ratio. Numerous methods have been put forward in developing MWFLs, including the slicing of amplified spontaneous emission (ASE) [1] generated by a gain medium or by employing non-linear effects such as scattered Brillouin scattering (SBS) [2–4].

Recently, however, the changing needs of various applications have brought about the development of switchable wavelength fibre lasers (SWFLs). SWFLs are essentially MWFLs with the ability to select particular wavelengths amongst a set number of discrete wavelengths to be transmitted, via the use of a wavelength selective filtering mechanism such as cascaded fibre Bragg gratings (FBGs) [5] and compact FBGs written on birefringence fibres [6]. SWFLs have also been demonstrated using wavelength selective mechanisms based on photonics crystal fibres (PCFs) [7] and Sagnac loop mirrors (SLMs) [8]. The benefit of SWFL systems is that they allow users to switch between several discrete wavelengths without the need for tedious tuning procedures while at the same time being robust.

A further advancement of the SWFL is the dual wavelength fibre laser (DWFL). The DWFL is essentially the same as the SWFL except that the DWFL allows the generation of two discrete switchable wavelengths at the same time, compared with the single wavelength generated by the SWFL. DWFLs have gained increasing interest for use in various specialised applications such as the generation of high-bit-rate soliton pulses [9], differential absorption measurement of trace gases [10], photonic generation of microwave carriers [11] and also the realisation of microwave photonic filters [12]. DWFLs are also important as a backup source for dense wavelength division multiplexing (DWDM) system applications because their dual wavelength output allows them to power two sources at the same time, compared to the SWFL which can only power a single source.

DWFLs and SWFLs, as with most MWFLs, use erbium doped fibres (EDFs) as the linear gain medium to achieve lasing wavelengths. This is because the EDF provides a large gain with high saturation power and a relatively low noise figure. However, the use of the EDF as the linear gain medium does have its drawbacks as the erbium ions exhibit homogeneous broadening characteristics at room temperature, thus leading to mode competition and subsequently suppression between the lasing wavelengths (which is more pronounced in DWFLs than in SWFLs). Furthermore, the homogeneous broadening characteristics of the erbium ions combined with the high intensity amplified

*Corresponding author. Email: mohdzamani@um.edu.my; harith@um.edu.my

ISSN 0950–0340 print/ISSN 1362–3044 online

DOI: 10.1080/09500340903289136
http://www.informaworld.com

Abstract: In this paper, a design of a quad-wavelength fiber laser (QWFL) operating in two different regions namely the O-band covering from 1302 nm to1317.4 nm and C-band from 1530.5 nm to 1548.0 nm is presented. Two different ASE sources from semiconductor optical amplifiers (SOAs) are used, one at 1310 nm and the other at1550 nm. By using a 1×24 channels arrayed waveguide grating (AWG) with 100 GHz interchannel spacing, the system is capable of generating 24 different wavelengths in more than 24 ways of quad-wavelength fiber laser with 0.6 nm and 0.8 nm of interval channel for O-band and C-band regions, respectively.

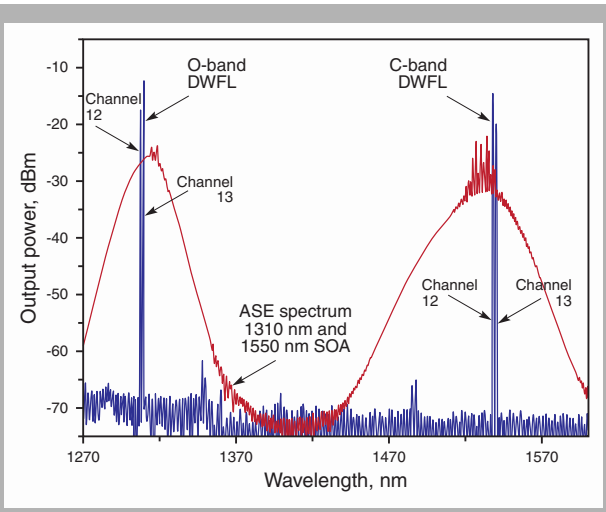

O-band and C-band DWFL with 325 nm span, showing the quad-wavelength outputs with superimposed ASE of the O-band and C-band

A compact O-plus C-band switchable quad-wavelength fiber laser using arrayed waveguide grating

A.A. Latif, [1] *M.Z. Zulkifli,* [1] *N.A. Hassan,* [1] *S.W. Harun,* [2] *Z.A. Ghani,* [3] *and H. Ahmad* [1,*]

[1] Photonics Laboratory, Department of Physics, University of Malaya, Kuala Lumpur 50603, Malaysia
[2] Department of Electrical Engineering, Faculty of Engineering, University of Malaya, Kuala Lumpur 50603, Malaysia
[3] Faculty of Applied Sciences, Universiti Teknologi Mara (UiTM), Shah Alam 40450, Selangor, Malaysia

Received: 11 March 2010, Revised: 5 April 2010, Accepted: 8 April 2010
Published online: 1 June 2010

Key words: semiconductor optical amplifier; arrayed waveguide grating; quad-wavelength fiber laser

1. Introduction

Single-wavelength laser has found many applications as a possible source in an optical network and also as a source for calibrating optical components. There is an immediate need for the tunability of this single wavelength fiber laser that can provide new opportunities as a tunable source for replacement parts in dense wavelength division multiplexing (DWDM) network systems. There are many methods of tuning or switching the output of a fiber laser. Notable methods include using fiber Bragg grating together with acousto-optic super lattice modulator [1], few mode FBGs [2,3], using AWG and broadband FBG [4], optical injection technique [5], using highly non-linear fiber and polarization controller [6–8], and using bismuth doped fiber [9].

Of late, there is also interest in dual wavelength output from a fiber laser for application in the areas of fiber optics sensors, optical spectroscopy and microwaves photonics systems. Dual wavelength output with reasonable output powers can also be a source for generating terahertz radiation. There are many approaches for dual wavelength out-

* Corresponding author: e-mail: harith@um.edu.my, harithba@gmail.com

Optics Communications 285 (2012) 1326–1330

Contents lists available at SciVerse ScienceDirect

Optics Communications

journal homepage: www.elsevier.com/locate/optcom

Synchronous tunable wavelength spacing dual-wavelength SOA fiber ring laser using Fiber Bragg grating pair in a hybrid tuning package

S.S. Chong, H. Ahmad, M.Z. Zulkifli *, A.A. Latif, W.Y. Chong, S.W. Harun

ARTICLE INFO

Article history:
Received 15 November 2010
Received in revised form 27 July 2011
Accepted 18 October 2011
Available online 7 November 2011

Keywords:
Dual-wavelength fiber laser
Fiber Bragg gratings
Semiconductor optical amplifier

ABSTRACT

A Dual-Wavelength Semiconductor Optical Amplifier (DW-SOA) based fiber ring laser with synchronous wavelength tunability is proposed and experimentally demonstrated. The SOA gain medium strongly suppresses mode competition, thus allowing stable dual-wavelength laser oscillation. The wavelength spacing of the two lasers can be tuned synchronously using a modified hybrid-tuning package incorporating a pair of Fiber Bragg Gratings (FBGs). The DW-SOA demonstrates a laser output with a wavelength spacing of between 0.10 and 8.30 nm (wavelength shift inequality of 0.08 to 0.75 nm). The relationship between the applied strain and wavelength shift of the two tuning modes is also analyzed.

1. Introduction

Since the first tunable Fiber Bragg Grating (FBG) using mechanical stress was demonstrated [1], the tunability of FBG has seen a tremendous amount of applications in various fields, including potential applications in tunable fiber laser sources, fiber sensors, and Wavelength Division Multiplexing (WDM) optical communication systems [2–4]. Recently, Single-Longitudinal Mode (SLM) fiber lasers capable of generating dual wavelength outputs with tunable wavelength spacing have attracted considerable interest in research and development, especially for the photonics generation of microwave signals [5]. Numerous efforts in developing tunable dual-wavelength fiber lasers have been proposed and demonstrated [5–11], and these systems are able to generate a dual-wavelength output with channel spacings of as narrow as 27 pm [9] to as wide as 15 nm [10]. The use of separate FBGs to generate a dual-wavelength SLM output from a fiber laser has also been demonstrated [11], with the output having tunable wavelength spacing between 0.1 and 1.3 nm.

While the progress into dual-wavelength fiber lasers is substantial, issues on the stability and power of the dual-wavelength output still arise. Typically, most fiber lasers utilize Erbium Doped Fibers (EDFs) as the gain medium; primarily because it is a well-known technology that is highly compatible with current fiber optic systems and also inexpensive. However, EDFs suffer from homogeneous line broadening and cross-gain saturation that in turn leads to mode competition and subsequently prevents the generation of the dual-wavelength output. In this regard, efforts have now focused on Semiconductor Optical Amplifiers (SOAs) as the gain medium due to its inhomogeneous broadening effect that eliminates the problem of mode competition [5,8]. Consequently, it is a more desirable candidate than the EDF for the generation of stable dual-wavelength output from fiber lasers.

In this paper, we propose and demonstrate a dual-wavelength SOA based fiber laser with the capability to conduct synchronous tuning of the channel spacing. The proposed system utilizes an SOA as the gain medium and a pair of FBGs to provide tunability in the channel spacing. The wavelength spacing can be tuned synchronously from 0.10 nm to 8.30 nm (with a wavelength shift inequality of 0.08 to 0.75 nm) and produces a stable dual-wavelength output. This system has a significant potential in the photonic generation of microwave signals in the 13 GHz to 1 THz frequency range.

2. Theory

The tuning of the channel spacing in this work is accomplished via the application of strain to the FBGs based on a lateral bending beam technique utilizing a hybrid material substrate [12]. The wavelength shift due to the axial strain applied on the FBGs is given as [12]:

$$\Delta\lambda = (1-\rho_e)\varepsilon_z \lambda_B \quad (1)$$

where $\rho_e = 0.22$ is the photo-elastic coefficient, ε_z is the applied strain in the z-direction and λ_B is the Bragg resonance wavelength. The two FBGs are mounted on both sides of the hybrid material so that one experiences compressive strain while the other experiences tensile strain when mechanical bending is applied to the material (note that the strains are experienced simultaneously, thus giving the synchronous tuning capabilities). Fig. 1 shows illustration of the synchronous FBG pair tuning setup.

* Corresponding author. Tel.: +60 3 79677133; fax: +60 3 79674290.
E-mail address: mohdzamani@um.edu.my (M.Z. Zulkifli).

0030-4018/$ – see front matter © 2011 Elsevier B.V. All rights reserved.
doi:10.1016/j.optcom.2011.10.044

Optics & Laser Technology 43 (2011) 550–554

Contents lists available at ScienceDirect

Optics & Laser Technology

journal homepage: www.elsevier.com/locate/optlastec

Flat and compact switchable dual wavelength output at 1060 nm from ytterbium doped fiber laser with an AWG as a wavelength selector

H. Ahmad [a,*], A.A. Latif [a], S.F. Norizan [a], M.Z. Zulkifli [a], S.W. Harun [b]

[a] Photonics Laboratory, Department of Physics, University of Malaya, 5060 Kuala Lumpur, Malaysia
[b] Department of Electrical Engineering, Faculty of Engineering, University of Malaya, 50603 Kuala Lumpur, Malaysia

ARTICLE INFO

Article history:
Received 18 February 2010
Received in revised form
8 July 2010
Accepted 29 July 2010
Available online 21 August 2010

Keywords:
Dual-wavelength fiber lasers
Cavity loss
Ytterbium doped fiber lasers

ABSTRACT

A dual-wavelength ytterbium doped fiber laser with a narrowest spacing of 0.53 nm and widest spacing of 12.2 nm at 1064 nm is presented in this paper. An arrayed waveguide grating (AWG) together with an optical channel selector (OCS) have also been incorporated in the proposed setup that works as a switchable mechanism giving 23 different wavelength tunings. Producing an average output power of −8 dB m and side mode suppression ratio (SMSR) of 59.65 dB, this dual-wavelength fiber laser is quite stable with an output power variance as low as 0.47 dB giving it an advantage due to its switching ability and stable dual-wavelength output powers.

1. Introduction

Fiber lasers have become a huge research area of interest especially as an alternative to solid state and semiconductor lasers due to their high beam quality, narrow bandwidth, good thermal management and their high reliability. This attention has led to the development of multiwavelength fiber lasers that have a variety of applications in optical sensing, precise spectroscopy, characterization of photonics components, and as sources for dense wavelength division multiplexing systems [1,2]. However, recently there has been an increased focus on the development of dual wavelength fiber laser (DWFL) sources. The demand for DWFL is increasing due to the needs of specific applications that can only be provided by the DWFL. Applications in the areas of high-bit-rate soliton pulses [3], differential absorption measurements of trace gases [4], photonic generation of microwave carriers [5] and also the realization of microwave photonic filters [6] are becoming important with the development of DWFL.

Current developments of DWFLs are focused towards the 1550 nm wavelength region using gain mediums such as semiconductor optical amplifier (SOA) [7], bismuth–erbium doped fiber (Bi-EDF) amplifiers [8], Raman fiber amplifiers [9] and erbium doped fiber amplifiers (EDFAs) [10]. However, the semiconductor optical amplifiers (SOAs) are the most preferred medium due to its inhomogeneous nature that provides the necessary platform for dual-wavelength operations but comes with the disadvantage of output instability and associated gain dependence on the polarization state of the input beam. The erbium doped fiber provides a very well studied gain medium for dual-wavelength generation but the homogeneous nature of the gain medium restricts the well controlled generation of dual-wavelength fiber laser. Various techniques such as careful gain or loss equalization [11,12], introducing a filter [13,14], use of an elliptical core EDF [15], multimode fiber Bragg grating [16] and other methods are available in the literature. Using these techniques a well controlled output of multiwavelengths dual-wavelength can be generated for application as mentioned earlier.

With the advent of terahertz technology and applications, various approaches of generating terahertz output are explored. One approach of interest will be to have a dual output at 1064 nm and applying the techniques of different frequency generation in nonlinear crystal output in the range of 0.5–1 THz [17].

In this paper, we report the generation of dual-wavelength output at 1060 nm region using ytterbium doped fiber (YDF) as a gain medium. The advantage of YDF is the high absorption coefficient that results in a very short length of fiber for amplification. In ytterbium doped fiber the spectral output is homogeneous having the same characteristic as in the erbium doped fiber. Techniques such as polarization hole burning (PHB) are used to generate dual wavelength output in ytterbium doped fiber [18]. In this reference, the authors use the few-mode fiber gratings (FMFGs) to provide the switchable dual-wavelength output from the ytterbium doped fibers with a separation of 0.9 nm. There are no results providing the tunability of the two wavelengths. In this paper, we also report a novel method of producing switchable dual wavelength output using an arrayed

* Corresponding author. Tel.: +60 3 79674290; fax: +60 3 79676770.
E-mail address: harith@um.edu.my (H. Ahmad).

0030-3992/$ - see front matter © 2010 Elsevier Ltd. All rights reserved.
doi:10.1016/j.optlastec.2010.07.013

CHAPTER 5

1. Awang NA, Ahmad H, **Latif AA**, Zulkifli MZ, Harun SW. Four-wave mixing in dual wavelength fiber laser utilizing SOA for wavelength conversion. Optik. 2011;122(9):754-7.

2. Ahmad, H., **Latif, A. A.**, Zulkifli, M. Z., Awang, N. A., & Harun, S. W. (2012). Temperature Sensing Using Frequency Beating Technique From Single-Longitudinal Mode Fiber Laser. IEEE Sensors Journal, *12*(7), 2496-2500.

Optik 122 (2011) 754–757

Contents lists available at ScienceDirect

Optik

journal homepage: www.elsevier.de/ijleo

Four-wave mixing in dual wavelength fiber laser utilizing SOA for wavelength conversion

N.A. Awang[a], H. Ahmad[a,*], A.A. Latif[a], M.Z. Zulkifli[a], S.W. Harun[b]

[a] Photonics Laboratory, Department of Physics, University of Malaya, 50603 Kuala Lumpur, Malaysia
[b] Department of Electrical Engineering, Faculty of Engineering, University of Malaya, 50603 Kuala Lumpur, Malaysia

ARTICLE INFO

Article history:
Received 4 November 2009
Accepted 27 May 2010

Keywords:
Four-wave mixing
Dual wavelength fiber laser
Semiconductor optical amplifier
Bi-EDF doped fiber

ABSTRACT

In this paper, a novel configuration of a wavelength converter is set forth by utilizing a semiconductor optical amplifier (SOA) as a nonlinear gain medium to generate a four-wave mixing (FWM) effect by using a dual wavelength bi-erbium-doped fiber laser that uses an Arrayed Waveguide Grating (AWG) together with two optical channel selector (OSC) as selective elements to function as a dual wavelength switchable pump power. The four-wave mixing (FWM) is produced with a wavelength detuning of 7 nm from the pump and signal which used is as the converted signal at wavelength 1532.8 nm or 1534.5 nm for transferring data from the input signal at wavelength 1547.0 nm. Thus, even though the conversion efficiency is as low as −43 dB, it is still possible for applications as a wavelength converter.

1. Introduction

Four-wave mixing (FWM) in semiconductor optical amplifiers (SOA) is useful depending on the application such as wavelength converter [1], supercontinuum generation [2], fast optical switching [3] and sub-carrier multiplexed radio over fiber [4]. The generation of the FWM effect is associated with the nonlinearity of the SOA. It is principally caused by carrier density pulsation, carrier heating and spectra hole burning changes induced by the amplifier input signal [1]. The mechanism of generating FWM is based on wavelength detuning where in the detuning above a few nm; the mechanism called a carrier density modulation happens [4]. Such a mechanism falls within the category of interband effects that change the carrier density due to the depletion caused by stimulated emission. For wavelength detuning below a few nm, the FWM generated is based off the intraband effect where it is associated with two phenomenon; spectra hole burning (SHB) and carrier heating (CH). In the SHB mechanism, an optical input signal create holes and changes the intraband carrier distribution producing modulation of the occupation probability of carriers within the energy band. The CH phenomena on the other hand is caused when free carriers at low energy levels are removed by stimulated emission or transferred to a higher level due to free carrier absorption [4].

Recently, the FWM effect in SOAs has become a promising technique with regards to wavelength converters. Wavelength converters are important tool in future WDM-based high speed optical networks because it provides simultaneous conversion of a single data channel into different channels without the necessity of multiple optical–electronic-optical transponders. Basically the wavelength converter utilizing the FWM technique has two schemes, the co-polarized pump scheme and orthogonal polarized pump scheme [5]. A typical dual wavelength laser source is injected to the nonlinear medium by incorporating two external laser sources such as a tunable laser source (TLS) as a pump source for the wavelength conversion. Recently, we have reported a simple configuration dual wavelength fiber laser by utilizing 24 Channel Arrayed Waveguide Gratings (AWG) as a wavelength selector in a two-cavity configuration that produces dual wavelength outputs by controlling both of the cavity losses to cope with the homogeneous broadening effect that comes from the Erbium-doped fiber, by now an infamously well known obstacle in producing dual and/or multiwavelength laser sources by using EDF as an active medium [6]. In this paper, we propose and demonstrate the conversion of wavelengths by the FWM effect by using an orthogonal polarized pump scheme in a dual wavelength fiber laser. This scheme represents a larger wavelength detuning range of input signal, pump signal and converted signal.

2. Experimental setup

The proposed experimental setup is shown in Fig. 1 below:

This experimental setup consists of two ring cavities that shares the same gain medium, a 14 m long Erbium-doped fiber (EDF), a 48 cm Bismuth-Erbium-doped fiber (Bi-EDF) and a 1550 nm SOA

* Corresponding author. Tel.: +60 3 79674290; fax: +60 3 79676770.
E-mail address: harith@um.edu.my (H. Ahmad).

0030-4026/$ – see front matter © 2010 Elsevier GmbH. All rights reserved.
doi:10.1016/j.ijleo.2010.05.018

Temperature Sensing Using Frequency Beating Technique From Single-Longitudinal Mode Fiber Laser

Harith Ahmad, Amirah A. Latif, Mohd. Zamani Zulkifli, Noor Azura Awang, and Sulaiman Wadi Harun

***Abstract*— In this paper, a high-resolution fiber temperature sensor is proposed and demonstrated using the frequency beating technique. The sensor uses a constant wavelength (CW) at 1539.96 nm as the reference signal for the frequency beating technique. The sensor signal is provided by a fiber Bragg grating (FBG) tuned single-longitudinal mode (SLM) fiber laser, which consists of a 0.5-m long highly doped Zirconium–Erbium doped with an erbium concentration of 3000 ppm as the gain medium. The signal of the SLM, which is generated by the FBG in response to external temperature changes, is mixed with the CW signal using a 3-dB fused coupler into a 6-GHz photodetector to generate frequency beating. The typical response of the system is about 1.3 GHz/°C, with nominal temperature measurement resolutions of 0.0023 °C being achieved, taking into account the resolution bandwidth of 3 MHz of the radio frequency spectrum analyzer.**

***Index Terms*— Dual-wavelength pulse, erbium-doped fiber, frequency generation, saturable absorber.**

I. Introduction

RECENTLY, there has been significant interest in the development of high resolution temperature sensors capable of detecting and measuring minute shifts in temperature for a wide variety of applications such as nano-biotechnology [1], micro-fluidic mechanics [2], thermal drift measurement in electronic equipment [3] and even the measurement of small temperature changes that arise from enzyme catalysis reactions [4, 5]. Traditionally, such temperature measurements can be done by conventional technologies such as thermistors, thermocouples, Resistance Temperature Detector (RTDs) and Platinum Resistance Temperature (PRT) sensors, which have resolutions ranging from 0.1 °C to 0.001 °C [6–8]. However, these sensors work on the electrical and mechanical responses to heat stimuli, and as a result very costly and fragile, as well as extremely sensitive to electromagnetic and environmental interference [9]. This severely limits their usage in various applications, in particular the above-mentioned.

In this regard, fiber based sensors have been seen as a highly potential alternative to develop compact and cost-efficient [10–12] temperature sensors which are electronically passive and resistant to electromagnetic interference. Various approaches to develop fiber based sensors have been explored, including the use of Fiber Bragg Gratings (FBGs) that are able to provide resolutions of up to 0.1 °C [10] as well as demodulation techniques using narrow band distributed feedback lasers [11] and FBG based extrinsic Fizeau sensors [12], which give resolutions as high as 0.05 °C to 0.07 °C. Besides this, other demodulation schemes such as optical filtering [13, 14], and also using interferometry techniques [15] have been explored. Recently, there has been a report of using a PbO-GeO_2-SiO_2 based fibers to enhance the sensitivity, with added material complexity.

Although FBG based fiber sensors present the most suitable candidate for the development of a commercially viable high-resolution temperature sensor, due to their low cost and low complexity as compared to other optical approaches, but they have limited temperature resolutions of approximately 0.01 °C [9]. In order to increase the resolution of FBG based sensors, frequency beating techniques using dual-wavelength continuous wave lasers in conjunction with FBGs are now being explored as a possibility. The success of the frequency beating technique for high-resolution sensor measurements has already been demonstrated for strain measurement [16, 17] using a dual-wavelength fiber laser. In this paper, we propose and demonstrate a similar technique for temperature measurement, using a dual-wavelength fiber laser that consists of a Constant Wavelength (CW) signal as the reference signal and an FBG tuned Single Longitudinal Mode Fiber Laser (SLM-FL) which acts as the sensor element. Measurements obtained by this technique are taken in the frequency domain by a Radio Frequency Spectrum Analyzer (RF-SA) with a very high resolution of 0.0023 °C. As to the knowledge of the authors, this is the first time this technique is applied to temperature measurement.

II. Experimental Setup

The experimental setup is shown in Figure 1, which consists of (a) an SLM-FL capable of generating a stable dual-wavelength output to be used in a (b) dual-wavelength

Manuscript received September 17, 2011; revised November 20, 2011; accepted December 22, 2011. Date of publication April 4, 2012; date of current version May 31, 2012. This work was supported in part by the University of Malaya under HIR Grant Terahertz, UM.C/HIR/MOHE/SC/01, MOHE. The associate editor coordinating the review of this paper and approving it for publication was Prof. Istvan Barsony.

H. Ahmad, A. A. Latif, M. Z. Zulkifli, and N. A. Awang are with the Photonics Research Centre, Department of Physics, University of Malaya, Kuala Lumpur 50603, Malaysia (e-mail: harith@um.edu.my; ammaug17@yahoo.com; mohdzamani82@yahoo.com; noorazura_msf@yahoo.com).

S. W. Harun is with the Department of Electrical Engineering, Faculty of Engineering, University of Malaya, Kuala Lumpur 50603, Malaysia (e-mail: swharun@um.edu.my).

Digital Object Identifier 10.1109/JSEN.2012.2191401

APPENDIX B:

REPRINT OF SELECTED PAPERS PUBLISHED BASED ON THE DEVELOPED TECHNIQUES FROM THE RESEARCH WORK

Optics & Laser Technology 44 (2012) 2168–2174

Contents lists available at SciVerse ScienceDirect

Optics & Laser Technology

journal homepage: www.elsevier.com/locate/optlastec

Wide-band fanned-out supercontinuum source covering O-, E-, S-, C-, L- and U-bands

H. Ahmad [a,*], A.A. Latif [a], N.A. Awang [a], M.Z. Zulkifli [a], K. Thambiratnam [a], Z.A. Ghani [c], S.W. Harun [a,b]

[a] Photonics Research Centre, Physics Department, University of Malaya, 50603 Kuala Lumpur, Malaysia
[b] Department of Electrical Engineering, Faculty of Engineering, University of Malaya, 50603 Kuala Lumpur, Malaysia
[c] Faculty of Applied Sciences, Universiti Teknologi MARA UiTM, Shah Alam 40450, Selangor Darul Ehsan, Malaysia

ARTICLE INFO

Article history:
Received 5 January 2012
Received in revised form
14 February 2012
Accepted 6 March 2012
Available online 28 March 2012

Keywords:
Supercontinuum
Bi–EDF
Mode-locked fiber laser

ABSTRACT

A wide-band supercontinuum source generated by mode-locked pulses injected into a Highly Non-Linear Fiber (HNLF) is proposed and demonstrated. A 49 cm long Bismuth–Erbium Doped Fiber (Bi–EDF) pumped by two 1480 nm laser diodes acts as the active gain medium for a ring fiber laser, from which mode-locked pulses are obtained using the Non-Polarization Rotation (NPR) technique. The mode-locked pulses are then injected into a 100 m long HLNF with a dispersion of 0.15 ps/nm km at 1550 nm to generate a supercontinuum spectrum spanning from 1340 nm to more than 1680 nm with a pulse width of 0.08 ps and an average power of −17 dBm. The supercontinuum spectrum is sliced using a 24 channel Arrayed Waveguide Grating (AWG) with a channel spacing of 100 GHz to obtain a fanned-out laser output covering the O-, E-, S-, C-, L- and U-bands. The lasing wavelengths obtained have an average pulse width of 9 ps with only minor fluctuations and a mode-locked repetition rate of 40 MHz, and is sufficiently stable to be used in a variety of sensing and communication applications, most notably as cost-effective sources for Fiber-to-the-Home (FTTH) networks.

1. Introduction

The application of the Supercontinuum (SC) sources cuts across many fields such as optical frequency metrology [1,2], time-resolved spectroscopy [3], optical sensing [4,5] and Dense Wavelength Division Multiplexing (DWDM) communication systems [6]. Optical Time Division Multiplexing (OTDM) has played a major role in realising high capacity and high bit-rates in point-to-point data transportation [7].

SC sources have wide-spectral range and high repetition rates, and can be used as pulse sources for the generation of picosecond pulses without the detrimental effect of timing jitters, which can find applications in photonics networks that employ OTDM riding on DWDM systems. Among the SC sources, those based on fibers are most effective in obtaining a broad-band spectrum with bandwidths exceeding 150 nm. In realising sources for communications networks, the SC spectrum needs to be sliced into various components and generally, those fiber based SC sources have a nearly flat *amplitude* spectrum over a wide-bandwidth, giving channel power equalization. Another requirement will be to have output pulses with similar spectral distributions, temporal pulse-widths and nearly uniform power levels across the whole spectrum.

Various techniques have been proposed to tune and split the SC spectrum into multi-channels of desired wavelengths, such as using tunable bandpass filters with a bandwidth of about 1 nm [8–11]. However, the limitation of this approach is that only a single wavelength can be generated at a time. In order to meet the requirements for sources in DWDM systems multiple signals are required, and the use of Arrayed Waveguide Gratings (AWG) can be a preferred alternative. AWGs allow for the generation of multiple wavelengths at a single time, and also have the advantage of a narrower channel spacing, giving values such as 200 GHz (1.6 nm), 100 GHz (0.8 nm) and of late 50 GHz (0.4 nm) and also 25 GHz (0.2 nm). There have been earlier reports of the use of AWGs to slice SC spectra as reported in [12–15], however, they have many limitations such as limited bandwidth within the C-band region spanning from around 1520 nm to around 1570 nm and also require complicated setups such as modulated Distributed Feedback (DFB) laser diodes, ring fiber lasers with boosters and some are actively mode-locked.

In this work, a novel approach is being proposed using a highly doped Bismuth–Erbium doped fiber in a ring configuration and mode-locked using the Non-linear Polarization Rotation (NPR) technique, which has a similar behavior as a saturable absorber. The SC is generated using a length of Highly Non-Linear Fiber (HLNF) with the output being sliced and fanned-out by a 1×24 AWG with a channel spacing of 100 GHz. The output spans from 1340 nm to more than 1680 nm, covering the entire band stretching from O-, E-, S-, C-, L- and U-bands. The measured repetition rate of the pulses is about 40 MHz which can be further increased by

* Corresponding author. Tel.: +603 79677133; fax: +603 79674146.
E-mail address: harith@um.edu.my (H. Ahmad).

0030-3992/$ - see front matter © 2012 Published by Elsevier Ltd.
http://dx.doi.org/10.1016/j.optlastec.2012.03.007

Journal of Modern Optics
Publication details, including instructions for authors and subscription information:
http://www.tandfonline.com/loi/tmop20

Wavelength conversion based on FWM in a HNLF by using a tunable dual-wavelength erbium doped fibre laser source

N.A. Awang [a b], H. Ahmad [a], A.A. Latif [a], M.Z. Zulkifli [a], Z.A. Ghani [c] & S.W. Harun [d]

[a] Photonics Laboratory, Department of Physics, University of Malaya, 50603 Kuala Lumpur, Malaysia

[b] Faculty of Science, Art and Heritage, Universiti Tun Hussein Onn Malaysia, 86400 Batu Pahat, Johor, Malaysia

[c] Faculty of Applied Sciences, MARA University of Technology, 40450 Shah Alam, Malaysia

[d] Department of Electrical Engineering, Faculty of Engineering, University of Malaya, 50603 Kuala Lumpur, Malaysia

Version of record first published: 06 Feb 2011

To cite this article: N.A. Awang, H. Ahmad, A.A. Latif, M.Z. Zulkifli, Z.A. Ghani & S.W. Harun (2011): Wavelength conversion based on FWM in a HNLF by using a tunable dual-wavelength erbium doped fibre laser source, Journal of Modern Optics, 58:7, 566-572

To link to this article: http://dx.doi.org/10.1080/09500340.2011.552796

Journal of Modern Optics
Publication details, including instructions for authors and subscription information:
http://www.tandfonline.com/loi/tmop20

Tunable single longitudinal mode S-band fiber laser using a 3 m length of erbium-doped fiber

H. Ahmad [a], M.Z. Zulkifli [a], A.A. Latif [a], M.H. Jemangin [a], S.S. Chong [a] & S.W. Harun [b]

[a] Photonics Research Center, Department of Physics, University of Malaya, 50603 Kuala Lumpur, Malaysia

[b] Department of Electrical Engineering, Faculty of Engineering, University of Malaya, 50603 Kuala Lumpur, Malaysia

Version of record first published: 19 Oct 2011

To cite this article: H. Ahmad, M.Z. Zulkifli, A.A. Latif, M.H. Jemangin, S.S. Chong & S.W. Harun (2012): Tunable single longitudinal mode S-band fiber laser using a 3 m length of erbium-doped fiber, Journal of Modern Optics, 59:3, 268-273

To link to this article: http://dx.doi.org/10.1080/09500340.2011.626900

Journal of Modern Optics
Publication details, including instructions for authors and subscription information:
http://www.tandfonline.com/loi/tmop20

O-band to C-band wavelength converter by using four-wave mixing effect in 1310nm SOA

N.A. Awang [a], H. Ahmad [a], A.A. Latif [a], M.Z. Zulkifli [a], Z.A. Ghani [c] & S.W. Harun [b]

[a] Photonics Laboratory, Department of Physics, University of Malaya, 50603 Kuala Lumpur, Malaysia

[b] Department of Electrical Engineering, Faculty of Engineering, University of Malaya, 50603 Kuala Lumpur, Malaysia

[c] Faculty of Applied Sciences, Universiti Teknologi Mara (UiTM), 40450 Shah Alam, Selangor, Malaysia

Version of record first published: 11 Nov 2010

To cite this article: N.A. Awang, H. Ahmad, A.A. Latif, M.Z. Zulkifli, Z.A. Ghani & S.W. Harun (2010): O-band to C-band wavelength converter by using four-wave mixing effect in 1310nm SOA, Journal of Modern Optics, 57:21, 2147-2153

To link to this article: http://dx.doi.org/10.1080/09500340.2010.529953